

Mode of Action Studies with Phthalate Acid Monoesters: Pharmacokinetic and  
Pharmacodynamic Factors Affecting Steroidogenesis

Rebecca Ann Clewell

A dissertation submitted to the faculty of the University of North Carolina at Chapel Hill in  
partial fulfillment of the requirements for the degree of Doctor of Philosophy in the  
Department of Environmental Science and Engineering.

Chapel Hill  
2009

Approved by:

Louise Ball, PhD

Melvin Andersen, PhD

Rebecca Fry, PhD

Noelle Granger, PhD

Ivan Rusyn, PhD

Russell Thomas, PhD

## ABSTRACT

REBECCA CLEWELL: Mode of Action Studies with Phthalate Acid Monoesters:  
Pharmacokinetic and Pharmacodynamic Factors Affecting Steroidogenesis  
(Under the direction of Melvin Andersen and Louise Ball)

The use of phthalate esters in plastics and resulting human exposure has led to concern over potential adverse effects in fetal development. This project provided data and quantitative tools to improve phthalate risk assessments. *In vivo*, *in vitro* and *in silico* experiments evaluated pharmacokinetic and pharmacodynamic factors responsible for anti-androgenic effects of phthalate esters. For pharmacokinetics, plasma and tissue metabolite levels were measured in maternal and fetal rats following DBP administration. A physiologically based pharmacokinetic (PBPK) model was developed for DBP distribution in rat gestation, tested against a variety of data across life-stages, doses and exposure routes, and accurately predicted maternal and fetal plasma MBP levels for acute and repeated dosing. The validated model permitted direct correlation of testes phthalate concentrations and testosterone. When extended to DEHP, the model also predicted MEHP kinetics. For pharmacodynamic evaluation, monoester concentrations were measured in the fetal testes after repeated doses of BBP, DEP, DBP, DEHP, and DMP. An *in vitro* assay tested the effect of inhibition of steroidogenesis directly in the Leydig cell. The differential ability of the monoesters to cause developmental toxicity was found to result from differences in their pharmacodynamic potency. Finally, we attempted to identify the molecular target for the phthalates in the Leydig cell. The phospholipase A<sub>2</sub> (PLA<sub>2</sub>) inhibitor CQ and MEHP had a

similar ability to inhibit testosterone production, steroidogenic gene expression and AA release in the LH-stimulated (MA-10) Leydig cell. Both compounds interfered with translocation of fluorescently tagged cPLA<sub>2</sub> in human HEK-cells after activation by a calcium ionophore, providing at least indirect evidence that inhibition of AA release by cPLA<sub>2</sub> is likely to be involved in phthalate anti-androgenic effects. When CQ was administered to the pregnant rat, fetal testes testosterone levels were reduced in a dose-dependent manner. CQ also down-regulated steroidogenic genes as noted with active phthalate administration. Our results strongly indicate that cPLA<sub>2</sub> is a key target of these phthalates in relation to decreased testosterone production. The improved understanding of phthalate dose-response and mechanism of action, together with *in vitro* derived potencies of phthalates for testosterone inhibition, should greatly improve cumulative risk assessments for the phthalates.

## ACKNOWLEDGEMENTS

I am truly grateful for the guidance and support of my research advisor, Dr. Mel Andersen, who gave me a lot of leeway to make this project my own, but also consistently challenged me to try a lot of new and often uncomfortable kinds of science. These experiments weren't ever easy, and were often frustrating, but I learned more than I ever expected. Miraculously, this PBPK modeler and former chemist finally feels comfortable in a molecular biology lab. I am a better scientist for this experience and I know that the skills I learned here will benefit me and those I work with in the future.

I am also thankful for the guidance of my thesis committee, Drs. Louise Ball, Rusty Thomas, Ivan Rusyn, Noelle Granger and Rebecca Fry who encouraged and challenged me all along the way. Dr. Ball also helped me navigate my way through the university guidelines and requirements, which are much more confusing than any GCPR pathway.

I'd also like to express my gratitude to the Hamner Institutes for Health Sciences for financial support and use of their excellent resources and to Drs. Kevin Gaido, Susan Borghoff, Jerry Campbell and Kamin Johnson, and Susan Ross who've taught and encouraged me and helped make these experiments and models happen.

Finally, my family and friends have always encouraged me throughout my career and in my decision to go back to school: Amy, Carl, Chris, my niece and nephews who are more precious than any thesis, Joel, Tina and my fellow potters. Ya'll kept me sane! My parents in particular have been ridiculously supportive: I love you and I can't ever thank you enough.

## TABLE OF CONTENTS

LIST OF TABLES.....	xi
LIST OF FIGURES.....	xii
LIST OF ABBREVIATIONS AND SYMBOLS.....	xvi
Chapter	
I. INTRODUCTION.....	1
A. PHTHALATE ESTERS.....	2
<i>Commercial use and population exposure</i> .....	2
<i>Metabolism, distribution and excretion of phthalates</i> .....	3
<i>Hepatic effects and enzyme induction</i> .....	4
<i>Effects of phthalates on testosterone-mediated sexual development</i> .....	6
<i>Phthalate kinetics and dose-response for fetal effects</i> .....	7
<i>Testosterone synthesis and potential mechanisms for phthalate disruption</i> .....	9
B. PHTHALATE RISK ASSESSMENT AND LEGISLATION.....	11
C. STUDY OBJECTIVE.....	12
II. Kinetics of Selected Di-n-butyl Phthalate Metabolites and Fetal Testosterone Following Repeated and Single Administration in Pregnant Rats.....	16
A. ABSTRACT.....	17
B. INTRODUCTION.....	18
C. METHODS.....	21

<i>Animals</i> .....	21
<i>Dosing solutions and treatment</i> .....	21
<i>MBP and MBP-G sample preparation</i> .....	22
<i>Testosterone sample preparation</i> .....	23
<i>Calibration and quality control standards</i> .....	24
<i>MBP/MBP-G analysis with liquid chromatography/mass spectrometry</i> .....	24
<i>Testosterone analysis with gas chromatography/mass spectrometry</i> .....	26
<i>Bicinchoninic acid assay</i> .....	27
<i>Pharmacokinetic analysis</i> .....	27
A. RESULTS.....	28
<i>MBP pharmacokinetics after repeated dosing</i> .....	28
<i>MBP-G pharmacokinetics after repeated dosing</i> .....	29
<i>Single versus repeated dosing</i> .....	31
<i>Testosterone response in fetal testes</i> .....	32
B. DISCUSSION.....	35
III. Tissue Exposures to Free and Glucuronidated Monobutylphthalate in the Pregnant and Fetal Rat Following Exposure to Di-n-butyl Phthalate: Evaluation with a PBPK Model.....	49
A. ABSTRACT.....	50
B. INTRODUCTION.....	51
C. METHODS.....	55
<i>Pharmacokinetic studies in vivo</i> .....	55
<i>PBPK model structure</i> .....	56
<i>Adult male rat model</i> .....	57
<i>Modifications for gestation</i> .....	59
<i>Parameterization in the adult male rat PBPK mode</i> .....	60
<i>PBPK model validation in the adult male rat</i> .....	64
<i>Application of adult male rat DBP PBPK model to gestation</i> .....	64
<i>Extrapolation of acute DBP gestation PBPK model to multiple         day exposures</i> .....	69
<i>Sensitivity analysis of model parameters</i> .....	69
D. RESULTS.....	71

<i>Pharmacokinetic studies in vivo</i> .....	71
<i>PBPK model validation in the adult male rat</i> .....	72
<i>Application of adult male rat DBP PBPK model to gestation</i> .....	73
<i>Extrapolation of acute DBP gestation PBPK model to multiple day exposures</i> .....	75
<i>Sensitivity analysis</i> .....	77
<i>Using the multiple exposure model to interpret effects data</i> .....	78
D. DISCUSSION.....	80
E. CONCLUSION.....	84
F. ADDITIONAL RESEARCH.....	85
Extrapolation of the Published PBPK Model to Describe DEHP kinetics...	85
<i>Changes to the model structure</i> .....	85
<i>DEHP model parameterization</i> .....	86
<i>DEHP model validation</i> .....	88
<i>Comparing internal dose associated with DEHP and DBP disruption of sexual development in rats</i> .....	89
IV. Phthalate Esters: Pharmacokinetic and Pharmacodynamic Factors Affecting Potency for Testosterone-Mediated Developmental Effects.....	112
A. ABSTRACT.....	113
B. INTRODUCTION.....	114
C. METHODS.....	116
Examination of pharmacokinetic differences among phthalates.....	116
<i>Animals</i> .....	116
<i>Treatment</i> .....	117
<i>Phthalate Analysis</i> .....	117
Development of an <i>in vitro</i> assay for phthalate inhibition of steroidogenesis.....	118
<i>Cell culture</i> .....	118

<i>Progesterone and testosterone inhibition</i> .....	118
<i>Protein content and viability analysis</i> .....	119
<i>Real-time quantitative PCR</i> .....	119
Examination of pharmacodynamic differences among phthalates.....	120
D. RESULTS.....	121
<i>Examination of pharmacokinetic differences among phthalates</i> .....	121
<i>Validation of an in vitro assay for phthalate inhibition of steroidogenesis</i> .....	121
<i>Examination of pharmacodynamic differences among phthalates</i> .....	124
<i>Predictive use of the MA-10 inhibition assay</i> .....	124
E. DISCUSSION.....	125
F. CONCLUSION.....	128
V. Evaluation of Cytosolic Phospholipase A <sub>2</sub> as a Potential Target of Steroid Inhibiting Phthalates.....	136
A. ABSTRACT.....	137
B. INTRODUCTION.....	138
C. METHODS.....	140
<i>Inhibition of testosterone synthesis in MA-10 cells</i> .....	140
<i>Protein assay</i> .....	140
<i>Quantitative RT-PCR</i> .....	141
<i>Inhibition of AA release in MA-10 cells</i> .....	142
<i>Calcium stimulated EGFP-cPLA<sub>2</sub> translocation</i> .....	142
<i>Confocal microscopy</i> .....	143
D. RESULTS AND DISCUSSION.....	144
<i>MEHP and CQ have similar effects on testosterone production and steroidogenic gene expression in MA-10 cells</i> .....	144
<i>MEHP and CQ inhibit LH-stimulated AA release in MA-10 cells</i> .....	145
<i>MEHP and CQ interfere with calcium stimulated translocation of EGFP-cPLA<sub>2</sub> to the perinuclear region</i> .....	146



E. CONCLUSIONS.....	148
VI. <i>In Utero</i> Exposure to Chloroquine Alters Sexual Development in the Male Fetal Rat.....	158
A. ABSTRACT.....	159
B. INTRODUCTION.....	160
C. METHODS.....	162
<i>Animals</i> .....	162
<i>Dosing solutions</i> .....	162
<i>Treatment</i> .....	163
<i>CQ analysis in dosing solutions</i> .....	164
<i>CQ analysis in serum samples</i> .....	164
<i>Maternal serum hormone analysis</i> .....	166
<i>Fetal testosterone analysis</i> .....	166
<i>Bicinchoninic acid assay</i> .....	166
<i>Histopathology</i> .....	167
<i>Clinical chemistry</i> .....	167
<i>Microarray hybridization</i> .....	168
<i>Microarray analyses</i> .....	168
<i>Quantitative RT-PCR</i> .....	169
D. RESULTS.....	170
<i>Analytical chemistry</i> .....	170
<i>Body weight changes and toxicity</i> .....	170
<i>Effect of CQ on hormone homeostasis and male fetus sexual development</i> .....	171
E. DISCUSSION.....	175
F. ADDITIONAL RESEARCH.....	178
Dose-Response Evaluation of Chloroquine Effects on Testosterone and Steroidogenic Gene Expression in the Fetal Rat Testes.....	178
<i>Chloroquine administration to pregnant rats and necropsy</i> .....	178
<i>Analysis of fetal testes testosterone and steroidogenic gene expression</i> .....	179

<i>Conclusions on chloroquine in vivo studies</i> .....	180
VII. GENERAL DISCUSSION.....	194
A. SUMMARY OF EXPERIMENTS.....	195
B. USING DOSE-RESPONSE MODELING TO EVALUATE POTENTIAL MOLECULAR TARGETS OF THE PHTHALATE MONOESTERS IN THE LEYDIG CELL.....	198
C. STUDY LIMITATIONS FUTURE DIRECTIONS.....	202
REFERENCES.....	209

## LIST OF TABLES

### Table

2.1.	Calculated Pharmacokinetic Parameters for MBP and MBP-G in Maternal Plasma, Fetal Plasma, and Amniotic Fluid after Repeated Doses of 50, 100, and 500 mg/kg/day from GD 12 to GD 19 calculated with WinNonlin®.....	42
3.1.	Physiological Parameters.....	91
3.2.	Kinetic Parameters.....	92
6.1.	Body Weights and Markers of Liver Toxicity.....	182
6.2.	Significantly altered genes in the testes of GD 19 male rat after CQ exposure (adjusted $p < 0.05$ ).....	183
6.3.	Characterized genes with changes in fetal testis expression of at least 1.5 fold after maternal CQ treatment.....	184
7.1.	Estimated potency of phthalates: Comparison across biological endpoints.....	208

## LIST OF FIGURES

Figure		
1.1.	Chemical structure of common phthalate esters.....	15
2.1.	Concentration of MBP after the last dose of DBP administered from GD 12-19.....	42
2.2.	Concentration of MBP-G after the last dose of DBP administered from GD 12-19.....	43
2.3.	MBP and MBP-G concentrations after single (GD 19) or repeated doses (GD 12-19) of 500 mg/kg DBP.....	44
2.4.	MBP and testosterone in fetal testes from dams exposed to 50, 100, or 500 mg DBP/kg/day from GD 12-19.....	45
2.5.	Testosterone recovery 4 and 24 hours after the last dose of DBP at 50, 100, or 500 mg/kg/day from GD 12-19.....	46
2.6.	MBP and testosterone in fetal testes from dams exposed to a single dose of 500 mg DBP/kg/day on GD 19.....	47
2.7.	Dose-response for testes testosterone in the GD 19 fetus after administration of 50, 100, or 500 mg DBP/kg/day to the pregnant dam.....	48
3.1.	Model structure for DBP kinetics in the pregnant rat.....	94
3.2.	Development and Validation for the Adult Male, Pregnant and Fetal Rat Model.....	95
3.3.	Total radioactivity, DBP and metabolites in plasma and urine of the male rat after a 10 mg/kg iv dose of <sup>14</sup> C-DBP.....	96
3.4.	Free MBP in the blood of the adult male rat after exposure to DBP via intravenous injection or oral gavage.....	97
3.5.	Maternal Plasma free MBP and MBP-G after a single 100mg/kg DBP oral dose on GD 20.....	98
3.6.	MBP and MBP-G in maternal plasma fetal plasma, and amniotic fluid after a single dose of 50, 100, or 250 mg/kg DBP on GD 20.....	99
3.7.	Free MBP and MBP-G in the maternal and fetal plasma, amniotic fluid, and fetal testes after a single oral dose of 500 mg/kg DBP on GD19.....	100

3.8.	Model predicted MBP and MBP-G in maternal blood, whole fetus, and placenta on GD 14.....	101
3.9.	Maternal plasma concentrations of free MBP and MBP-G after a single <i>iv</i> dose of MBP on GD 19.....	102
3.10.	MBP and MBP-G in maternal plasma and placenta tissue after the last daily dose of 50, 100 or 500 mg/kg-day administered from GD 12-19.....	103
3.11.	MBP and MBP-G in fetal plasma and fetal testes, and amniotic fluid after the last dose of 50, 100, or 500 mg/kg-day administered from GD 12-19.....	104
3.12.	Calculated sensitivity coefficient for model parameters with respect to maternal plasma MBP AUC 24 hrs after a single oral dose of 10 or 500 mg/kg DBP on GD 20.....	105
3.13.	DBP dose response: Predicted average daily concentration of MBP in maternal and fetal plasma and fetal testes at external doses ranging from 1 to 550 mg DBP/kg-day from GD12.....	106
3.14.	Revised PBPK model structure to describe both DEHP and DBP kinetics in the pregnant rat.....	107
3.15.	Free MEHP in the blood of the adult male rat after an <i>iv</i> dose of 20 or 50 mg/kg MEHP.....	108
3.16.	Free MEHP in the (A) blood of adult male rat after an oral dose of 70, 100, or 400 mg/kg MEHP or (B) excreta of adult mat rat after an oral dose of 70 mg/kg MEHP.....	109
3.17.	Free MEHP in the blood of adult rats after an (A) <i>iv</i> dose of 100 mg/kg DEHP, or (B) oral dose of 30, 300, or 500 mg/kg DEHP.....	110
3.18.	Free MEHP in the (A) maternal blood or (B) placenta and fetal tissues after the last oral dose of 30 or 500 mg/kg/day administered from GD 14 – 19.....	111
4.1.	Measured monoester concentrations in the fetal testes from dams given daily oral doses of DMP, DEP, DBP, DEHP, or BBP from GD 12-19.....	129
4.2.	PG Concentration in the medium of MA-10 cells treated with 100 ng/mL LH and varying concentrations of MEHP.....	130

4.3.	Genes encoding proteins in the Leydig cell steroidogenic pathway.....	131
4.4.	Expression of selected steroidogenic genes in MA-10 cells.....	132
4.5.	Testosterone concentration in the medium of MA-10 cells treated with 100 ng/mL LH and varying concentrations of MEHP.....	133
4.6.	Monobutyl, monoethyl, and monomethyl phthalate inhibition of LH-stimulated testosterone synthesis in MA-10 Leydig cells.....	134
4.7.	Mono-n-octyl and monobenzyl phthalate inhibition of LH-stimulated testosterone synthesis in MA-10 Leydig cells.....	135
5.1.	Two-pathway model for co-regulation of testosterone synthesis in the Leydig cell.....	149
5.2.	Effect of MEHP and CQ on LH-stimulated testosterone synthesis in MA-10 cells.....	150
5.3.	Effect of MEHP and CQ on steroidogenic gene expression in MA-10 cells.....	151
5.4.	LH stimulation of arachidonic acid release in MA-10 cells.....	152
5.5.	Effect of MEHP and CQ on LH-stimulated arachidonic acid release in MA-10 cells.....	153
5.6.	Activation, translocation and phospholipase activity of cPLA <sub>2</sub> .....	154
5.7.	Calcium stimulated translocation of EGFP-cPLA <sub>2</sub> in control cells.....	155
5.8.	Inhibition of EGFP-cPLA <sub>2</sub> translocation by MEHP and CQ.....	156
5.9.	Two-dimensional structures of the natural ligand for cPLA <sub>2</sub> , phosphatidylcholine, and potential inhibitors CQ and MEHP.....	157
6.1.	Sections of maternal or fetal liver after exposure to 0 or 100 mg/kg/day CQ.....	185
6.2.	Lipid accumulation in the maternal or fetal liver after exposure to 0 or 100 mg/kg/day CQ.....	186
6.3.	Maternal serum estradiol and progesterone levels on GD 19 after maternal CQ exposure to 0 or 100 mg/kg/day from GD 16 – 18.....	187

6.4.	Fetal testes testosterone levels on GD 19 after maternal CQ exposure to 0 or 100 mg/kg/day from GD 16 – 18.....	188
6.5.	Effect of CQ treatment on fetal anogenital distance (AGD) after maternal exposure to 0 or 100 mg/kg/day from GD 16-18.....	189
6.6.	Testicular artery after maternal CQ administration at 0 or 100 mg/kg/day from GD 16-18.....	190
6.7.	Effect of CQ treatment on expression of selected steroidogenic genes in fetal testes testosterone after maternal administration of 0 or 100 mg/kg/day from GD 16-18.....	191
6.8.	Testosterone in fetal testes after maternal CQ administration at 0, 10, 50, or 100 mg/kg/day from GD 16-18.....	192
6.9.	Expression of selected steroidogenic genes in fetal testes after maternal CQ administration at 0, 10, 50, or 100 mg/kg/day from GD 16-18.....	193

## LIST OF ABBREVIATIONS AND SYMBOLS

AA	arachidonic acid
AGD	anogenital distance
ALP	alkaline phosphatase
ALT	alanine aminotransferase
AUC	area under the curve
AUC/D	dose normalized area under the curve
BBP	butylbenzyl phthalate
BW	body weight
c-AMP	cyclic adenosine monophosphate (cyclic AMP)
CAT	carnitine acetyltransferase
Cl <sub>Gc</sub>	clearance value for urinary excretion of MBP-G
Cl <sub>Oc</sub>	clearance value for urinary excretion of MBP-O
C <sub>max</sub>	peak concentration
C <sub>max</sub> /D	dose normalized peak concentration
cPLA <sub>2</sub>	cytosolic phospholipase A <sub>2</sub>
CQ	chloroquine
Cre	creatinine
CYP	cytochrome P450
DBP	di-n-butyl phthalate
DEP	diethyl phthalate
DEHP	di-2,4-ethylhexyl phthalate
DMP	dimethylphthalate
DMSO	dimethylsulfoxide



DNA	deoxyribonucleic acid
DnOP	di-n-octyl phthalate
E2	estradiol
ED <sub>50</sub>	external dose causing 50% inhibition/activation
ELISA	enzyme-linked immunosorbent assay
GD	gestation day
hr	hour
IC <sub>50</sub>	internal concentration causing 50% inhibition/activation
iv	intravenous administration
kad	rate of oral uptake of DBP in the intestine
kam	rate of oral uptake of MBP in the intestine
kbc	rate constant for hydrolysis of DBP in the blood
kbdc	rate constant for DBP excretion into bile
kbgc	rate constant for MBP-G excretion into bile
kbmc	rate constant for MBP excretion into bile
kc	rate constant for hydrolysis of DBP in the liver
kfc	rate constant for fecal excretion of DBP, MBP, and MBP-G
kg	kilogram
kgic	rate constant for movement of DBP, MBP, and MBP-G in gut
khydc	rate constant for hydrolysis of MBP-G in the gut
khydrAc	rate constant for hydrolysis of MBP-G in the amniotic fluid
khydrfc	rate constant for hydrolysis of MBP-G in fetus
KmG	affinity constant for DBP hydrolysis in the gut lumen
KmL	affinity constant for MBP glucuronidation in the liver
KmLf	affinity constant for MBP glucuronidation in the fetal liver

KmO	affinity constant for MBP oxidative metabolism in the liver
KmU	affinity constant for MBP excretion into the urine
ktransM1c	rate constant for MBP transfer from fetus to amniotic fluid
ktransM2c	rate constant for MBP transfer from amniotic fluid to fetus
ktransGc	rate constant for MBP-G transfer from fetus to amniotic fluid
LH	luteinizing hormone
LOQ	limit of quantitation
MA-10	mouse tumor Leydig cell line
MBP	mono-n-butyl phthalate
MBP-G	mono-n-butyl phthalate glucuronide
MBP-O	combined oxidative metabolites of mono-n-butyl phthalate
MBeP	monobenzyl phthalate
MEHP	monoethylhexyl phthalate
MEP	monoethyl phthalate
mg	milligram
mg/kg/day	milligram dosed per kilogram bodyweight per day
μL	microliter
mL	milliliter
μM	micromolar (micromoles per liter)
MMP	monomethyl phthalate
MnOP	mono-n-octyl phthalate
MRT	mean retention time
PAFetc	permeability area cross product for MBP in the fetus
PAFTc	permeability area cross product for MBP in the fetal testes
PAGFetc	permeability area cross product for MBP-G in the fetus

PAGFTc	permeability area cross product for MBP-G in the fetal testes
PAGLc	permeability area cross product for MBP-G in the liver
PAGPlc	permeability area cross product for MBP-G in the placenta
PAGSc	permeability area cross product for MBP-G in maternal tissues
PALc	permeability area cross product for the liver
PARc	permeability area cross product for the richly perfused tissues
PASc	permeability area cross product for the slowly perfused tissues
PBPK	physiologically based pharmacokinetic
PBS	phosphate buffered saline
PD	pharmacodynamic
PG	progesterone
PGFet	fetus:maternal blood partition coefficient for MBP-G
PGFT	testes:fetal blood partition coefficient for MBP-G
PGL	liver:blood partition coefficient for MBP-G
PGPI	placenta:blood partition coefficient for MBP-G
PGT	tissue:blood partition coefficient for MBP-G
PK	pharmacokinetic
PKA	protein kinase A
PL	liver:blood partition coefficient for DBP
PLA <sub>2</sub>	phospholipase A <sub>2</sub>
PMFet	fetus:maternal blood partition coefficient for MBP
PMFT	testes:fetal blood partition coefficient for MBP
PMG	gut tissue:blood partition coefficient for MBP
PML	liver:blood partition coefficient for MBP
PMPi	placenta:blood partition coefficient for MBP

PMR	richly perfused tissue:blood partition coefficient for MBP
PMS	slowly perfused tissue:blood partition coefficient for MBP
PMT	tissue:blood partition coefficient for MBP
po	per os; oral administration
PP	peroxisome proliferator
PPAR	peroxisome proliferator activated receptor
PT	tissue:blood partition coefficient for DBP
QCc	cardiac output
QFc	fractional blood flow to fat
QGc	fractional blood flow to gastrointestinal tract
QLc	fractional blood flow to liver
QMc	fractional blood flow to mammary gland
QPlc	fractional blood flow to placenta
QRc	fractional blood flow to richly perfused tissues
QSc	fractional blood flow to slowly perfused tissues
RIA	radioimmunoassay
RNA	ribonucleic acid
RT-PCR	real time polymerase chain reaction
SFM	serum free medium
ST	seminiferous tubule
T	testosterone
$T_{1/2}$	half-life
$T_{max}$	time of peak concentration
UDPGT	uridine 5'-diphospho-glucuronosyltransferase
VAFc	fractional volume of amniotic fluid

V <sub>Bc</sub>	fractional volume of perfused tissues
V <sub>Dc_f</sub>	fractional volume of distribution in the fetus
V <sub>Fc</sub>	fractional volume of fat
V <sub>fet</sub>	fractional volume of fetus
V <sub>FT</sub>	fractional volume of fetal testes
V <sub>GC1c</sub>	fractional volume of upper gut contents
V <sub>GC2c</sub>	fractional volume of lower gut contents
V <sub>GIc</sub>	fractional volume of gastrointestinal tract
V <sub>Lc</sub>	fractional volume of liver
V <sub>maxGc</sub>	maximum capacity for DBP hydrolysis in the gut lumen
V <sub>maxLc</sub>	maximum capacity for MBP glucuronidation in the liver
V <sub>maxLfc</sub>	maximum capacity for MBP glucuronidation in the fetal liver
V <sub>maxOc</sub>	maximum capacity for MBP oxidative metabolism in the liver
V <sub>maxUc</sub>	maximum capacity for MBP excretion into the urine
V <sub>Mc</sub>	fractional volume of mammary gland
V <sub>Plasc</sub>	fractional volume of plasma
V <sub>Plc</sub>	fractional volume of placenta
V <sub>Rc</sub>	fractional volume of richly perfused tissue
V <sub>Sc</sub>	fractional volume of slowly perfused tissue

## **CHAPTER 1**

### **INTRODUCTION**

## **A. PHTHALATE ESTERS**

### **Commercial Use and Population Exposure**

The phthalic acids are a family of dialkyl esters that are primarily used as softeners in plastic products, but may also be found in paint, glue, putty, pharmaceutical products and cosmetics [1, 2]. Phthalates are not chemically bound to the plastics and as a result, they may leach from the surface over time. Human exposure primarily occurs via the oral route. Phthalates from plastic food and liquid containers may leach into the packaged contents to be ingested with the food. Dermal exposure is also possible, through clothes and beauty care products (perfume, cosmetics). Inhalation of some phthalates, such as di-2,4-ethylhexyl phthalate (DEHP), may occur due to association with dust particles. The presence of DEHP in blood storage bags and iv tubing could also result in relatively high exposures to transfusion patients.

Though the relative source contributions have not been characterized in the United States, a recent study in Europe found that food sources accounted for 40-90% of the overall exposure to di-n-butyl phthalate (DBP) and DEHP; inhalation and dermal exposures are dominant sources of diethyl (DEP) and dimethyl phthalate (DMP) [3]. Biomonitoring studies have identified the metabolites of DBP and several other phthalates in the urine of the US population including adults, children, infants, and pregnant women [4-6]. The most recent NHANES study, which tested a cross section of human urine samples obtained from children aged six to adults, reported measurable metabolite concentrations for 6 of the 7 tested phthalates [7]. Estimated exposure to two of the more prevalent phthalates, DEHP and DBP, is in the range of 2-6 and 1-4  $\mu\text{g}/\text{kg}/\text{day}$ , respectively [5, 8].

## **Metabolism, Distribution, and Excretion of Phthalates**

Phthalates are manufactured as dialkyl esters and typical human exposure is to this form. The diesters are then rapidly and efficiently metabolized to their monoalkyl form, regardless of the route of exposure, by a variety of non-specific hydrolases in GI, skin, blood, liver, kidney and lung [9]. The parent diester and monoester metabolites for some of the more common phthalates are shown in Figure 1.1. These monoester metabolites are thought to be the active species responsible for reported effects in animal toxicity studies. Differences in alkyl chain length and degree of branching can have significant effects on the metabolism, distribution and excretion of the monoesters [10]. The shorter chain phthalates are excreted mainly as the unchanged monoester. Increased length and branching, however, leads to more extensive metabolism. Monobutyl phthalate (MBP), the monoester metabolite of DBP, is excreted primarily as the free monoester or as its glucuronide conjugate. Oxidative metabolites make up only a small portion of the total excreted MBP [11]. On the other hand, monoethylhexyl phthalate (MEHP; the monoester metabolite of DEHP) undergoes extensive oxidative alkyl group metabolism in both the rat and human. Unchanged MEHP makes up only a small portion of the excreted dose [12, 13].

Differences in metabolism can have significant effects on the kinetic behavior of the monoesters and ultimately on the target tissue dose. In general, the *in vivo* kinetics of the various phthalates are poorly characterized. With the exception of DEHP and DBP, very little quantitative information has been collected on metabolism and distribution in the rat or human. Often, the published kinetic information is limited to qualitative analyses of excreted metabolites or blood concentrations at a handful of time-points.



## **Hepatic Effects and Enzyme Induction**

Some of the phthalates (*i.e.*, DEHP) are peroxisome proliferators (PPs), which induce liver tumors in rodents through the activation of peroxisome proliferator activated receptors (PPAR). PPARs are a nuclear hormone receptor superfamily of ligand-activated transcription factors [14]. After forming a heterodimer with retinoid X-receptor (RXR) in the cytoplasm, the ligand/PPAR/RXR complex is transported to the nucleus where it binds a particular sequence within the promoter region on target genes (PPAR response element; PPRE) and initiates gene transcription [14-17]. PPAR $\alpha$  appears to be responsible for the majority of hepatic effects observed with PP administration in rodents.

Several key events have been identified in the development of liver tumors following sustained PP treatment: 1) PPAR $\alpha$  activation; 2) up-regulated transcription of genes involved in peroxisome proliferation, lipid metabolism, and cell cycle/apoptosis; 3) increased fatty acid  $\beta$ -oxidation and oxidative stress; 4) hepatomegaly (enlarged liver); 5) stimulation of non-parenchymal cells and inhibition of gap junction intercellular communication; and finally 6) increased cell proliferation and decreased apoptosis leading to proliferation of DNA-damaged cells, hyperplasia and hepatic tumors [14, 18, 19].

Many of the genes up-regulated by PPARs are involved in fatty acid metabolism. Peroxisomal acyl-coA oxidase, an enzyme associated with  $\beta$ -oxidation of long chain fatty acids and very long chain fatty acids, can be increased by as much as 15-fold with PP treatment [20]. Similarly, the expression of cytochrome P450 4A (CYP4A) enzymes has been shown to increase more than 20-fold after PP treatment [21]. The CYP4A superfamily is responsible for  $\omega$  and  $\omega$ -1 oxidation of fatty acids. Induction of these and other enzymes

that mediate lipid and cholesterol metabolism leads to reduced serum cholesterol and triglyceride levels – an effect which led to the classification of many PPs as hypolipidemic drugs [22].

The phthalates differ significantly in their PP activity [23]. DEHP induces peroxisome proliferation, acyl-coA oxidase activity and CYP4A expression in rodents [24, 25]. *In vitro*, MEHP binds both PPAR $\alpha$  and PPAR $\gamma$ , and up-regulates expression of PP associated enzymes, including acyl-coA oxidase. MBP, the monoester metabolite of DBP, however, does not bind either PPAR $\alpha$  or  $\gamma$  *in vitro* [26]. While DBP induces CYP4A and acyl-coA oxidase *in vivo*, the doses of DBP required to induce these enzymes are much higher than those of DEHP [25].

The carcinogenicity of PPs varies widely among species. In contrast to rats and mice, where PPAR activation is associated with hepatocarcinogenicity, chronic exposure to PPs has not been shown to lead to tumors in humans or non-human primates [19]. Several reasons for the different susceptibility of rodents and humans have been suggested, including reduced levels of PPAR $\alpha$  in the human liver [27, 28] and differences in PPRE activity [29]. Recent studies in humanized mouse models (PPAR $\alpha$ -/- mice expressing human PPAR $\alpha$ ) showed that activation of human PPAR $\alpha$  up-regulates enzymes associated with lipid metabolism, but does not lead to tumor development [30, 31]. Based on observed differences in species susceptibility, the International Agency for Research on Cancer (IARC) has categorized DEHP as a Class 3 carcinogen (no evidence of cancer causing potential in humans).

## Effects of phthalates on testosterone-mediated sexual development

Treatment of rats with some of the longer chain alkyl phthalates, including DEHP and DBP, has identified these as potential reproductive toxicants in rats [32-34]. High doses administered during gestation ( $\geq 100$  mg/kg/day) leads to reduced anogenital distance (AGD), nipple retention, hypospadias (malformed penis), delayed testes descent, and vaginal pouch development in the male rat pup. Many of these effects are associated with reduced in fetal testosterone production. In studies specifically designed to test the effect of phthalates on fetal testes development, DBP, DEHP, butylbenzyl phthalate (BBP) and dipentyl phthalate caused significant reduction in a large number of genes involved in steroid synthesis. Phthalates also cause cryptorchidism (undescended testes), increased multinucleated gonocytes in the fetal testes, increased seminiferous tubule diameter and Sertoli-germ cell detachment. These effects do not appear to be dependent on alterations in testosterone production, however [35].

The similarity between the steroidogenic pathway in rats (where toxicity has been observed) and humans [36] and the widespread exposure to phthalates has led to a high degree of public concern regarding perinatal exposure through medical devices and childcare products (*i.e.*, iv tubing, bottles, pacifiers, and infant toys). Recently, several epidemiology studies have been performed in an effort to identify effects of phthalate exposure in the human. Studies in adult men reported a negative association between MEHP and serum testosterone, estradiol [37] and semen quality [38]. Findings in children, however, have been less clear. Studies comparing maternal urine metabolite concentrations of several phthalates to neonatal AGD and several sex hormone markers have had conflicting results. Swan *et al.* [39] reported a negative correlation between AGD and maternal urine levels of several

phthalates, including the known anti-androgen MBP and the DEP metabolite MEP, which is not endocrine active in animal studies. No correlation was found between AGD and MEHP. Main *et al.* [40] measured several markers of sex hormone homeostasis in male infants and compared observed changes to phthalate concentrations in maternal breast milk. The results showed no direct correlation between maternal phthalate exposure and serum total testosterone. However, some differences were noted in other indices. MBP was negatively correlated to free testosterone, MEP, a similar inactive phthalate (monomethyl phthalate; MMP), and MBP were positively correlated to LH:free testosterone ratio. MEHP was not significantly correlated to any of the measured indices. More recently, a study found a negative correlation between urine MBP levels and AGD in female, but not male, infants [38]. While the authors interpreted these results as evidence of phthalate effects on human sexual development, the conclusions have been met with a fair amount of controversy in the scientific community. Primary concerns about the interpretation of these studies include the inability to account for confounders and the findings of significant associations between phthalates that do not affect sexual development or testosterone production in laboratory animals [41].

### **Phthalate kinetics in gestation and dose-response for fetal effects**

Despite the number of *in vivo* effects studies, little information is available regarding phthalate disposition during gestation. In fact, with the exception of DBP, no data has been published on fetal phthalate concentrations. A few studies are available that examined DBP kinetics during gestation. Fennell [42] obtained time-course data for MBP and MBP-glucuronide (MBP-G) in maternal and fetal plasma and amniotic fluid after a single dose of

50, 100, or 250 mg DBP/kg on gestation day (GD) 20. Saillenfait [43] also measured MBP and MBP-G kinetics in maternal plasma, placenta, fetal plasma, and amniotic fluid in rats given single oral dose of 500 or 1500 mg <sup>14</sup>C-DBP/kg on GD 14. Calafat [44] identified MBP as well as MBP-G in the amniotic fluid and urine of rats after repeated DBP exposures. DEHP kinetic data have been published for the blood and excreta of the pregnant dam, but not the fetus itself [44, 45].

While developmental effects have been associated with multiple day phthalate exposures [46, 47], most of the published kinetic studies in gestation have focused on acute metabolite kinetics [42, 48, 49]. Repeated DEHP and DBP administration to adult male rats induces hepatic expression and activity of CYP4A isozymes, which catalyze ω-hydroxylation of fatty acids [24, 25, 50, 51]. Exposure to DBP at 500 mg/kg/day from GD 12-19 has also been shown to induce CYP2B1, 3A1 and 4A1 mRNA and protein expression in the liver of the pregnant rat and fetus and uridine 5'-diphosphoglucuronosyltransferase (UDPGT) mRNA in the dams [52]. The effect of the up-regulation of CYP enzyme and UDPGT expression on DBP and/or MBP kinetics has not been previously examined. Studies on the effect of P450 enzyme induction on body burden of the MEHP have had variable results: some showed slightly greater clearance after repeated dosing [45, 53] while others showed no difference [54].

There is currently very little data regarding the fetal phthalate concentrations associated with developmental effects. Prior to the current work, the available studies related fetal/pup effects to the maternal administered dose. Because of non-linearities expected in metabolism and its induction and limited data on placental transfer, it was not previously possible to relate the developmental effects to the phthalate concentration in the fetus.

## **Testosterone synthesis and potential mechanisms for phthalate disruption**

Testosterone (T) synthesis is stimulated by the release of luteinizing hormone (LH) from the pituitary, which binds to a G-protein coupled receptor (GCPR) on the surface of the Leydig cell. Release of the G-protein increases intracellular levels of cyclic AMP (c-AMP), activating protein kinase A (PKA) and several transcription factors, including those regulating steroid acute regulatory (StAR) protein expression. StAR protein plays an important role in steroidogenesis by facilitating cholesterol transport into the mitochondria. GCPR binding also leads to activation of cytosolic phospholipase A<sub>2</sub> (cPLA<sub>2</sub>) and the release of arachidonic acid (AA), which also stimulates transcription of genes required for steroidogenesis, including StAR. The c-AMP pathway appears to be dominant in the adult Leydig cell, though both the c-AMP and AA pathways are necessary for the maintenance of normal T levels [55]. The interdependence of these two pathways is not well characterized, though a few studies have shown that AA release occurs either downstream or independently from c-AMP [55-57].

While phthalate inhibition of steroid synthesis has been shown to occur through direct interaction in the Leydig cell, the molecular target for these anions has not yet been identified. Because of the known PP activity of some phthalates, and presence of PPAR $\alpha$  and  $\delta$  in the testes, PPAR activation has been identified as a potential mechanism of testicular toxicity [26, 58]. Studies in knockout mice show that PPAR $\alpha$  is involved in DEHP-dependent testicular toxicity, though PPAR $\alpha$  alone cannot account for the full range of effects seen in testes of male mice [58]. Furthermore, the trend seen when comparing the potency of different phthalates is not consistent with PPAR as a regulator of testicular

toxicity. While DEHP and DBP cause similar effects on fetal sexual development and testosterone production, they have different abilities to activate PPAR [25]. In transfected COS cells [59], MEHP was a potent activator of mouse PPAR $\alpha$  ( $IC_{50} = 0.6 \mu M$ ), but MBP showed no significant activation at concentrations up to 300  $\mu M$ .

A second potential target, PLA<sub>2</sub>, was identified based on the studies recognizing its metabolic product AA as a necessary signaling molecule in Leydig cell steroidogenesis together with the historical data on MEHP's ability to inhibit AA release in platelets [60]. While the AA pathway appears to be secondary to the c-AMP/PKA pathway, AA inhibition does cause decreased steroidogenesis *in vitro* [55, 61] and negatively effects male sexual development *in vivo* [62]. As opposed to PPAR [59], preliminary studies in our laboratory showed that MEHP and MBP have a similar ability to inhibit AA cPLA<sub>2</sub> activity (see Chapter 5). Additionally, *in vivo* studies have shown decreased cPLA<sub>2</sub> activity in the testes of male fetal rats exposed to DEHP during gestation [63].

## **B. PHTHALATE RISK ASSESSMENT AND LEGISLATION**

Despite the lack of clear evidence for developmental effects in humans, the consistent findings in animals have led to several legislative acts aimed at reducing children's risk of endocrine disruption. In 2005, the European Union banned the use of six phthalate esters in plastics manufactured for use in children's toys and childcare products. California state legislature followed suit in 2007 and in 2008, the United States Senate banned the use of three phthalates in toys and childcare products, BBP, DEHP and DBP. They also placed a temporary ban on three additional phthalates pending further study. US public health agencies have yet to recommend standards for the plasticizers based on potential developmental effects. Both the Environmental Protection Agency (EPA) and the Food and Drug Administration are currently evaluating the available data. Previous recommendations by the EPA predate the developmental toxicity studies and are based on effects in adult rats, such as increased liver weight (BBP, DEHP) and mortality (DBP), which occur after long-term dosing at 470, 19 and 600 mg/kg/day, respectively. Development of a quantitative estimate of human risk to phthalate-induced developmental effects, however, is severely limited by insufficient relevant data. To determine the relevance of rodent toxicity studies to the human population, a better understanding is needed of the fetal dose required to cause the adverse effects and of molecular targets by which the phthalates exert their effect.



### C. STUDY OBJECTIVE

The purpose of this project was to improve the current understanding of the pharmacokinetic and pharmacodynamic factors governing the testosterone-dependent effects in the fetal rat upon administration of certain phthalates, such as DEHP and DBP. In order to better define both the chemical kinetics and the mechanism of action of the phthalates, a variety of *in vivo*, *in vitro* and *in silico* approaches were employed. Ultimately, the goal of this work was to provide both data and predictive tools (PBPK models) that could be used to improve accuracy of current and future risk assessment efforts. This thesis describes a series of experiments designed to answer specific questions regarding the pharmacokinetic and pharmacokinetic determinants of phthalate developmental toxicity:

#### a) Pharmacokinetic evaluations

The *in vivo* kinetic studies in Chapter 2 examine the distribution of DBP and its major metabolites (MBP and MBP-glucuronide; MBP-G) in the pregnant and fetal rat after a single dose of 500 mg/kg on gestation day (GD) 19 or repeated doses of 50, 100, or 500 mg/kg/day from GD 12-19. The dose regimens used in this study are designed specifically to correlate fetal testosterone reduction to internal measures of dose, including maternal plasma, fetal plasma and fetal testes MBP concentrations. Because these studies are also intended to support the development of a PBPK model for DBP in the pregnant and fetal rat, time-course data were collected for MBP and MBP-G in maternal plasma, placenta, fetal plasma, testes and amniotic fluid at each dose.

Development of a quantitative physiological pharmacokinetic model which relates external dose to maternal, fetal, and target tissue (fetal testes) concentrations of MBP and

MEHP, the active metabolites of DBP and DEHP, respectively, is described in Chapter 3. PBPK models are useful tools for describing the relationship between external dose and time-dependent tissue concentrations quantitatively. The models described in Chapter 3 are based on a variety of *in vitro* and *in vivo* data taken from the published literature and from the studies described in Chapter 2.

#### b) Pharmacodynamic Evaluations

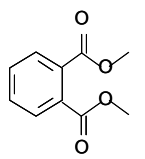
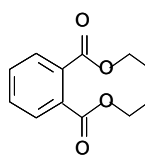
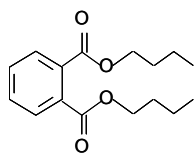
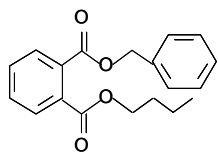
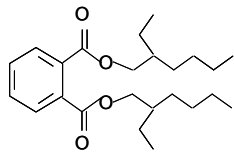
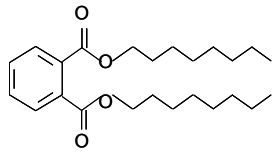
Chapter 4 describes a series of studies designed to determine whether the difference in potency among phthalates is a result of PK or PD differences. The monoester metabolites of several phthalates (both endocrine active and inactive) are reported for the fetal testes following maternal dosing to determine differences in fetal exposure. Additionally, an *in vitro* assay was developed to evaluate the effect of several phthalates directly in the Leydig cell, the steroidogenic cell in the testes.

The use of the *in vitro* assay to determine the molecular target for the phthalates is presented in Chapter 5. These experiments evaluate the potential role of arachidonic acid release by cPLA<sub>2</sub> in phthalate inhibition of steroidogenesis. Additionally, the effect of phthalate exposure on cPLA<sub>2</sub> activation and translocation using confocal microscopy and fluorescently tagged protein is described.

Finally, an *in vivo* experiment designed to test the role of arachidonic acid on fetal sexual development is reported in Chapter 6. Administration of chloroquine (CQ), a known inhibitor of AA release, and resulting changes in several markers of fetal testes

development are described. The design of this experiment is based on the premise that the AA inhibitor should have similar effects on fetal steroidogenesis as the phthalates, if AA does mediate phthalate anti-androgen activity. Taken together, our studies indicate a key role of cPLA2 as a target for the phthalate monoesters developmental toxicity.

**Figure 1.1. Chemical structure of common phthalate esters.**

<b>Structure</b>	<b>Diester</b>	<b>Monoester Metabolite</b>
	Dimethyl phthalate (DMP)	Monomethyl phthalate (MMP)
	Diethyl phthalate (DEP)	Monoethyl phthalate (MEP)
	Di-n-butyl phthalate (DBP)	Mono-n-butyl phthalate (MBP)
	Butylbenzyl phthalate (BBP)	Monobutyl phthalate (MBP) Monobenzyl phthalate (MBeP)
	Diethylhexyl phthalate (DEHP)	Monoethylhexyl phthalate (MEHP)
	Di-n-octyl phthalate (DOP)	Mono-n-octyl phthalate (MOP)

## **CHAPTER 2**

**Kinetics of selected di-n-butyl phthalate metabolites and fetal testosterone following repeated and single administration in pregnant rats**

**The text of this chapter is reproduced with permission from**

***Toxicology 255 (2008) 80-90.***

**© 2008**

**Elsevier, Inc.**

## A. ABSTRACT

Human exposure to phthalic acid diesters occurs through a variety of pathways as a result of their widespread use in consumer products and plastics. Repeated doses of di-n-butyl phthalate (DBP) from gestation day (GD) 12-19 disrupt testosterone synthesis and male sexual development in the fetal rat. Currently little is known about the disposition of DBP metabolites, such as monobutyl phthalate (MBP) and its glucuronide conjugate (MBP-G), during gestation after repeated exposure to DBP. In order to gain a better understanding of the effect of repeated dosing on maternal and fetal metabolism and distribution, pregnant Sprague-Dawley rats were given a single dose of 500 mg/kg DBP on GD 19 or daily doses of 50, 100, and 500 mg/kg/day from GD 12-19 via corn oil gavage. Dose-response evaluation revealed a non-linear increase in maternal and fetal plasma concentrations of MBP. Maternal and fetal MBP levels were slightly lower in animals after eight days of dosing at 500 mg/kg/day. Fetal plasma MBP levels closely followed maternal plasma, while the appearance and elimination of MBP-G in fetal plasma were significantly delayed. MBP-G accumulated over time in the amniotic fluid. Inhibition of testosterone was rapid in fetal testes when exposed to DBP (500 mg/kg/day) on GD 19. Within 24 hrs, the level of inhibition in the fetus was similar between animals exposed to a single or multiple daily doses of 500 mg/kg/day. Examination of testosterone time-course data indicates a rapid recovery to normal levels within 24 hrs post-dosing at DBP doses of 50 and 100 mg/kg/day, with a rebound to higher than normal concentrations at later time-points. MBP kinetics in fetal testes allows direct comparison of active metabolite concentrations and testosterone response in the fetal testes.

## B. INTRODUCTION

Phthalate esters are found in drinking water, food, and personal care products and are used in the coating of some medications [1, 3, 64]. Though relative source contributions have not been characterized in the United States, a recent study in Europe found that food sources accounted for 40-90% of the overall di-n-butyl phthalate (DBP) exposure [3]. Biomonitoring studies have identified the metabolites of DBP and several other phthalates in the urine of the US population including adults, children, infants, and pregnant women [4-6]. Some of these phthalates, including (DBP), are developmental toxicants in rats and mice [32-34, 65-68]. Exposure to DBP between gestation days (GD) 12 and 19 disrupts male rat sexual development, as evidenced by reduced anogenital distance, nipple retention, hypospadias, delayed testes descent, and vaginal pouch development in male pups [69]. The anti-androgenic effects of DBP are thought to result from inhibition of fetal testosterone synthesis by the monoester metabolite, monobutyl phthalate (MBP) [33, 70-72]. Repeated doses of DBP cause reduced testosterone levels in the blood of adult male rats [70, 72, 73] and in the testes of male fetuses from rats exposed to doses as low as 50 mg/kg-day from GD 12 – 19 [46]. To date, studies have not been performed to determine target tissue phthalate concentrations associated with these observed effects.

MBP, the active metabolite of DBP, is formed by intestinal hydrolases upon ingestion and is quickly absorbed in the gut [11]. MBP can be excreted unchanged in the urine, undergo oxidative metabolism (primarily  $\omega$  and  $\omega$ -1-hydroxylation), or be conjugated to glucuronic acid by uridine 5'-diphospho-glucuronosyltransferase (UDPGT) [74]. Glucuronide conjugation is a major route of clearance for MBP in the rat, particularly at

higher doses where developmental effects have been found. Urinary MBP-glucuronide (MBP-G) was shown to account for 17% of the dose 24 hrs after 10 mg/kg iv or 36% of the dose after a single 2000 mg/kg oral administration [49, 75].

A few studies are available which examined DBP kinetics during gestation. Fennell [42] fetal plasma and amniotic fluid after a single dose of 50, 100, or 250 mg DBP/kg on GD 20. Saillenfait [43] also measured MBP and MBP-G kinetics in maternal plasma, placenta, fetal plasma, and amniotic fluid in rats given single oral dose of 500 or 1500 mg <sup>14</sup>C-DBP/kg on GD 14. Both studies showed similar kinetics to that of the male rat, with more than 77% of the dose excreted in the urine in 24 hrs. Both free MBP and MBP-G were found in the fetal rat plasma and amniotic fluid after maternal DBP exposure. Calafat [44] also identified MBP as well as MBP-G in the amniotic fluid and urine of rats after repeated DBP exposures.

Despite the fact that the developmental effects of DBP have been associated with multiple day exposures (with the exception of testosterone reduction) [46, 47], previous studies in gestation have focused on acute metabolite kinetics [42, 48, 49]. As is true with the related phthalate ester diethylhexyl phthalate (DEHP), DBP administration to adult male rats induces expression and activity of CYP4A isozymes, which catalyze  $\omega$ -hydroxylation of fatty acids [24, 25, 50]. Exposure to DBP at 500 mg/kg/day from GD 12-19 also induces CYP2B1, 3A1 and 4A1 mRNA and protein expression in the liver of pregnant rats and in the fetal liver. UGT mRNA was also up-regulated in these dams [52]. The effect of the up-regulation of P450 and UGT expression on DBP and/or MBP kinetics has not been previously examined. Studies on the effect of P450 induction on body burden of the DEHP monoester, monoethylhexyl phthalate, have had variable results: some showed slightly greater clearance after repeated dosing [45, 53] and while others showed no difference [54].



The purpose of this study was (1) to develop a better understanding of maternal and fetal DBP kinetics under exposure conditions where developmental effects have been observed and (2) to directly relate fetal concentrations of the active metabolite (MBP) with changes in testes testosterone concentration. Thus, pregnant rats were given daily doses of DBP at 50, 100, and 500 mg/kg/day on GD 12 -19 MBP and MBP-G kinetics were measured in maternal and fetal plasma, placenta, and amniotic fluid for two days post-dose. To test whether MBP metabolism is significantly altered after multiple high dose exposures, a study was also performed in which maternal and fetal kinetics were examined after a single dose of 500 mg/kg on GD 19. The fetal testes were collected and measured for both MBP and testosterone. These were quantified in order to evaluate the dose-response relationship between the MBP and testosterone, a sensitive marker for disruption of sexual development in the target tissue.

## C. METHODS

### Animals

Pregnant Sprague-Dawley (CrI:CD(SD)) rats (sperm plug positive GD 0) were obtained from Charles River Laboratories (Raleigh, NC) and housed in the Animal Care Facility of the The Hamner Institutes for Health Sciences, which is accredited by the Association for Assessment and Accreditation of Laboratory Animal Care International. Rats were acclimated in a temperature- and humidity-controlled, HEPA-filtered environment on a 12 hr light-dark cycle. NIH rodent diet (NIH-07, Zeigler Bros., Gardner, PA) and reverse-osmosis water were provided *ad libitum*. This study was approved by The Hamner Institute's Animal Care and Use Committee.

### Dosing Solutions and Treatment

Dosing solutions of DBP at concentrations of 50, 100 and 500 mg/mL were prepared in corn oil (Sigma-Aldrich, St. Louis, MO) and administered to rats at a volume of 1 mL/kg. The actual concentrations of DBP in the dosing solutions were  $48 \pm 0.4$ ,  $89 \pm 10$ , and  $502 \pm 9$  mg/mL (mean  $\pm$  SE) by gas chromatography using a method described by Fennell et al. (2004) [42]. Time points of tissue collection were selected based on the rapid pharmacokinetics of MBP and the pharmacodynamics of testosterone changes in fetal testes following administration of DBP. In the repeated dose study, pregnant rats (n=4/dose group/time point) were administered a daily dose of DBP (0, 50, 100 or 500 mg/kg) from GD 12-19. At 0.25, 0.5, 0.75, 1, 2, 4, 8, 12, 24, and 48 hrs after the final dose, rats were euthanized by CO<sub>2</sub> asphyxiation and exsanguination. In the single dose study, pregnant Sprague-Dawley rats (n=4/dose group/time point) were administered 1.0 mL/kg of corn oil

on GD 12 – 18 and corn oil (0 mg/kg) or DBP (500 mg/kg) on GD 19. Maternal rats were euthanized with CO<sub>2</sub> followed by exsanguination at 0.5, 1, 2, 24 and 48 hrs post-dosing. Litter sizes varied from 12 -17 fetuses per dam. Fetuses were delivered by caesarean section and amniotic fluid was collected from 4 fetuses, selected randomly. Amniotic fluid that was visibly clear of blood or other contaminants was pooled by litter, snap frozen in an ethanol/dry ice bath, and stored at -80°C. Fetal blood was collected from the jugular vein using heparinized capillary tubes and pooled by litter in glass centrifuge tubes. Placentas were pooled by litter, snap frozen an ethanol/dry ice bath and stored at -80°C. Testes from each male fetus were stored separately. Maternal livers taken from the 500 mg/kg dose groups were snap frozen in an ethanol/dry ice bath and stored at -80°C. Maternal blood was obtained at the time of sacrifice by cardiac puncture. Plasma was separated from maternal and fetal whole blood by centrifugation and stored at -80°C.

### **MBP and MBP-G Sample Preparation**

MBP and MBP-G were extracted from plasma, amniotic fluid, and tissues prior to analysis based on previously described methods Saillenfait [42, 48]. Aliquots (25 µl) of plasma or amniotic fluid (pooled by litter) were thawed, vortexed, and added to a solution containing internal standard <sup>13</sup>C<sub>4</sub>-MBP (25 µL, Cambridge Isotope Laboratories, Andover, MA), HPLC-grade water (25 µL, Burdick and Jackson), and 0.1% (v/v) formic acid in acetonitrile (425 µL, EMD Chemicals Inc., Gibbstown, NJ). Samples were shaken for 6 min at 4°C, vortexed, and centrifuged at 1900 x g at 4°C. The supernatant was transferred to a glass vial with a deactivated siliconized glass insert.

Fetal testes were pooled by litter and homogenized in 1% PBS (500  $\mu$ L per testes pair) with a Mixer Mill 300 for 5 minutes at 30 Hz. The homogenate was divided into two 200  $\mu$ L fractions; the first fraction was prepared for analysis of MBP and MBP-G, the second was prepared for testosterone analysis. The fraction designated for MBP/MBP-G analysis (200  $\mu$ L) was transferred to a 2.0 mL microcentrifuge tube and 200  $\mu$ L of 1% formic acid/water and 25  $\mu$ L of  $^{13}$ C-MBP (6 mg/mL) were added to the tube. The sample was vortexed and then centrifuged at 1900 x g for 6 min at 4°C. The supernatant was loaded onto an LC-18 SPE column (Honeywell Burdick and Jackson, Morristown, NJ) that had been rinsed twice with 0.1% formic acid in methanol (1 mL/rinse) followed by two rinses with 0.1% formic acid in water (1 mL/rinse). After loading the sample, the column was washed with a 3:1 mixture of 0.1% formic acid in water and 0.1% formic acid in methanol. MBP and MBP-G were then eluted with 2 mL of 0.1% formic acid in methanol added in 2 increments of 1 mL. Eluted samples were evaporated to dryness under nitrogen and reconstituted in 200  $\mu$ L of 0.1% formic acid in ACN/H<sub>2</sub>O (90%/10%) for injection on the LC-MS/MS.

### **Testosterone Sample Preparation**

The second fraction of the testes homogenate (200  $\mu$ L) was added to  $^{13}$ C<sub>2</sub>-testosterone (Cambridge Isotope Labs, 10  $\mu$ L), diluted with 4 M urea (Sigma-Aldrich, 200  $\mu$ L), and heated to 60°C for 30 min [76]. Samples were cooled to room temperature, transferred to LC-18 SPE columns previously conditioned with methanol and water, and rinsed with 25% methanol. Methanol (100%) was used to elute the testosterone. Samples were dried under

nitrogen, reconstituted in 25  $\mu$ L chloroform and testosterone was derivatized with n-heptafluorobutyrylimidazole (HFBI, Indofine, Hillsborough, NJ) for 4 hrs at 60°C.

### **Calibration and quality control standards**

MBP (TCI America, Portland, OR) was dissolved in acetonitrile/water (1:1, v/v) at 2 mg/mL. MBP-G was purified from urine from rats dosed with 50 mg/kg MBP as described previously [48]. Calibration standards consisted of the stock solution, control plasma, and extraction buffer, and were prepared daily. Preliminary studies indicated that control plasma could be used as the biological matrix in preparation of the calibration curves for maternal plasma, fetal plasma, amniotic fluid, and fetal testes. Calibration curves for MBP and MBP-G consisted of 12 serial dilutions of MBP (0.1-200  $\mu$ g/mL) and MBP-G (0.04-90  $\mu$ g/mL). Testosterone (Steraloids, Newport, RI) was dissolved in chloroform and standards were prepared individually (no serial dilution) with concentrations ranging from 0 to 20 ng/mL.

### **MBP/ MBP-G Analysis with Liquid Chromatography/Mass Spectrometry (LC-MS/MS)**

LC-MS/MS (Applied Biosystems, Foster City, CA) was used to quantify MBP and MBP-G in plasma, amniotic fluid, and tissues. The LC was a Series 200 from Perkin Elmer (Norwalk, CT) and consisted of 2 MicroPumps, autosampler, and on-line Vacuum Degasser. Chromatography was performed on a Luna<sup>®</sup> phenyl-hexyl column (50 mm\*2 mm\*3  $\mu$ m) with a SecurityGuard<sup>™</sup> phenyl(phenylpropyl) guard column (Phenomenex, Torrance, CA). The mobile phase consisted of 0.1% formic acid in HPLC-grade water and acetonitrile. The acetonitrile gradient was increased from 30 to 95% over 3 min, with a 5-min post-run equilibration time.

MS analysis (Applied Biosystems API 3000) was conducted in negative ion mode with a turbo ionspray interface. Curtain, nebulizing, and collision gases were set in the PE Sciex Analyst 1.1 software at 11 (nitrogen), 7 (air), and 3 (nitrogen), respectively. Turbospray gas was nitrogen at 7 L/min at 375°C. The nebulizing, declustering, and focusing potentials were -4000 V, -25 V and -90 V. Quantitation was performed using selected reaction monitoring of precursor-product ion transitions at m/z 221.1 to 77.1 for MBP, m/z 225.1 to 79.1 for <sup>13</sup>C<sub>4</sub>-MBP, and m/z 397.1 to 221.1 for MBP-G. Collision energy was optimized to -25 eV for MBP and <sup>13</sup>C<sub>4</sub>-MBP and -22 eV for MBP-G. Data acquisition and initial analysis used PE Sciex Analyst 1.1 software.

Background levels of MBP and MBP-G were calculated by averaging daily plasma from control animals. Peak area counts were calculated by subtracting blanks and comparing to calibration standards, both averaged by analysis date. Samples were randomly placed into queue. Visually outlying results and random samples were verified by reextraction and/or reanalysis.

Limits of detection (LOD) for MBP and MBP-G were determined to be 6 and 1 ng/mL, respectively, using standard solutions. However, in control plasma samples both MBP and MBP-G levels were above the LOD (control levels: MBP = 0.26 ± 0.30 mg/L; MBP-G = 0.003 ± 0.003 mg/L). The method limit of quantitation (LOQ) was therefore determined from standards prepared in control plasma, yielding values of 0.26 and 0.003 mg/L (or 0.0024 and 0.0011 mg/L minus background from controls) for MBP and MBP-G, respectively. The LOQs for placenta, amniotic fluid and testes were calculated from the lowest point in the linear portion of the standard curve and adjusted for dilution during sample preparation. The resulting values for the LOQ for MBP and MBP-G were 2.4 and 1.1

mg/L in the fetal testes, and 0.0024 and 0.0011 mg/L in the placenta and amniotic fluid when adjusted for background levels. The potential source of the MBP background has not been determined, though internal studies have shown little to no detectable contamination from laboratory supplies. For example, there were no significant differences in MBP background following extraction and analysis using glass as compared to plastic lab supplies. Control animals were used to normalize MBP levels and to negate any phthalate contamination from laboratory supplies.

### **Testosterone Analysis with Gas Chromatography/Mass Spectrometry (GC-MS)**

Testosterone was quantified using an Agilent 6890 gas chromatograph (GC) coupled to an Agilent 5973 inert mass spectrometer (MS). GC separations were carried out by injecting 1  $\mu$ l onto a DB-5 column (30 m \* 0.25 mm, 0.25  $\mu$ m) (J&W Scientific, Folsom, CA) with an injector temperature of 280°C (split-less mode) and a carrier gas (helium) flow of 0.9 mL/min. The GC temperature program was 150°C for 0.5 min, ramped to 300°C at 10°C/min, and held at 300°C for 1.5 min before returning to 150°C. The mass selective detector was run in negative chemical ionization mode with methane as the reagent gas. Quantitation was conducted using selective ion monitoring of the 464 and 466 atomic mass unit ions for testosterone and  $^{13}\text{C}_2$ -testosterone, respectively. Data were collected and integrated using Agilent Chemstation software.

### **Bicinchoninic Acid (BCA) Protein Assay**

Protein concentration in fetal testes homogenate (10  $\mu$ L) was quantified using a commercially-available Bicinchoninic acid (BCA) method (Pierce, Rockford, IL).

### **Pharmacokinetic Analysis**

Pharmacokinetic parameters for MBP and MBP-G in the maternal and fetal plasma from the repeated dosing study were calculated in WinNonlin® version 4.5 (Pharsight, Mountain View, CA). Data were averaged by time point and dose group and modeled using noncompartmental analysis with extravascular administration and no weighting. The data from the single dose study did not contain a sufficient number of time points to carry out a comparable analysis.



## D. RESULTS

### MBP Pharmacokinetics after Repeated Dosing:

The dosing regimen of repeated dosing study was carried out in the same manner as [46], which showed a dose-dependent decrease in fetal testes testosterone concentrations. MBP and MBP-G were quantified in maternal plasma, maternal liver, placenta, amniotic fluid, and fetal plasma and testes using LC-MS/MS. Elution times for MBP-G, <sup>13</sup>C<sub>4</sub>-MBP, and MBP were comparable to previous LC-MS/MS results [46]. Concentration time courses were collected for MBP in maternal and fetal tissues after daily exposure to DBP from GD 12 to 19 (Figure 2.1). MBP in maternal plasma, placenta, and fetal plasma was mostly eliminated after 24 hrs. In the 50 mg/kg/day group, tissue distribution of free MBP occurred rapidly. Both placenta and fetal serum kinetics closely followed the maternal plasma, though the fetal plasma showed a slight delay in the time to reach peak concentration ( $T_{max} = 1$  vs. 0.75 hr). Fetal plasma levels were consistently lower (~60%) than maternal plasma. Placental tissue concentrations also remained lower than the plasma; peak MBP concentrations in the placenta were 15% of peak plasma levels in the 50 mg/kg/day dams.

Plasma and placenta MBP kinetics were qualitatively similar in the 100 and 500 mg/kg/day groups when compared to the 50 mg/kg/day group (Figure 2.1), with nearly complete clearance within 24 hrs and rapid, but limited, distribution into the placenta and fetal plasma. The half-life for MBP in maternal and fetal plasma was also similar across doses (Table 2.1). However, some pharmacokinetic parameters calculated from a noncompartmental model for maternal and fetal plasma (Table 2.1) did indicate the existence of dose-dependent differences.

The dose normalized area under the curve (AUC/D) was nearly 2-fold higher in the plasma of the 100 and 500 mg/kg/day dams than 50 mg/kg/day. In contrast, the dose normalized maximum concentration ( $C_{\max}/D$ ), time of peak concentration ( $T_{\max}$ ), and mean residence time (MRT) were similar between the 50 and 100 groups, but differed in the 500 mg/kg/day group. The  $C_{\max}/D$  was reduced nearly 3-fold at 500 mg/kg/day, while  $T_{\max}$  and MRT were increased more than 2-fold in the 500 mg/kg/day group. Fetal MBP parameters showed the same trends as the dam, with increased values for AUC/D (2-fold) and  $T_{\max}$  (4-fold) at 500 mg/kg/day. However, dose-dependent changes in  $C_{\max}/D$  and MRT in the fetus were minor (<20%).

Amniotic fluid MBP levels were not linearly correlated with either the maternal or fetal plasma when examined across doses (Figure 2.1). As opposed to the fetal plasma, where the AUC/D remained constant at the lower doses (50 – 100 mg/kg/day), amniotic fluid AUC/D increased 2-fold between the 50 and 100 mg/kg/day groups and another 3.4-fold between 100 and 500 mg/kg/day. Furthermore, while the half-life for MBP in the plasma did not change, the  $T_{1/2}$  in the amniotic fluid decreased with increasing dose (11.7 – 4.1 hr).

### **MBP-G Pharmacokinetics after Repeated Dosing:**

Concentrations of MBP-G in the maternal plasma, placenta, fetal plasma and amniotic fluid were also measured (Figure 2.2). The nearly complete elimination of MBP-G from maternal plasma within 24 hrs, and the low MBP-G concentrations at the 15 min time point, indicated that MBP-G was not accumulated with repeated dosing. In the 50 mg/kg/day dose group, MBP-G appeared rapidly in the maternal blood and placenta, with  $T_{\max}$  values similar to MBP (Table 2.1). However, appearance of MBP-G in the fetal plasma was slower

than free MBP (Figure 2.2), with peak concentrations occurring between 4 and 12 hrs post-dosing (as opposed to 1-2 hrs for MBP). Clearance of MBP-G from the fetal blood was somewhat slower than free MBP with a calculated  $T_{1/2}$  of 8.2 hrs (versus 5.2 hrs for free MBP).

When compared across dose groups, the trends seen in MBP-G kinetics were similar for maternal plasma, fetal plasma and placenta, *i.e.*, rapid appearance in maternal blood and placenta, delayed appearance in fetal plasma and amniotic fluid, no indication of accumulation in maternal or fetal plasma. However, as noted with free MBP, examination of the kinetic parameters (Table 2.1) revealed some dose-dependent differences in the chemical distribution and clearance. Trends seen in many of the MBP-G parameters were similar to those described above for MBP in the maternal plasma:  $T_{max}$ , AUC/D and  $MRT_{inf}$  increased at doses above 50 mg/kg/day and  $T_{1/2}$  did not change with dose. Notably, the difference in AUC/D in fetal plasma was more pronounced than was seen with either metabolite in the dam or with fetal MBP. The AUC/D increased nearly 6-fold between the plasma from the 50 and 500 mg/kg/day dose groups.

Amniotic fluid MBP-G levels were non-linear with respect to both external dose and fetal plasma MBP-G (Figure 2.2). MBP-G concentrations in the amniotic fluid were similar to the fetal plasma at 50 and 100 mg/kg/day. However, the AUC was approximately 2-fold greater in amniotic fluid than fetal plasma at 500 mg/kg/day.

## Single versus Repeated Dosing

Previous studies in pregnant rats showed induction of P450 expression in the liver of dams and fetuses exposed to 500, but not 50 mg/kg/day DBP from GD 12-19. UDPGT expression was also increased in the maternal liver [52]. To test whether these changes in enzyme expression translate to altered metabolite kinetics, maternal and fetal plasma and amniotic fluid were collected after a single DBP dose (500 mg/kg) and the MBP and MBP-G concentrations at 0.5, 1, 2, and 24 hrs post-dosing were compared to repeated dosing results. Use of the single dose study for comparison is based on the assumption that there would be insufficient time to induce these enzymes in the absence of pre-exposure. Livers were also collected from dams in the single and repeated (500 mg/kg/day) dose study in order to directly measure the effect of repeated dosing on liver metabolite concentrations.

Maternal and fetal plasma MBP levels were consistently lower with repeated doses compared to a single dose (Figure 2.3A-B), suggesting that metabolism of MBP was induced with multiple exposures. Peak maternal and fetal plasma MBP concentrations from animals exposed from GD 12-19 were 67% and 55% compared to those given a single dose. Maternal liver MBP levels were also reduced after multiple exposures; the  $C_{max}$  for MBP after multiple doses was 72% of the single dose (Figure 2.3C). Maternal liver MBP-G concentrations were not significantly different in the single and repeated dose groups (Figure 2.3C). MBP concentrations in the amniotic fluid were also reduced with repeated doses of 500 mg/kg DBP (Figure 2.3D). MBP-G, however, was not decreased (Figure 2.3D). In fact, the amniotic fluid MBP-G concentrations were consistently higher in the repeated dosing study than the single dose.

## **Testosterone Response in Fetal Testes**

In order to directly compare target tissue dose of MBP and testosterone concentration for DBP administration that results in developmental effects, fetal testes were collected from rats from both the repeated and single dose studies. Testes were pooled by litter, homogenized and split into two aliquots. One aliquot was analyzed for MBP and MBP-G and the other was analyzed for testosterone (Figures 2.4 – 2.6). Fetal testosterone levels were not expected to undergo the same diurnal cycling seen in the adult; plasma levels increase during gestation to peak levels at GD 18, followed by a slight decrease until birth [77]. In order to account for changes in testosterone levels with prenatal age, controls were taken on the day of sacrifice (0.5 hr) and on each subsequent day (24 and 48 hr post-dosing). A 12 hr control was also collected in the 50 mg/kg/day study (Figure 2.4A). The small tissue volume and the amount of dilution necessary to run the same sample through both the phthalate and testosterone analysis resulted in many of the samples being below the LOQ for MBP and MBP-G.

All testes samples in the lowest dose (50 mg/kg/day) were below LOQ for MBP and MBP-G and testosterone levels were significantly lower than controls only at the 12 hr time point (Figure 2.4A). At 100 mg/kg/day (Figure 2.4B), MBP was measurable for the first 4 hrs following the final administration of DBP and the testes showed significant decrease (43%) in testosterone at 0.5 hr post-dosing (GD 19). Testosterone levels recovered to control levels by 24 hrs post-dosing (GD 20) and at 48 hrs (GD 21) fetal testosterone levels for the 100 mg/kg/day group exceeded control levels ( $p < 0.05$ ). At the highest DBP dose (500 mg/kg/day), MBP was measurable up to 12 hrs after the final dose and testosterone was significantly decreased, with testosterone levels at 25 and 19% of controls on GD 19 and 20

(Figure 2.4C). Mean testosterone concentrations in testes of this high dose group remained low on GD 21 (48 hrs post-dosing), but were not statistically different from control values ( $p > 0.05$ ). More time points were taken for DBP treated animals than controls, as described in the Methods section. Figure 2.5 shows relative changes in testosterone at all time-points collected in DBP treated rats versus estimated control values calculated by linear interpolation of the available time-points. Because control values were not available for every time point, the statistical significance could not be determined for time points other than those shown in Figure 2.4. Nonetheless, the time courses for the 50, 100 and 500 mg/kg/day dose groups clearly show a pattern of testosterone reduction followed by recovery after cessation of dosing. In lower doses, 24 hrs is sufficient for complete recovery of normal testosterone levels, while the highest dose would require more time to reach control levels.

Testes MBP levels did not differ significantly ( $p > 0.05$ ) between animals given a single 500 mg/kg dose and those dosed daily from GD 12-19 (Figure 2.6A). Testosterone levels were significantly reduced on GD 20 (24 hrs post-dosing) but not GD 19 or 21 (0.5 and 48 hrs post-dosing) in the fetal testes of dams given a single dose of 500 mg/kg (Figure 2.6B). Mean changes in testosterone levels were less pronounced after a single dose as compared to repeated dosing. The testes testosterone concentrations after a single or repeated dose of 500 mg/kg day were 40 vs. 19% of control at 24 hrs and 76 vs. 55% of control at 48 hrs post-dosing.

In order to directly relate the internal dose for the active phthalate metabolite concentration to measured changes in testosterone, the average testosterone concentration (0.5 – 24 hr) was calculated for GD 19 using WinNonlin® and plotted against the calculated  $AUC_{inf}$  for MBP in the plasma of the same fetuses. Fetal plasma MBP was used instead of

testes levels as they were above LOQ for all time-points on GD 19. Figure 2.7 illustrates the fetal plasma MBP concentration-dependent decrease in fetal testosterone.

## E. DISCUSSION

DBP causes a variety of developmental effects in the male fetuses of rats exposed during the critical window for testosterone-dependent sexual development (GD 12-19). It is thought to exert its effect through inhibition of testosterone synthesis by the free monoester metabolite MBP. Thus, it is important to understand both 1) metabolite disposition with repeated DBP exposures during the critical period of gestation; and 2) how target tissue MBP concentrations relate to changes in fetal testes testosterone levels. In this study, MBP and its primary metabolite, MBP-G, were measured in maternal and fetal plasma, placenta and amniotic fluid after DBP doses where developmental effects have been found.

Analysis of the dose-response data from the repeated dosing study indicated dose-dependence in several pharmacokinetic parameters in maternal and fetal plasma, including AUC/D,  $T_{max}$ , MRT and  $C_{max}/D$ . While these differences were generally subtle (~ 2-fold), they are supported by their reproducibility across studies in both the pregnant [42] and non-pregnant rat (NIEHS, 1994). Fennell et al. [42] reported an increase in AUC/D in pregnant rats given a single dose of 250 mg/kg DBP versus those dosed with 50 or 100 mg/kg [42]. Evaluation of published data in male rats [78] using WinNonlin® revealed increases in AUC/D (3.7-fold),  $T_{max}$  (2-fold), and MRT (1.8-fold) and a decrease (3-fold) in  $C_{max}/D$  after administration of 43 or 857 mg DBP/kg via oral gavage. The reproducible increase in  $T_{max}$  and corresponding decrease in  $C_{max}/D$  seen at the higher doses, suggests that uptake of the monoester is dose limited. This is likely due to saturation of the intestinal lipases, which convert the poorly absorbed diester to the rapidly absorbed monoester phthalate [9]. Despite this reduced uptake, AUC/D and MRT are increased at higher doses, suggesting that metabolite clearance is also saturated.



Amniotic fluid showed notably different dose-response trends compared to either maternal or fetal plasma. The calculated AUC/D for MBP and MBP-G for amniotic fluid showed greater increases across doses than would be expected from fetal plasma levels. Both metabolites also exhibited a decrease in  $T_{1/2}$  that is not recapitulated in the plasma. The reason for the different dose-response in the amniotic fluid and the fetal plasma are not known, though the existence of these differences suggest that amniotic fluid kinetics are governed by more complex processes than simple passive exchange with either the maternal or fetal plasma. Both trends are reiterated in the data of Fennell et al. [42], who noted decreasing  $T_{1/2}$  (11 – 6.2 hr) and increasing AUC/D (1.54 – 2.56) in the amniotic fluid after a single dose of 50, 100, or 250 mg/kg DBP. Similar increases (nearly 10-fold) to the current study were also seen in AUC/D for amniotic fluid MBP-G between the 50 and 250 mg/kg dose. However, Fennell et al. [42] also noted a much longer  $T_{1/2}$  than was observed in present study. The data in Fennell et al. [42] was taken on GD 20 rather than GD 19. It is not clear whether the timing of gestation and development of UDPGT activity would account for this difference between the studies. The relatively high concentrations of MBP-G in amniotic fluid at 15 min and 24 hrs post-dosing indicate that MBP-G may be accumulating in the amniotic fluid.

The results from the repeated dosing study indicate there is no bioaccumulation of MBP or MBP-G in the dam or fetus, with the possible exception of MBP-G in the amniotic fluid. This conclusion is supported by previous radiolabeled studies in male rats showing little to no residual activity 24 hrs after a single DBP dose [11]. The fact that MBP-G, but not MBP, accumulates in the amniotic fluid suggests that MBP-G may require hydrolysis before re-entering fetal circulation. Fennell et al. [42] showed amniotic fluid MBP-G

underwent pH-dependent rearrangement, which was not present in the plasma. These rearranged glucuronides are more resistant to hydrolysis via  $\beta$ -glucuronidase than the original congeners. Resistance of MBP-G toward hydrolysis may account for the anomalous kinetics of the amniotic fluid.

The reduced MBP and MBP-G concentrations in the tissues of animals dosed repeatedly with 500 mg/kg DBP from GD 12-19 versus those administered a single dose on GD 19 indicates that there is some induction of oxidative metabolism with repeated high dose administration. Peak MBP concentrations in the maternal and fetal plasma were reduced by nearly 50% after eight days of dosing. Despite the increase in UGT expression in the maternal liver at 500 mg/kg/day [52], the current results do not indicate a corresponding increase in glucuronide conjugation. Peak MBP-G levels were not elevated in either the maternal or fetal plasma, or in the liver of the maternal rat. In fact, like MBP, MBP-G plasma levels were reduced in animals given several, rather than one, 500 mg/kg dose.

The difference between the single and repeated 500 mg/kg/day dose studies may be explained by increased oxidative metabolism, which was not directly measured in this study. Wyde *et al.* [52] demonstrated increased mRNA and protein expression of more than one family of the P450 enzymes, including CYP4A, after repeated exposures to DBP at these levels. CYP4A is the primary P450 involved in  $\omega$ -hydroxylation of fatty acids and is thought to play a role in metabolism of MEHP, a phthalate that is similar in structure to MBP [24]. The current study, together with studies of repeated DEHP exposures [45, 53, 54] indicates that oxidative metabolism is likely to be induced with repeated high doses of some phthalates, but the effect on overall kinetics is small. In the current study, the difference in

peak plasma levels was less than a factor of two between repeated and a single 500 mg/kg DBP dose. While the half-lives could not be compared, MBP levels at the 24 hr time-points were not statistically different between the single and repeated dose studies.

Fetal MBP-G may arise either from delivery via maternal blood or through fetal metabolism. The presence of MBP-G in plasma of the GD 19 fetus could, but does not necessarily, indicate placental transfer of the glucuronide conjugate. UGTs become active in the fetal liver as early as GD 16 in the rat [79]. The slow appearance of MBP-G in the fetus versus the dam may indicate that fetal MBP-G is derived from conjugation in the fetus rather than placental transfer, especially since clearance of MBP-G is not slowed to the same extent as its appearance in the fetus. However, without additional data it is not possible to definitively state if fetal MBP-G levels are a product of maternal or fetal conjugation.

Decreases in testosterone levels after repeated dosing was similar to previous studies. Lehmann et al. [46] reported a mean decrease of 24, 33, and 94% in fetal testes testosterone levels 2 hr after the final dose of 50, 100, and 500 mg/kg/day, respectively, administered from GD 12-19. In the current study, the closest comparable time-point with corresponding controls was 0.5 hr. The testes testosterone concentration was reduced by 17, 33, and 75% in the 50, 100, and 500 mg/kg/day groups with respect to the control animals. Changes in testosterone concentration were rapid in fetal testes after a single DBP dose of 500 mg/kg. Within 24 hrs, the decrease in testosterone was equal to that seen in the repeated dose study. Recovery time was also similar in the single and repeated dose groups. Evaluation of the testosterone time-course data showed a return to control levels within 24 hrs for doses  $\leq$  100 mg/kg/day. The 100 mg/kg/day group returned to levels that were significantly greater than the pretreatment controls, indicating a tendency of the system to over-compensate for

temporary decreases in the hormone. This trend may have also been true for animals given 500 mg/kg/day. However, because animals at the highest dose took longer to recover, it would have been necessary to measure testosterone at time-points greater than 48 hr after dosing to see this response.

Repeated DBP exposures during the period of sexual development can interfere with normal testosterone-dependent development, with the following effects occurring at doses at 100 – 500 mg/kg/day: hypospadias (cleft penis), nipple retention, reduced anogenital distance (AGD), cryptorchidism, seminiferous tubule degeneration, testis interstitial cell proliferation, and malformed epididymis, seminal vesicle, vas deferens and ventral prostate [47]. The current study correlates testosterone inhibition at these exposures to target tissue levels of MBP and MBP-G. At exposures where effects are seen (100 and 500 mg/kg/day) peak fetal testes MBP concentrations were 72 and 152  $\mu$ M. Although method sensitivity prohibits the calculation of testes MBP AUCs using traditional noncompartmental analyses, they can be correlated to maternal plasma average daily MBP concentrations of 5, 11, and 60 mg/L.

This study provides the first description of DBP disposition after repeated dosing in gestation that directly correspond to exposures associated with reduced testosterone in the fetal rat, which has been repeatedly shown to cause delayed sexual development of the male rat both in our laboratory [34, 46, 47, 68, 80] and others [32, 33, 63]. Examination of the 50, 100 and 500 mg/kg/day groups confirms the dose-dependent differences in plasma pharmacokinetics noted in previous acute studies [42]. A comparison of the pharmacokinetic and testosterone response in animals given single or multiple doses of 500 mg/kg DBP shows little difference between the two groups, though the statistically significant decreases in MBP

tissue concentrations at early time-points indicated that there may be some up-regulation of oxidative metabolism at repeated high doses. This study further supports the direct correlation of fetal testosterone response to fetal metabolite levels.

**Table 2.1. Calculated Pharmacokinetic Parameters for MBP and MBP-G in Maternal Plasma, Fetal Plasma, and Amniotic Fluid after Repeated Doses of 50, 100, and 500 mg/kg/day from GD 12 to GD 19 calculated with WinNonlin®.**

	<u>50 mg/kg/day</u>		<u>100 mg/kg/day</u>		<u>500 mg/kg/day</u>	
	<u>MBP</u>	<u>MBP-G</u>	<u>MBP</u>	<u>MBP-G</u>	<u>MBP</u>	<u>MBP-G</u>
<b>Maternal Plasma</b>						
Tmax (hr)	0.75	1.0	1.0	1.0	2.0	4.0
Cmax (mg/L)	169	27	502	80	959	131
Cmax/D						
( $\mu\text{mol/L-mg/kg}$ dosed)	0.94	0.15	1.39	0.22	0.53	0.07
T <sub>1/2</sub> (hr)	3.3	3.5	4.5	2.4	3.0	3.5
AUCinf						
( $\mu\text{mol-hr/L}$ )	591	107	1839	405	12271	2110
AUCinf/D						
( $\mu\text{mol-hr/L-mg/kg}$ dosed)	3.3	0.6	5.1	1.1	6.8	1.2
MRTinf (h)	3.5	4.2	3.8	4.1	7.7	8.7
<b>Fetal Plasma</b>						
Tmax (hr)	1.0	4.0	1.0	4.0	4.0	12.0
Cmax (mg/L)	48	3	142	29	386	169
Cmax/D						
( $\mu\text{mol/L-mg/kg}$ dosed)	0.27	0.02	0.39	0.08	0.21	0.09
T <sub>1/2</sub> (hr)	5.2	8.2	5.9	3.7	4.8	5.5
AUCinf						
( $\mu\text{mol-hr/L}$ )	241	41	833	235	5082	2564
AUCinf/D						
( $\mu\text{mol-hr/L-mg/kg}$ dosed)	1.3	0.2	2.3	0.7	2.8	1.4
MRTinf (h)	7.4	12.2	6.4	7.2	8.9	11.8
<b>Amniotic Fluid</b>						
Tmax (hr)	4.0	8.0	4.0	8.0	4.0	12.0
Cmax (mg/L)	9	1	38	13	810	321
Cmax/D						
( $\mu\text{mol/L-mg/kg}$ dosed)	0.05	0.01	0.10	0.04	0.45	0.18
T <sub>1/2</sub> (hr)	11.7	17.4	9.4	7.8	4.1	13.5
AUCinf						
( $\mu\text{mol-hr/L}$ )	151	37	581	210	9930	7943
AUCinf/D						
( $\mu\text{mol-hr/L-mg/kg}$ dosed)	0.8	0.2	1.6	0.6	5.5	4.4
MRTinf (h)	18.2	27.3	14.4	14.6	9.3	22.7

**Figure 2.1. Concentration of MBP after the last dose of DBP administered from GD 12-19.**

Values represent mean  $\pm$  SE of four dams given ( $\blacktriangledown$ ) 50, (O) 100, or ( $\blacksquare$ ) 500 mg/kg/day.

Placenta, amniotic fluid and fetal plasma samples were pooled by litter before analysis.

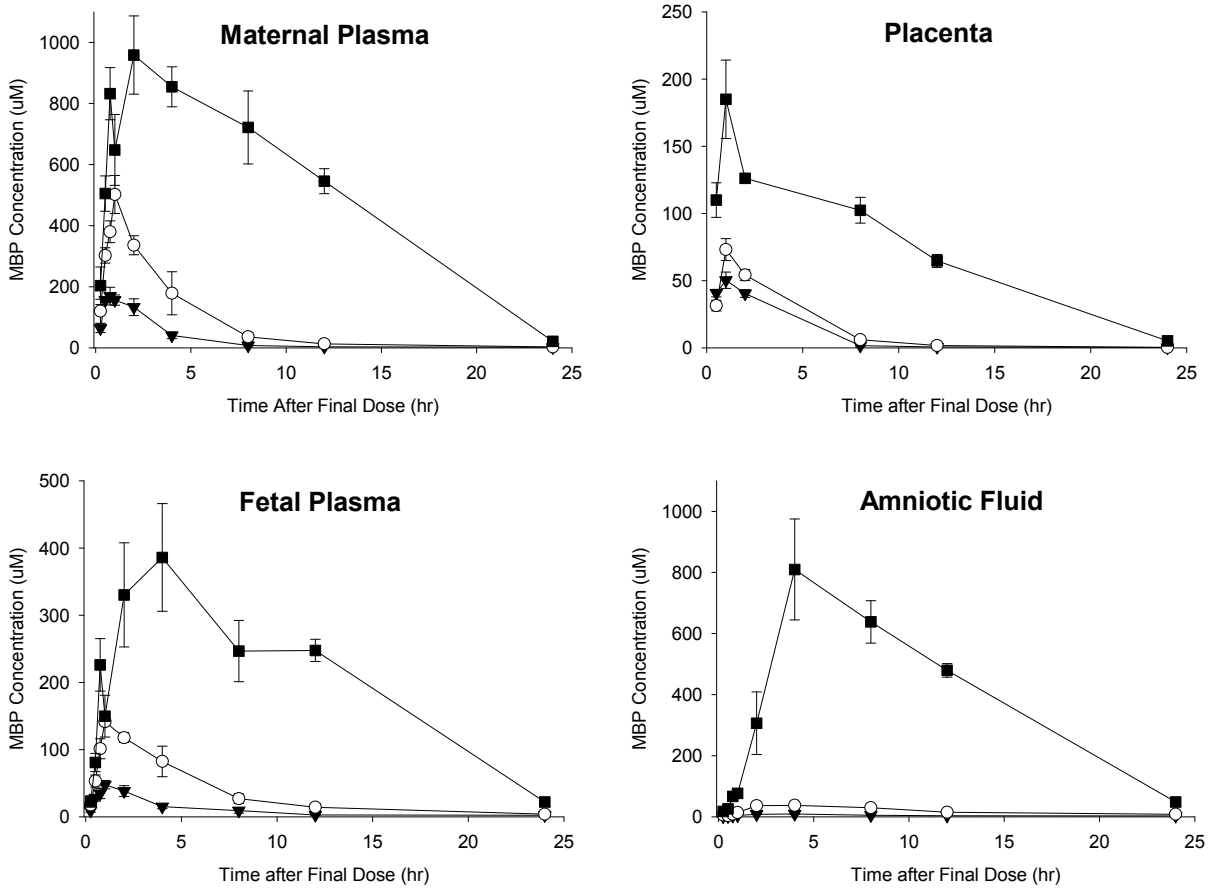


**Figure 2.2. Concentration of MBP-G after the last dose of DBP administered from GD 12-19.**

Values represent mean  $\pm$  SE of four dams given ( $\blacktriangledown$ ) 50, (O) 100, or ( $\blacksquare$ ) 500 mg/kg/day.

Placenta, amniotic fluid and fetal plasma samples were pooled by litter before analysis.

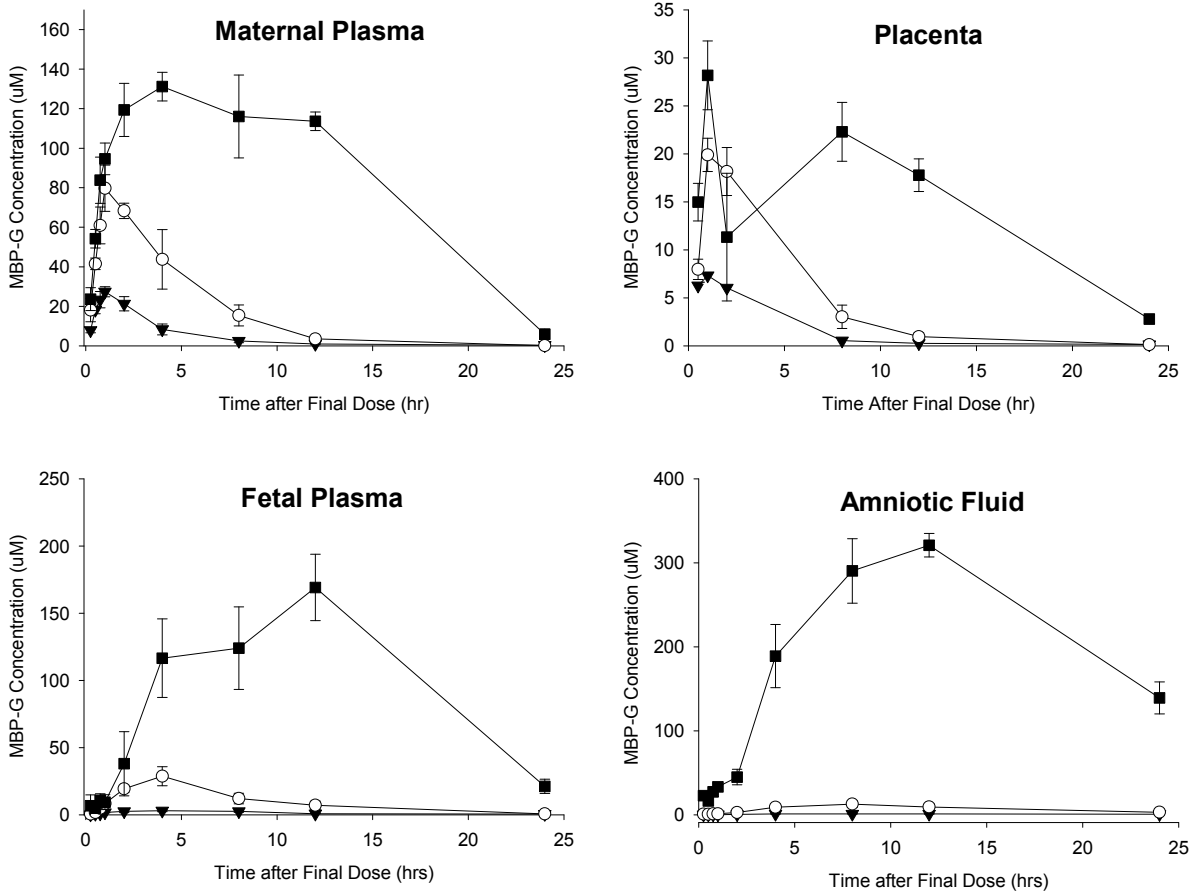




**Figure 2.3. MBP and MBP-G concentrations after single (GD 19) or repeated doses (GD 12-19) of 500 mg/kg DBP.**

Values represent mean  $\pm$  SE for four dams. \* $p < 0.05$ , two-tailed student's t test. Placenta, amniotic fluid and fetal plasma samples were pooled by litter before analysis.

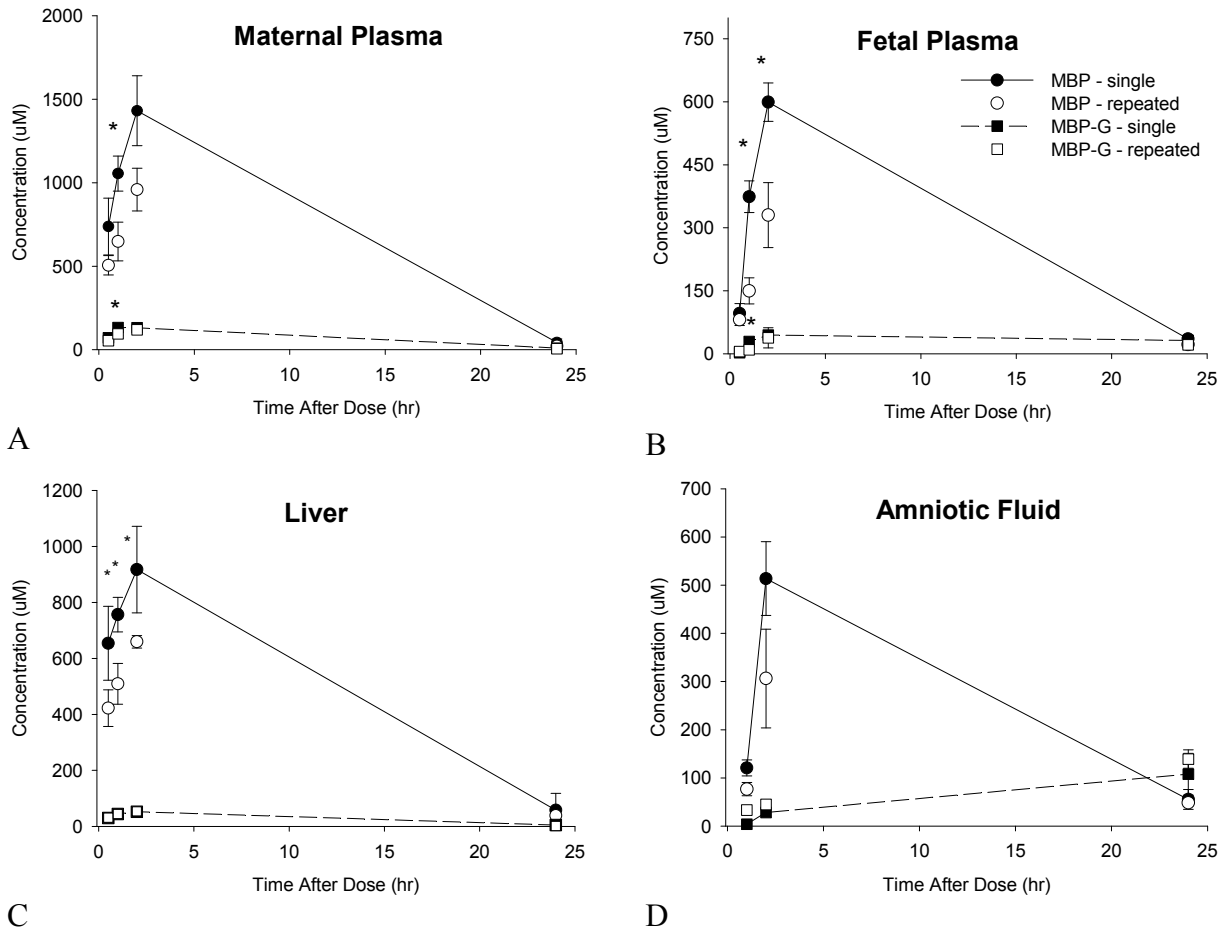


**Figure 2.4 MBP and testosterone in fetal testes from dams exposed to (A) 50, (B) 100, or (C) 500 mg DBP/kg/day from GD 12-19.**

Circles represent mean measured MBP concentration in the fetal testes. White bars represent testosterone from control animals. Grey bars represent testosterone from DBP treated animals expressed as percent control. Values represent mean  $\pm$  SE for the fetal testes (pooled by litter) from 3-4 dams. \* $p < 0.05$ , two-tailed student's t test. MBP concentrations are shown only for the (B) 100 and (C) 500 mg/kg/day dose groups. Sample concentrations were below the LOQ for all time-points in the 50 mg/kg/day dose group.

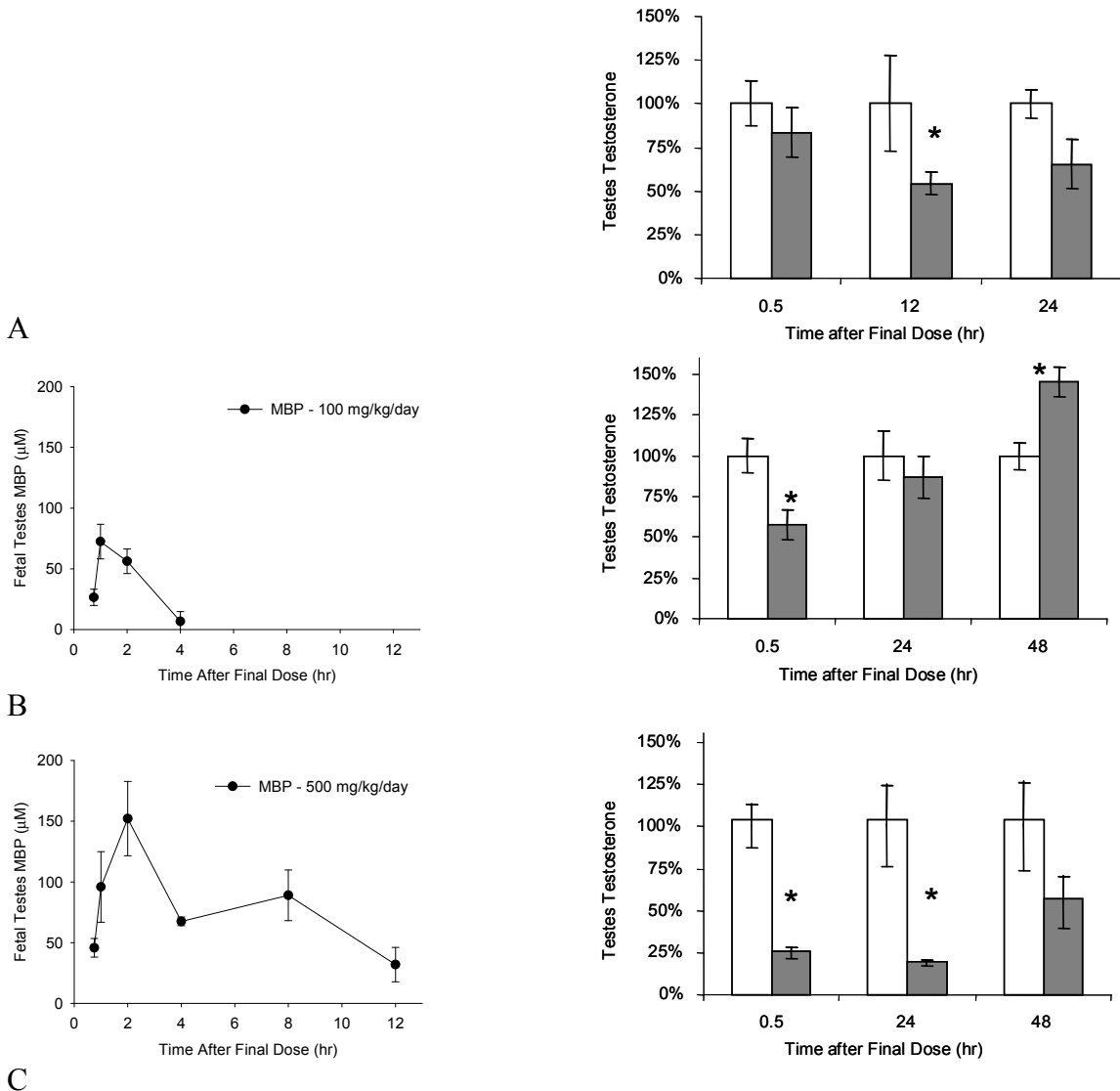


**Figure 2.5. Testosterone recovery (A) 4 and (B) 24 hours after the last dose of DBP at 50, 100, or 500 mg/kg/day from GD 12-19.**

For time-points where direct controls were not available, control testosterone values were estimated from linear interpolation between measured points. Values represent mean  $\pm$  SE for the fetal testes (pooled by litter) from 3-4 dams. Statistical differences were calculated only for samples with comparable controls and are shown in Figure 4.

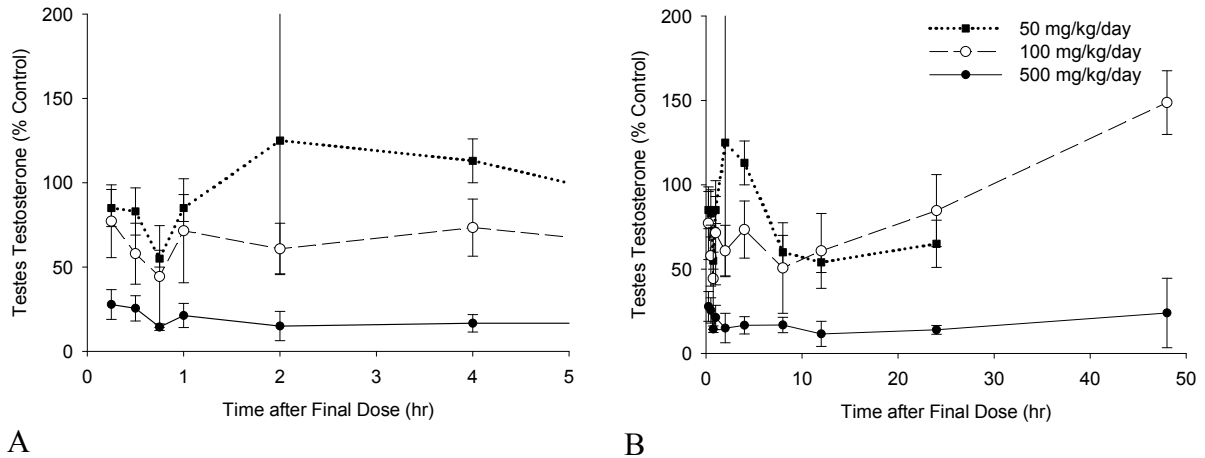


**Figure 2.6. MBP and testosterone in fetal testes from dams exposed to a single dose of 500 mg DBP/kg/day on GD 19.**

Circles represent mean measured MBP concentration in the fetal testes. Bars represent testosterone from control (white) and DBP treated (grey) animals expressed as percent control. Values represent mean  $\pm$  SE for the fetal testes (pooled by litter) from 3-4 dams. \*p < 0.05, two-tailed student's t test.

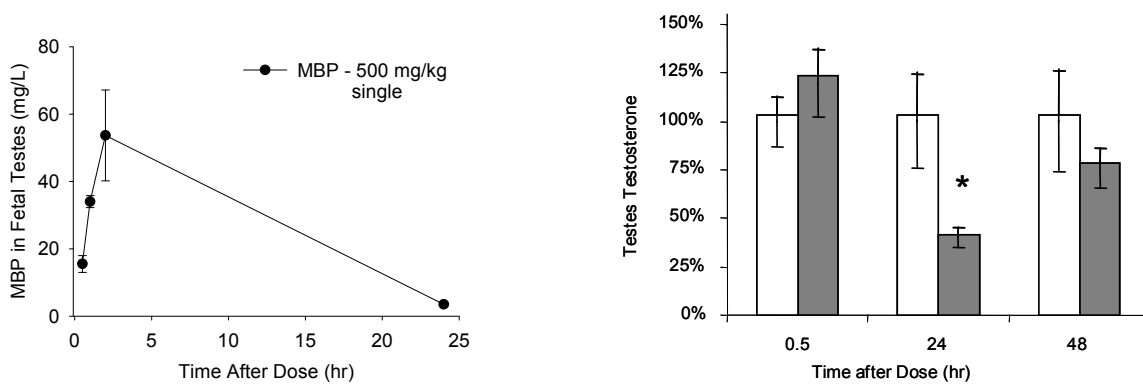
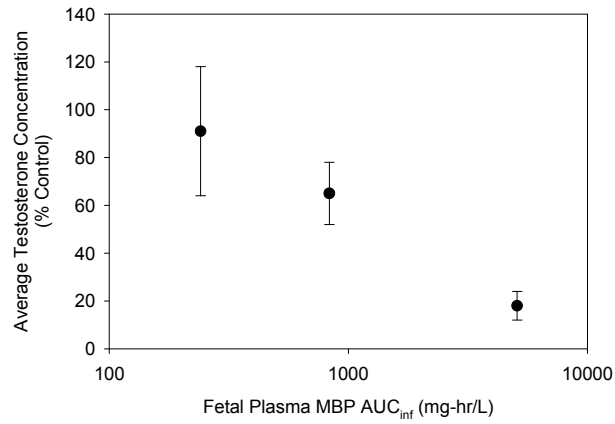


**Figure 2.7. Dose-response for testes testosterone in the GD 19 fetus after administration of 50, 100, or 500 mg DBP/kg/day to the pregnant dam.**

Circles and cross-bars represent the mean  $\pm$  SD of the percentage of control testosterone with respect to fetal plasma MBP.



## CHAPTER 3

**Tissue exposures to free and glucuronidated monobutylphthalate in the pregnant and fetal rat following exposure to di-n-butylphthalate: Evaluation with a PBPK model**

The text of sections A – F of this chapter is reproduced with permission from

*Toxicological Sciences* 103 (2008) 241-259

© 2008

Oxford University Press

Supplemental Materials are published on-line at:

<http://toxsci.oxfordjournals.org/cgi/content/full/kfn054/DC1>

## A. ABSTRACT

Human exposure to phthalic acid diesters occurs through a variety of pathways as a result of their widespread use in plastics. Repeated doses of di-n-butyl phthalate (DBP) from GD 12-19 disrupt testosterone synthesis and male sexual development in the fetal rat. To gain a better understanding of the relationship of the target tissue (testes) dose to observed developmental effects, the pharmacokinetics of monobutyl phthalate (MBP) and its glucuronide (MBP-G) were examined in pregnant and fetal rats following single and repeated administration of DBP from GD 12-19. These data, together with results from previously published studies, were used to develop a physiologically based pharmacokinetic (PBPK) model for DBP and its metabolites in the male, pregnant and fetal rat. The model structure accounts for the major metabolic (hydrolysis, glucuronidation, oxidative metabolism) and transport processes (enterohepatic recirculation, urinary and fecal excretion, placental transfer). Extrapolation of the validated adult male rat model to gestation successfully predicts MBP and MBP-G levels in maternal plasma, placenta and urine, as well as the fetal plasma and testes. Sensitivity analysis indicates that plasma MBP kinetics are particularly sensitive to glucuronidation and enterohepatic recirculation: a decrease in the UDPGT capacity during gestation results in an increased MBP residence time, and saturation of UDPGT at the highest doses ( $> 100$  mg/kg/day) causes a flattening out of the plasma time-course data. Oxidative metabolism plays a significant role in elimination only at low doses ( $<50$  mg/kg DBP). Insights gained from modeling of the rat data will be used to support development of a human PBPK model for DBP.

## B. INTRODUCTION

Phthalate esters are found in drinking water, food, personal care products and are used in the coating of some medications [1, 3, 64]. Although the relative source contributions have not been well characterized in the United States, a recent study in Europeans found that oral exposure through food sources accounted for 40-90% of the overall DBP exposure [3]. Metabolites of several phthalates have been found in the urine of the US population, including adults, children, infants, and pregnant women [4-6, 81, 82], with the highest levels in women of child-bearing age. Some of these phthalates, including di-n-butylphthalate (DBP), are developmental toxicants in rats and mice [32-34, 65, 66, 68]. Exposure of pregnant rats to DBP impairs development of male reproductive tissues, as evidenced by reduced anogenital distance, nipple retention, hypospadias, delayed testes descent, and vaginal pouch development in male pups [47, 83]. While the mechanism of action of DBP has not been fully elucidated, these anti-androgenic effects result, at least in part, from the ability of the monoester metabolite (MBP) to inhibit testosterone production in the fetal rat testes [33, 70-72]. Repeated doses of DBP have been shown to reduce testosterone levels in the blood of adult male rats [63, 70, 72, 84] in the testes of male fetuses from pregnant rats exposed to doses as low as 50 mg/kg/day from gestation day (GD) 12 – 19 [46].

In the environment, phthalates exist primarily as their dialkyl esters [1]. After ingestion, they are rapidly hydrolyzed to the monoester and released into systemic circulation [9, 85]. Monobutyl phthalate (MBP) is the most prevalent metabolite of DBP in rat and is thought to be the principal biologically active species [11, 69]. MBP can be excreted unchanged in the urine, further metabolized via oxidation, or conjugated to glucuronic acid



by uridine 5'-diphospho-glucuronosyltransferase (UDPGT). Oxidation of MBP occurs primarily through  $\omega$  and  $\omega$ -1 sidechain cleavage [74]. The resulting oxidative metabolites may be further oxidized (with a terminal product of phthalic acid), conjugated by UDPGT, or excreted in urine [74]. Glucuronidation appears to be a major route of clearance for MBP in the rat: MBP-glucuronide (MBP-G) accounted for greater than 20% of the total urinary metabolites and approximately 17% of the administered dose in rats after 1 – 10 mg/kg DBP iv [49]. Both free MBP and MBP-G have been identified in the fetal rat plasma after maternal exposure to DBP [42, 43, 48], though the processes driving fetal MBP kinetics (placental transport, glucuronide conjugation) are not well-characterized. While placental transfer of glucuronidated xenobiotics is typically inefficient [86-88], the presence of MBP-G in the rat fetus suggests that it may be important to understanding fetal MBP exposure.

The combination of multiple non-linear metabolic processes leads to rather complex behavior of DBP and its metabolites *in vivo*, making it difficult to predict a priori the pharmacokinetics of these chemicals at different doses. Inherent changes in physiology and biochemistry during pregnancy further compound this issue. Yet, in order to evaluate the risk associated with exposure to DBP, it is necessary to have a quantitative understanding of the dose-response of the active compound (MBP) at the target organ (fetal testis). The purpose of this research was two-fold: 1) to gain a quantitative understanding of the relationship of fetal plasma and testes metabolite concentrations to external DBP doses, and 2) to identify the biochemical processes that are the major determinants of metabolite kinetics. In order to accomplish these goals, two *in vivo* studies were performed in which the distribution of MBP and MBP-G in the pregnant rat and fetus was measured after single or repeated doses of DBP. These data were then used to inform the development of a

physiologically based pharmacokinetic (PBPK) model for DBP and its metabolites during gestation.

The structure of the PBPK model was determined based on three primary considerations: 1) its intended use, 2) the available data, and 3) previous investigations into DBP kinetics using PBPK models. The ultimate goal of our work was to develop a single model description that could be used with confidence to predict DBP, MBP, and MBP-G distribution and elimination in the pregnant and fetal rat under a variety of dosing scenarios, particularly those associated with observed developmental effects (repeated oral dosing). While a few studies were available in the literature with information on DBP disposition during gestation [42-44, 48], some significant data gaps still existed. In particular, urinary, fecal, and biliary excretion and the potential differences in kinetics after multiple exposures had not been characterized in the pregnant rat. Since more complete information on metabolite kinetics (including bile, urine and feces) was available in the adult male than the pregnant rat, the model was initially parameterized for the adult male and then extended to gestation using the published and newly obtained kinetic data.

A previous PBPK model for DBP was also available in the literature [89] and was used to inform the current model structure. Keys et al. [89] evaluated the ability of four different models (flow-limited, diffusion-limited, pH-trapping, and enterohepatic recirculation) to recapitulate blood levels of MBP after iv and oral dosing. The data available to Keys et al. [89] and the goal of their work required that the models be kept relatively simple in structure (few adjustable parameters), precluding any description of the MBP metabolism or characterization of excreted products. In order to describe not only DBP and MBP, but also the glucuronide conjugate and oxidative metabolites of MBP in the

plasma, urine, feces and developing fetus, a more comprehensive model is needed. By including all major metabolic (hydrolysis, oxidation, glucuronidation) and transport (biliary excretion, tissue partitioning, urinary and fecal excretion) processes, the current model provides both a means for investigating the processes driving kinetics and a platform for future use in risk assessment applications including extrapolation across doses, exposure routes and eventually species.

## C. METHODS

### Pharmacokinetic Studies *In Vivo*

Pregnant Sprague-Dawley (CrI:CD(SD)) rats (Charles River Laboratories, Raleigh, NC) were housed in a temperature- and humidity-controlled, HEPA-filtered environment on a 12 hr light-dark cycle. Rats were provided NIH rodent diet (NIH-07, Zeigler Bros., Gardner, PA) and reverse-osmosis water ad libitum. Dosing solutions were prepared by mixing DBP and corn oil (Sigma-Aldrich, St. Louis, MO). DBP concentrations in the dosing solutions were verified to be  $48 \pm 0.4$ ,  $89 \pm 10$ , and  $502 \pm 9$  mg/mL (mean  $\pm$  SE) by gas chromatography with the method of Fennell et al. [42].

In the single dose study, GD 19 pregnant Sprague-Dawley rats (sperm positive on GD 0) were administered a single oral dose of DBP (0 or 500 mg/kg) in corn oil (1.0 mL/kg). Rats were euthanized with CO<sub>2</sub> at 0.5, 1, 2, and 24 hrs post-dosing. In the repeated dose study, pregnant rats were given a daily dose of DBP (0, 50, 100 or 500 mg/kg) dissolved in corn oil (1.0 mL/kg) from GD 12 through 19. At 0.25, 0.5, 0.75, 1, 2, 4, 8, 12, 24, and 48 hrs after the final dose, rats were euthanized by CO<sub>2</sub>. Maternal blood was drawn by cardiac puncture. Fetal blood was collected using heparinized capillary tubes and pooled by litter in glass centrifuge tubes. Plasma was separated from whole blood by centrifugation at 1900 x g at 4°C and stored at -80°C. Placenta samples and amniotic fluid that was visibly clear of blood or other contaminants were pooled by litter. Testes from each male fetus were stored separately. All amniotic fluid and tissue samples were snap frozen in liquid nitrogen and stored at -80°C. Tissues were prepared and analyzed for MBP and MBP-G as described in the Supplemental Materials (SM-1).

Area under the curve (AUC<sub>t-inf</sub>), half-life ( $T_{1/2}$ ), and mean residence time (MRT<sub>t-inf</sub>) for MBP and MBP-G in the maternal and fetal plasma data from the repeated dosing study were calculated in WinNonlin (Pharsight, Mountain View, CA). Data were averaged by time point and dose group and modeled using a noncompartmental analysis with extravascular administration and no weighting. The data from the single dose study did not contain a sufficient number of time-points to carry out a comparable analysis.

### **PBPK Model Structure**

Keys et al. [89] showed that a simple flow-limited model was sufficient for the description of DBP in the blood, while transport-limited tissue distribution and enterohepatic recirculation were important determinants of short-term MBP kinetics. These insights were used to inform the initial model structure. However, as the current model was intended to describe several aspects of DBP metabolite kinetics that were not addressed in the Keys model (MBP-G in plasma, fecal and urinary excretion products, and most importantly, fetal exposure), decisions regarding the current model structure were ultimately based on available disposition data. Defining the structure of the model was an iterative process, wherein the behavior of the data was used to develop an initial model, which was then tested by simulating additional data sets. Failure to recapitulate data led to revisions of the mechanistic hypotheses and model restructuring. For example, in the most preliminary version, only DBP, MBP and MBP-G were specified in the model. However, when simulations were performed for the data of Payan et al. [49], it was clear that urinary clearance and total plasma radioactivity could not be accurately described without including a description of the oxidative metabolites. Thus, the model was extended to include a simple description of the

combined oxidative metabolites in the plasma and urine, which allowed the whole data set to be reproduced.

The final model (Figure 3.1) contains four inter-connected sub-models, each with the necessary amount of detail to adequately describe its chemical species: DBP, MBP, MBP-G, and the combined oxidative metabolites (MBP-O). The individual sub-models interact at sites of metabolism (hydrolysis of the diester, glucuronidation, hydrolysis of the glucuronide, and oxidation). The models for each chemical species in the adult rat are described below, followed by the modifications made to describe gestation. PBPK model simulations were performed using ACSL 11.0 (Advanced Continuous Simulation Language, AEGIS Technologies Group, Inc., Huntsville, AL). Examples of model equations are shown in the Supplemental Materials (SM-2).

### **Adult Male Rat Model**

#### *Intact DBP*

Enzymes responsible for the hydrolysis of DBP are present in the intestinal mucosa, plasma and liver [11, 85]. Hydrolysis of DBP in the plasma (kbc) and liver (kc) is described as a first order rate as none of the tested doses were sufficient to overwhelm hydrolysis. Hydrolysis of the DBP in the upper GI (stomach  $\pm$  small intestine; GC1), on the other hand, is described as a saturable process based on the *in vitro* data of Rowland et al. [85] and the apparent saturation of oral uptake at the highest doses (~500 mg/kg) [78]. *In vitro* studies suggest that DBP is poorly absorbed in the gut, though a small amount may enter circulation intact, particularly at doses where hydrolysis is overwhelmed [9]. Unabsorbed DBP may also be passed in to the lower intestine (GC2) and cleared in the feces. Oral absorption is

described as a first order process ( $k_{ad}$ ). Transport between the upper intestine (G1) and lower intestine (G2) compartments ( $k_{gic}$ ) is a first order rate. Fecal excretion ( $k_{fc}$ ) is described using a clearance rate (L/hr). DBP that is taken up into the gut wall is passed to the liver via the portal blood where it is hydrolyzed, released into systemic circulation with the plasma or excreted into the bile [11]. Biliary transfer of DBP into the duodenum is modeled as a clearance rate ( $k_{bdc}$ ) from the liver to the upper intestine (GC1). Efficient hydrolysis ensures that essentially 100% of the DBP is de-esterified before it can be taken up into the bile. However, competition between these processes (particularly after saturation of intestinal lipases at  $> 500$  mg/kg doses) is included in the model in order to describe the wide range of published data. Transport of DBP into the tissues is assumed to be flow limited.

#### *Free MBP*

Oral absorption is described as a first order process ( $k_{am}$ ). Movement through the GI and fecal excretion are clearance rates. Unlike DBP, MBP is readily absorbed in the gut wall and passed to liver via the portal blood. Glucuronidation and oxidation of free MBP in the liver are described using saturable kinetics. Free MBP may also be excreted into the bile or released into systemic circulation. Transfer of MBP in the bile is described in the same manner as DBP, using a clearance rate ( $k_{bmc}$ ) from the liver to the upper intestine (GC1). The MBP may then be reabsorbed or transported ( $k_{gic}$ ) into the lower intestine (GC2). Absorption may occur in both the upper and lower intestine compartments. Free MBP that is not absorbed in the intestine is cleared via the feces ( $k_{fc}$ ). Transport of MBP into the tissues from the plasma is modeled using diffusion-limitation. Secretion of free MBP into the urine is a saturable process, based on non-linear behavior of excretion data at low doses [49].

### *MBP-glucuronide*

MBP-G formed in the liver ( $V_{maxLc}$ ,  $K_{mL}$ ) may be excreted into the bile or released into systemic circulation. Biliary transfer of MBP-G is modeled as described for free MBP above. MBP-G then travels through the intestine ( $k_{gic}$ ) and is either hydrolyzed to MBP via  $\beta$ -glucuronidase ( $k_{hydrc}$ ) in the lower intestine (GC2) or passed in the feces using first order clearance rates. In the model, the hydrolysis of MBP-G is the rate limiting step for reabsorption of conjugated MBP from the bile. Distribution of MBP-G into the tissues is modeled using flow-limitation, assuming distribution with body water. Urinary excretion of MBP-G is modeled as a first order clearance rate from the plasma compartment.

### *Oxidative Metabolites of MBP.*

MBP-O formed by P450 metabolism ( $V_{maxOc}$ ,  $K_{mO}$ ) in the liver is released into the body via the venous blood. A one-compartment volume of distribution model is used to describe the combined oxidative metabolites. Distribution is assumed to be the body water compartment. Urinary excretion is modeled as a first order clearance rate from the central compartment.

### **Modifications for Gestation**

During gestation, both MBP and MBP-G are allowed to move freely between the arterial and placental plasma. Transfer of MBP between the placental plasma and the fetal plasma is described as diffusion-limited [90]. Versions of the model were tested which did or did not allow MBP-G to cross the placenta (described below). Based on the fit of the



model simulations to available data, the final model does not include placental transfer of MBP-G. Based on fetal MBP kinetic data, as well as published data on UDPGT and  $\beta$ -glucuronidase activities in fetal tissues [79, 91, 92], glucuronidation of MBP and hydrolysis of MBP-G are included in both dam and fetus. Transfer of MBP and MBP-G between the fetus and amniotic fluid are described as first-order processes. Transfer between the fetal plasma and testes tissue is described using diffusion-limited transport.

### **Parameterization in the Adult Male Rat PBPK Model**

#### *Physiological Parameters*

Physiological parameters were obtained from measured values in the literature (Table 3.1). Adult male rat, body weight, cardiac output, and fractional tissue volumes and blood flows were available from Brown et al. [93]. Fractional tissue volumes were scaled by BW and blood flows were scaled by  $BW^{0.75}$ .

#### *Kinetic Parameters*

Final values for the kinetic parameters are given in Table 3.2. The majority of the data presented in this paper was obtained from Sprague-Dawley rats. However two of the studies in the adult male rat were performed in Wistar-Furth rats [7, 78]. While some variability may exist for parameters between these strains, it was not possible to tease out differences in biochemical parameters between rat strains based on the limited data currently available. Therefore kinetic parameters were kept the same for both strains and scaled allometrically as is typical for intra- and inter-species extrapolation [94].  $PA$ ,  $V_{max}$ , and clearance constants were scaled by  $BW^{0.75}$ . With the exception of metabolism parameters,

fetal parameters were scaled in a similar manner to the maternal parameters; PA's were scaled by  $v_{fet}^{0.75}$  and then multiplied by the total number of fetuses (n=8) to obtain the value for the litter. Metabolism parameters (glucuronide conjugation and hydrolysis;  $V_{maxLf}$  and  $k_{hydrfc}$ ) were scaled by adjusting the adult value by the ratio of the fetal:adult liver weight, since the fetal liver weight is not linearly correlated with body weight. The value for the total litter was then calculated by multiplying by the number of fetuses (n=8). Whenever possible parameters were taken from published values or calculated from *in vitro* studies. Nonetheless, the lack of specific tissue and metabolism data required that many of the model parameters be fitted to *in vivo* kinetic data.

#### *Measured Parameters*

Tissue:plasma partition coefficients were obtained from radiolabeled DBP studies [95], and as such, represent total phthalate rather than a specific compound. However, since free MBP is expected to be the primary chemical form in the tissues, the total radioactivity should be a reasonable predictor of MBP partitioning. Tissue:plasma ratios obtained from early time-points (4 hrs post-dosing) of radiolabeled studies were generally similar to the values obtained from vial equilibration studies performed by Keys et al. [89] (PMR = 1.3 v. 1.2), with the exception of the partition coefficient for the slowly perfused tissue (muscle). Since their vial equilibration studies yielded questionable results for the muscle, Keys et al. [89] used their published values for MEHP as a surrogate for MBP partitioning in the slowly perfused tissue (PMS). While muscle was not measured in Williams & Blanchfield [95], another study indicated that muscle:blood ratios were similar to the other richly perfused tissues 24 hrs post-dosing [11]. Both the *in vitro* value for MEHP and the value described

above for MBP in the richly perfused tissue at 4 hr post-dosing were tried as surrogates for the PMS by running the model against iv plasma data [78] and slowly perfused tissue data (not shown) [11]. The value for PMR (1.3) provided a better visual fit to the data and was therefore used in the model.

The affinity constant ( $K_m$ ) for hydrolysis in the gut was calculated from the data of Rowland et al. [85]. Rowland and coauthors spiked 1 mL aliquots of rat stomach contents with various concentrations of DBP and measured remaining DBP after 16 hrs. The  $K_m$  for hydrolyzing enzymes ( $K_{mG} = 350$  mg/L) in the intestine was calculated by fitting a one-compartment model to the data in Berkeley Madonna (University of California, Berkeley, CA).

#### *Fitted and Calculated Parameters*

For parameters that were not measured experimentally, the values were estimated by adjusting the parameters to obtain the best visual fit of the model to time-course data. At this stage of model development and evaluation, a statistical program was not used to estimate model parameters, although such an exercise would be particularly useful in conjunction with further applications (*e.g.*, extrapolation to the human). For the duration of this paper, fitting of parameters refers to the manual process of determining one set of parameters that could consistently recapitulate a large base of diverse data. In order to minimize uncertainty in parameters, a sequential approach was followed so that the most pertinent data sets were used for each parameter. This approach to model parameterization is illustrated in Figure 3.2 and is described below.

Time-course data on plasma MBP levels after a single iv dose (8 mg/kg) of the monoester [78] were used to develop initial estimates of values for the parameters governing liver metabolism and diffusion-limitation in the richly and slowly perfused tissues (PARc and PAsC). First approximations of these parameters were based on this iv data set because it represented the simplest possible dosing scenario, and was therefore dependent upon the least number of adjustable parameters. However, as this study measured only plasma MBP concentrations, additional data were needed to refine the parameters driving elimination and enterohepatic recirculation.

Payan et al. [49] provided a more comprehensive data set, which was ideal for estimating elimination and metabolism parameters. Both iv and dermal exposure data were presented. However, as the dermal data could not be used in the model without significant changes to the structure that were not pertinent to the current work, only the iv data were used. The iv study included plasma DBP, MBP, MBP-G and total  $^{14}\text{C}$  levels after a single iv dose of either 1 or 10 mg/kg  $^{14}\text{C}$ -DBP to adult male rats. Elimination of MBP, MBP-G and total  $^{14}\text{C}$  was measured over 72 hrs in the urine. Bile cannulation or a sham operation (controls) was performed on a subset of rats dosed with 1 mg/kg  $^{14}\text{C}$ -DBP and the total amount of  $^{14}\text{C}$  excreted in the bile and/or feces and urine was measured at 30 hr. Metabolism parameters (glucuronide conjugation, oxidation), and urinary clearance rates were adjusted to fit DBP, MBP, MBP-G and total  $^{14}\text{C}$  in the plasma and urine at the 1 mg/kg dose. Based on the increased water solubility of glucuronide conjugates, it was assumed for the sake of simplicity that MBP-G would be distributed with the water ( $VD = 0.65$ ). The partition coefficient for MBP-G in the tissue (PGT) was then calculated from the VD, blood volume (VB) and combined tissue volume (VT) to be 0.3 ( $PGT = (VD-VB)/VT$ ). Bile cannula

studies were simulated by turning off transfer of DBP, MBP and MBP-G from the liver to the upper intestine and biliary transport parameters (kbg, kbm, kbd) were fit to the bile excretion data. The rates of MBP-G hydrolysis in the gut (Khydrc) and fecal excretion (kfgc, kfdc, kfmc) and movement in the gut (kgic) were then adjusted to reproduce fecal excretion and plasma data in sham-operated rats.

With the above parameters constrained, the first order rate of MBP oral absorption (kam) was determined. Kam was fit to plasma MBP data obtained from adult male rats after a single oral bolus of 34 mg/kg MBP [78]. Absorption of unchanged DBP was then calculated based on *in vitro* data using everted gut preparations [9]. The measured rate for DBP absorption was 67-fold less than MBP. Using this measured ratio and the previously determined value for MBP absorption (20 hr<sup>-1</sup>), a value of 0.3 hr<sup>-1</sup> was calculated for kad.

### **PBPK Model Validation in the Adult Male Rat**

Validation of the model structure and the final parameters was performed using separate data sets from those used for parameterization [49, 78]. No parameters were changed to improve model fits to the “validation” data.

### **Application of Adult Male Rat DBP PBPK Model to Gestation**

#### *Physiological Parameters:*

During gestation, mammary gland (VM) and fat (VF) tissue growth were described as a linear processes based on the data of [96-99], as described in Clewell et al. [99]. Placental volume (VPI) was described as the sum of the yolk sac and chorioallantoic placenta based on the model of O’Flaherty et al. [100]. Growth equations were available in the cited papers.

The total body weight of the dam was made equal to the initial body weight plus the change in volume of the uterus, fat, mammary gland, placenta, and fetus. Fetal volume ( $V_{\text{fet}}$ ) was described using the equations of O’Flaherty et al. [100]. Growth of fetal testes is proportional to the total body weight, accounting for approximately 0.1% of the total fetal volume from GD16 through the end of gestation [72, 101, 102]. Changes in amniotic fluid volume were described using a TABLE function in ACSL, with linear interpolation between data points [103, 104].

Maternal cardiac output was described as the sum of initial cardiac output [93] and the change in blood flow to the placenta, mammary and fat tissues, per the approach of O’Flaherty et al. [100]. Changes in the fractional cardiac output to the mammary gland, fat and yolk sac were assumed to be proportional to changes in tissue volumes, with the exception of the chorioallantoic placenta which increased more rapidly than the tissue volume. Chemical transport within the fetus was modeled using diffusion, rather than blood-flow limitation. Thus, no assumptions were made as to proportional blood flows to fetal tissues.

### *Kinetic Parameters*

Two kinetic parameters were adjusted before using the model in the pregnant dam based on published *in vitro* studies:  $V_{\text{maxGc}}$  and  $V_{\text{maxLc}}$ .  $V_{\text{maxGc}}$ , the maximum capacity for DBP hydrolysis in the intestine, was decreased based on *in vitro* metabolism studies. Rowland et al. [85] measured the disappearance of DBP in 1 mL aliquots of small intestine contents from adult male and female rats (33 – 40 days old). Their studies showed a sex difference in the ability to hydrolyze DBP, with the females metabolizing only 60% as much

as the males. This sex difference was accounted for in the model by reducing the unscaled value for  $V_{maxGc}$  (90 vs. 150 mg/hr/kg) for all simulations of female rats. The parameter was then scaled by  $BW^{0.75}$  to account for differences in body weight.

$V_{maxLc}$ , the maximum capacity for glucuronide conjugation in the liver, was also reduced in simulations of pregnant rats. *In vitro* studies in livers of non-pregnant female and pregnant rats showed that UDPGT activity for a variety of substrates (steroidal and non-steroidal) was decreased by approximately 50% during gestation (GD 19-20) [91, 105]. This difference in activity was included in the model by reducing the unscaled value of  $V_{maxLc}$  by 50% (150 vs. 300 mg/hr/kg) during gestation, which was scaled by  $BW^{0.75}$  to account for changes in body weight. All other maternal parameters were scaled allometrically from the adult male rat.

Parameters describing transfer between the dam and fetus, and the fetus and amniotic fluid were fit to published placenta, fetal plasma, and amniotic fluid time-course data [42]. Because no previous data were available for MBP concentrations in the placenta tissue or fetal testes, the partition coefficients ( $P_{mpl}$ ,  $P_{mft}$ ) for these tissues were fit to the data from the single dose data from the current studies (500 mg/kg).

Two possible explanations were considered for the presence of MBP-G in the fetus [42]: (1) MBP-G is not significantly transported in the placenta and fetal MBP-G must be formed in the fetus itself, or 2) maternally formed MBP-G is able to cross the placenta. Alternative versions of the model were developed and tested with the MBP-G time course data to determine which one described the data more accurately. In the first version, glucuronide conjugation and hydrolysis of MBP-G was described in the central compartment of the fetus (plasma). Fetal metabolism parameters were estimated from *in vitro* data

described below. In the second version of the model, placental transfer of MBP-G was described in the same manner as free MBP, in addition to fetal UGT and  $\beta$ -glucuronidase activity. The partition coefficient and permeability area cross product were adjusted to achieve the best visual fit to the fetal plasma MBP-G time course data.

During fetal development, rat UDPGTs are classified into two distinct classes based on the preferred substrates. Steroidal UDPGTs are characterized by a low activity in the fetal liver, with a rapid increase to adult levels after birth. Non-steroidal UDPGTs show a peak in activity on GD 19 at nearly adult levels, followed by a drop in activity at birth and a subsequent increase in adolescent rats [79, 92]. Although studies haven't been performed specifically on glucuronidation of MBP in fetal livers, studies with a similar chemical, monoethylhexyl phthalate, showed that it is metabolized by steroidal UDPGTs [106]. Therefore, the fetal UDPGT activity in the model was estimated from the ratio of measured fetal:adult UDPGT activities towards several steroidal substrates from measured *in vitro* values. The *in vitro* activity averaged for the measured steroidal substrates was 0.6, 1.3, 2.5, 11.8, and 11.4% of the adult male rat value per mg microsomal protein on GD 17, 18, 19, 20 and 21 [79, 92]. These relative activities were used to calculate the value for maximum capacity of fetal UDPGT according to Equation 1. The amount of microsomal protein in the liver of the Sprague-Dawley fetus (~7.3 mg/g liver) was obtained from Alcorn et al. [107], as it was not reported in the Lucier and McDaniel [92] or Wishart [79, 92] studies. The final values for  $V_{maxLf}$  (0.05, 0.12, 0.6, 3.0, and 4.4 mg/hr) were coded into the model using a TABLE function, which employs linear interpolation to estimate parameter values between defined points. Fetal  $\beta$ -glucuronidase activity (khydrfc) was found to be 20% of the adult value based on measured activities per mg microsomal protein *in vitro* for various substrates



[91, 108].  $K_{hydrf}$  was estimated from the adult male rat value in the same manner as  $V_{maxLf}$ .

$$V_{maxLf} = V_{maxL} \times RA_{fL} \times MPC \times LW \times \text{numfet}$$

where  $V_{maxL}$  is the maximum capacity for glucuronide in the adult male rat (after scaling for BW),  $RA_{fL}$  is the *in vitro* relative activity expressed as the ratio of fetal to maternal activity per mg microsomal protein), MPC is the ratio of microsomal protein content of the fetal to maternal liver (mg/g liver), LW is the ratio of the fetal:maternal liver weight (g), and numfet is the number of fetuses per litter.

After setting the parameters, testing the model against the data of Fennell et al. [42] and deciding on a final model for the fetal MBP-G, the gestation model was then tested with additional data sets from single dose studies on different days of gestation and alternate dose routes: current studies (GD 19, po); Saillenfait et al., 1998 (GD14, po) [43], and Kremer et al., 2005 (GD 19, iv) [48]. Saillenfait et al. [43] treated GD 14 Sprague-Dawley rats with a single oral dose of 500 or 1500 mg/kg  $^{14}\text{C}$ -DBP in mineral oil. Total radioactivity,  $^{14}\text{C}$ -MBP and  $^{14}\text{C}$ -MBP-G were measured in the maternal plasma, placenta, amniotic fluid and whole fetus at 0.5, 1, 2, 4, 6, 8, 24, and 48 hrs post-dosing. Total radioactivity in the maternal urine and feces was also measured at 24 and 48 hrs post-dosing. Kremer et al. [48] performed a time-course study in GD 19 Sprague-Dawley rats after a single iv dose of 10, 30, or 50 mg/kg MBP. Serial samples were collected from cannulated rats, and MBP and MBP-G plasma concentrations were measured at 0.08, 0.25, 0.5, 0.75, 1, 1.5, 2, 4, and 8 hrs post-dosing.

## **Extrapolation of Acute DBP Gestation PBPK Model to Multiple Day Exposures**

The ability to describe repeated dosing scenarios was tested by running the model against the repeated dosing data from the current studies without adjusting any of the model parameters determined from the single dose data. The model was also tested with the data of Calafat et al. [44], who measured free MBP in the amniotic fluid of GD 18 Sprague-Dawley rats. Dams received an oral dose of 0, 100, or 250 mg/kg DBP once daily from GD 12- 17. Amniotic fluid was pooled by litter and collected at the time of sacrifice (GD 18). Urine catch samples were also collected on GD 17 (approximately 6 hrs post-dosing). However, since the urine samples were presented as concentrations and volumes were not included, they could not be used straightforwardly in the model.

## **Sensitivity Analysis of Model Parameters**

A normalized sensitivity analysis was run on the gestation model to examine the relative influence of each of the parameters on model output. The model was run to determine the change in the average plasma MBP concentrations (24 hr AUC: area under the curve) resulting from a 1% change in the value of each kinetic parameter. In an effort to determine the effect of metabolic saturation on relative parameter importance, the sensitivity analysis was performed at two nominal doses of DBP, representing unsaturated and saturated states (10 and 500 mg-kg, respectively). The following equation shows the calculation of the sensitivity coefficient.

$$\text{Sensitivity Coefficient} = \frac{(A - B)/B}{(C - D)/D}$$

Where A is the plasma AUC with 1% increased parameter value, B is the plasma AUC at the starting parameter value, C is the parameter value after 1% increase and D is the original parameter value.

## D. RESULTS

In order to relate tissue concentration of DBP metabolites to observed effects during fetal development, the distribution of MBP and MBP-G in the pregnant rat and fetus were determined after a single dose of 500 mg/kg DBP and repeated doses of DBP at a low (50 mg/kg), medium (100 mg/kg) and high (500 mg/kg) doses. In addition to allowing direct comparison of external and tissue dose, these data also supported the development of a PBPK model that was used to evaluate the relative importance of transport and metabolic processes in the pharmacokinetic behavior of DBP across doses, providing a robust platform for future risk assessment applications.

### **Pharmacokinetic Studies *In Vivo***

The repeated dosing study was designed to reproduce the experimental conditions of the published DBP effects studies in order to gain a better understanding of internal dose associated with observed effects. In this case, maternal and fetal plasma, placenta and amniotic fluid MBP levels may be used as surrogates for fetal dose. Concentration time-course data collected in this present study appear in the Supplemental Materials (SM-3, Tables S1-S4). Some key aspects of disposition of DBP and its metabolites were noted from the initial PK analysis of the data (SM-3, Table S5).

Dose-dependent differences in AUC/D, C<sub>max</sub>, T<sub>1/2</sub>, and MRT illustrate the non-linear behavior of MBP in the repeated dosing study (SM-3), leading to some preliminary hypotheses about dose-dependent kinetics. For example, the fact that the apparent parameter differences in maternal plasma MBP do not take place at the same dose may suggest that more than one saturable process is driving MBP dose-response. Differences (~2-

fold) in  $C_{max}/D$ ,  $T_{1/2}$  and MRT between the 100 and 500 mg/kg/day groups, may be explained by saturation of DBP intestinal hydrolysis and prolonged absorption of MBP. AUC/D, on the other hand, increases from 2.6 to 4.8 between the 50 and 100 mg/kg/day groups, suggesting that a second saturable process (possibly clearance) may be involved. Nonetheless, the parameters are certainly affected by a combination of many factors and these simple PK models do not lend themselves to in-depth analysis of the processes driving dose-dependent kinetics. PBPK models that incorporate the various biochemical pathways into their description are better suited to mechanistic investigations. The model described in this paper was specifically designed for this purpose. The PBPK model also allows comparison of studies with fewer data points (*i.e.*, the single dose study, testes data), where classical PK analysis cannot be performed.

### **PBPK Model Validation in the Adult Male Rat**

The results of model development and parameterization in the adult male rat are provided in the Supplemental Materials (SM-4). The final model differed significantly in structure from the previous model of Keys et al. [89], primarily as a result of the current need to describe additional metabolites in tissues and urine and to facilitate extension to gestation. Differences between the two models are summarized in the Supplemental Materials (SM-4; Table S6). Before extending the model to gestation, the final model structure and parameter values were tested by simulating data in the male rat that were not used for parameterization. No parameters were altered to fit the validation data. Plasma and urine metabolite kinetics were well-described by the model for iv doses of 10 mg/kg  $^{14}C$ -DBP (Figure 3.3). Predicted fecal and urinary excretion were 9 and 89% of the total dose compared to the measured

values of  $10.9 \pm 1.1$  and  $85.8 \pm 2.4$  %, respectively [49]. The model also reproduced plasma MBP kinetics after a single iv dose of 20 mg/kg DBP or an oral dose of 50 or 200 mg/kg DBP [7] (Figure 3.4).

### **Application of Adult Male Rat DBP PBPK Model to Gestation**

The reduced value for  $V_{maxLc}$  based on *in vitro* data improved the fit of the model to maternal plasma simulations of the data of Fennell et al. [42] (Figure 3.5). Increasing the value for  $k_{hydrc}$  would provide similar benefits to model fit. However, literature suggests that  $\beta$ -glucuronidase activity is not increased in the maternal liver during gestation [109]. Therefore, the value for  $k_{hydrc}$  was not changed in the gestation model. The reduced capacity for diester hydrolysis in the female versus the male (90 vs. 150 mg/hr/kg) did not affect plasma appreciably at these dose levels (50 – 250 mg/kg DBP). No additional parameters were changed to obtain the fits shown in Figure 3.6A.

Fetal plasma MBP data from this same study [42] were used to fit the permeability area cross product and partition coefficient for placental-fetal transfer of MBP (PAF<sub>etc</sub>, PMF<sub>et</sub>), and first order transfer rates between the fetal plasma and amniotic fluid ( $k_{transm1c}$ ,  $k_{transm2c}$ ) (Figure 3.6B-C).

Two descriptions of fetal MBP-G kinetics were tested with the model. The first version assumed fetal MBP-G is formed and hydrolyzed in situ. Using this description, together with the literature-derived parameters for glucuronide conjugation and hydrolysis, the model successfully described the slower appearance of MBP-G in the fetal plasma as compared to MBP (Figure 3.6B). The second version of the model included the possibility of diffusion-limited transfer of MBP-G between the mother and fetus. Addition of placental

transfer did not improve the fit of the model to the published data over that which assumes all MBP-G is formed in the fetus. In fact, any attempt to include transfer to or from the fetus caused the model to over-predict MBP-G uptake or clearance in fetal plasma, respectively (not shown). Thus, the placental transfer was not included in the final version of the model. This description is supported by the ability of the model to reproduce the non-linear behavior of fetal MBP-G across doses, as well as the changes in fetal MBP-G levels across different days of fetal development. Nonetheless, additional studies (*i.e.*, *ex vivo* placenta perfusion) are needed to definitively rule out placental transport of the glucuronide.

The utility of the gestation model for extrapolation across doses, routes and gestational age was tested against a combination of data from our laboratory and published studies: single oral DBP dose on GD 19 (current study; Figure 3.7) single oral DBP dose on GD14 (Figure 3.8), and single iv MBP dose on GD 19 (Figure 3.9). Model simulations were consistent with single dose kinetics in the maternal and fetal plasma, and placenta across dose routes (iv vs. po) and dose levels (10 mg/kg MBP – 500 mg/kg DBP) without changing any of the previously determined parameters. The success in simulating the trend of the data from GD 14 to 20 supports the approach used to estimate parameters that are changing throughout gestation. In particular, maternal glucuronide levels in gestation (reduced versus predictions in male rat) and the increase in fetal glucuronidation capacity with gestational age are reproduced using the  $V_{max}$  values calculated from the *in vitro* activity measured for steroidal substrates.

The model adequately captures the kinetic behavior of MBP and MBP-G in the amniotic fluid at the lower doses (50 – 250 mg/kg) 19 – 20. However, they were not as concordant for GD 14 (not shown). The data of Saillenfait et al. [43] suggested that

clearance of both MBP and MBP-G is much faster in the GD 14 fetus. It was not possible to fit that particular data set without making large changes (>10-fold) in the fetal/amniotic fluid transport parameters. Without additional support for a time-dependent difference in amniotic fluid transfer, this change was not made to the model. In contrast, amniotic fluid MBP and MBP-G levels from the current single dose studies indicated reduced clearance at the 500 mg/kg dose on GD 19 (Figure 3.7C). The model is able to predict amniotic fluid after doses of 50 – 250 mg/kg DBP, but under-predicts amniotic fluid levels at 500 mg/kg. The reason for this non-linear relationship between the fetal plasma and amniotic fluid is not currently known.

Fetal testes parameters were fitted to the data from the current single dose study (Figure 3.7D), as no previous data were available for this tissue. Both MBP and MBP-G appear to be distributed with body water. Partition coefficients were 0.3 and permeability area cross products were 1 L/hr/kg, suggesting rapid equilibration with the plasma.

Model predictions for 24 hr urinary (77% of dose) and fecal (15% of dose) excretion in the GD 20 rat were similar to the measured values in the naïve female rat ( $77 \pm 8$  and  $7 \pm 3.5\%$  of dose, respectively) after a 100 mg/kg oral DBP dose [42]. Model predicted excretion did not differ between the non-pregnant and GD 20 rat.

### **Extrapolation of Acute DBP Gestation PBPK Model to Multiple Day Exposures**

In general, the model was able to predict maternal and fetal plasma and placenta kinetic behavior at the 50, 100, and 500 mg/kg/day doses from the current repeated dose studies (Figures 3.10-3.11) without changing any kinetic parameters. While the model falls outside of the standard deviations for some time points, it consistently captures the kinetic



behavior of MBP and MBP-G, including the slowed uptake and clearance of MBP at high doses (Figure 3.10A) and the apparent accumulation of MBP-G in the fetal plasma and amniotic fluid over time (Figure 3.11). The majority of the fetal testes samples had MBP and MBP-G concentrations that were below the method limit of quantitation, with the exception of the 0.5 - 2 hr time points in the 100 mg/kg/day group and the 0.5 - 12 hr time points in the 500 mg/kg/day groups. Model simulations based on flow-limited transfer of MBP and MBP-G between the fetal plasma and testes are shown versus the data in Figure 3.11B. The lack of analytical sensitivity precludes testing of the model at lower doses. However, the ability to predict uptake and peak concentrations within a factor of two from the mean at 100 and 500 mg/kg/day, suggests that fetal testes concentrations are linearly correlated with fetal plasma levels. Additionally, the ability of the flow-limited model to describe single and repeated dose data (Figures 3.7B and 3.11B) suggests that MBP does not accumulate in the fetal testes over time. In fact, the testes concentrations are consistently lower than fetal plasma levels ( $P_{mft} = 0.3$ ), which are linearly correlated with maternal plasma MBP concentrations.

The repeated dosing data clearly exhibits dose-dependent kinetics (Figures 3.10-3.11; Table S5). This behavior was seen consistently across data sets [43, 78]. The model successfully simulated the dose-response trend in the plasma, indicating that the model structure has components consistent with the biological determinants of metabolite kinetics. Visual examination of the model fit with varying parameter values showed that saturation of glucuronidation in the maternal liver is primarily responsible for the reduced clearance at DBP doses  $\geq 500$  mg/kg. Intestinal DBP hydrolysis is also saturated at the high dose, leading to slower absorption and a prolonged period of uptake, evidenced by the increased

T<sub>max</sub>. Reduced absorption also leads to increased pre-systemic loss through fecal excretion in the model, which has a negative effect on plasma AUC.

The model prediction of both MBP and MBP-G is within a factor of two of most of the measured amniotic fluid concentrations at the 50 and 100 mg/kg/day doses (Figure 3.11C). However, as was noted in the single dose simulations, amniotic fluid concentrations are severely under-predicted by the model at the 500 mg/kg/day dose. Measured MBP and MBP-G in the amniotic fluid of the 500 mg/kg/day dose group are approximately 5 times higher than would be expected based on the lower dose groups assuming a linear dose-response. It is possible that a dose-dependent biokinetic difference (saturable transport/hydrolysis within the amniotic fluid, transporter mediated uptake in the fetus, *etc.*) could be responsible for this observed behavior. Additional studies are needed to better define the mechanisms of chemical transport between fetus and amniotic fluid in order to better understand observed kinetics across doses.

The data of Calafat et al. [44] were simulated (not shown here) by providing a daily maternal oral dose of 100 or 250 mg/kg DBP from GD 12 – 17. The simulation was allowed to run to the reported day of sacrifice (GD 18). The model-predicted amniotic fluid MBP concentrations (1.6 and 6.5 mg/L) were within the range of the measured values for both the 100 (0.3 – 2.4 mg/L) and the 250 mg/kg/day (3.8 – 22.3 mg/L) dose groups.

### **Sensitivity Analysis**

Sensitivity analysis performed at 10 and 500 mg/kg DBP revealed a dose-dependent difference in model sensitivity to some of the chemical specific parameters (Figure 3.12). At 10 mg/kg, the plasma MBP concentrations are more sensitive to parameters governing

oxidative metabolism ( $K_{mO}$ ,  $V_{maxOc}$ ) of MBP. At the higher dose (500 mg/kg), where oxidative metabolism is saturated, the model predictions of plasma MBP levels are more sensitive to parameters describing elimination and recirculation of the glucuronide conjugate. Oral absorption also becomes important at 500 mg/kg/day;  $V_{maxGc}$  and  $k_{ad}$  are positively correlated to plasma levels and  $k_{gic}$  is negatively correlated. This suggests that upon saturation of hydrolysis ( $V_{maxGc}$ ), inefficient absorption of the diester and clearance via fecal excretion increases presystemic loss, and reduces maternal exposure. As expected, fetal plasma MBP levels are influenced by the same parameters governing maternal plasma concentrations.  $P_{mfet}$ , the parameter governing partitioning between maternal and fetal plasma, had the largest effect on fetal AUC, with a sensitivity coefficient of 0.9. The AUC for MBP in the fetal testes showed the same dependence on maternal parameters as illustrated in Figure 3.12, in addition to  $P_{mfet}$  and the testes:plasma partition coefficient ( $P_{mft}$ ). Maternal plasma levels are not affected by changes in  $P_{mfet}$  or  $P_{mft}$ .

### **Using the Multiple Exposure Model to Interpret Effects Data**

Several studies have shown that exposure to DBP during the period of sexual development in the fetal rat may lead to delayed development of the male reproductive tract. Dose response examinations showed several overt effects in the male offspring from dams exposed to >500 mg/kg/day from GD 12-21, including hypospadias (cleft penis), nipple retention, reduced anogenital distance (AGD), cryptorchidism, seminiferous tubule degeneration, testis interstitial cell proliferation, and malformed epididymis, seminal vesicle, vas deferens and ventral prostate [47]. Of these effects, only nipple retention and reduced AGD have been found lower doses (100 and 250 mg/kg/day, respectively). Delayed

preputial separation has been noted in some studies at doses > 100 mg/kg/day, but not in others at doses up to 500 mg/kg/day [34, 47]. All of these adverse effects occur in concert with decreased testes testosterone concentration, which may provide a more sensitive marker for disruption of androgen-dependent development [33, 46, 83].

Although these effects have been well-studied with regard to external DBP dose, there is currently no information on the internal (fetal) dose expected from these exposures. In order to illustrate how this PBPK model may be used to relate external DBP to internal MBP dose in multiple day studies, the model was run with the repeated exposure parameters at 16 different dose levels, ranging from 1 to 550 mg/kg/day. The AUC for the last day of dosing was then used to calculate the average concentration in the maternal and fetal plasma, and fetal testes (daily AUC/24 hrs). The predicted dose response is illustrated in Figure 3.13, together with reported lowest observed adverse effect levels (LOAELs) for several landmarks of male sexual development. Model predictions suggest that the average daily MBP concentration in the fetal rat testes must reach levels of approximately 1, 2 and 18 mg/L in order to cause noticeable changes in testosterone production, nipple retention or more overt effects (*i.e.*, reduced AGD), respectively. Using the model, these testes concentrations may also be correlated to fetal and maternal plasma, which are often used as surrogates for fetal dose in the human. Maternal plasma MBP concentrations associated with reduced testosterone, nipple retention and reproductive tract malformations in the rat fetus are 5, 11, and 60 mg/L.

## E. DISCUSSION

Few data are available in which controlled doses of phthalates have been administered to human subjects [110]. In order to interpret such data and develop realistic estimates of fetus and/or fetal testes exposure, models such as the one provided here must be able to relate external dose to plasma, tissue and urine kinetics. PBPK models use animal and *in vitro* data to build a platform that can be used to predict human kinetics by accounting for differences in physiology and, where necessary, biochemistry (*i.e.*, enzyme activities). In order to maximize the utility of this model in future applications to humans, this model included descriptions of MBP, MBP-G, and oxidative metabolites in the plasma and tissues of interest as well as the urine, feces and bile. Detailed radiolabeled studies allowed parameterization to be performed against specific data. The resulting model described metabolite distribution and excretion in adult male rats over doses spanning more than three orders of magnitude (1 mg/kg to > 500 mg/kg), regardless of the form of the chemical used (MBP, DBP) or the route of exposure (iv, po).

Successful extrapolation of the male rat model to describe kinetics in the pregnant rat suggests that - with the exception of glucuronidation and intestinal hydrolysis - the metabolic and chemical transport processes do not change significantly as a result of pregnancy. Reduced hydrolysis of the diester in the intestine of the female rat had little effect on maternal kinetics other than the initial uptake at the highest dose (500 mg/kg). The reduced capacity for glucuronide conjugation does affect plasma kinetics, causing a notable increase in free MBP residence time in both maternal and fetal plasma. This dose-dependent behavior could have important implications for perinatal toxicity. As glucuronidation plays a major role in the elimination of many xenobiotics, a decrease in capacity during gestation could

result in increased fetal exposure to a variety of chemicals. This finding emphasizes that understanding the determinants of chemical kinetics in the adult male will not be sufficient for assessing exposure to the pregnant female or fetus.

The comprehensive nature of this model allows a thorough investigation into the transport and metabolic processes that are responsible for the overall observed kinetics. Because all of the major metabolic (hydrolysis, oxidation, glucuronidation) and transport (biliary excretion, tissue partitioning, urinary and fecal excretion) processes are included in the model, it is possible to examine the effect of these individual processes on chemical behavior. This was accomplished both through a quantitative sensitivity analysis and through manual manipulation of model parameters coupled with observation of the effect on fits to the data. Model analysis indicates that saturation of diester hydrolysis is responsible for the prolonged absorption observed at doses  $> 100$  mg/kg, and reduced phthalate exposure due to the poor absorption and subsequent presystemic loss of DBP. In fact, saturation of diester hydrolysis may mitigate the effect of reduced clearance on the plasma AUC to some extent. Saturation of glucuronidation appears to be responsible for reduced clearance of MBP the higher doses (100 -500 mg DBP/kg/day). This conclusion is particularly interesting in light of the available toxicity data, as many of the more serious developmental effects have been seen only at doses at or above 500 mg/kg. Reduced anogenital distance, for example, which is a source of concern due to its indication of impaired sexual development in both the rat and human [67] is only seen at doses  $>250$  mg/kg/day. This effect may in fact be a result of reduced clearance of MBP due to saturation of glucuronidation. Saturation of the oxidation pathway and renal uptake of MBP occur at much lower doses than saturation of

glucuronide conjugation (< 50 mg/kg). Thus, these pathways do not appear to be responsible for slowed clearance at high doses.

In the attempt to describe plasma kinetics at low doses (1 mg/kg DBP), it became clear that the oxidative metabolites are more important to overall kinetics than has previously been assumed based on high dose toxicity studies. In fact, these metabolites are predicted to make up approximately 40% of the excreted metabolites at the 1 mg/kg dose. The oxidative metabolites of monophthalates may still be active and could play a significant role in human toxicity, as they have been shown to constitute the largest fraction of the urinary metabolites after human exposure to DEHP, a phthalic acid diester with a similar toxicological profile to DBP [81]. While the current model attempts to account for these metabolites by including a generic compartment and urinary clearance of “other” metabolites, the description could only be tested by comparing MBP, MBP-G, and total radioactivity measurements simultaneously. The lack of data for validation of oxidative metabolites remains an important gap in the pool of information available for phthalate risk assessment efforts.

In addition to saturable metabolism and renal uptake, enterohepatic recirculation has a significant effect on the retention of MBP and MBP-G in the plasma. Greater than 40% of a given dose is transferred into the bile, and nearly 90% of those bile metabolites are then reabsorbed in the intestine and re-released into circulation. When re-uptake is absent in the model, clearance of both MBP and MBP-G from the plasma is increased and the free MBP and oxidative metabolites make up only a small fraction of urinary excretion. Thus, extensive enterohepatic recirculation in the rat increases internal exposure to the active metabolite (free MBP).

Insights provided by the model into the processes driving MBP kinetics (enterohepatic recirculation, glucuronidation) are not only helpful to understanding DBP dose-response, but may also help to improve accuracy of model extrapolation to other chemicals and other species through the design of targeted experiments. The successful description of UDPGT-dependent MBP kinetics across life-stages based on *in vitro* data bodes well for further applications of this model. A similar approach may be useful with other phthalates (*i.e.*, DEHP) in rats and, more importantly, in other species. *In vitro* metabolism studies require less time, money, and animals than traditional *in vivo* studies and are much more feasible in the human than *in vivo* dosing.

Inclusion of several possible biomarkers (plasma, urine, amniotic fluid MBP) in the model allows evaluation of their usefulness as fetal dose surrogates. Failure of the model to describe amniotic fluid metabolites across doses suggests that more complex processes are involved in uptake and clearance of MBP and MBP-G in the amniotic fluid and fetus than simple passive diffusion. In fact, the tendency to concentrate MBP-G speaks to potentially limited clearance. A better understanding of amniotic transport and/or metabolism is needed before it could be used with confidence as a surrogate for fetal dose. With the current model, however, it is possible to determine fetal MBP exposure from a variety of surrogates, including external dose, and maternal plasma and urine. Thus, this model provides a means of estimating fetal dose from easily obtained biological samples.



## **F. CONCLUSION**

This paper illustrates the extension of a model for DBP in the adult male rat to describe gestation through the inclusion of maternal and fetal growth and a simple description of placental transport, made possible by newly generated data. By incorporating important biochemical processes, it was possible to test how the changes in metabolism during pregnancy may affect fetal exposure. The use of realistic, data-validated kinetic and physiological parameters also reduces uncertainty in use of the model to predict target tissue exposure across doses, routes, developmental stages and even species. This validated model can now serve as a basis for extrapolation across species, life-stages, and exposure scenarios (acute v. repeated dosing) to provide quantitative measures of target tissue dosimetry in the population of interest.

## **G. ADDITIONAL RESEARCH**

### **Extrapolation of the Published PBPK Model to Describe DEHP Kinetics**

#### *Changes to the Model Structure*

The initial structure was taken from published models for di-n-butyl phthalate (DBP) in the non-pregnant, pregnant and fetal rat. In applying this model to DEHP, very few changes had to be made to the original model structure. In particular, a slightly more detailed kinetic description of the combined oxidative metabolism of the monoester was required to fit the metabolite excretion data for DEHP. The revised model structure used to describe disposition of DEHP in the pregnant and fetal rat is shown in Figure 3.14.

In the original DBP model, a one-compartment volume of distribution model was used to describe the combined oxidative metabolites. This description was sufficient for DBP, due the fact that the majority of the dose exists as free MBP or MBP-G in the rat. However, in the case of DEHP, the metabolite profile is substantially different. The majority of the dose (>90%) undergoes oxidation, free MEHP is only a minor metabolite, and the glucuronide conjugate does not exist at detectable levels. The description of the oxidative metabolites was expanded to better describe these kinetic data.

Oxidative metabolism is described in the liver using a saturable Michealis-Menten equation. The oxidized monoesters are then excreted into the bile or released into systemic circulation. Biliary metabolites are released into the upper intestine (GC1), where they may be reabsorbed (described as a first order rate) or passed in the feces (described as a first order clearance rate). A three compartment model was used to describe the oxidative metabolites in the blood, liver and other tissues. Distribution of MEHP-O into the tissues was modeled using flow-limitation, assuming distribution with body water. Urinary excretion was modeled

using first order clearance from the plasma compartment. Because the oxidative metabolites play only a small role in DBP kinetics, these changes to the model structure had little effect on DBP model fits.

#### *DEHP Model Parameterization*

The physiological parameters were not altered for the DEHP model. However, it was necessary to adjust some of the chemical-specific parameters to fit the available kinetic data for DEHP. In fact, when the DBP model was run “as is” against the MEHP iv and DEHP po data, the model over-predicted serum MEHP levels by an order of magnitude (not shown). Several observations can be made about the kinetic differences in the two phthalates based on available *in vitro* and *in vivo* data. (1) DEHP is not hydrolyzed as efficiently as DBP in the gut [85], which leads to a greater loss of unmetabolized diester in the feces and measurable concentrations of the diester in the blood. (2) Both DEHP and MEHP are more poorly absorbed from the gut than DBP and MBP. (3) The high lipophilicity of DEHP and the reduced hydrolysis in the blood (compared to DBP) results in reduced clearance of the diester from blood after iv dosing. (4) Metabolism of the monoester is also quite different for the two phthalates. A large portion of MBP is removed via glucuronidation; oxidation is important at low doses only [49]. In contrast, oxidation, not glucuronidation, is the dominant metabolic pathway for MEHP. Oxidative metabolites make up >90% of the total urinary metabolites, while glucuronide conjugates of MEHP have not been detected in the urine or plasma of rats after DEHP dosing [111].

Based on these observations, UGT activity ( $V_{maxLc}$ ) was turned off in the DEHP model. The  $V_{max}$  for oxidative metabolism ( $V_{maxOc} = 28$  mg/hr-kg BW) was adjusted by

visually fitting the model simulations to MEHP *iv* data in the adult male rat [53]. The rate of oral absorption of MEHP ( $k_{am} = 0.4 \text{ hr}^{-1}$ ) was adjusted based on the fit of the model to MEHP oral gavage studies [54]. The maximum capacity for hydrolysis in the gut ( $V_{maxGc} = 80 \text{ mg/hr-kg BW}$ ), oral absorption of DEHP ( $k_{ad} = 0.015 \text{ hr}^{-1}$ ), and intestinal clearance of DEHP ( $k_{gic1} = 0.1 \text{ L/hr}$ ) and the other metabolites ( $k_{gic2} = 0.05 \text{ L/hr}$ ), and the urinary excretion rate of MEHP ( $V_{mxUc} = 1 \text{ mg/hr-kg BW}$ ,  $K_{mU} = 450 \text{ mg/L}$ ) were fit to DEHP oral gavage data (blood, feces, urine) in the non-pregnant female rat [45]. All other parameters were kept the same as DBP.

Like DBP, only one kinetic parameter was adjusted before using the adult rat model for the pregnant dam:  $V_{maxOc}$ . Because glucuronidation is set to zero in the DEHP model, it was not necessary to adjust that parameter for the reduced capacity for glucuronide conjugation during gestation [91, 105]. However, similar studies with hepatic microsomes obtained from pregnant and non-pregnant rats showed approximately 40% reduction in the capacity of oxidative metabolism in the pregnant rat liver regardless of the substrate used [112]. Therefore, the maximum capacity for oxidative metabolism of MEHP ( $V_{maxOc}$ ) was reduced by 40% when applied to the pregnant rat. All other maternal parameters were scaled allometrically from the adult male rat. Since MEHP is not significantly glucuronidated and oxidative metabolism is negligible in the rat fetus, both  $V_{maxGc_f}$  and  $V_{maxOc_f}$  were set to zero. Transfer of MEHP between the maternal and fetal blood, and between the fetal blood and amniotic fluid were assumed to be the same as MBP.

### *DEHP Model Validation*

There is a much larger database of kinetic studies with DEHP than DBP in the adult male rat, primarily due to the fact that DEHP has long been investigated for its ability to induce liver tumors through peroxisome proliferation. In order to test adequacy of the revised model structure for predictive use, the model was tested against several data sets from the literature. Final model simulations are shown versus various data sets after iv and oral doses of MEHP or DEHP in the non-pregnant rat in Figures 3.15-3.17. Like DBP, the DEHP oral dosing data displays non-linear kinetics, with reduced uptake of the 400 mg/kg dose.

The model is able to reproduce the oral dose data by incorporating saturable hydrolysis of the diester in the gut, and the lower absorption rate of the diester versus the monoester seen *in vitro* [9]. The model appears to under-predict clearance of MEHP from the blood after iv dosing of DEHP in early time points (Figure 3.17A), despite its ability to predict peak concentrations and later time-points. It is likely that this rapid disappearance from the blood represents a fast redistribution of the diester into the tissues, followed by a slow release, which would account for the slow clearance at later time-points. Including a description of DEHP binding in the tissues would improve the fit to the iv blood data. However, since there is no tissue data available with which to validate the assumption of binding or the chosen parameters, this additional complexity was not added to the model. Nonetheless, the model is able to reproduce both peak concentrations and the delayed clearance from the blood at later time points. More importantly, the model adequately predicts the dose-dependent kinetics from oral dosing, which is the primary route of exposure in the human.

Studies of DEHP kinetics during gestation are less abundant than those in the male rat. In fact, to date only one published study provides information on DEHP metabolites in the pregnant rat [45]. This study provides time-course information on DEHP and MEHP in the maternal blood, feces and urine. Data were also collected for a single time-point (2 hr post-dosing) in the fetal blood, carcass and testes (J. Filser, personal communication). The fetal data allows testing of the assumption that placental MEHP transfer would be similar to MBP. Model predictions are shown with data from the pregnant and fetal rat in Figure 3.18.

#### *Comparing Internal Dose Associated with DEHP and DBP Disruption of Sexual Development in Rats*

Because there are significant differences in DEHP and DBP kinetics, external dose is clearly a poor indicator of relative potency among the phthalates. The differences in metabolism and clearance can affect fetal dose in ways that cannot be accounted for with a qualitative approach. With the use of quantitative biological models, however, it is possible to predict the levels of the active metabolites in the tissues of interest, enabling the determination of more relevant dose metrics than external dose.

The DEHP and DBP models were run using the dosing scenarios that correspond to published inhibition data in order to predict fetal serum MEHP and MBP concentrations associated with testosterone reduction. The external dose required to cause 50% inhibition ( $ED_{50}$ ) of fetal testosterone was estimated from published dose-response studies to be 35 and 63 mg/kg/day for DBP and DEHP, respectively (Chapter 2) [46, 72, 113]. Based only on the administered dose, DBP appears to be more potent than DEHP with regard to testosterone inhibition.

These phthalate PBPK models were used to convert the ED<sub>50s</sub> to internal concentrations (IC<sub>50</sub>) by determining the area under the curve (AUC) for the monophthalates in the fetal blood (μmol-hr/kg BW) and dividing by time. When the phthalate models were run at these doses for the amount of time used in the studies (4 – 7 days), the IC<sub>50s</sub> for MEHP and MBP were very similar, despite the difference in the external dose. Calculated IC<sub>50</sub> values were 1.9 and 1.4 μM for MBP and MEHP, respectively, indicating that the active metabolites of DBP and DEHP have a similar potency for testosterone inhibition.

**Table 3.1. Physiological Parameters**

Physiological Parameter			Source
	Adult Male	Gestation	
<b>Tissue Volumes (%BW)</b>			
Body Weight $BW$ (kg)	0.280	0.280 - 0.361	[100]
Slowly Perfused $VSc$ (%BW <sub>1</sub> )	60.4	57.4 – 52.7	[93]
Richly Perfused $VRc$ (%BW <sub>1</sub> )	4	2.9 – 2.4	[93]
Fat $VFc$ (%BW)	7	10.0 - 11.0	[93, 98]
Liver $VLc$ (%BW <sub>1</sub> )	3.4	3.4	[93]
GI Tract $VGlc$ (%BW)	3.6	3.60	[93]
Upper GI Contents $VG1c$ (%BW)	3.9	3.9	[114]
Lower GI Contents $VG2c$ (%BW)	3.2	3.2	[114]
Mammary Gland $VMc$ (%BW)	---	1.0 - 5.5	[97]
Plasma $VPlasc$ (%BW)	4.7	4.7	[93, 115]
Placenta $VPlc$ (%BW)	---	0.0 -2.57	[100]
Fetal Volume $Vfet$ (kg)	---	0.0 – 0.0045	[100] (individual fetus)
Volume of Distribution in Fetus $VDc_f$ (%Vfet)	---	0.65	[93]
Fetal testes volume (%Vfet)	---	0.1	[72, 101, 102]
Amniotic Fluid $VAFc$ (mL/fetus)	---	0 – 0.56	[103, 104]
Placenta $VPlc$ (%BW)	---	0.0 -2.57	[100]
Body $VBc$ (%BW)	85-89	85-89	<i>Sum of fat, rich, slow perfused ± GI</i>
<b>Blood Flows (%QC)</b>			
Cardiac Output $QCc$ (L/hr/kg)	14	14	[100, 116]
Slowly Perfused $QSc$ (%QC)	17.0	17 – 15.9	[93]
Richly Perfused $QRc$ (%QC)	56	55.8 – 53.5	[93]
Fat $QFc$ (%QC)	7	7 - 8.1	[93]
Liver $QLc$ (%QC)	4	4	[93]
GI $QGc$ (%QC)	16	16	[93]
Mammary $QMc$ (%QC)	---	0.2 - 1.2	[96]
Placenta $QPlc$ (%QC)	---	0.0 - 12.3	[100]



**Table 3.2. Kinetic Parameters**

<b>Parameter</b>	<b>Value</b>	<b>Source</b>
<b>Partition Coefficients (unitless)</b>		
DBP Liver:Plasma <i>PL</i>	21.8	[89]; personal communication
DBP Body (Tissues):Plasma <i>PT</i>	1.0	[89]Keys et al., 2000;
MBP Gut Tissue:Plasma <i>PMG</i>	1.0	[95]Williams & Blanchfield, 1975
MBP Liver:Plasma <i>PML</i>	1.3	[95]Williams & Blanchfield, 1975
MBP Richly Perfused Tissues:Plasma <i>PMR</i>	1.3	same as liver
MBP Slowly Perfused Tissues:Plasma <i>PMS</i>	1.2	[11, 95]
MBP Maternal Placenta Tissue:Plasma <i>PMPi</i>	0.3	Fitted - Current Data
MBP Fetus:Maternal Plasma <i>PMFet</i>	0.7	Fitted-[42]
MBP Testes:Fetal Central Compartment <i>PMFT</i>	0.3	Fitted - Current Data
MBP-G Liver:Plasma <i>PGL</i>	0.3	Vol of distribution = 0.65
MBP-G Body Tissue:Plasma <i>PGT</i>	0.3	Vol of distribution = 0.65
MBP-G Placenta Tissue:Plasma <i>PGPi</i>	0.3	Vol of distribution = 0.65
MBP-G Fetus:Maternal Plasma <i>PGFet</i>	---	Fitted - [42]
MBP-G Testes:Fetal Central Compartment <i>PGFT</i>	0.3	same as maternal tissue:plasma
<b>Max Capacity, Vmaxc (mg/hr/kg)</b>		
Hydrolysis of DBP in GI Lumen <i>VmaxGc</i>	150 (♂), 90 (♀)	Fitted (♂) - [78], (♀)- [9]
Glucuronidation of MBP in Liver <i>VmaxLc</i>	300 (N); 150 (P)	*Fitted (N)- [49] (P)-[92]
Glucuronidation of MBP in Fetal Liver (/fetus) <i>VmaxLfc</i>	0 - 44	[79, 92]
Oxidation of MBP in Maternal Liver <i>VmaxOc</i>	1	Fitted -[49]
Uptake of MBP in Urine <i>VmaxUc</i>	5	Fitted - [49]
<b>Affinity Constants, Km (mg/L)</b>		
Hydrolysis of DBP in GI Lumen <i>KmG</i>	350	[85]
Glucuronidation of MBP in Liver <i>KmL</i>	300	Fitted - [49]
Glucuronidation of MBP in Fetal Liver <i>KmLF</i>	300	Same as adult value
Oxidation of MBP in Maternal Liver <i>KmO</i>	5	Fitted - [49]
Uptake of MBP into Urine <i>KmU</i>	45	Fitted - [49]
<b>Permeability Area Cross Products, (L/hr/kg)</b>		
MBP Liver <i>PALc</i>	1	Fitted - [78]
MBP Richly Perfused Tissue <i>PARc</i>	1	Fitted - [78]
MBP Slowly Perfused Tissue <i>PASc</i>	0.15	Fitted - [78]
MBP Fetus:Maternal Plasma (/fetus) <i>PAFetc</i>	0.05	Fitted -[42]
MBP Testes:Fetal Central Compartment (/fetus) <i>PAFTc</i>	1	Fitted – Current Data
MBP-G Maternal Tissues (/fetus) ( <i>PAGSc, PAGLc, PAGPlc</i> )	1	Fitted – [42]
MBP-G Fetus:Maternal Plasma (/fetus) <i>PAGFTc</i>	---	Fitted – [42]
MBP-G Testes:Fetal Central Compartment (/fetus) <i>PAGFTc</i>	1	Fitted – Current Data

<b>Metabolism Rates (/hr)</b>		
Hydrolysis of DBP in Blood <i>kbc</i>	16	Fitted - [49]
Hydrolysis of DBP in Liver <i>kc</i>	16	Fitted - [49]
<b>Fetal-Amniotic Fluid Transport (L/hr/kg/fetus)</b>		
MBP Transfer from Fetus (Central Compartment) to Amniotic Fluid <i>KtransM1c</i>	0.005	Fitted - [42]
MBP Transfer from Amniotic Fluid to Fetus (Central Compartment) <i>KtransM2c</i>	0.01	Fitted - [42]
MBP-G Transfer from Fetus (Central Compartment) to Amniotic Fluid <i>KtransGc</i>	0.003	Fitted - [42]
Hydrolysis of MBP-G in Amniotic Fluid <i>KhydrAc</i>	0.0025	Fitted - [42]
<b>Clearance Rates (L/hr/kg)</b>		
MBP-G Urinary Excretion <i>ClGc</i>	0.35	Fitted - [49]
MBP-O Urinary Excretion <i>ClOc</i>	0.1	Fitted - [49]
DBP, MBP, MBP-G Fecal Excretion <i>kfc</i>	0.012	Fitted - [49]
<b>Enterohepatic Recirculation</b>		
Liver DBP Passed to Bile <i>kbdc</i> (L/hr/kg)	0.1	Fitted - [49]
Liver MBP Passed to Bile <i>kbmc</i> (L/hr/kg)	0.1	Fitted - [49]
Liver MBP-G Passed to Bile <i>kbgc</i> (L/hr/kg)	0.76	Fitted - [49]
Movement in GI Contents <i>kgic</i> (/hr)	0.01	Fitted - [49, 78]
Hydrolysis of MBP-G in Maternal GI <i>khydrC</i> (L/hr/kg)	0.3	Fitted - [9, 49]
Hydrolysis of MBP-G in Fetus <i>khydrfc</i> (L/hr/kg)	0.13	[91, 108]
<b>Oral Uptake (/hr)</b>		
DBP Absorption in Stomach and Intestine <i>kad</i>	0.75	Calculated: kam and White et al. [9]
MBP Absorption in Stomach and Intestine <i>kam</i>	20	Fitted - [78]

\* N = Non-pregnant rat, P = Pregnant rat

**Figure 3.1. Model structure for DBP kinetics in the pregnant rat.**

Adult male rat model is identical with the exception of the placenta/fetus compartments. Dashed arrows indicate first order processes and clearance rates. Bold dashed arrows represent saturable processes. Solid arrows represent blood flows to the tissue compartments. The solid arrows represent flow-limited (DBP) and diffusion-limited (MBP, MBP-G) transport into the tissues.

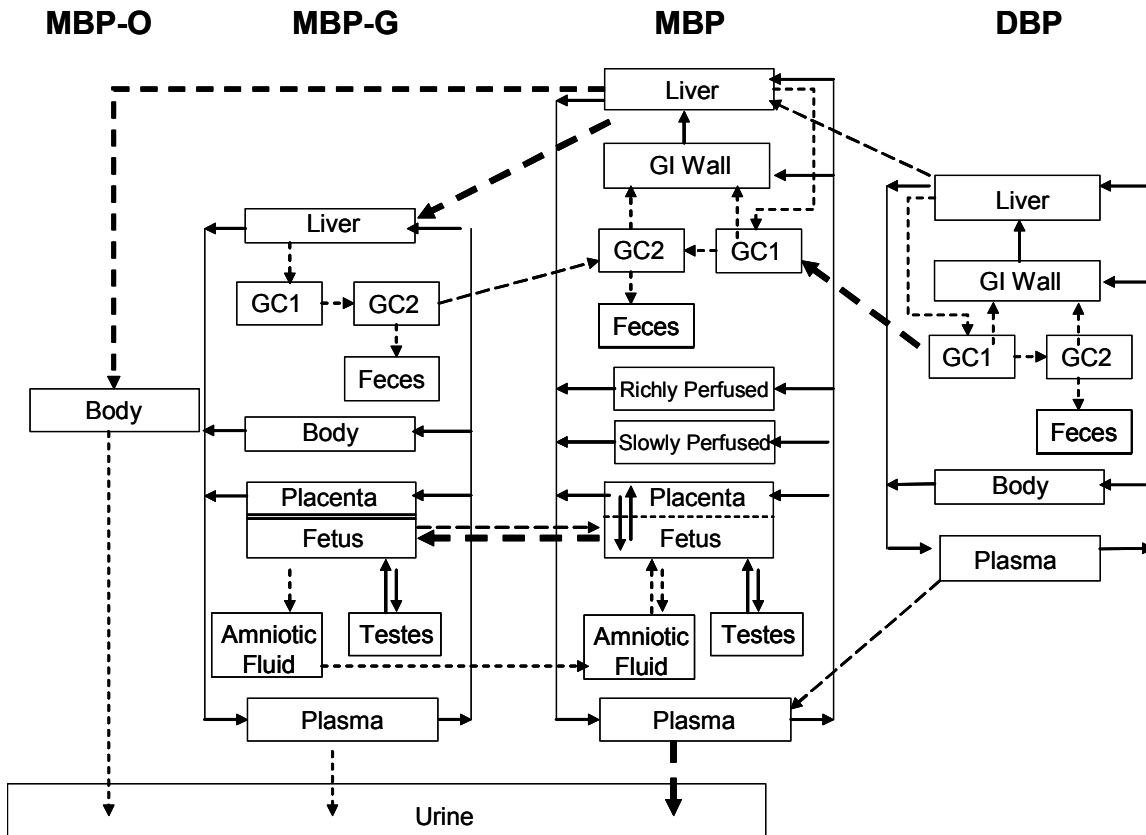


**Figure 3.2. Model Development and Validation for the Adult Male, Pregnant and Fetal Rat**

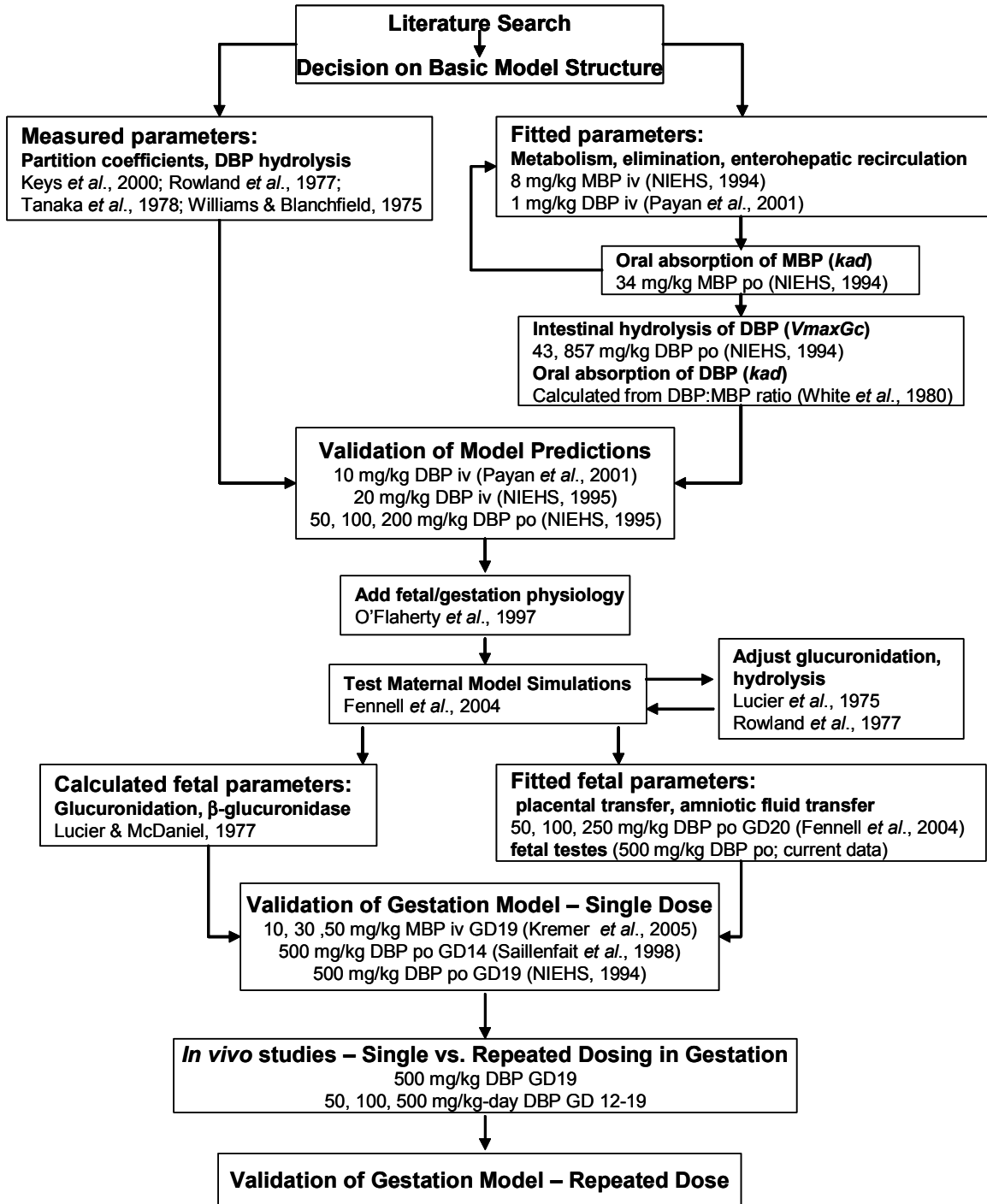
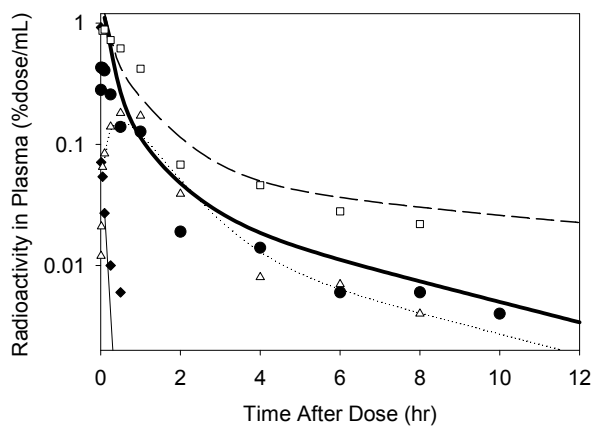
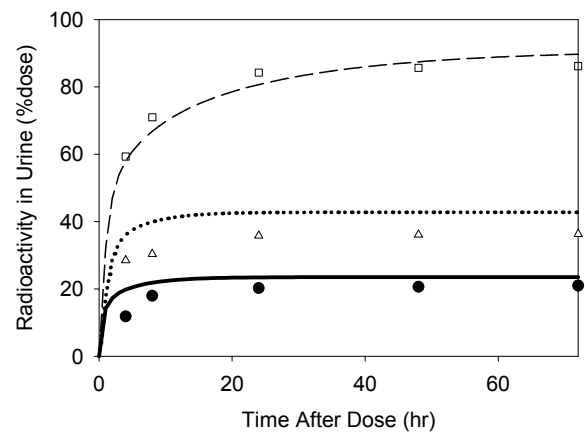


**Figure 3.3. Total radioactivity, DBP and metabolites in (A) plasma and (B) urine of the male rat after a 10 mg/kg iv dose of  $^{14}\text{C}$ -DBP.**

Lines represent model simulation, points represent mean measured values [49]. Figure illustrates total radioactivity (dashed line,  $\square$ ), unchanged DBP (thin solid line,  $\blacklozenge$ ), MBP (bold line,  $\bullet$ ), and MBP-G (dotted line,  $\Delta$ ). For visual clarity, only the means of the data are shown.



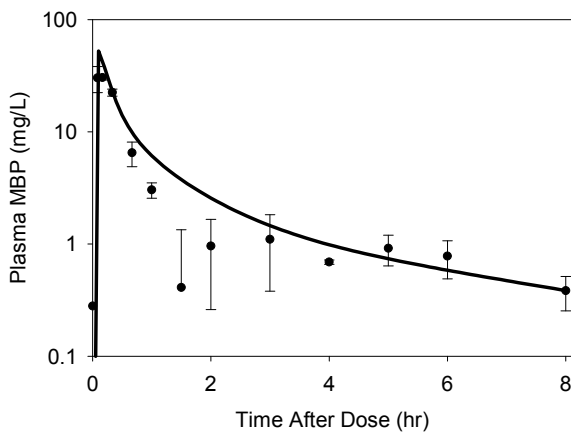
A



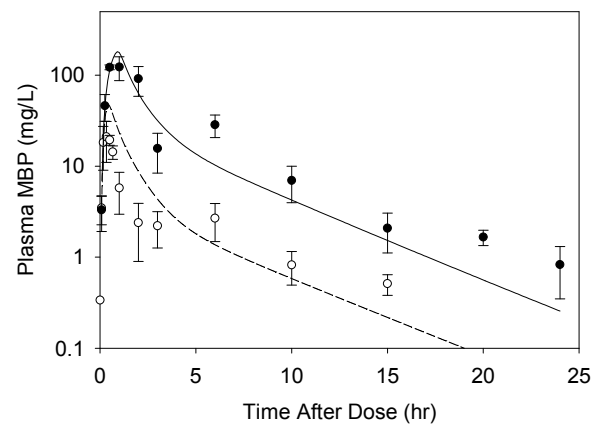
B

**Figure 3.4. Free MBP in the blood of the adult male rat after exposure to DBP via (A) intravenous injection or (B) oral gavage.**

Lines indicate model predictions, points and cross-bars represent the mean  $\pm$  SD of the measured data (n=3) [7]. Where available, standard deviations of data are indicated by cross bars. (A) Plasma MBP after 20 mg/kg DBP iv dose. (B) Plasma MBP after a single oral gavage of 50 (dashed line) or 200 (solid line) mg/kg DBP.



A



B

**Figure 3.5. Maternal Plasma (A) free MBP and (B) MBP-G after a single 100mg/kg DBP oral dose on GD 20.**

Solid line indicates model prediction using lower value for  $V_{maxLc}$  based on *in vitro* UGT activity data from pregnant rats. Dashed line illustrates model prediction using the same  $V_{maxLc}$  value as the male rat. Circles and cross-bars represent the mean  $\pm$  SD of measured values [42].

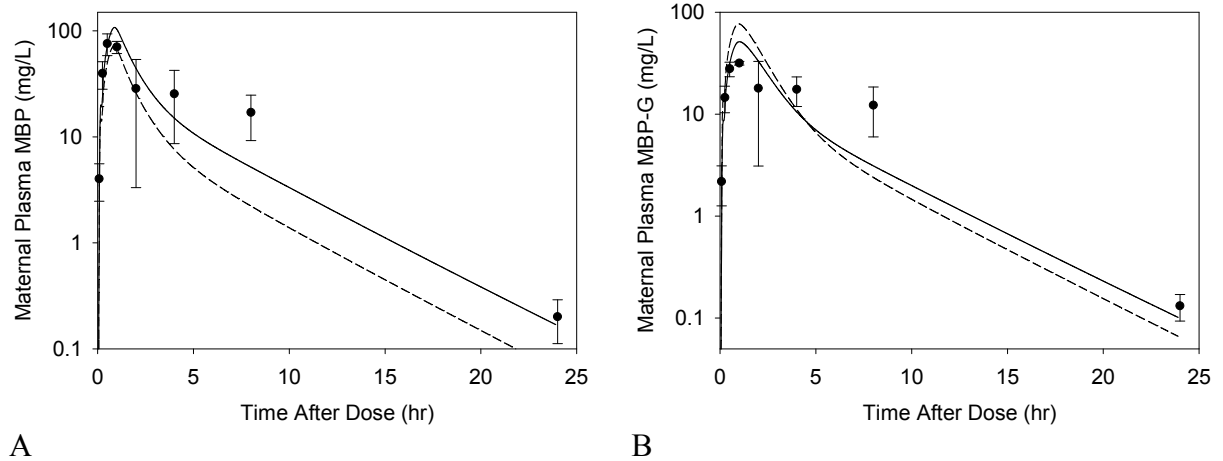


**Figure 3.6. MBP (left) and MBP-G (right) in (A) maternal plasma (B) fetal plasma, and (C) amniotic fluid after a single dose of 50, 100, or 250 mg/kg DBP on GD 20.**

Crossbars show the standard deviation of the measured data of Fennell et al. [42]. Lines indicate model predictions at 50 (small dashed), 100 (large dashed) and 250 (solid) mg/kg DBP.

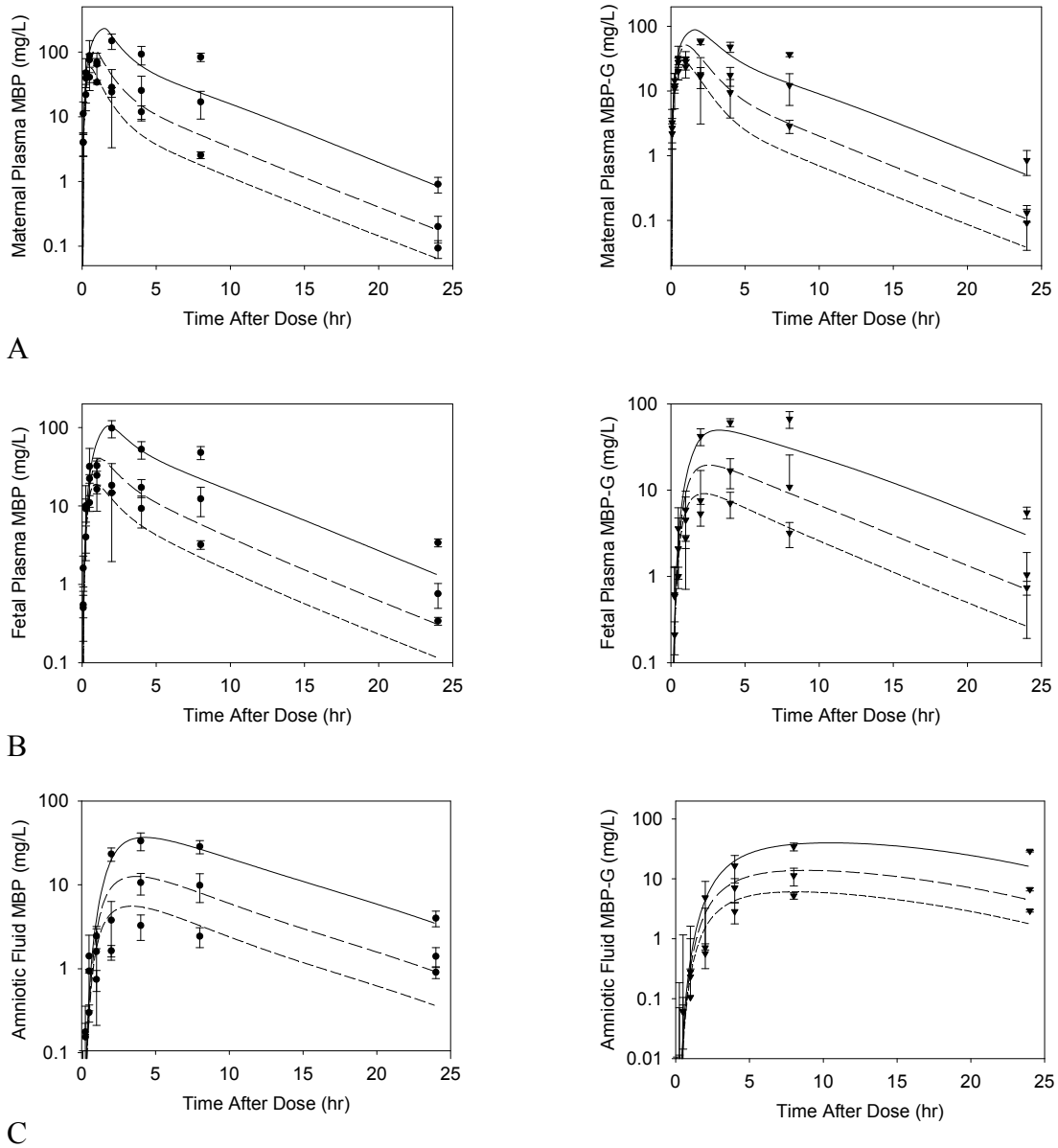




**Figure 3.7. Free MBP and MBP-G in the (A) maternal and (B) fetal plasma (C) amniotic fluid, and (D) fetal testes after a single oral dose of 500 mg/kg DBP on GD19.** Solid lines and circles represent free MBP. Dashed lines and triangles represent MBP-G. Cross bars represent the mean  $\pm$  SD from the current studies. Fetal plasma and amniotic fluid were pooled by litter.

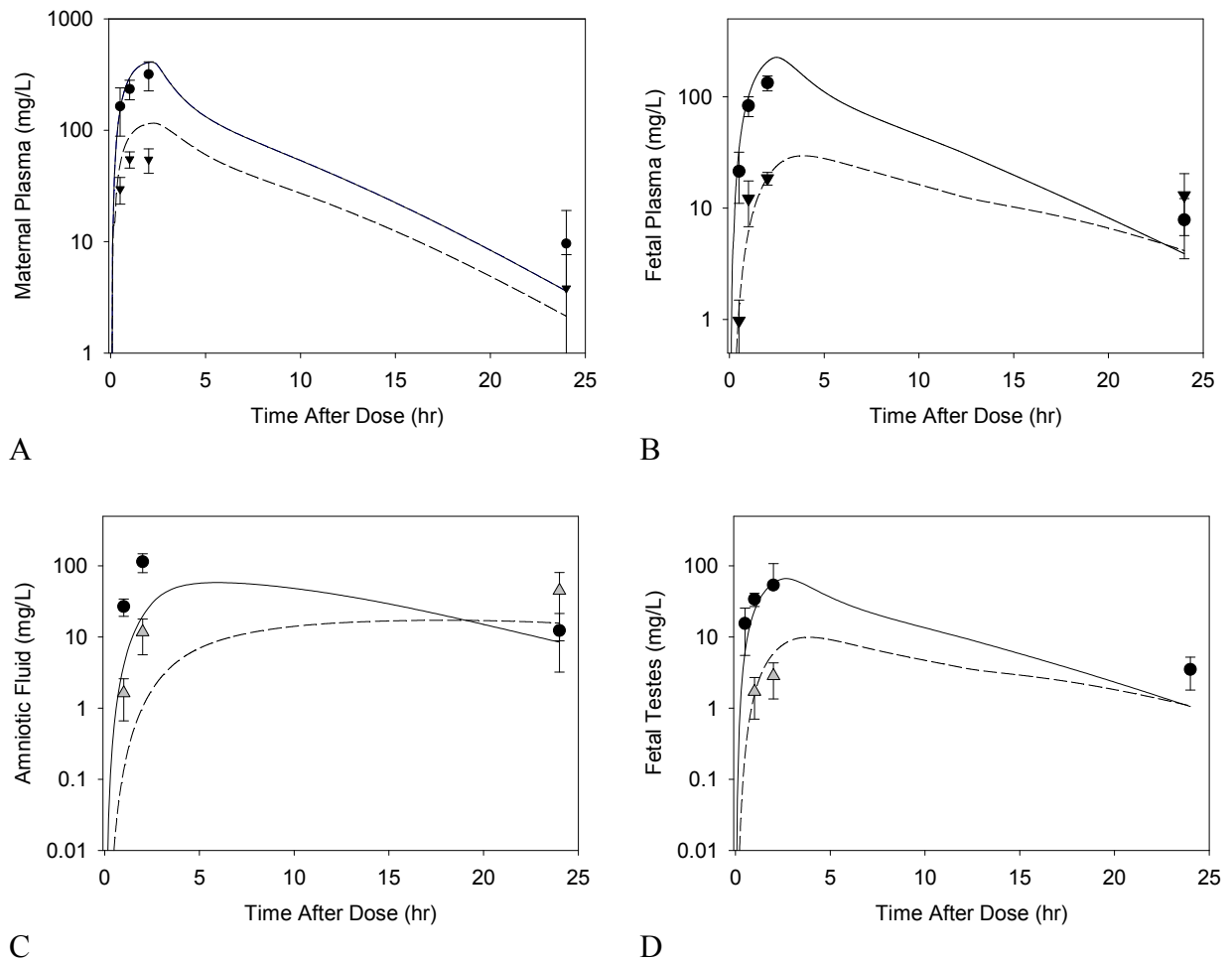


**Figure 3.8. Model predicted (A) MBP and (B) MBP-G in maternal blood, whole fetus, and placenta on GD 14.**

Data is shown for the mean MBP and MBP-G concentrations in maternal blood (x, solid line), whole fetus ( $\square$ , dashed line), or placenta ( $\bullet$ , dotted line) after a single oral dose of 500 mg/kg  $^{14}\text{C}$ -DBP to the dam[43]. Only the mean values could be determined from the published graphs and are indicated by points. Lines represent model predictions.

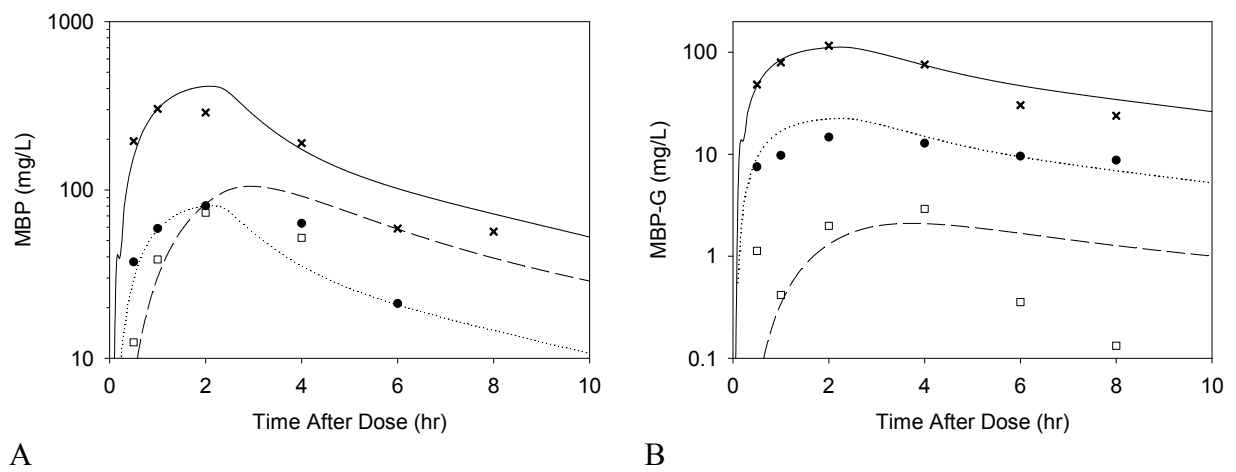


**Figure 3.9. Maternal plasma concentrations of (A) free MBP and (B) MBP-G after a single iv dose of MBP on GD 19.**

Solid lines indicate model predictions. Mean MBP and MBP-G concentrations were measured after single iv dose of 10 ( $\blacktriangle$ ), 30 ( $\bullet$ ), or 50 ( $\blacksquare$ ) mg/kg MBP [48]. For visual clarity, only the means of the data are shown.

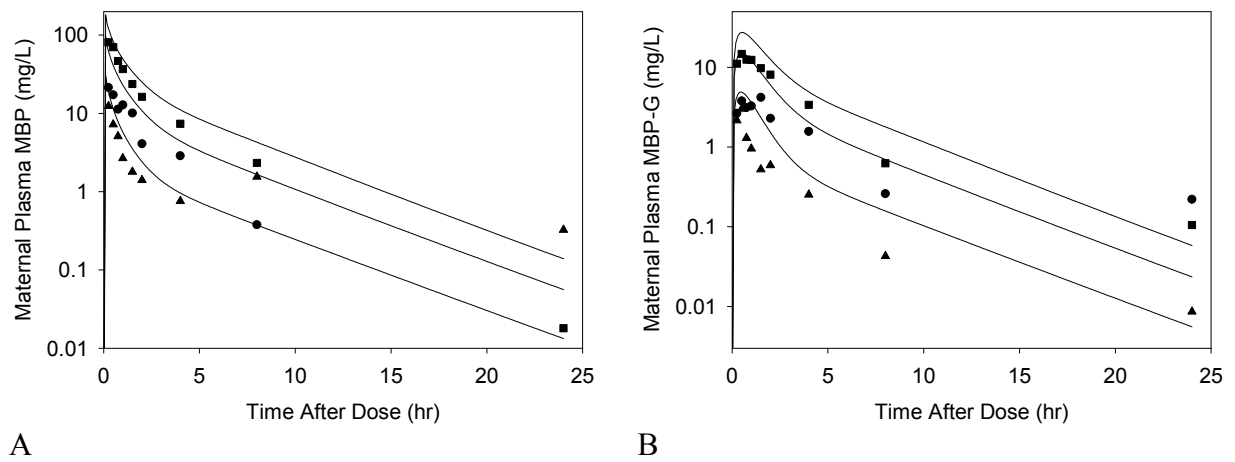


**Figure 3.10. MBP (left) and MBP-G (right) in (A) maternal plasma and (B) placenta tissue after the last daily dose of 50 (▲), 100 (○), or 500 (■) mg/kg-day administered from GD 12-19.**

Lines represent model predictions. Cross bars represent the mean  $\pm$  SD from the current studies. Placenta tissue was pooled for each dam.

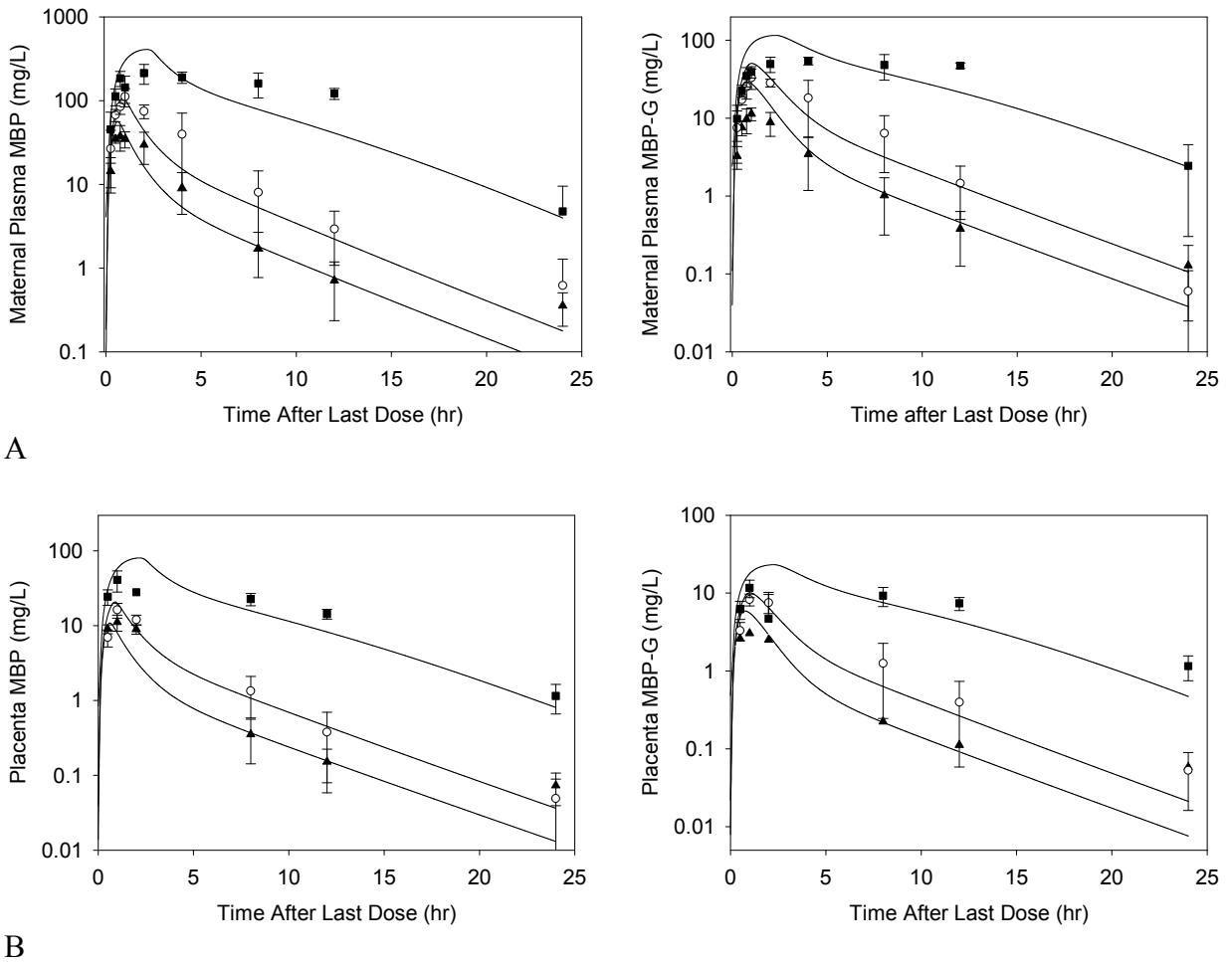


**Figure 3.11. MBP (left) and MBP-G (right) in (A) fetal plasma and (B) fetal testes, and (C) amniotic fluid after the last dose of 50 (▲), 100 (○), or 500 (■) mg/kg-day administered from GD 12-19.**

Lines represent model simulations. Cross bars represent the mean  $\pm$  SD from the current studies. Fetal plasma and amniotic fluid were taken from each fetus and pooled for the entire litter. Fetal testes were pooled for all the males in a litter.

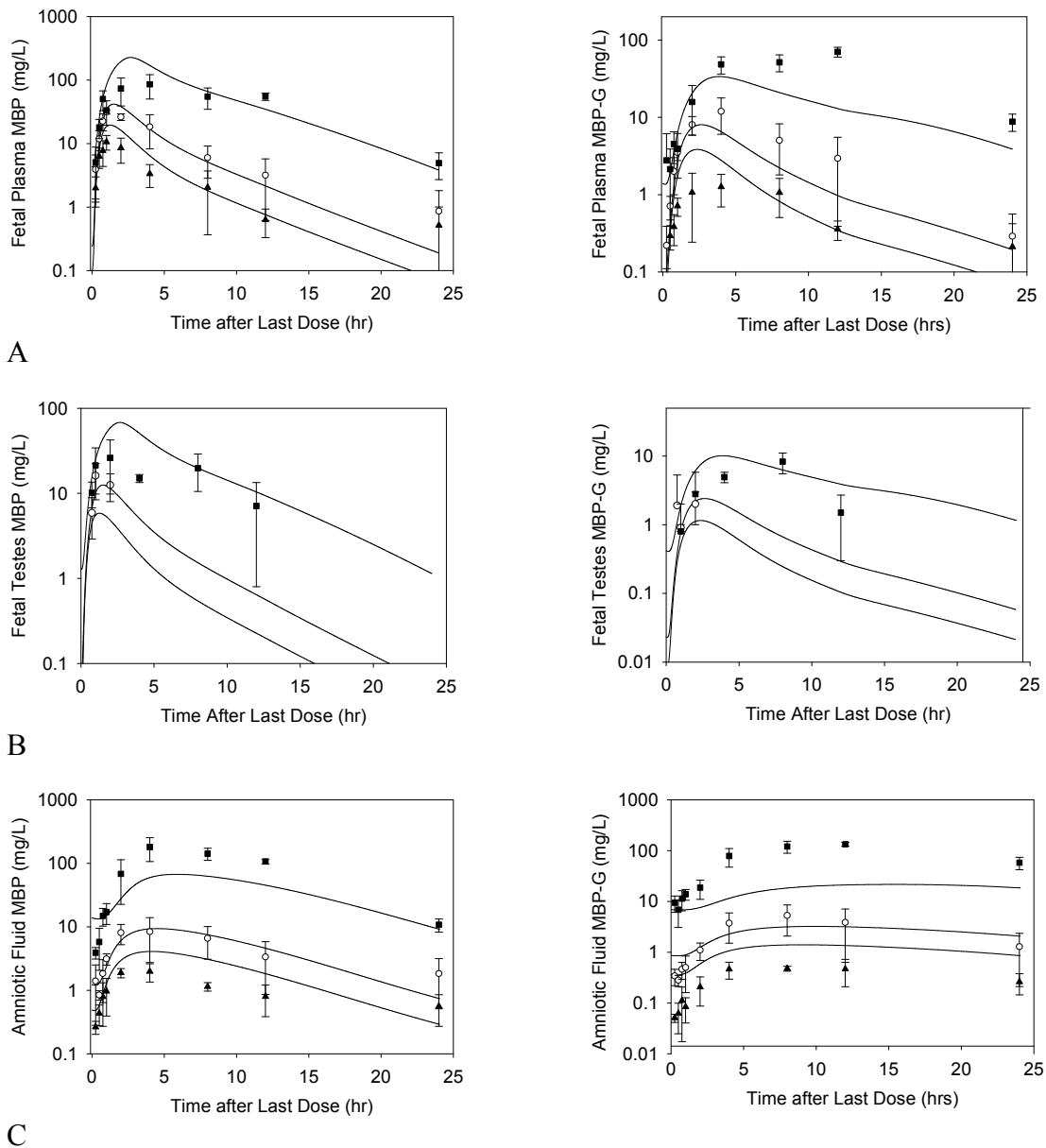


**Figure 3.12. Calculated sensitivity coefficient for model parameters with respect to maternal Plasma MBP AUC 24 hrs after a single oral dose of 10 (white bars) or 500 mg/kg DBP (black bars) on GD 20.**

Only those parameters with absolute values greater than 0.1 are shown. Coefficients for fetal parameters are not shown, with the exception of *Pmfet* (sensitivity coefficient = 0.9 in fetus), predicted fetal plasma levels show the same trends in parameter sensitivity coefficients as are seen in the dam.

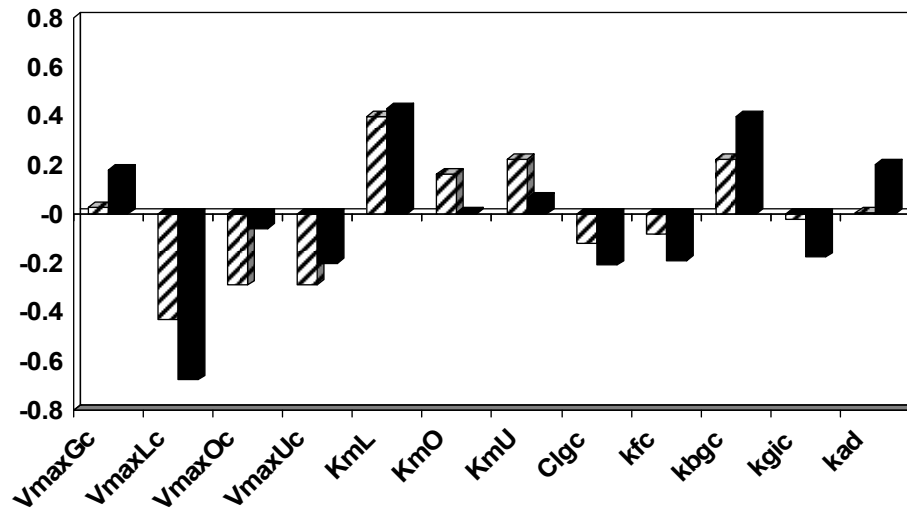


**Figure 3.13. DBP dose response: Predicted average daily concentration of MBP in maternal and fetal plasma and fetal testes at external doses ranging from 1 to 550 mg DBP/kg-day from GD12.**

Lines represent the average MBP concentrations in the maternal plasma (solid), fetal plasma (dashed) and fetal testes (dash-dotted) predicted by the model across doses. Points and drop bars represent the published LOAELs for the identified effects from the studies of Lehmann et al. [46] and Mylchreest et al. [34, 47, 68].

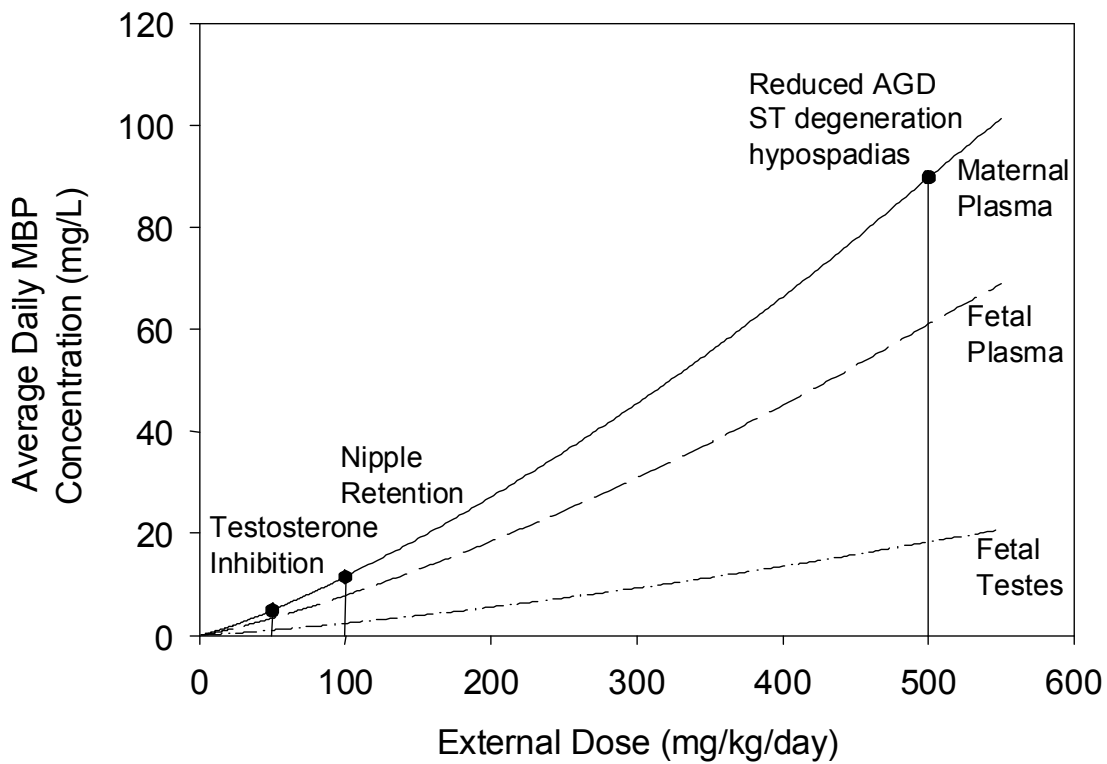


**Figure 3.14. Revised PBPK model structure to describe both DEHP and DBP kinetics in the pregnant rat.** Adult male rat model is identical with the exception of the placenta/fetus compartments. Dashed arrows indicate first order processes. Bold dashed arrows represent saturable processes. Solid arrows represent blood flows to the tissue compartments and are diffusion limited.

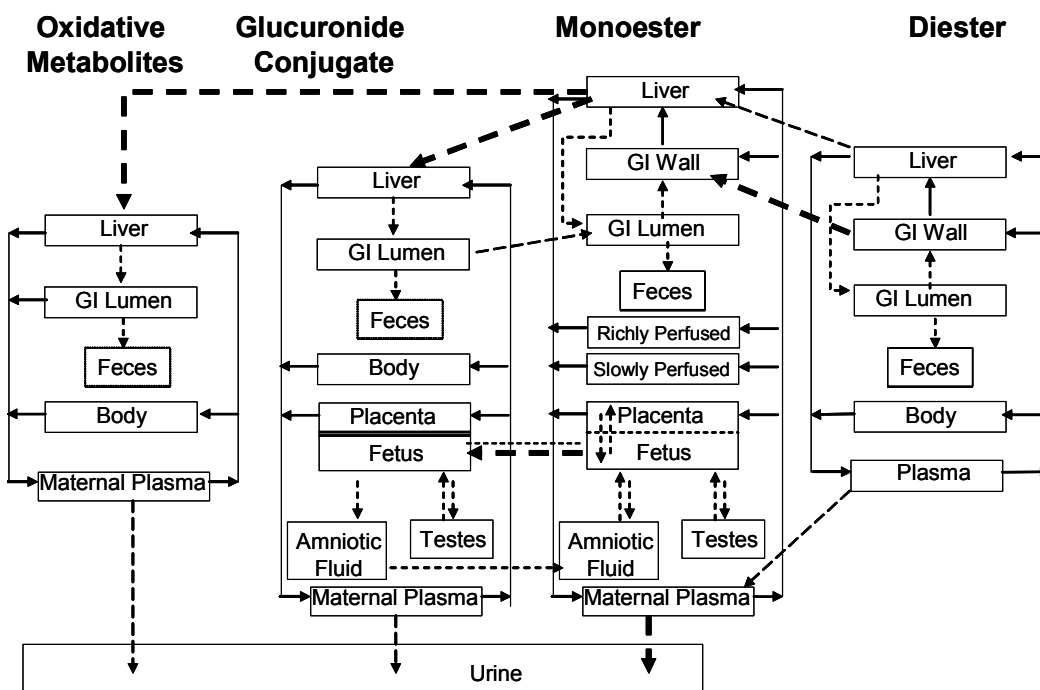




**Figure 3.15. Free MEHP in the blood of the adult male rat after an iv dose of 20 or 50 mg/kg MEHP.** Lines indicate model simulations. Points represent measurements from individual animals administered (●) 20 mg/kg MEHP [117], (▼) 50 mg/kg MEHP [53], or (Δ) 50 mg/kg MEHP [45].

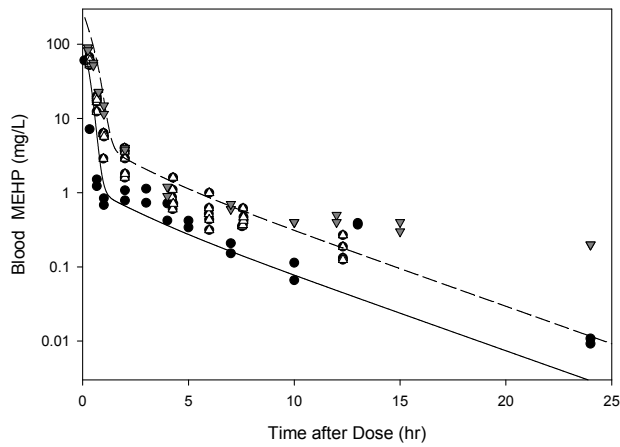


**Figure 3.16. Free MEHP in the (A) blood of adult male rat after an oral dose of 70, 100, or 400 mg/kg MEHP or (B) excreta of adult mat rat after an oral dose of 70 mg/kg MEHP . (A) Lines indicate model simulations. Points represent measurements from individual animals administered (o) 70 mg/kg MEHP [118], (■) 100 mg/kg MEHP [53], or (●) 400 mg/kg MEHP [54]. (B) Bars represent model simulations (gray) or mean  $\pm$  SD of measured (black) MEHP in the urine and feces rats administered 70 mg/kg MEHP [118].**

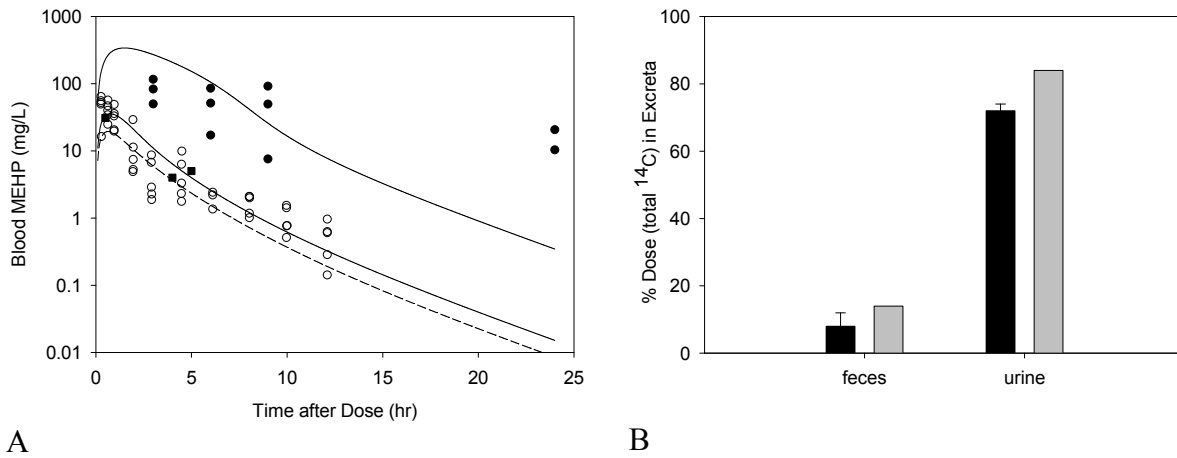
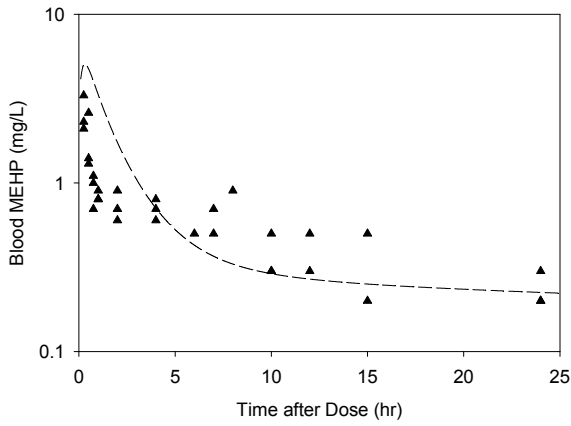
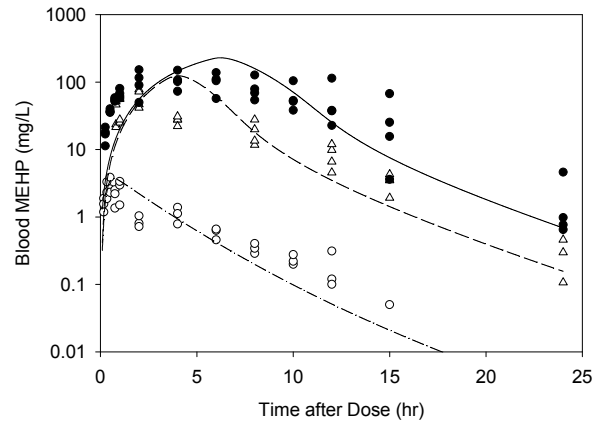


**Figure 3.17. Free MEHP in the blood of adult rats after an (A) iv dose of 100 mg/kg DEHP, or (B) oral dose of 30, 300, or 500 mg/kg DEHP. Line indicates model simulation. Points represent measurements from individual animals administered (A) 100 mg/kg DEHP iv [45] or (B) (o) 30 mg/kg, ( $\Delta$ ) 300 mg/kg, or ( $\bullet$ ) 500 mg/kg DEHP po [45].**

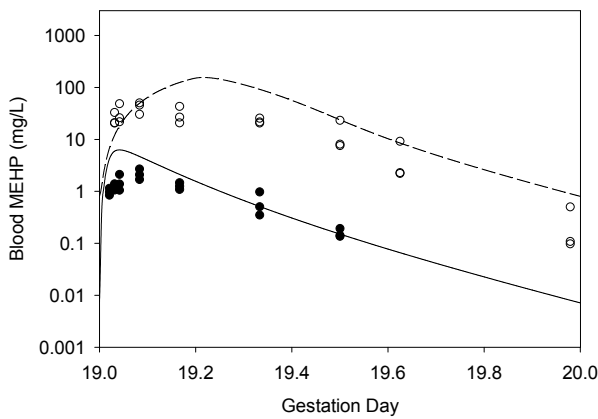


A

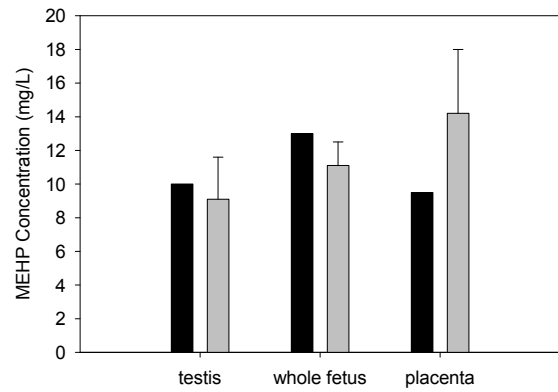


B

**Figure 3.18. Free MEHP in the (A) maternal blood or (B) placenta and fetal tissues after the last oral dose of 30 or 500 mg/kg/day administered from GD 14 - 19.** (A) Lines indicate model simulations. Points represent measurements from individual animals administered (●) 30 mg/kg/day or (○) 500 mg/kg/day DEHP po [45]. (B) Bars represent model simulations (black) or mean  $\pm$  SD of measured concentrations (gray) in the placenta and fetal tissues 2 hrs after the last daily dose of 500 mg/kg/day (J. Filser, personal communication).



A



B

## CHAPTER 4

### **Phthalate Esters: Pharmacokinetic and Pharmacodynamic Factors Affecting Potency for Testosterone-Mediated Developmental Effects**

This chapter is expected to be submitted for publication in *Toxicology In Vitro* in May 2009.

## A. ABSTRACT

Human exposure to phthalates occurs as mixtures of diesters with varying activity towards testosterone-dependent development. Dibutyl (DBP), diethylhexyl (DEHP), and butylbenzyl (BBP) phthalate disrupt sexual development in the fetal rat. Dimethyl (DMP) and diethyl (DEP) phthalate do not. This difference in potency may result from pharmacokinetic (PK) or pharmacodynamic (PD) differences. These five phthalates were administered to pregnant rats (500 mg/kg-d, GD12-19) and the fetal testes were analyzed for the corresponding monoester (MMP, MEP, MBP, MEHP, MBeP). Fetal testes MMP and MEP levels were 2 - 40-fold higher than MBP and MEHP. BBP exposure led to very low concentrations of MBeP, but similar MBP levels as seen with DBP dosing. An *in vitro* assay in MA-10 cells was developed to determine the direct effect of monophthalates on Leydig cell function. The MA-10 cell, a tumor line thought previously to have a functioning steroidogenic pathway that ended at progesterone, produced testosterone after stimulation with luteinizing hormone (LH). LH stimulated testosterone production was inhibited by MEHP at concentrations as low as 1  $\mu$ M. When evaluated by RT-PCR, expression of genes associated with cholesterol transport and steroid synthesis at steps in the pathway both before and after progesterone were significantly decreased at MEHP concentrations of 100  $\mu$ M. Five additional phthalates were tested with the *in vitro* assay. MBP and mono-n-octyl phthalate showed similar inhibition to MEHP, while MMP, MEP and MBeP did not affect testosterone. These studies indicate that phthalates activity *in vivo* is dependent upon pharmacodynamic, not kinetic, differences in phthalates of varying alkyl chain length.

## B. INTRODUCTION

Exposure to phthalate esters occurs through drinking water, food, personal care products. Some of these esters are also used as a coating for medications [64]. Metabolites of several phthalates are found in the urine of the US population at all age ranges from infants to adults, and in pregnant women [6]. Some phthalates, such as di-(2,4)-ethylhexyl phthalate (DEHP), di-n-butyl phthalate (DBP), and butylbenzyl phthalate (BBP) disrupt male sexual development in the rat. Administration of DBP, DEHP, or BBP to pregnant rats causes reduced anogenital distance (AGD), nipple retention, hypospadias, delayed testes descent, and vaginal pouch development in the male offspring [33, 47]. Several other phthalate esters, however, including diethyl phthalate (DMP), dimethyl phthalate (DEP), and dioctyl terephthalate [33] do not affect sexual development of the male rat. Neither DEP nor DMP caused down-regulation of steroidogenic genes or inhibition of testosterone production in the fetal rat testes.

The monoester metabolites are the biologically active forms of the phthalate diesters. DBP and DEHP and their monoesters, MBP and MEHP, have been studied extensively *in vivo* in an effort to elucidate their mechanism of action. While the molecular target(s) has not been identified, the monoester metabolites of the endocrine active phthalates have been shown to inhibit testosterone synthesis by direct interaction with the testes, reducing the steroidogenic response to luteinizing hormone (LH) stimulation [72, 119]. Inactive phthalates, such as DEP and DMP, do not reduce fetal testosterone. It is not clear why some phthalates disrupt testosterone-dependent development and others do not. The difference in potency may result from the length and extent of branching in the alkyl chains [33]. The

structural differences in the monoalkylesters could affect metabolite kinetics, as well as their ability to interfere with steroidogenesis.

The purpose of this study was to determine whether differences in phthalate potency *in vivo* result from pharmacokinetic (PK) or pharmacodynamic (PD) factors. Two studies were performed with representative endocrine active and inactive phthalates: 1) phthalate monoester concentrations were measured in the testes of male fetuses from exposed pregnant rats, and 2) an *in vitro* assay was developed and used to measure directly the effect of the various phthalates on Leydig cell steroidogenesis.



## C. METHODS

Six different phthalates were chosen to represent compounds with different potencies for steroidogenic effects. Two of the tested phthalates are known inhibitors of male rat sexual development: DEHP (MEHP), DBP (MBP). Two of the tested phthalates do not disrupt reproductive tract development *in vivo*: DEP (MEP) and DMP (MMP). Effects of butylbenzyl phthalate (BBP) exposure are similar to those of DEHP and DBP [33, 80]. However, it is not known which metabolite is responsible for the anti-androgenic effects, as BBP may be metabolized to MBP or MBeP. The *in vivo* activity of two of the phthalates: di-n-octyl (DnOP) and dibenzyl phthalate (DBeP) has not been tested.

### **Examination of Pharmacokinetic Differences among Phthalates**

#### *Animals*

Pregnant Sprague-Dawley (CrI:CD(SD)) rats (sperm plug positive GD 0) were obtained from Charles River Laboratories (Raleigh, NC) and housed in the Animal Care Facility of the The Hamner Institutes for Health Sciences, which is accredited by the Association for Assessment and Accreditation of Laboratory Animal Care International. Rats were acclimated in a temperature- and humidity-controlled, HEPA-filtered environment on a 12 hr light-dark cycle. NIH rodent diet (NIH-07, Zeigler Bros., Gardner, PA) and reverse-osmosis water were provided *ad libitum*. This study was approved by The Hamner Institute's Animal Care and Use Committee.

### *Treatment*

Animal exposures, sacrifice and tissue collection has been described previously [80]. Briefly, dosing solutions (500 mg/mL) were prepared by mixing DEHP, DBP, BBP, DEP or DMP and corn oil (Sigma-Aldrich, St. Louis, MO). Pregnant rats were given corn oil (1.0 mL/kg/day) or one of the phthalates (500 mg/kg/day) dissolved in corn oil (1.0 mL/kg) from GD 12 through 19. The dams were euthanized by CO<sub>2</sub> asphyxiation and exsanguination 2 hrs after the final dose. Fetuses were delivered by caesarean section and sex was determined by internal inspection of gonads. Testes from each male fetus were collected, snap frozen in liquid nitrogen, and stored individually at -80°C. Testes samples that were not used for gene expression data provided in Liu et al. [80] were generously provided to us for measurement of phthalate concentrations.

### *Phthalate Analysis*

The monoester phthalates (MEHP, MBP, MBeP, MEP, and MMP) were extracted from testes prior to analysis using a previously described method for MBP (Chapter 2). Each testes pair was homogenized in 1% PBS (500 µL) with a Mixer Mill 300 for 5 minutes at 30 Hz/s. The homogenate was transferred to a 2.0 mL microcentrifuge tube and 200 µL of 1% formic acid/water and 25 µL of [<sup>13</sup>C]-MBP (6 mg/mL) were added to the tube. The sample was vortexed for 5 seconds and then centrifuged at 1900 x g for 6 min at 4°C. The supernatant was loaded onto an LC-18 SPE column (Honeywell Burdick and Jackson, Morristown, NJ) that had been pre-activated with a water solution of 2 mL of 0.1 formic acid, added in two 1 mL increments. After passing 2 mL of a 0.1% formic acid in water/0.1 formic acid in methanol (75%/25%) in 1 mL increments, the monoester was eluted with a

methanol solution of 0.1% formic acid (2 mL) in 1 mL increments. The samples were evaporated to dryness under nitrogen and reconstituted in 200  $\mu$ L of 0.1% formic acid in ACN/H<sub>2</sub>O (90%/10%) for analysis by LC-MS/MS, performed according to previously published methods [42].

## **Development of an *In Vitro* assay for Phthalate Inhibition of Steroidogenesis**

### *Cell Culture*

Mouse Leydig tumor (MA-10) cells were obtained from Dr. Mario Ascoli (Department of Pharmacology, University of Iowa, College of Medicine, Iowa City). Stock cells were grown in 150 mm tissue-culture dishes as described by Ascoli et al. [120] in complete medium (Waymouth's MB 752/1 supplemented with 15% horse serum, 2% L-glutamine, 20 mM HEPES, and 50  $\mu$ g/mL Gentamicin). For all cell culture experiments, dishes were coated with a 0.1% solution of gelatin for 30 min before plating cells. All incubations were performed at 37°C in a humidity-controlled atmosphere of 5% CO<sub>2</sub>-air.

### *Progesterone and Testosterone Inhibition*

Cells were plated in 24-well plates at a density of  $1 \times 10^5$  cells/well in 0.5 mL complete medium and allowed to incubate for 24 hrs. The medium was then removed and replaced with serum-free medium (SFM) containing 0 (0.1% DMSO), 1, 3, 10, 30, 100, 300, 1000  $\mu$ M MEHP. After 24 hrs, the medium was replaced with SFM containing the same inhibitor concentration supplemented with a maximum stimulating concentration of LH (100 ng/mL). The medium was collected after 6 hrs and stored at -20°C. PG and testosterone in

the medium were measured using ELISA assays (Neogen Corporation, Lexington, KY) according to the manufacturer's directions.

#### *Protein Content and Viability Analysis*

Cells were collected from each well and combined for each dose. Each well was treated with 100  $\mu$ L of lysis buffer (0.1 M Tris-HCl (pH= 8.0), 0.05 M EDTA, 0.1 M NaCl, 1% sodium dodecyl sulfate, 1% sarcosyl) supplemented with HALT Protease Inhibitor Cocktail (10  $\mu$ L/1 mL buffer) (Thermo Fisher Scientific Inc., Rockford, IL) and the cells were dislodged using a cell scraper. The resulting lysate was homogenized and stored at -80°C prior to analysis. Total protein content was measured using a bicinchoninic acid (BCA) assay (Sigma-Aldrich) according to the manufacturer's directions. Cell viability was also tested in triplicate using the ATPlite luminescence assay (Perkin Elmer, Boston, MA) according to manufacturer's instructions.

#### *Quantitative RT-PCR*

MA-10 cells were plated at a density of  $3 \times 10^6$  cells/well in 100 mm cell culture dishes (CellStar) in 20 mL complete medium. 24 hrs after plating, medium was replaced with 20 mL SFM containing 0 (DMSO) or 100  $\mu$ M MEHP. Cells were incubated for 24 hrs and medium was replaced with SFM containing the same inhibitor concentration supplemented with PBS (no treatment control) or a maximum stimulating concentration of LH (100 ng/mL). After 6 hrs, medium was aspirated from the plate, cells were washed with  $\text{Ca}^{++}/\text{Mg}^{++}$ -free PBS and removed from the plate using a disposable cell scraper. Total RNA was isolated from the cells of each cell culture dish using an RNeasy Mini Kit (Qiagen,

Valencia, CA). cDNA was prepared for each sample using the High Capacity cDNA kit (Applied Biosystems, Foster City, CA) according to the manufacturer's protocol. Reverse transcription (RT) reactions were performed on the Taqman 7900HT system (Applied Biosystems, Foster City, CA). Taqman gene expression assays for mouse *Cyp17A1*, *GAPDH*, *P450scc*, *SR-BI*, and *Star* were purchased from Applied Biosystems (Foster City, CA). Samples were run in triplicate and the change in expression of target genes were normalized to *GAPDH*. The fold change for each gene normalized to GAPDH and relative to expression in no treatment control (NTC) samples was determined by the  $2^{-\Delta\Delta Ct}$  method [121].

### **Examination of Pharmacodynamic Differences among Phthalates**

The ability of five additional phthalates to inhibit testosterone synthesis in the MA-10 cell was examined using the method described for MEHP above. MBP (TCI America), MEP (Accustandard), and MNOP, MBEP, and MMP (Sigma-Aldrich) were dissolved separately in DMSO to obtain stock solutions (1 M) for each of the phthalates. Cells were pre-treated with 0, 1, 3, 10, 30, or 100  $\mu$ M of an individual phthalate for 24 hrs in SFM. Cells were then stimulated with 100 ng/mL LH in the presence of the inhibitor (or DMSO) and medium was collected for hormone analysis. Cell protein content was assayed for all tested compounds at each dose. Cell viability assays were also run for each treatment in triplicate using the ATPlite luminescence assay (Perkin Elmer, Boston, MA).

## D. RESULTS

### Examination of Pharmacokinetic Differences among Phthalates.

Despite the number of *in vivo* effect studies, little information is available regarding phthalate disposition during gestation. In fact, active metabolite (MBP) concentrations in the target tissue (fetal testes) have only been published for DBP (Chapter 2). Thus, the first question in interpreting the effect studies is whether the fetus is exposed to the active metabolites. Testes were collected from fetuses of dams exposed to 500 mg/kg/day DMP, DEP, BBP, DBP, or DEHP from gestation day (GD) 12- 19, and their free monoester metabolites, MMP, MEP, MBP or MBeP, MBP and MEHP, respectively, were measured using HPLC/MS-MS (Figure 4.1).

All of the monoesters were found in the fetal testes after maternal exposure to the dialkyl esters. MMP and MEP, the monoesters derived from the two “inactive” phthalates were present at the highest concentrations, with mean concentrations of 396 and 409  $\mu\text{M}$ , respectively. Mean testes concentrations of MBP (189  $\mu\text{M}$ ) indicate that it is also efficiently transported into the fetus. MEHP, on the other hand, was present at much lower concentrations (12  $\mu\text{M}$ ) than MBP (189  $\mu\text{M}$ ), despite the fact that both DBP and DEHP are potent inhibitors of fetal development at this administered dose (500 mg/kg/day). In rats exposed to BBP, MBP was the major metabolite found in the testes: the mean concentration (124  $\mu\text{M}$ ) was 5-fold greater than MBeP (21  $\mu\text{M}$ ).

### Validation of an *in vitro* assay for phthalate inhibition of steroidogenesis

The PD effect of interest for the phthalates is delayed sexual development of the fetal rat [33, 80]. Inhibition of testosterone production in the Leydig cell of the fetal testes has

been shown to precede the more overt physiological effects, such as nipple retention and hypospadias [46, 72, 113] and may be a useful early marker of sexual development disruption. To test whether the phthalates have different potencies for steroid inhibition, an assay was needed that allows direct exposure of the Leydig cell and a measurable biomarker. To this end, an assay in the murine Leydig tumor (MA-10) cell line was developed based on the method of Dees et al. [122], who reported inhibition of progesterone production after stimulation with human chorionic gonadotropin. MA-10 cells are known to produce progesterone (PG; the testosterone precursor) in response to stimulation by luteinizing hormone. The MA-10 cell has been widely used as a model for studying the steroidogenic pathway in the Leydig cell, measuring alterations in PG in a variety of conditions [55].

Based on previous reports that PG was the terminal point in MA-10 steroid synthesis, initial assay development focused on the ability of MEHP, a known inhibitor of steroid production, to inhibit LH-stimulated PG production. Treatment of MA-10 cells was found to inhibit PG production at doses concentrations  $\geq 1 \mu\text{M}$  (Figure 4.2). Cell viability assessed via intracellular ATP and total protein content were  $> 90\%$  of control values at doses up to  $100 \mu\text{M}$ . At  $300$  and  $1000 \mu\text{M}$ , reduced viability ( $< 90\%$  of control) was observed.

Gene array studies performed on whole testes samples obtained from the fetal rat after gestational phthalate exposure [46, 80, 123] revealed consistent down-regulation of genes associated with steroidogenesis in the Leydig cell, including genes that encode proteins at multiple points in the biosynthesis pathway for testosterone. Some of the key genes identified in these studies include *scavenger receptor class B family 1 (SR-B1)*, *steroid acute regulatory protein (StAR)*, *cytochrome P450 17a1 (Cyp17a1)*, and *P450 side chain cleavage (P450scc)* (Figure 4.3). *SR-B1* and *StAR* encode proteins responsible for the transport of

cholesterol into the cell and across the mitochondrial membrane, respectively. P450scc is required for the conversion of cholesterol to pregnenolone, which is then metabolized by Cyp17a1 over several steps to form androstenedione, the immediate precursor to testosterone.

Expression of *SR-B1*, *StAR*, *Cyp17a1* and *P450scc* were evaluated in MA-10 cells by quantitative RT-PCR. All four genes were significantly up-regulated within 6 hrs of LH stimulation compared to controls (Figure 4.4A). When pre-treated with 100  $\mu$ M MEHP, *Cyp17a1*, *P450scc*, *SR-B1* and *StAR* were decreased relative to LH stimulated cells (Figure 4.4B).

*Cyp17a1* changes were particularly interesting due to the fact that the enzyme is responsible for metabolism of PG, indicating that the enzymes necessary for synthesis of the subsequent steroids, androstenedione and testosterone, are present in the MA-10 cell. In response to these observations, medium from control and LH-stimulated MA-10 cells was analyzed for testosterone by ELISA assay. The ELISA assay has less than 1% cross reactivity with the precursor steroids, including progesterone, pregnenolone, 17-hydroxyprogesterone, and androstenedione. The MA-10 cells were found to produce testosterone in response to LH-stimulation. At 100 ng/mL LH, testosterone concentration in the medium was  $0.27 \pm 0.3$  ng/mL (vs.  $<0.01$  ng/mL in no treatment controls). When the cells were pre-treated with MEHP, testosterone production was reduced in a dose-dependent manner. MEHP concentrations as low as 1  $\mu$ M resulted statistically significant ( $p < 0.05$ ) testosterone inhibition (Figure 4.5)



### **Examination of pharmacodynamic differences among phthalates.**

MEHP induced inhibition of testosterone and steroidogenic gene expression in the MA-10 cell is consistent with *in vivo* phthalate effects, indicating that this assay may provide a reasonable model for the action of phthalate monoesters on Leydig cell function. Because the *in vitro* assay eliminates PK differences inherent in *in vivo* studies, the MA-10 *in vitro* assay was used to compare the PD behavior of different phthalates (Figure 4.6). The dose-response curve for MBP, another endocrine active phthalate, was remarkably similar to that of MEHP, with significant inhibition at 3  $\mu\text{M}$ . In contrast, neither MMP nor MEP inhibited testosterone synthesis significantly at concentrations up to 100  $\mu\text{M}$ .

### **Predictive use of the MA-10 inhibition assay.**

A reliable *in vitro* assay for phthalate-induced inhibition of steroidogenesis would improve our ability to identify endocrine active phthalates while reducing the need for in life animal testing. The proposed MA-10 assay was used to predict the anti-androgenic activity of mono-n-octyl phthalate (MnOP) and monobenzyl phthalate (MBeP), two esters with unknown activity *in vivo* (Figure 4.7). Neither DnOP nor MnOP have been tested in rat developmental studies and MBeP has only been tested in a mixture with MBP (BBP administration). MnOP treatment of MA-10 cells caused similar inhibition of testosterone to MEHP and MBP. MBeP, on the other hand, did not show appreciable inhibition of testosterone at any of the measured concentrations ( $\leq 100 \mu\text{M}$ ).

## E. DISCUSSION

Comparative *in vivo* studies in pregnant rats have identified several phthalates, including DBP, DEHP, and BBP, that induce developmental responses in male offspring. These active phthalates have similar effects on male reproductive tract development, testosterone production and gene expression in the fetal testes. Other phthalates, however, including DMP and DEP do not have the same effects *in vivo*. The data presented here for monoester phthalate concentrations in the fetal testes demonstrates for the first time that these differences in phthalate potency are not a result of varying kinetic properties (*i.e.*, lack of fetal exposure). MEP and MMP are efficiently transferred to the fetus. Thus, their inability to disrupt sexual development indicates that MMP and MEP do not share the same mode of action as the endocrine active phthalates (*i.e.*, MBP).

Use of an *in vitro* Leydig cell assay allows this hypothesis to be tested quantitatively, through examination of the steroidogenic effects of phthalates directly in the cell. Several important differences exist between the MA-10 cell line and the cell of interest *in vivo*. The MA-10 is a tumor derived cell line obtained from the adult male mouse. The most striking *in vivo* effects, however, occur in the fetal rat. The fetal mouse does not exhibit the same T dependent effects *in vivo* that are seen in the rat, despite receiving a similar fetal dose [35]. Nonetheless, phthalates have been shown to cause similar [122] steroidogenic and morphological effects in the MA-10 [122] and primary rat Leydig cell [119]. Treatment with endocrine active phthalates (MEHP, MBP) caused reductions in LH-stimulated steroidogenesis, mitochondrial swelling and vesiculation of the golgi apparatus in both the MA-10 and the primary rat Leydig cell. Gene expression data from the current study were also consistent with the fetal rat *in vivo* data, showing down-regulation of steroidogenic

genes involved in both cholesterol transport (*SR-B1*, *StAR*) and metabolism (*Cyp17a1*, *P450scc*). The similarities in cellular response to phthalate exposure indicates that the MA-10 cell should be a reasonable model of phthalate effects on the Leydig cell itself despite species and age-related differences observed in whole animal studies.

Concentrations required to inhibit testosterone synthesis in the MA-10 cell were similar to those expected in the fetus. Dose-response studies with DBP have shown that external doses between 50 and 500 mg/kg/day significantly reduced fetal testes testosterone levels [46] (Chapter 2). Based on recent PK studies and physiologically based PK (PBPK) modeling (Chapters 2-3), fetal MBP concentrations associated with reduced testosterone have been estimated to be in the low micromolar range (2-9  $\mu\text{M}$ ). Likewise, the current study equates testes concentrations of 12  $\mu\text{M}$  MEHP with the external doses of 500 mg DEHP/kg/day, which cause > 50% reduction in fetal testes testosterone content [113]. The *in vitro* assay also accurately identified phthalates that are without effects on androgen synthesis – neither MMP nor MEP was able to repress testosterone synthesis *in vitro*. This observation is in agreement with data from isolated rat Leydig cells [119] and *in vivo* studies where DEP and DMP did not cause the reproductive [33] or gene expression changes [80], despite significant exposure of the fetus to the monoester metabolites verified in this study.

Application of this *in vitro* assay to other phthalates enables the classification of various phthalate metabolites according to their ability to inhibit steroid production, supporting a more informed assessment of human risk. MnOP has not been tested in the fetal rat. It reduced testosterone synthesis in the MA-10 cell, indicating that it likely shares the same mechanism of action as MBP and MEHP. This conclusion is consistent with studies in the adult rat, showing similar effects of DEHP and DnOP administration in the Leydig cells

of adult rats *in vivo*, as well as reduced testosterone production in cultured rat Leydig cells (Jones et al., 1993). Interestingly, MBeP did not inhibit steroidogenesis *in vitro*, despite the fact that BBP has been shown to be a potent anti-androgen in fetal rats [33, 46]. The lack of effect *in vitro*, together with the testes metabolite data showing minimal transfer of MBeP to the fetus, indicates that the observed fetal effects after administration of BBP are due to the preferential hydrolysis of BBP to MBP in the rat [124].

The use of this MA-10 assay to evaluate mixed exposures would be particularly useful in the effort to predict cumulative human risk, since human exposure occurs as a mixture of both endocrine active and inactive compounds. *In vivo* efforts to evaluate mixed exposures are limited by the expense incurred for the many sets of exposures required and the challenges in accounting for differences in pharmacokinetics when rats are dosed with multiple compounds at high doses that produce dose-dependent changes in kinetics (Chapter 3). A reliable *in vitro* test would also allow examination of relative potencies and the combined effect of oxidative metabolites in addition to the intact monoesters. MEHP, for example, is only a minor metabolite of DEHP in the blood of the rat [12]. In the human, blood concentrations of potentially endocrine active oxidative metabolites such as mono(2-ethyl-5-oxohexyl) phthalate and mono(2-ethyl-5-hydroxyhexyl) phthalate are similar to MEHP [81]. A better understanding of the relative potency of the monoester derivatives and their combined effect on the Leydig cell would be valuable in predicting human risk and in determining the most informative measure of human exposure for biomonitoring data collection.

## F. CONCLUSION

Together, our studies provide insight on both the PK and PD factors responsible for the phthalate-induced inhibition of steroidogenesis observed in animal studies, and indicate how these animal studies may be used to estimate human risk. For example, because MBP and MEHP are commonly found in human urine, and have anti-androgenic activity in the fetal rat and *in vitro*, both would need to be included in a cumulative phthalate risk assessment. Despite the lack of information on DnOP fetal development, it would also be advisable to account for its potential exposure in a cumulative risk assessment, as its primary metabolite reduces Leydig cell steroid production. Limited studies indicate that tissue and plasma kinetics of MnOP are similar to MEHP [125]. MEP and MMP, on the other hand, should be excluded from calculations of total phthalate exposure in relation to fetal testes effects as they do not share the same mode of action. BBP is an interesting case, in that despite the adverse effects seen in rat developmental studies, it might still be excluded from a cumulative risk assessment in the human. The observed effects in the rat are clearly driven by MBP concentrations. The human, however, preferentially hydrolyzes BBP to MBeP [110], which does not exhibit anti-androgenic activity *in vitro*. In this case, species PK differences indicate that the human would be less susceptible than the rat to developmental toxicity from BBP exposure.

**Figure 4.1. Measured monoester concentrations in the fetal testes from dams given daily oral doses of DMP, DEP, DBP, DEHP, or BBP from GD 12-19.**

Testes were collected 2 hrs after the final dose. Bars represent mean  $\pm$  SD from 3 fetuses of 2-3 dams.

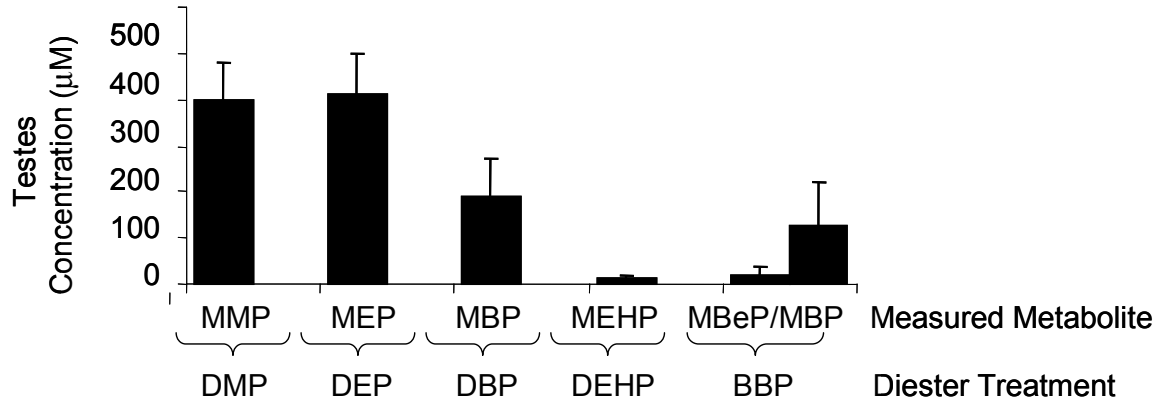


**Figure 4.2. Progesterone concentration in the medium of MA-10 cells treated with 100 ng/mL LH and varying concentrations of MEHP.**

Bars represent mean  $\pm$  SE from 3 separate experiments performed in triplicate. \* $p < 0.05$  analyzed by 1-Way ANOVA with Dunnett's post-test. 300 and 1000  $\mu$ M concentrations caused cell loss. 1 – 100 mM MEHP did not cause cellular toxicity as assessed by total protein and ATP content ( $>90\%$  of control).

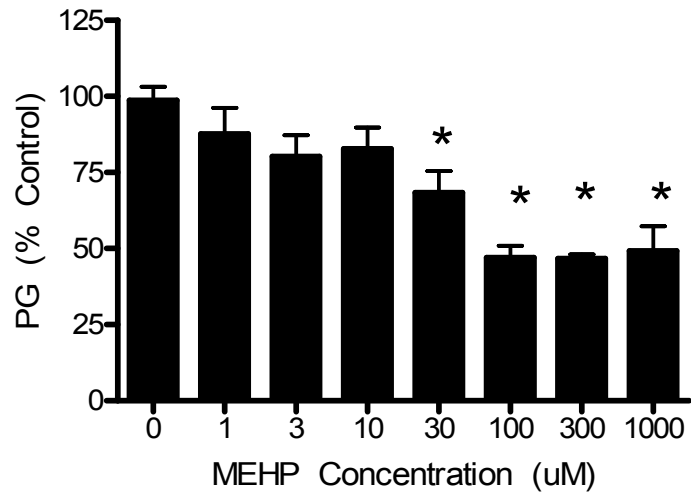


**Figure 4.3. Genes encoding proteins in the Leydig cell steroidogenic pathway.**

Broken lines represent transport proteins, solid arrows represent enzymatic proteins.

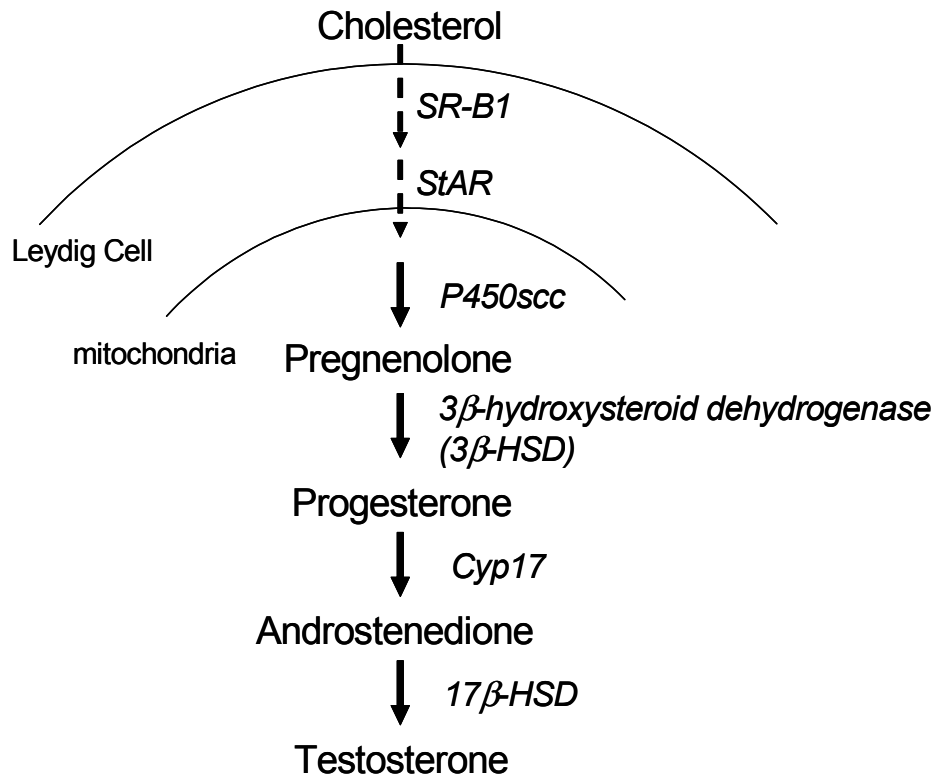
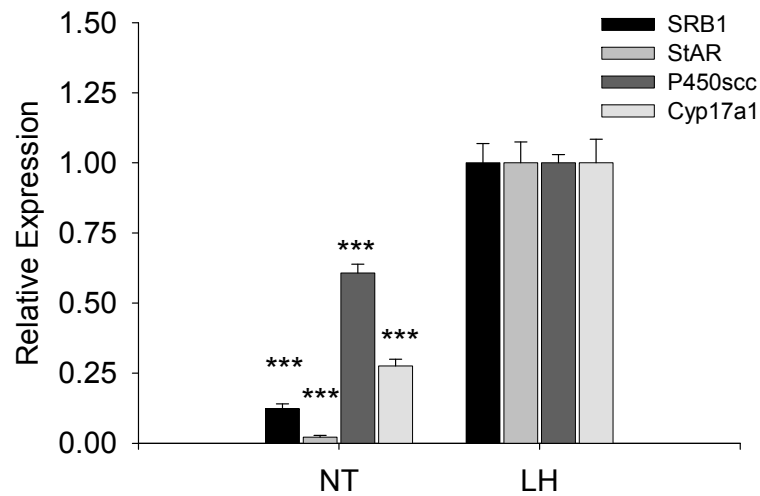


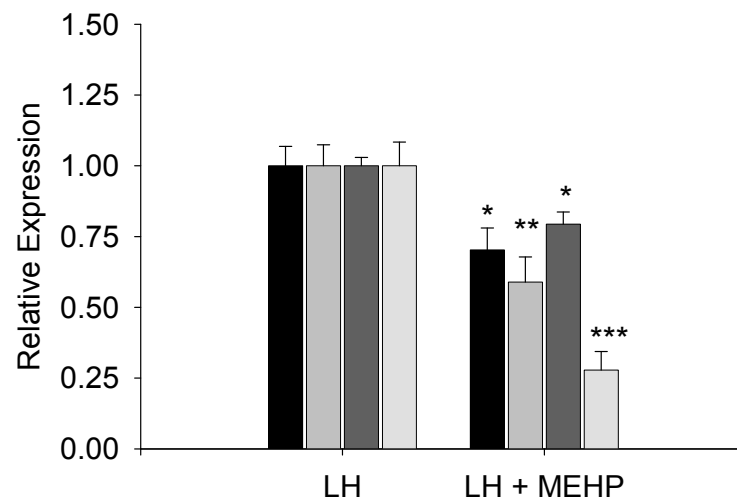


**Figure 4.4. Expression of selected steroidogenic genes in MA-10 cells.**

Bars represent mean  $\pm$  SE (n=6) of the values measured via RT-PCR. \*p< 0.005, \*\*p=0.0005, \*\*\*p<0.0001 Student's t-test for comparison of (A) no treatment (NT) vs. LH control or (B) LH control vs. MEHP (100  $\mu$ M) treated groups.



**A**



**B**

**Figure 4.5. Testosterone concentration in the medium of MA-10 cells treated with 100 ng/mL LH and varying concentrations of MEHP.**

Bars represent mean  $\pm$  SE from 3 separate experiments performed in triplicate. \* $p < 0.05$  analyzed by 1-Way ANOVA with Dunnett's post-test. 300 and 1000  $\mu$ M concentrations caused cell loss. 1 – 100  $\mu$ M MEHP did not cause cellular toxicity as assessed by total protein and ATP content (>90%).

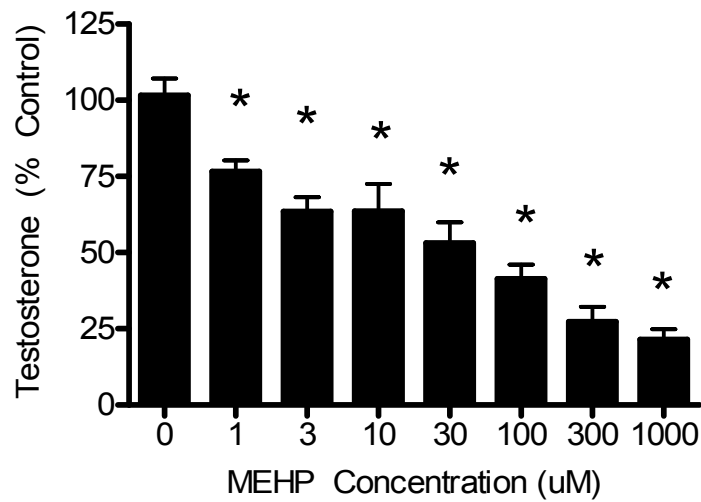


**Figure 4.6. Monobutyl, monoethyl, and monomethyl phthalate inhibition of LH-stimulated testosterone synthesis in MA-10 Leydig cells.**

Bars represent mean  $\pm$  SE from 3 separate experiments performed in triplicate. \* $p < 0.05$  analyzed by 1-Way ANOVA with Dunnett's post-test. Cell viability was  $> 90\%$  based on total protein and ATP content.

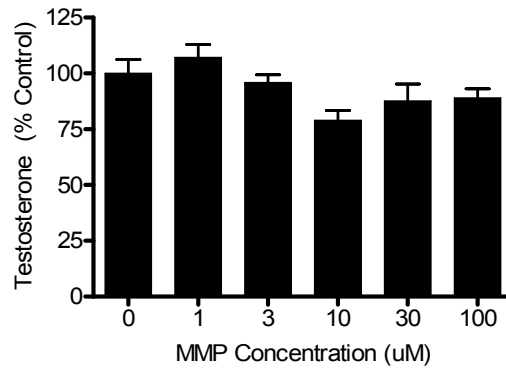
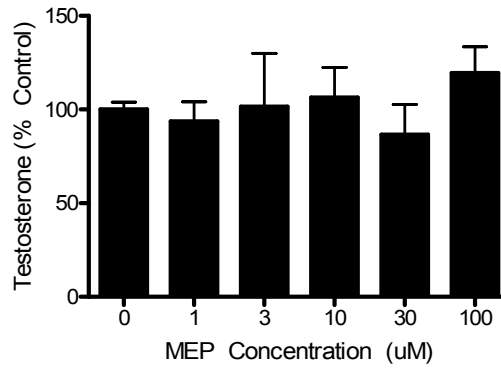
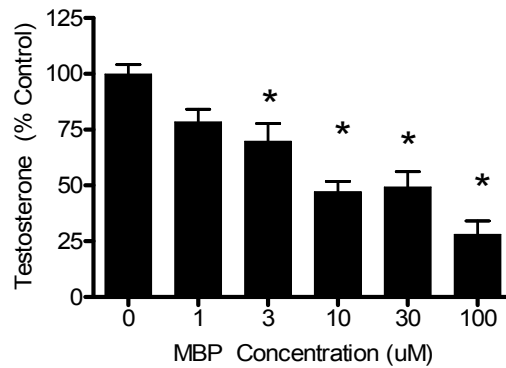
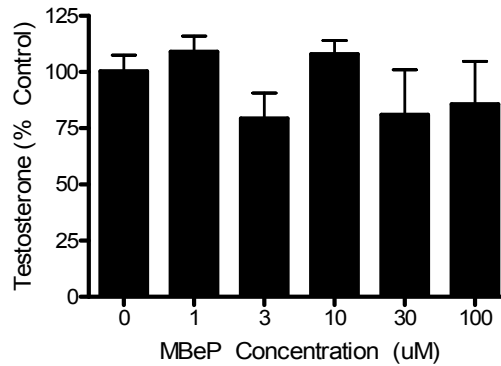
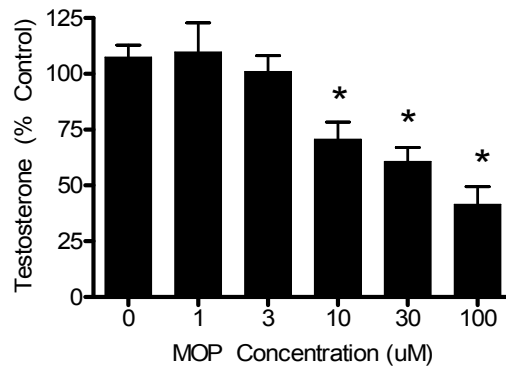


**Figure 4.7. Mono-n-octyl and monobenzyl phthalate inhibition of LH-stimulated testosterone synthesis in MA-10 Leydig cells.**

Bars represent mean  $\pm$  SE from 3 separate experiments performed in triplicate. \* $p < 0.05$  analyzed by 1-Way ANOVA with Dunnett's post-test. Cell viability was  $> 90\%$  based on total protein and ATP content.



## **CHAPTER 5**

### **Evaluation of Cytosolic Phospholipase A<sub>2</sub> as a Potential Target of Steroid Inhibiting Phthalates**

This chapter is expected to be submitted for publication in *Biology of Reproduction* or a similar peer-reviewed journal in June 2009.

## A. ABSTRACT

Phthalate monoesters disrupt sexual development in the male rat fetus, at least in part, through the inhibition of testosterone synthesis in the Leydig cell. Several of the phthalates, including monoethylhexyl phthalate, inhibit testosterone synthesis *in vivo* and *in vitro*. The mechanism of this inhibition, however, remains unknown. The purpose of this study was to attempt to identify molecular targets for MEHP in the Leydig cell. Studies in mouse MA-10 Leydig cell line showed similar effects on steroidogenic gene expression and testosterone production when pretreated with MEHP or chloroquine (CQ), a known inhibitor of arachidonic acid (AA) release. LH-stimulated release of AA from MA-10 cells was also inhibited to a similar extent by MEHP and CQ, indicating that MEHP also interferes with the arachidonic pathway, which is a co-regulator of steroid synthesis. HEK 293 cells overexpressing EGFP-cPLA<sub>2</sub> were used to determine the effect of MEHP treatment on cPLA<sub>2</sub> activation by calcium. Both MEHP and CQ interfered with translocation of the activated cPLA<sub>2</sub> to the nuclear membrane and endoplasmic reticulum. These studies support the conclusion that MEHP may disrupt steroid signaling in the Leydig cell by inhibiting arachidonic acid release by cPLA<sub>2</sub> and induction of steroid hormone production by AA.

## B. INTRODUCTION

Phthalate esters are widely used as plasticizers, and are ubiquitous drinking water contaminants. Epidemiological studies have shown evidence of phthalate exposure in the urine from samples from every subset of the US population [4, 5, 82]. Some of the longer chain alkyl phthalates, such as di-(2,4-ethylhexyl)phthalate (DEHP), have been identified as potential reproductive toxicants in rats [32, 33, 68]. Effects of gestational exposure to DEHP are similar to those induced by androgen receptor (AR) inhibitors: nipple retention, hypospadias, delayed testes descent, and vaginal pouch development in the male rat pup. Rather than interacting with the AR, however, the phthalates appear to exert their anti-androgenic effect through inhibition of testosterone synthesis in the Leydig cell [33, 46, 84, 113, 126]. The mechanism of this inhibition, however, is unknown.

Luteinizing hormone (LH) stimulates testosterone synthesis through binding and activation of a specific G-coupled protein receptor on the surface of the Leydig cell. In the adult Leydig cell (ALC), the primary regulatory pathway for steroidogenesis is regulated by the LH-stimulated release of cyclic AMP (c-AMP), which activates protein kinase A (PKA) and up-regulates transcription of certain steroidogenic genes, such as those encoding steroid acute regulatory (StAR) protein, and the cytochrome P450 enzymes side chain cleavage (P450<sub>scc</sub>) and 17a1 (Cyp17a1). LH also stimulates a secondary signaling cascade, which uses arachidonic acid (AA) as a second messenger. This pathway has similar down-stream effects to the better known c-AMP/PKA cascade, yet appears to be independent (or at least downstream) of c-AMP. AA release up-regulates StAR transcription and steroid production without altering c-AMP levels [55-57]. Figure 5.1 illustrates this two-pathway model for testosterone regulation.

Several *in vitro* studies have examined the effect of MBP on the LH regulatory pathway and found that disruption occurs prior to StAR gene transcription up-regulation [46, 127]. Yet, phthalate treatment does not affect intracellular c-AMP levels [55], indicating that the monoesters act either independently or downstream of c-AMP. In the classic literature, MEHP was shown to inhibit AA release in activated platelets [60]. This observation, together with histological studies showing decreased lipid metabolism in MA-10 cells with MEHP treatment [122], indicates that the phthalates may target the AA pathway rather than the more dominant c-AMP cascade. The purpose of this project was to determine the site of interaction between the monophthalate esters and this signaling cascade, focusing on the release of AA by LH regulation of cytosolic phospholipase A<sub>2</sub> (cPLA<sub>2</sub>).



## **C. METHODS**

### **Inhibition of Testosterone in MA-10 Cells**

MA-10 cells were obtained from Dr. Mario Ascoli (Department of Pharmacology, University of Iowa, College of Medicine, Iowa City). For all cell culture experiments, dishes were coated with a 0.1% solution of gelatin for 30 min before plating cells. All incubations were performed at 37°C in a humidity-controlled atmosphere of 5% CO<sub>2</sub>-air. Cells were plated in 24-well plates at a density of 1 x 10<sup>5</sup> cells/well in 0.5 mL complete medium (Waymouth's MB 752/1 supplemented with 15% horse serum, 2% L-glutamine, 20 mM HEPES, and 50 µg/mL Gentamicin) and allowed to incubate for 24 hrs. The medium was then removed and replaced with serum-free medium (SFM) containing 0 (DMSO), MEHP, or the PLA<sub>2</sub> inhibitor CQ. After 24 hrs, the medium was replaced with SFM containing the same inhibitor concentration supplemented with a maximum stimulating concentration of LH (100 ng/mL). The medium was collected after 6 hrs and stored at -20°C. Testosterone was measured using an ELISA assays (Neogen Corporation, Lexington, KY) according to the manufacturer's directions.

### **Protein Assay**

Cells from each well were treated with 100 µL of lysis buffer (0.1 M Tris-HCl (pH= 8.0), 0.05 M EDTA, 0.1 M NaCl, 1% sodium dodecyl sulfate, 1% sarcosyl) supplemented with HALT Protease Inhibitor Cocktail (10 µL/1 mL buffer) (Thermo Fisher Scientific Inc., Rockford, IL) and the cells were dislodged using a cell scraper. The resulting lysate was homogenized and stored at -80°C prior to analysis. Total protein content was measured using

a bicinchoninic acid (BCA) assay (Sigma-Aldrich) according to the manufacturer's directions.

### **Quantitative RT-PCR**

MA-10 cells were plated at a density of  $3 \times 10^6$  cells/well in 100 mm cell culture dishes (CellStar) in 20 mL complete medium. 24 hrs after plating, medium was replaced with 20 mL SFM containing 0 (DMSO), 100  $\mu$ M MEHP or 10  $\mu$ M CQ. Cells were incubated for 24 hrs and medium was replaced with SFM containing the same inhibitor concentration supplemented with PBS (no treatment control) or a maximum stimulating concentration of LH (100 ng/mL). After 6 hrs, medium was aspirated from the plate, cells were washed with  $\text{Ca}^{++}/\text{Mg}^{++}$ -free PBS and removed from the plate using a disposable cell scraper. Total RNA was isolated from the cells of each cell culture dish using an RNeasy Mini Kit (Qiagen, Valencia, CA). cDNA was prepared for each sample using the High Capacity cDNA kit (Applied Biosystems, Foster City, CA) according to the manufacturer's protocol. Reverse transcription (RT) reactions were performed on the Taqman 7900HT system (Applied Biosystems, Foster City, CA). Taqman gene expression assays for mouse *Cyp17A1*, *GAPDH*, *P450scc*, *SR-B1*, and *StAR* were purchased from Applied Biosystems (Foster City, CA). Samples were run in triplicate and changes in expression of target genes were normalized to *GAPDH*. The fold change for each gene normalized to *GAPDH* and relative to expression in no treatment control (NTC) samples was determined by the  $2^{-\Delta\Delta\text{Ct}}$  method [121].

### **Inhibition of AA Release in MA-10 Cells**

PLA<sub>2</sub> activity was evaluated by measuring the cellular release of radiolabeled AA [128]. MA-10 cells were plated in 24-well plates at a density of  $1 \times 10^5$  cells/well in 0.5 mL complete medium. After 24 hrs, the medium was replaced with SFM containing 0.3  $\mu$ Ci/mL radiolabeled arachidonic acid (5,6,8,9,11,12,14,15-<sup>3</sup>H) (Perkin Elmer, Inc.) for 18 hrs. Cells were washed once with 0.1% fatty acid-free BSA/PBS and twice with Ca<sup>++</sup>-free PBS. SFM containing 0, 1, 3, 10, or 30  $\mu$ M MEHP or CQ in DMSO was then added to the cells. 30 min after application of the inhibitor, LH (100 ng/mL) was added to all wells other than the no treatment (NT) controls. 1 min after addition of LH, the medium was transferred to scintillation vials. Cells were removed from the plate using 0.25% trypsin/EDTA and transferred to separate scintillation vials. Total radioactivity in the medium and cell lysate was determined by scintillation counting.

### **Calcium Stimulated EGFP-cPLA<sub>2</sub> Translocation**

HEK 293 cells, stably transfected with pEGFP-cPLA<sub>2</sub> (human), were generously provided by Dr. Joseph O'Flaherty (Wake Forest University Health Sciences, Winston-Salem, NC). HEK cells were cultured at 37°C with 5% CO<sub>2</sub> in DMEM containing penicillin, streptomycin, L-glutamine, and 10% FBS (Invitrogen, Carlsbad, CA). Cells were plated at  $3.0 \times 10^5$  cells/well in two-chamber Nunc Lab-Tek II chambered cover glasses (Thermo Fisher Scientific, Rochester, NY) in DMEM with 10% FBS. After 18 hr, the medium was replaced with SFM plus DMSO, 100  $\mu$ M MEHP or 30  $\mu$ M CQ. Cells were visualized using confocal microscopy 60 min after changing to SFM. After an initial scan, cells were treated with 20  $\mu$ M calcium ionophore A23187 (Fisher Scientific, Pittsburg, PA).

## **Confocal Microscopy**

Fluorescence was detected with a Zeiss LSM 510 META laser scanning microscope (Carl Zeiss, International, Oberkochen, Germany) equipped with a 40x oil corrected lens, heated stage and incubation chamber. During microscopy, cells were maintained at 37°C and 5% CO<sub>2</sub> with a Zeiss CTI-Controller 3700 and Tempcontrol 37-2. EGFP was visualized using an Argon laser with a 488-nm laser line for excitation and a 520-nm band pass filter for emission. OFP was visualized using a He-Ne laser with a 552-nm laser line for excitation and a 570-nm band pass filter for emission.

## D. RESULTS AND DISCUSSION

### MEHP and CQ Have Similar Effects on Testosterone Production and Steroidogenic Gene Expression in MA-10 Cells

Unlike the phthalates, which showed no indication of cellular toxicity *in vitro* at concentrations up to 300  $\mu\text{M}$  (see Chapter 4), CQ induced toxicity at concentrations  $\geq 60$   $\mu\text{M}$ , as evidenced by reduced total protein ( $< 80\%$  of control). Nonetheless, CQ was found to be a highly effective inhibitor of steroidogenesis at non-toxic doses, with significant testosterone reduction at the lowest tested concentration - 1  $\mu\text{M}$  (Figure 5.2A). In fact, CQ was more potent testosterone inhibitor than MEHP. CQ was able to induce 67% inhibition at 10  $\mu\text{M}$ . MEHP required a 10-fold higher concentration to cause the same level of inhibition (Figure 5.2B).

At concentrations sufficient to cause  $\sim 65\%$  inhibition of testosterone, CQ and MEHP induced similar changes in the expression of genes required for steroidogenesis (Figure 5.3). Steroid acute regulatory protein (StAR) promotes the transport of intracellular cholesterol into the mitochondria, where the first step in its conversion to the active steroids takes place. *P450scc* and *Cyp17a1* encode enzymes responsible for the conversion of cholesterol to progesterone and testosterone. All three genes were up-regulated in the MA-10 cell upon stimulation with LH (see Chapter 4). LH stimulated expression of these genes was inhibited by pretreatment with 10  $\mu\text{M}$  CQ or 100  $\mu\text{M}$  MEHP. Down-regulation of *P450scc* by this concentration of CQ was not statistically significant, but the trend was consistent with MEHP, which caused only a 20% decrease (Figure 5.3).

The ability of CQ and MEHP to inhibit steroid production and steroidogenic gene expression is consistent with *in vivo* studies in the fetal rat. CQ and DEHP have been shown

to inhibit fetal testes testosterone production at maternal doses as low as 10 and 30 mg/kg/day, respectively. Significant down-regulation of several steroidogenic genes, including *StAR*, *P450scc* and *Cyp17a1*, is also associated with CQ and DEHP administration during gestation (Chapter 6) [80]. The similar effects on the steroidogenic pathway *in vivo* and in the MA-10 indicate that CQ and MEHP are likely to have a common target in the Leydig cell.

### **MEHP and CQ Inhibit LH-stimulated AA Release in MA-10 Cells**

CQ is known inhibitor of PLA<sub>2</sub> activity and AA release. MEHP has also been shown to prevent AA release from platelets *in vitro* [60]. In the Leydig cell, AA acts as a second messenger for LH, leading to increased transcription of steroidogenic genes, such as *StAR*, and increased steroid production. To test whether MEHP and CQ affect LH activation of the AA pathway, the release of membrane-incorporated <sup>3</sup>H-AA was measured in MA-10 cells. Treatment with LH (100 ng/mL) caused a rapid release of AA from MA-10 cells. At 1 minute, total radioactivity in the medium from LH stimulated cells was approximately 150% that of untreated cells (Figure 5.4). MEHP and CQ caused similar dose-related decreases in AA release after LH-stimulation (Figure 5.5) and abolished the burst of AA at doses in the low micromolar range (~10 μM).

The rapid response to inhibitor treatment indicates that MEHP and CQ disrupt AA signaling via interaction with PLA<sub>2</sub> protein, rather than at the transcriptional level. The PLA<sub>2</sub> enzymes consist of a broad group of proteins that catalyze the release of fatty acids from the membrane phospholipids sn-2 position [129]. cPLA<sub>2</sub>, specifically, is the essential component in the release of intracellular AA. Activation of this PLA<sub>2</sub> is regulated through

calcium ( $\text{Ca}^{++}$ ) binding and phosphorylation (Figure 5.6) [130]. The C2 domain located on the C-terminus of cPLA<sub>2</sub> binds to  $\text{Ca}^{++}$  ions, targeting the enzyme to phospholipid membranes of the endoplasmic reticulum (ER), golgi body and nuclear membrane. The cPLA<sub>2</sub> C2 domain binds the head group of phosphatidylcholine (PC), and through nucleophilic attack, the catalytic portion of the enzyme cleaves the phospholipid, releasing AA into the cell. Inhibition of AA release could be accomplished through inhibition of the initial binding of  $\text{Ca}^{++}$ , which is required for activation of the cytosolic protein, or through interference with the interaction between the activated protein and membrane phospholipids.

### **MEHP and CQ Interfere with Calcium Stimulated Translocation of EGFP-cPLA<sub>2</sub> to the Perinuclear Region**

The effect of MEHP and CQ on cPLA<sub>2</sub> activation and translocation was studied using HEK 293 cells stably transfected with EGFP-cPLA<sub>2</sub>. In the absence of inhibitor, translocation of the cytosolic protein to the perinuclear region was observed in cells over-expressing EGFP-cPLA<sub>2</sub> within 30 minutes of stimulation by the calcium ionophore A23187 (Figure 5.7A - C). In order to verify the location of the activated EGFP-cPLA<sub>2</sub>, HEK cells expressing EGFP-cPLA<sub>2</sub> were transiently transduced with a commercial ER marker containing the ER signal sequence of calreticulin coupled to orange fluorescent protein (OFP-ER) (Organelle Lights, Invitrogen, Carlsbad, CA) (Figure 5.7D - F). Prior to stimulation with the calcium ionophore, EGFP-cPLA<sub>2</sub> is not concentrated at the ER, but is dispersed throughout the cytoplasm. After activation with the calcium ionophore, colocalization of the EGF-cPLA<sub>2</sub> and OFP-ER marker is clearly observed (Figure 5.7G - I). EGFP-cPLA<sub>2</sub> becomes highly concentrated around the nucleus.

Pre-treatment with 100  $\mu$ M MEHP for 1 hr prior to stimulation with A23187 caused notable inhibition of cPLA<sub>2</sub> translocation to the perinuclear region (Figure 5.8). Interestingly, it appears that cPLA<sub>2</sub> is still activated in the presence of MEHP. However, rather than concentrating at the ER, small clusters of the EGFP-tagged protein are scattered throughout the cell. This speckled appearance is remarkably similar to the behavior reported in cells stimulated with arachidonic acid rather than calcium ionophore [168]. Wooten and coauthors reported that these sites of cPLA<sub>2</sub> concentration corresponded to organelles that were discrete from the golgi body and largely composed of lipids. CQ caused the same punctate behavior as MEHP in A23187 stimulated cells (Figure 5.8). Neither MEHP nor CQ affected distribution of EGFP-cPLA<sub>2</sub> in the absence of calcium ionophore (not shown). The fact that the cPLA<sub>2</sub> protein attempts to respond to calcium stimulation, but does not appear to bind the nuclear membrane indicates that the interaction between these inhibitors and cPLA<sub>2</sub> occurs after binding of Ca<sup>++</sup> to the C2 domain, but prior to binding to the phospholipid membrane.



## D. CONCLUSIONS

From the literature, it is apparent that the release of AA by PLA<sub>2</sub> is a regulatory step in testosterone production [55, 131, 132] and that MEHP can inhibit PLA<sub>2</sub> activity [60, 73]. Our studies show that MEHP and CQ, a known PLA<sub>2</sub> inhibitor, have similar effects on steroid synthesis, steroidogenic gene expression and LH-stimulated AA release in Leydig cells. Based on these studies, together with the ability of MEHP to inhibit translocation, but not activation, of cPLA<sub>2</sub>, we propose the following mechanism of action for MEHP in the Leydig cell. The longer chain alkyl phthalates mimic the shape of the phospholipid head group of phosphatidylcholine, bind Ca<sup>++</sup> activated C2 domain and preventing binding to the nuclear/ER membrane. Reduced AA may be responsible for diminished gene transcription and subsequent steroid synthesis, particularly in the fetal Leydig cell, where LH feedback is not fully established. Examination of the 2-dimensional chemical structures for the known PLA<sub>2</sub> inhibitors, CQ and quinacrine, and the testosterone inhibitor, MEHP, show striking similarity to the portion of PC that is thought to bind to the C2 domain of cPLA<sub>2</sub> (Figure 5.7). Additional studies are underway to better define the nature of the interaction between endocrine active phthalates like MEHP and cPLA<sub>2</sub>.

**Figure 5.1. Two-pathway model for Co-Regulation of Testosterone in the Leydig Cell.**

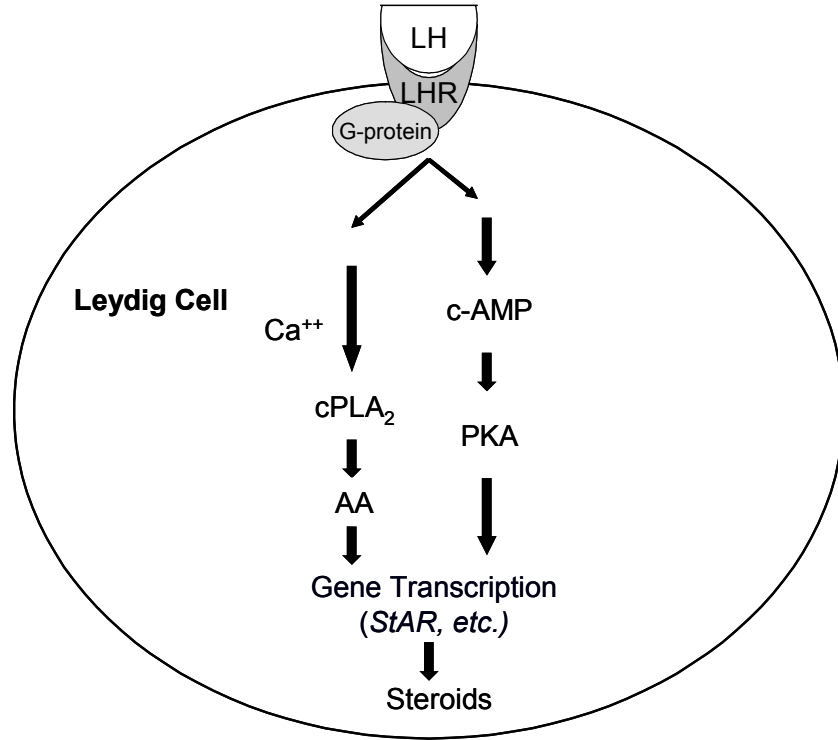


**Figure 5.2. Effect of MEHP and CQ on LH-stimulated testosterone synthesis in MA-10 cells.**

Cells pre-treated with DMSO or various concentrations of (A) MEHP or (B) CQ for 24 hr in SFM prior to stimulation with 100 ng/mL LH. Each data point represents the mean  $\pm$  SE from 3 separate experiments performed in triplicate. \* $p < 0.05$ , 1-Way ANOVA, Dunnetts post-test.

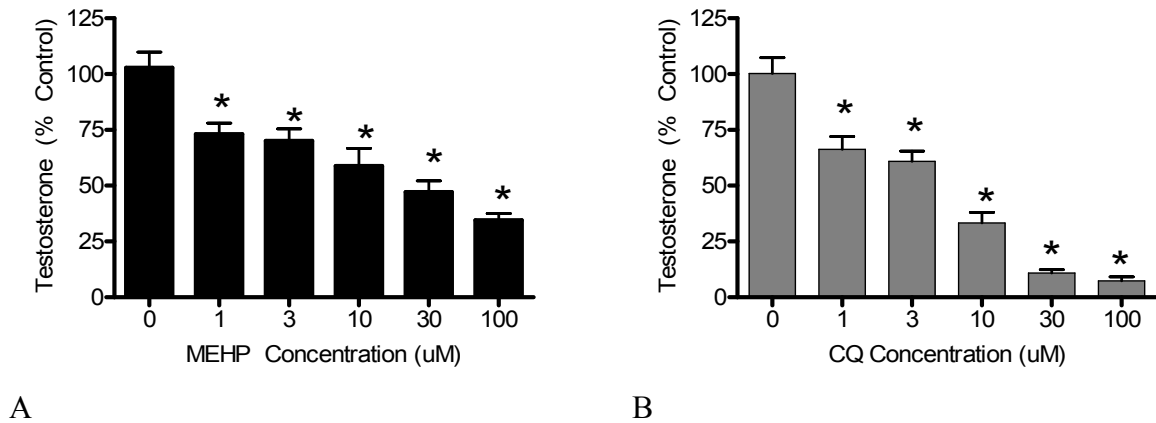


**Figure 5.3. Effect of MEHP and CQ on steroidogenic gene expression in MA-10 cells.**

Cells were pretreated with DMSO, 100  $\mu$ M MEHP, or 10  $\mu$ M CQ for 24 hr prior to stimulation with 100 ng/mL LH. Bars represent mean  $\pm$  SE (n=6) of the values measured via RT-PCR. \*p< 0.005, \*\*p=0.0005, \*\*\*p<0.0001 Student's t-test for treatment vs. LH control groups.

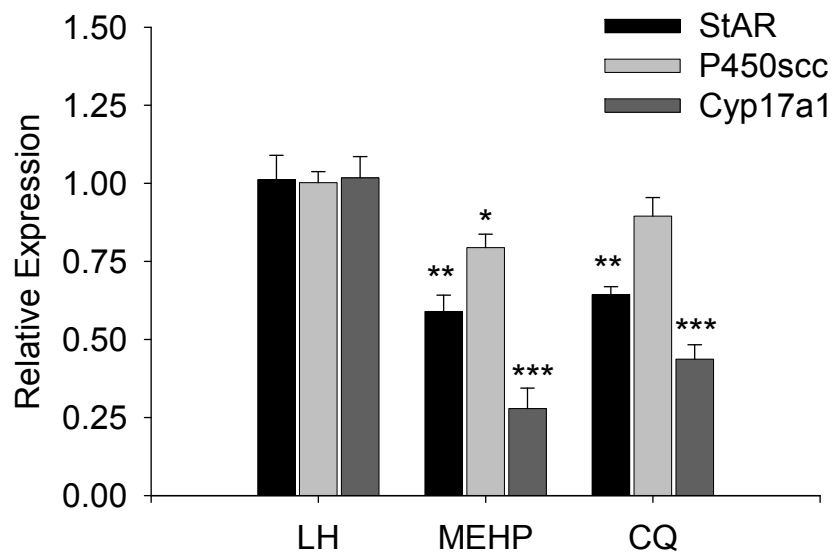


**Figure 5.4. LH Stimulation of Arachidonic Acid Release from MA-10 Cells.**

Cells were incubated with 0.3  $\mu\text{Ci}/\text{mL}$   $^3\text{H}$ -AA in serum free medium for 18 hrs, rinsed with  $\text{Ca}^{++}$ -free PBS, and incubated in SFM for 30 min. 1 min after stimulation with 100 ng/mL LH, medium was removed and analyzed for total radioactivity with a liquid scintillation counter. Data points represent mean  $\pm$  SE from 3 independent trials with treatments performed in triplicate. \*\*\* $p \leq 0.0001$ , student's t-test.

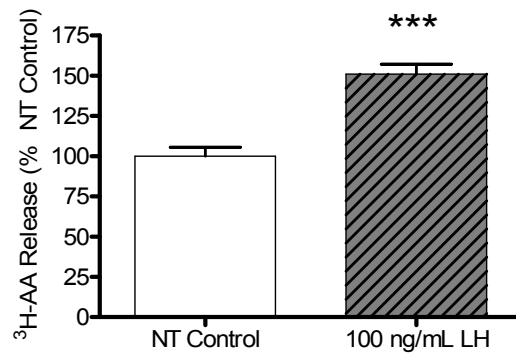


**Figure 5.5. Effect of MEHP and CQ on arachidonic acid release in MA-10 cells.**

Cells were incubated with 0.3 uCi/mL AA in serum free medium for 18 hrs. After washing with Ca<sup>++</sup> free PBS, cells were treated with inhibitor or DMSO in SFM for 30 min, followed by stimulation with 100 ng/mL LH. 1 min after LH, medium was removed and analyzed with a scintillation counter. Data points represent mean  $\pm$  SE of 3 independent trials with treatments performed in triplicate. \*p < 0.05, 1-Way ANOVA, Dunnett's post-test.

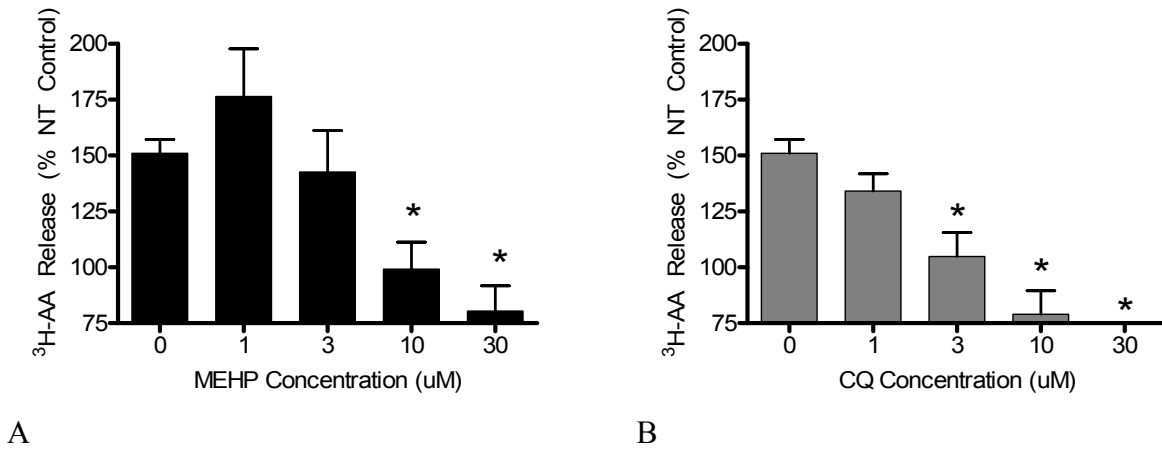


**Figure 5.6. Activation, translocation and phospholipase activity of cPLA<sub>2</sub>.**

Ca<sup>++</sup> ions bind the free C2 domain of resting cPLA<sub>2</sub>, resulting in a conformational change that allows the C2 domain to bind phospholipid head groups, particularly phosphatidylcholine (PC). Once bound, the catalytic region penetrates the phospholipid membrane and cleaves PC at the sn-2 position, releasing AA into the cell. Phosphorylation of membrane-bound cPLA<sub>2</sub> at serine-505 is not necessary for phospholipase activity, but acts to retain cPLA<sub>2</sub> at the membrane and increase AA release [133].

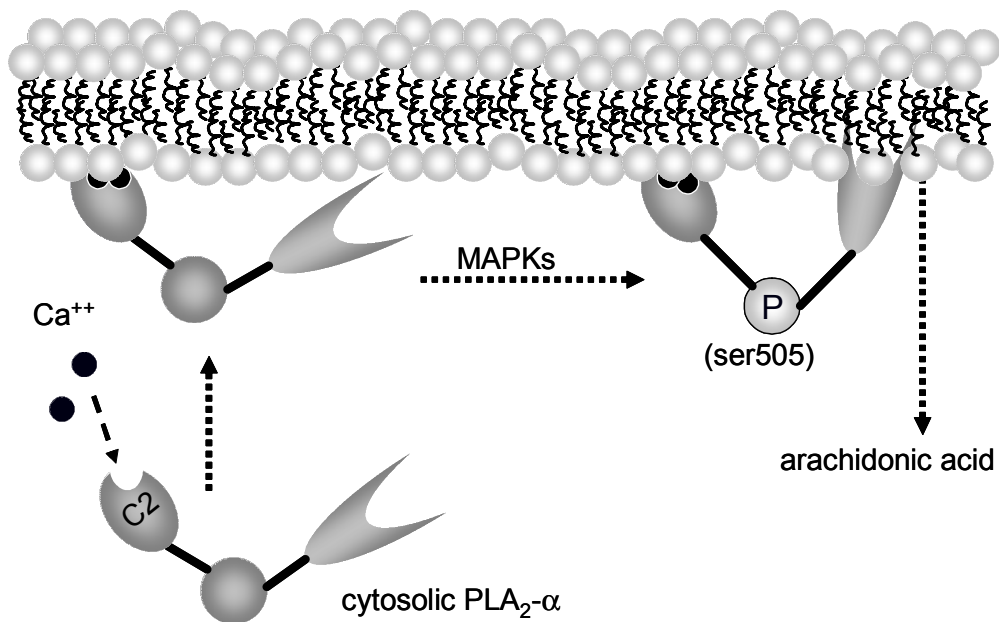


**Figure 5.7. Calcium stimulated translocation of EGFP-cPLA<sub>2</sub> in control cells.**

HEK 293 cells stably transfected with pEGFP-cPLA<sub>2</sub> and transiently transduced with an orange fluorescent protein-tagged endoplasmic reticulum (ER) marker. Cells were treated with vehicle for 1 hr and scanned just before (A, D, G), 14 minutes (B, E, H) or 30 minutes (C, F, I) after (C, F, I) stimulation with 20  $\mu$ M A23187. Panels A-C illustrate response of EGFP-cPLA<sub>2</sub> to calcium ionophore. Panels D-F show ER marker at 0, 14, and 30 minutes. Panels G-I show areas of overlap of the EGFP-cPLA<sub>2</sub> and OFP-ER marker in yellow.

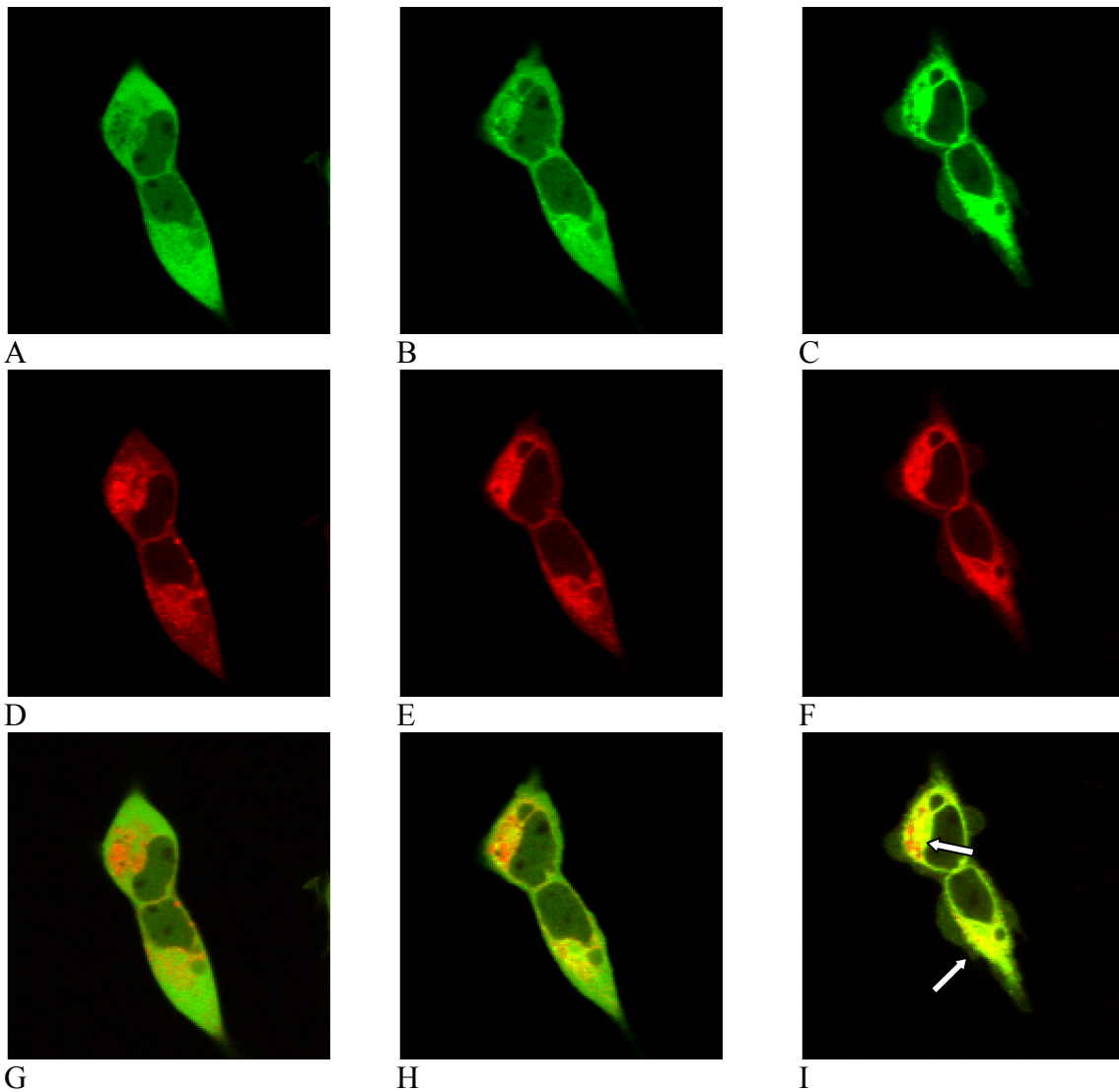




**Figure 5.8. Inhibition of EGFP-cPLA<sub>2</sub> translocation by MEHP and CQ.**

Control cells were treated with vehicle for 1 hr and scanned just before (A, C) or 30 minutes after (B, D) stimulation with A23187. MEHP treated cells were incubated in 100  $\mu$ M MEHP for 1 hr and scanned just before (E, G) or 30 min after (F, H) stimulation with A23187. CQ treated cells were incubated with 30  $\mu$ M CQ for 1 hr and scanned just before (I, K) or 30 min after (J, L) stimulation with A23187.

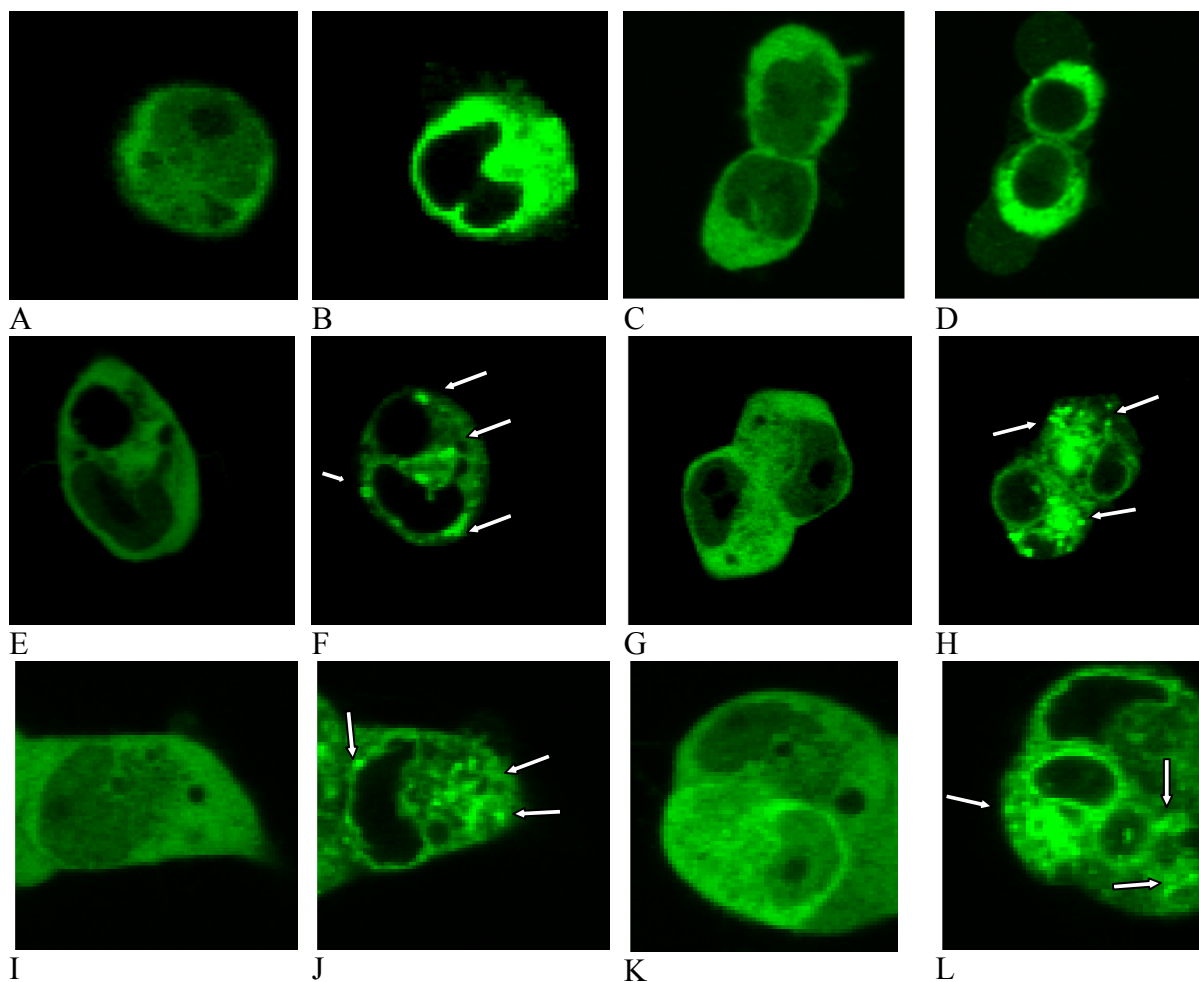
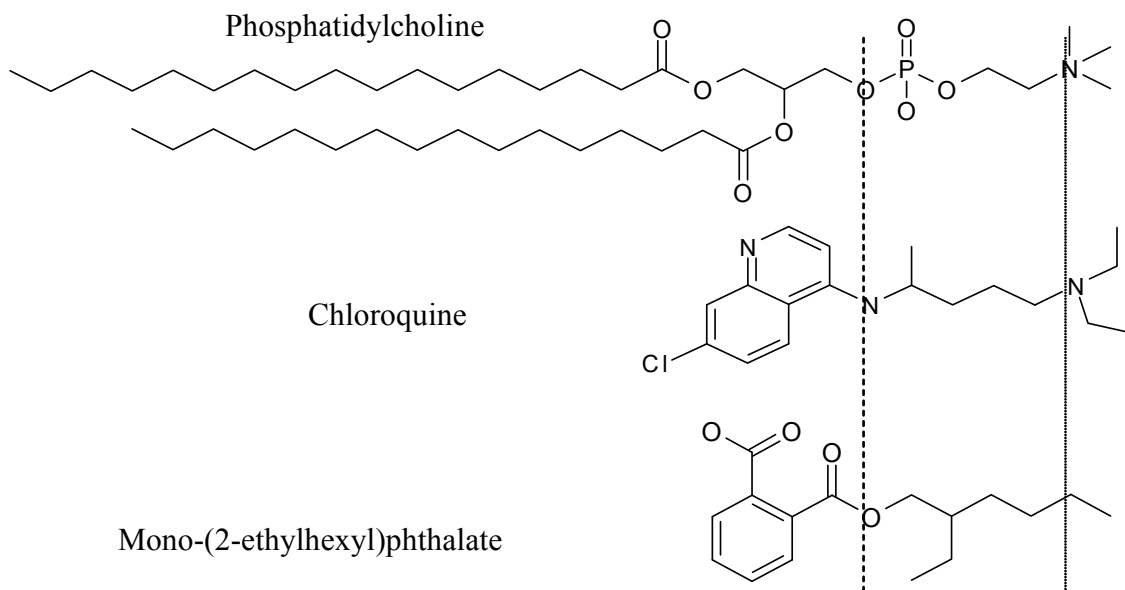


**Figure 5.9. Two-dimensional structures of the natural ligand for cPLA<sub>2</sub>, phosphatidylcholine, and potential inhibitors CQ and MEHP.**

Dotted lines indicate areas of structural similarities that may mediate binding of substrate, CQ, and MEHP to the C2 domain. The phospholipid is shown, without charges on the phosphate group or the quaternary nitrogen, esterified with aliphatic fatty acids. cPLA<sub>2</sub> catalyzes the release of arachidonic acid from the sn-2 position of the phospholipid.



## CHAPTER 6

### **In Utero Exposure to Chloroquine Alters Sexual Development in the Male Fetal Rat**

This chapter was submitted for publication in *Toxicology and Applied Pharmacology* in March 2009.

## A. ABSTRACT

Chloroquine (CQ), a drug that has been used extensively for the prevention and treatment of malaria, is currently considered safe for use during pregnancy. However, CQ has been shown to disrupt steroid homeostasis in adult rats and similar compounds, such as quinacrine, inhibit steroid production in the Leydig cell *in vitro*. To explore the effect of *in utero* CQ exposure on fetal male sexual development, pregnant Sprague-Dawley rats were given a daily dose of either 0 or 100 mg CQ/kg/day from GD 16-18 by oral gavage. Three days of CQ treatment resulted in reduced maternal and fetal weight on GD 19 and increased necrosis and steatosis in the maternal liver. Fetal livers also displayed mild lipid accumulation. Maternal serum progesterone was increased after CQ administration. Fetal testes testosterone, however, was significantly decreased. Examination of the fetal testes revealed significant alterations in vascularization and seminiferous tubule development after short-term CQ treatment. Anogenital distance was not altered. Microarray and RT-PCR showed down-regulation of several genes associated with cholesterol transport and steroid synthesis in the fetal testes. This study indicates that CQ inhibits testosterone synthesis and normal testis development in the rat fetus at human relevant doses.

## B. INTRODUCTION

Chloroquine (CQ) is a commonly prescribed drug in the treatment and prevention of malaria and several connective tissue disorders, including rheumatoid arthritis and lupus. For the treatment of malaria [134], CQ is typically administered in three doses over a period of three weeks (25 mg/kg/dose). Connective tissue disorders usually require lower doses (~ 5 mg/kg/day) that can continue for many years [135]. Negative side-effects associated with long-term CQ treatment range from rashes and gastrointestinal discomfort to retinopathy, a degenerative condition resulting from CQ accumulation in the eye [136]. In rare cases, CQ treatment can have more serious health effects, such as neuropathy, myopathy, and cardiomyopathy [135, 136].

CQ is generally considered safe for use in pregnant women based on lack of evidence of increased miscarriage or overt birth defects in offspring of exposed mothers [137]. Yet, despite its widespread use, few reproductive toxicity studies are available for CQ, particularly at doses that are relevant to human exposures. At doses as low as 10 - 40 mg/kg/day the offspring of rats treated during gestation and lactation have reduced body and organ weights and delayed lung development [138, 139]. Much higher doses (700 mg/kg once during gestation) produce liver toxicity in the offspring, whether CQ was administered in early or late gestation [140]. This same CQ dose administered for fifteen days in gestation caused severe structural defects, reduced weight and liquification of visceral organs in the fetus [141].

Many of the adverse effects of CQ exposure (*e.g.*, lipidosis) are associated with its ability to interfere with lipid metabolism [142, 143]. One molecular target of CQ is phospholipase A<sub>2</sub> (PLA<sub>2</sub>) [144]. CQ inhibits phospholipid metabolism by PLA<sub>2</sub>, leading to

reduced intracellular arachidonic acid (AA) – a second messenger involved in numerous signaling pathways. AA release is a necessary component of the Leydig cell's steroidogenic pathway [55, 61]. Thus, the ability of CQ to inhibit AA signaling may have downstream effects on steroid production. *In vivo*, CQ disrupts steroid homeostasis in both the adult male and female rat [145-147] and adversely affects fertility [148] as well as the structural integrity of the adult male testes at relatively low doses ( $\geq 0.57$  mg/kg/day) [146, 148, 149]. Since CQ is efficiently transferred to the fetus [150, 151], it may also interfere with steroidogenesis during fetal development, a time in which testosterone production is critical for normal sexual development. The effect of CQ on testosterone-dependent sexual development has not been reported. The purpose of the current study was to determine whether CQ affects testosterone production in the fetal rat and normal sexual development in male pups. Indicators of overt reproductive tract toxicity (reduced anogenital distance, testis morphology) and early markers of perturbation of steroidogenesis (testosterone production, steroidogenic gene changes) were examined in the fetal rat.

## C. METHODS

### Animals

Pregnant Sprague-Dawley (CrI:CD(SD)) rats (sperm plug positive GD 0) were obtained from Charles River Laboratories (Raleigh, NC) and housed in the Animal Care Facility of the The Hamner Institutes for Health Sciences, which is accredited by the Association for Assessment and Accreditation of Laboratory Animal Care International. Rats were acclimated in a temperature- and humidity-controlled, HEPA-filtered environment on a 12 hr light-dark cycle. NIH rodent diet (NIH-07, Zeigler Bros., Gardner, PA) and reverse-osmosis water were provided *ad libitum*. This study was approved by The Hamner Institute's Animal Care and Use Committee.

### Dosing Solutions

The stock solution was prepared by mixing chloroquine diphosphate salt (CQP) (CAS# 50-63-5; Sigma-Aldrich, St. Louis, MO) and reverse osmosis water to reach a nominal CQ (adjusted by molar ratio) concentration of 200 mg/mL. The dosing solution was prepared with a 1:2 dilution of the 200 mg CQ/mL stock solution in reverse osmosis water, for a nominal concentration of 100 mg CQ/mL. After adjusting for the molar ratio, CQ concentrations in the stock and dosing solutions were determined to be 203.5 and 98.7 mg CQ/mL using high performance liquid chromatography (HPLC) and UV-Vis detection [152]. No CQ was detected in the water used for control animals.

## Treatment

Pregnant rats (n = 6 per dose) were dosed once daily by oral gavage on gestation days (GD) 16-18 with reverse osmosis water or CQ. On GD 16, the dams in the treatment group were given a loading dose (1mL/kg) of 200 mg/kg CQ. This dose was followed by maintenance doses of 100 mg CQ/kg on GD 17 and 18. Maternal body weights were recorded daily at the time of dosing. All dams were euthanized by CO<sub>2</sub> asphyxiation and exsanguination on GD 19 (24 hrs after the final dose). Sacrifice times were randomized between the control and treatment group to minimize influence of time-dependent differences in hormone production on dose-response data. Maternal blood was collected via cardiac puncture. Serum was obtained from maternal blood by allowing the samples to sit at room temperature for 1.5 hrs, followed by centrifugation at 2500 rpm for 15 min (4°C). Serum samples were kept at 4°C until clinical chemistry was performed (< 2 hrs). Maternal liver was removed and two sections of the left lobe were processed for histopathology by either snap-freezing in liquid nitrogen or fixing in 10% formalin.

Fetuses were delivered by cesarean section, weighed and AGD was assessed using a dissecting microscope and micrometer lens (accuracy 0.05 mm). All fetuses were euthanized by decapitation, sexed by internal inspection of the reproductive organs, and testes were collected from the male fetuses. The testes pair of one male fetus from 5 control and 5 treated dams were processed for frozen sections. The trunk of 1 male fetus of each litter was fixed in modified Davidson's fixative after sexing, but before removal of the testes. The remaining fetal testes pairs were placed in separate cryogenic vials, snap-frozen in liquid nitrogen, and stored at -80°C. The liver of one male fetus per litter was collected and



processed for histopathology: one half was prepared for frozen section and the other half was fixed in 10% formalin, stained with hematoxylin and eosin and evaluated histologically.

### **CQ Analysis in Dosing Solutions**

Stock CQP solution was prepared by dissolving 10 mg CQP (Sigma-Aldrich, St. Louis, MO) in reverse osmosis water. Standard solutions (0 – 600 µg/mL) and quality control standards were prepared by diluting the stock solution with the appropriate amount of reverse osmosis water. CQP dosing solutions were diluted with water until they were within the linear range of the calibration curve (100 – 500 µg/mL). Diluted dose solutions and extracted tissue samples were analyzed on an Agilent 1100 HPLC with a spectrophotometric detector (Agilent, Palo Alto, CA). HPLC analysis used a reverse phase C-18 column (5 µm, 4.6 x 250 mm), and a solvent flow rate of 1.5 mL/min. Column temperature was maintained at 40°C. Separation was achieved using a 2 solvent (A: 0.1%formic acid in water, B: 0.1%formic acid in acetonitrile) gradient. The solvent was maintained at a 95/5% A/B for 1 min and then increased to 100% solvent B at 5 min. 100% Solvent B was maintained for 2.5 min, and then decreased over 0.5 min to reach the initial solvent mixture of 95% solvent A, 5% solvent B. Injection volume was 20 µL. Detector absorbance was set to 254 nm, with a 20 mm bandwidth. Peak area counts were calculated by subtracting background (determined from blank samples) and comparing to calibration standards, both averaged by analysis date.

### **CQ Analysis in Serum Samples**

Analysis of CQ in rat serum was performed using a published method (Lejuene et al., 2007) with some modifications. Serum (100 µL) was thawed, transferred to a polypropylene

tube with 200  $\mu$ L acetonitrile and vortexed to precipitate serum proteins. Samples were then acidified with 700  $\mu$ L 0.1% trifluoroacetic acid, vortexed, and cooled at 4°C for 15 min. Supernatant was collected after centrifugation (10,000 rpm for 4 min) and analyzed via LC/MS/MS (Applied Biosystems, Foster City, CA). The liquid chromatograph (Perkin Elmer Series 200, Norwalk, CT) was equipped with two MicroPumps, autosampler, and on-line Vacuum Degasser. Chromatography was performed on a Luna<sup>®</sup> phenyl-hexyl column (50 mm x 2 mm x 3  $\mu$ m). The mobile phase consisted of 0.1% formic acid in HPLC-grade water and acetonitrile. The acetonitrile content was increased from 25 to 100% over 7 min, with a 3 min post-run equilibration time. Column effluent was diverted to waste during pre-run and post-run equilibration using a Valco (Houston, TX) Model C2 6-port switching valve. Methanol-water (50:50, v:v) solvent was delivered using a make-up pump (Spectroflow 400, Kratos Analytical, Ramsey, NJ) when column effluent was diverted to waste.

MS analysis (Applied Biosystems API 3000) was conducted in positive ion mode with a turbo ionspray interface. Curtain, nebulizing, and collision gases were set in the PE Sciex Analyst 1.1 software at 10 (nitrogen), 7 (air), and 4 (nitrogen), respectively. Turbospray gas was nitrogen at 7 L/min at 375°C. The nebulizing potential, declustering potential, and focusing potential were 4600 V, 61 V and 200 V, respectively. Quantitation was performed using selected reaction monitoring of precursor-product ion transitions at m/z 320.4 to 246.9. Collision energy was optimized to 25 eV. Data acquisition and initial analysis used PE Sciex Analyst 1.1 software on a Dell Precision 360 computer (Austin, TX). Integration data were manually corrected, if necessary, and then transferred to Excel<sup>™</sup> (Microsoft<sup>®</sup>, Redmond, WA) for analysis.

### **Maternal Serum Hormone Analysis**

Maternal serum progesterone (PG) and estradiol (E2) levels were determined from individual dams using commercially available ELISA assay kits (Neogen Corporation, Lexington, KY) according to the manufacturer's directions. PG and E2 were extracted from 50  $\mu$ L of serum in 1000  $\mu$ L of diethyl ether (Sigma-Aldrich, St. Louis, MO). The organic layer was removed, dried under nitrogen and resuspended in 200 – 500  $\mu$ L steroid diluent provided with the ELISA kits. Samples were assayed in duplicate.

### **Fetal Testosterone Analysis**

Fetal testes testosterone concentration was determined from all fetuses remaining after samples were taken for histopathology and gene expression analysis. Testes from individual fetuses were assayed according to the method of Shultz et al. [123]. Each testes pair was homogenized in 100 mL of PBS-Gelatin buffer. The homogenate was then extracted three times with a total of 1 mL of a fresh mixture of ethyl acetate and chloroform (4:1). Extracts were dried under nitrogen and resuspended in 100  $\mu$ L steroid diluent (MP Biomedicals, Solon, OH). An aliquot (25 or 50  $\mu$ L) of each testes sample was analyzed using a Testosterone Double Antibody RAI kit (MP Biomedicals). Samples from different fetuses were not pooled.

### **Bicinchoninic Acid (BCA) Protein Assay**

Protein concentration in fetal testes homogenate (5  $\mu$ L) was quantified using a commercially available bicinchoninic acid (BCA) method (Sigma-Aldrich, St. Louis, MO).

## **Histopathology**

One pair of GD19 fetal testes per litter from control rats (n=6) and rats treated with 100mg/kg CQ (n=6) were immersion-fixed in modified Davidson's fixative for 24 hr and then embedded in paraffin. A section of the left lobe of the maternal liver and one half of the liver from one fetus per dam (n=5/dose) were fixed in 10% neutral buffered formalin and embedded in paraffin. Paraffin embedded sections (5  $\mu$ m) of livers and testes were prepared and stained with hematoxylin and eosin. Maternal and fetal liver morphology was evaluated subjectively for lesions. Centrilobular degeneration was graded on a scale of 1 to 4, where 1 indicated minimal degeneration and 4 indicated marked degeneration. Fetal testes seminiferous tubule diameter was evaluated quantitatively using Image Pro Plus software (version 4.5; Media Cybernetics, Carlsbad, CA).

The remaining portions of the maternal and fetal livers were frozen, sectioned with a microtome and placed on slides. One pair of fetal testes per litter from control (n=5) and CQ treated rats (n=5) were frozen as before, cut and placed on slides. Oil Red O staining of maternal liver, fetal liver and fetal testes frozen sections was performed as previously described [153]. Lipid staining was evaluated subjectively using a scale of 1 to 4, with a score of 1 indicating minimal and 4 indicating marked lipid staining.

## **Clinical Chemistry**

Serum samples were analyzed for alkaline phosphatase (ALP), alanine aminotransferase (ALT) and creatinine (Cre) using commercially available assay kits

according to the manufacturer's instructions (Pointe Scientific, Canton, MI). Samples were analyzed on a COBAS Fara II (Roche Diagnostics, Switzerland).

### **Microarray Hybridization**

RNA was isolated from the testes of one individual fetus from each dam. Testes were homogenized in RNA Stat-60 reagent (Tel-Test, Friendswood, TX) and processed using the RNeasy Mini Kit (Qiagen, Valencia, CA) according to the manufacturer's protocol. RNA concentration was determined spectrophotometrically and integrity was assessed using the Agilent 2100 Bioanalyzer (Agilent Technologies, Palo Alto, CA). Double stranded DNA was synthesized from 2.5 µg of total RNA using a one-cycle cDNA synthesis kit (Affymetrix, Santa Clara, CA). Biotin-labeled cRNA was transcribed from the cDNA using the Gene Chip IVT labeling kit (Affymetrix, Santa Clara, CA). Labeled cRNA (15 µl) was fragmented and hybridized to the Affymetrix Rat Genome 230 2.0 microarray, which allows for measurement of over 28,000 genes representing the entire rat genome. Each RNA sample was hybridized to a single microarray giving a total of 12 microarrays.

### **Microarray Analyses**

A robust singular value decomposition algorithm was used to summarize the expression levels based on the probe level data. After normalization, the first robust principal component of the perfect match was extracted and the mean of the fitted value was used as the signal intensity. A log<sub>2</sub> transformation was performed to stabilize the variance. A Student's t-test was performed to compare gene expression between the CQ treated and

control animals. Probability values were adjusted for multiple comparisons using a false discovery rate of 5% (FDR = 0.05).

### **Quantitative RT-PCR**

Total RNA was isolated from the testes of one fetus per litter from five control dams and five dams from the CQ treated group using RNA STAT-60 reagent (Tel-Test, Friendswood, TX) and the RNeasy Mini Kit (Qiagen, Valencia, CA). cDNA was prepared for each sample using the High Capacity cDNA kit (Applied Biosystems, Foster City, CA) according to the manufacturer's protocol. Polymerase chain reactions (PCR) were performed on the Taqman 7900HT system (Applied Biosystems, Foster City, CA). Taqman gene expression assays for rat *Cyp17A1* (RN00562601), *GAPDH* (4352338E), *Nppc* (RN00587070), *P450scc* (RN00568733), *SR-B1* (RN00580588), *StAR* (RN00580695) and *Tm7sf2* (RN01479184) were purchased from Applied Biosystems (Foster City, CA). Samples were run in triplicate and the change in expression of target genes was normalized to *GAPDH*. The fold change for each gene normalized to GAPDH and relative to expression in control testes was determined by the  $2^{-\Delta\Delta C_t}$  method [121].

## **D. RESULTS**

### **Analytical Chemistry**

Though CQ kinetics are not well defined, the relatively long half-life (~7 hrs) [167] indicated that CQ would be present in detectable levels in the serum of the rats 24 hrs after the final dose. CQ concentrations were therefore measured in maternal serum taken at the time of sacrifice in an attempt gain some understanding of internal dose associated with observed effects. Maternal serum CQ levels were  $1.6 \pm 0.4$  mg/L (mean  $\pm$  SE) in the 100 mg/kg/day dose group at 24 hrs post-dosing. CQ was not detected in the serum of control animals.

### **Body weight changes and liver toxicity**

Maternal body weight was significantly reduced after three days of CQ treatment (Table 6.1). The maternal liver weight was also reduced. However, the body weight adjusted liver weight (g liver/g BW) was not different between the treated and control groups. Fetal body and absolute liver weight also showed a small, but statistically significant ( $p < 0.001$ ) reduction in weight after CQ treatment (Table 6.1). Again, the fractional liver weight was not significantly different between the two groups. Some fetuses in the 100 mg/kg/day dose group displayed significant edema.

After three doses of 100 mg CQ/kg, the clinical chemistry did not indicate kidney or liver toxicity. Maternal serum ALT, ALP, and creatinine levels in exposed dams were not significantly different from controls (Table 6.1). Treatment effects were noted, however, upon histological examination of the maternal livers (Table 6.1). Three of the CQ treated

dams exhibited centrilobular degeneration that was not present in the control group (Figure 6.1A-B). Oil Red O staining revealed mild to moderate steatosis in 5 out of the 6 dams given CQ (Figure 6.2A-B). Examination of the fetal livers did not show evidence of necrosis after staining with hematoxylin and eosin (Figure 6.1C-D). Three of the six fetuses in the CQ treated group had increased liver lipid content (grade 1-2) when stained with Oil Red O (Figure 6.2C-D).

### **Effect of CQ on Hormone Homeostasis and Male Fetus Sexual Development**

Maternal and Fetal Hormone Measurement. To determine whether CQ affected hormone levels in the pregnant rat, maternal serum samples from control and CQ treated dams collected at the time of sacrifice (24 hrs after the final dose) were analyzed for estradiol (E2) and progesterone (PG). Serum E2 was reduced by 33% in CQ treated dams, though the difference was not statistically significant ( $p = 0.13$ , Student's t test). Interestingly, serum PG was significantly increased ( $p = 0.003$ ) in CQ treated dams (Figure 6.3). Testosterone was also measured in the testes of the male fetuses taken at the time of sacrifice. Testes testosterone was significantly reduced after CQ exposure (Figure 6.4).

Male Fetal Reproductive Tract Morphology and Testis Histopathology. Reduced anogenital distance (AGD) is a commonly used marker of feminization in male rats. In the current study, AGD was evaluated in both male and female pups (Figure 6.5). CQ treatment had no effect on AGD measured at GD 19 in either the male or female fetuses. Visual inspection of the gonads at the time of sacrifice revealed some changes in the testes vasculature after CQ exposure. Typically, by GD 19 the fetal rat testis has a visible, well-developed unbranched testicular artery displaying characteristic convolutions (Figure 6.6A).



In the CQ treated group, however, the testicular arteries were less organized. The coiling of the main artery was reduced and looping was less uniform (Figure 6.6B).

Cross sections from the testes of one male fetus of each litter were stained with hematoxylin and eosin and evaluated for CQ related changes in morphology. Three days of CQ treatment did not significantly affect the organization of the fetal testes. However, when the widths of the seminiferous tubules were measured, treatment effects were noted. Seminiferous tubules in the CQ treated testes were significantly larger in diameter than those of the control group ( $66 \pm 1$  vs.  $62 \pm 1$   $\mu\text{m}$ , mean  $\pm$  SE) ( $p < 0.005$ , Student's *t*).

Fetal Testes Gene Expression. Relative gene expression was examined in the fetal testes of the 0 and 100 mg CQ/kg/day groups using genome-wide Affymetrix microarrays. Of 28,000 genes on the array, only 6 genes were statistically different from controls (FDR adjusted  $p < 0.05$ ) (Table 6.2). Of the significantly altered genes in the 100 mg/kg/day group, 5 have been characterized, all of which were down-regulated. Argininosuccinate synthetase (*Ass*), saccharopine dehydrogenase (*Sccpdh*), coenzyme Q homologue (*CoQ*), and aldehyde dehydrogenase 1 family, member B1 (*Aldh1b1*) are associated with regulation of molecular oxygen. Serine/threonine kinase receptor associate protein (Strap) is a negative regulator of TGF $\beta$  signaling.

When the stringency of the tests for significance were relaxed to include all gene changes  $\geq 1.5$ -fold, trends were also seen in genes associated with cytoskeleton organization, extracellular matrix proteins, intracellular calcium binding/regulation, oxygen and nitric oxide regulation, and fatty acid, cholesterol and steroid synthesis (Table 6.3). Five genes associated with cholesterol and steroidogenesis were down-regulated with at least 1.5-fold change from control.

Transmembrane 7 superfamily member 2 (*Tm7sf2*) and steroid acute regulatory (*Star*) protein are involved in steroid synthesis. *Tm7sf2* encodes 3 $\beta$ -hydroxysterol- $\Delta^{14}$ -reductase (3 $\beta$ HSR), an enzyme required for the conversion of lanosterol to cholesterol [154]. StAR protein regulates the transport of cholesterol into the mitochondria where it is metabolized to pregnenolone [155].

Natriuretic peptide precursor type C (*Nppc*) and the prolactin receptor (*PRL*) are associated with external signaling of steroidogenesis. *Nppc* encodes C-type natriuretic peptide (CNP), which has been shown to stimulate fetal rat testosterone production *in vitro* [156]. In the testes, this peptide is localized in the Leydig cell [157]. Peptides such as CNP may be responsible for regulation of fetal testosterone production prior to pituitary secretion of luteinizing hormone [156]. The role of the pituitary hormone prolactin and its receptor in steroidogenesis is not well defined. However, secretion of prolactin has been shown to be regulated by estrogen levels, and administration of prolactin is associated with altered testosterone levels in the rat. In cultured fetal rat Leydig cells, prolactin induces testosterone production [158]. Other genes that showed at least 1.5-fold difference between fetal testes from the CQ treated and control groups, such as stanniocalcin 2 (*Stc2*), visinin-like 1 (*Vsnl1*), and pregnancy induced growth inhibitor (*Okl38*), have not been definitively linked to

steroidogenesis. However, the changes in expression of these genes in this study were consistent with studies of other steroid synthesis inhibitors (*e.g.*, phthalate esters;[131]).

RT-PCR was performed on fetal testes samples from 5 control and CQ treated animals to confirm the trend in steroidogenic genes indicated by the current microarray study. Confirmation with RT-PCR revealed statistically significant decreases in *Star*, *Tm7sf2* and *Nppc* with CQ treatment (Figure 6.7A), which were consistent with the fold-changes from the microarray study (Table 6.3).

The expression of three additional steroidogenic genes (*SR-B1*, *Cyp17A1*, and *P450scc*) were evaluated using RT-PCR in an effort to obtain more targeted information about the effect of prenatal CQ treatment on steroidogenesis in the fetal testes (Figure 6.7B). These genes are typically induced in the testosterone-producing cell and are consistently down-regulated in the testes of fetal rats after exposure to known inhibitors of steroid synthesis, such as the phthalate esters [46, 80, 123]. Scavenger receptor class B type 1 (SR-B1) regulates uptake of cholesterol into the Leydig cell [159], while *Cyp17A1* and *P450scc* are required for the conversion of cholesterol to testosterone. All three genes were significantly down-regulated ( $p < 0.05$ ) in the CQ exposed fetal testes when evaluated by RT-PCR. These gene changes were consistent with the microarray results: relative expression values for SR-B1, *P450scc* and *Cyp17a1* in CQ treated animals were 0.73, 0.87, and 0.71 when compared to controls.

## E. DISCUSSION

CQ was administered to late-term pregnant rats at doses that are comparable to those recommended for the pregnant human. After three days of exposure, maternal rats exhibited signs of general toxicity, including reduced weight gain and general lethargy. CQ treatment at 100 mg/kg/day was associated with morphological liver changes in the maternal rat, as evidenced by increased incidence of centrilobular degeneration and steatosis. Fetal rats in the CQ treated group also had reduced body weight when compared to controls, and mild lipidosis was noted in the histopathology of the fetal livers.

Clinical signs of toxicity were consistent with those presented in the literature. CQ is known to cause liver toxicity in rats when given at high doses or for long periods of time (>1 week) [160, 161]. Lipidosis, in particular, is a common result of CQ administration in the rat [142, 143]. While little work has been done to characterize CQ toxicity *in utero*, a recent study found that newborn rats exposed to CQ during gestation and lactation (10 mg/kg/day) had decreased liver weights, potentially indicating hepatotoxicity [140]. Our study confirms the CQ-induced reduction in liver weight. However, when adjusted for body weight, the relative liver weight was the same in control and treated rats. This, together with the lack of change in the morphology, indicates that the fetal liver is not a major target of CQ toxicity. Nonetheless, staining with Oil Red O does indicate some potential for development of fatty liver in the fetus.

The more significant finding in our study was the CQ-induced alteration in steroid hormone homeostasis in the both the dam and the male fetus after three days of treatment. In the maternal rat, the decrease in serum estradiol, while not statistically significant, is consistent with previous reports of reduced estrogen levels in female rats after four weeks of

treatment [147]. The effect of CQ on progesterone has not been evaluated previously. However, since this hormone is vital to maintenance of normal pregnancy, it was measured in the current study and was significantly increased after three days of CQ treatment. Fetal hormones were also affected by CQ treatment; fetal testes testosterone was significantly decreased 24 hrs after the last dose. Testosterone is synthesized in the male fetal testes independent of maternal regulation. Thus, the reduction in testosterone indicates a direct effect of CQ on the fetal testes.

AGD, a marker of disruption of male sexual development, was not reduced in the male fetuses of CQ treated animals. Inhibition of testosterone signaling by chemicals such as flutamide and di-n-butyl phthalate (DBP) from GD 12 - 19 has consistently been shown to result in reduced AGD in male rats [68, 162]. This decrease was not seen in the current study, despite the significant reduction in testes testosterone. It is possible that our dosing regimen was not optimal for detecting a difference in this parameter; dosing was started in late gestation and sacrifice performed on GD 19 rather than post-natal day 1 as is more typical [34, 162, 163]. Mychrest et al. [34] noted ~30% decrease in the AGD of post-natal day 1 male rats from DBP doses that caused > 90% reduction in fetal testosterone (500 mg/kg/day; Lehmann et al., 2004). A similar phthalate, di-isobutyl phthalate, caused only a 14% reduction in AGD on GD 19 with a comparable dose (600 mg/kg/day) [164]. Alterations in AGD are expected to be more noticeable if measured post-natally.

Despite the lack of change in AGD, early markers of sexual development were altered in the CQ treated fetus. Clear changes were seen in the testes vasculature after CQ treatment upon gross examination of the testes. Furthermore, the cord diameter was increased in the CQ treated testes. These changes indicate an effect of CQ treatment on normal development

of the testes. These alterations may represent some general effects on development.

However, when coupled with the concurrent reduction in testosterone and the expression of genes associated with structural and vascular regulation in the testis, these alterations are more likely to represent a direct action of CQ on testes development.

Our gene array studies, while limited in statistical power, indicated potential alterations in genes that are associated with steroid regulation in the testes, both at the level of cholesterol synthesis and in its conversion to testosterone. The trends in gene changes observed in this study were consistent with those seen with DBP, which is also an anti-androgenic chemical, indicating that CQ is able to reduce the production of testosterone in the fetal testes. More targeted analysis of testes samples with RT-PCR confirmed CQ-related decrease in 6 genes associated with steroidogenesis, including *StAR*, *SR-B1*, *P450scc*, *Cyp17*, *Tm7sf2*, and *Nppc*. These genes are also down-regulated with gestational phthalate treatment [80, 123], supporting the conclusion that CQ is able to interfere with fetal testosterone homeostasis through disruption of steroid synthesis.

This study demonstrated that the anti-malarial drug CQ disrupts sexual development in the male fetal rat at doses that are similar to those recommended for pregnant women. At doses just 4-fold higher than those used in the human, structural differences were present in the testes of the male fetus (increased tubule diameter) and significant reductions were found in testosterone content and mRNA of genes associated with cholesterol transport and steroid synthesis. On the basis of this study, further research is warranted on the effect of pre-natal CQ exposure on male sexual development and fertility.

## F. ADDITIONAL RESEARCH

### **Dose-Response Evaluation of Chloroquine Effects on Testosterone and Steroidogenic Gene Expression in the Fetal Rat Testes**

#### *Chloroquine Administration to Pregnant Animals and Tissue Collection*

Pregnant rats (n=3 per dose/study) were dosed once daily by oral gavage from gestational day (GD) 16-18 with reverse osmosis water or CQ. On GD 16, the dams were given a loading dose (1mL/kg) of 20, 100 or 200 mg/kg CQ. These doses were followed by maintenance doses of 10, 50, and 100 mg CQ/kg, respectively, on GD 17 and 18. This study was performed twice (for a total of 6 dams/dose group), in an effort to verify original observations in the first study (Group I), retain statistical power, and minimize variability due to the time of day at which animals were sacrificed and hormones measured. Rats in the second study (Group II) were mated, dosed and euthanized 1 day after those in Group I. Maternal body weights were recorded daily at the time of dosing. All dams were euthanized by CO<sub>2</sub> asphyxiation and exsanguination on GD 19 (24 hrs after the final dose). Sacrifice times were randomized across dose groups to minimize influence of time-dependent differences in hormone production on dose-response data. Maternal blood was collected via cardiac puncture. Fetuses were delivered by cesarean section, weighed and AGD was assessed using a dissecting microscope and a micrometer lens (accuracy 0.05mm). All fetuses were euthanized by decapitation, sexed by internal inspection of the reproductive organs, and testes were collected from the male fetuses. Each fetal testes pair was placed in a separate cryogenic vial, snap-frozen in liquid nitrogen, and stored at -80°C.

### *Analysis of Fetal Testes Testosterone and Steroidogenic Gene Expression*

Fetal testes testosterone concentration was determined from 3 individual fetuses from each litter in Group I and II following with the previously described method (Figure 6.8). Testosterone showed a dose-dependent decrease with CQ treatment. A 2-way ANOVA indicated that CQ treatment and study group were significant factors ( $p < 0.001$  and  $p < 0.003$ , respectively). Group I showed a greater reduction in testosterone than Group II. However both groups clearly had a negative dose-response. Testosterone was significantly reduced ( $p < 0.05$ ) in all treatment groups ( $\geq 10$  mg/kg/day) when compared to controls.

RT-PCR was performed on fetal testes samples from one testes pair from each litter in the control, 10, 50, and 100 mg/kg/day groups ( $n=6$ ) using the probes for genes indicated from the single dose CQ study and from published gene expression studies with the DBP and DEHP [46, 80]. In addition to the genes described above, 7-dehydrocholesterol reductase (*Dhcr7*) and emopamil binding protein (*EBP*) expression were examined. *Dhcr7* and *EBP* are required for de novo cholesterol synthesis, and are consistently down-regulated with steroid inhibitors [46, 80]. With the exception of *P450scc*, all of the examined genes (Figure 6.9) showed a dose-dependent decrease in expression following CQ exposure ( $p < 0.05$ , 2-way ANOVA with LS means student's *t* post-test). *Dhcr*, *StAR*, *Tm7sf2*, *Cyp17A1*, *P450scc*, and *Nppc* were significantly down-regulated at CQ doses of 50 and 100 mg/kg/day. The genes encoding *EBP* and the cholesterol transporter SR-B1, also showed decreasing trends with dose. However, only the 100 mg/kg/day group was significantly different from controls.



### *Conclusions on Chloroquine In Vivo Studies*

In addition to showing that CQ is able to disrupt fetal testosterone at doses that are within the range of those recommended for pregnant women (10 mg/kg/day), the second *in vivo* study demonstrated a clear dose-response for testosterone inhibition. The concurrent dose-related decrease in the expression of genes responsible for regulation of steroidogenesis indicates that CQ interferes with testosterone regulation through inhibition of synthesis. The ability of CQ, a known inhibitor of arachidonic acid release by PLA<sub>2</sub>s, to inhibit fetal testosterone synthesis *in vivo* supports our hypothesis that this enzyme is necessary for fetal rat steroidogenesis and may play a role in phthalate induced inhibition.

CQ treatment did not recapitulate all of the responses seen in rats exposed to DBP and DEHP during gestation. In particular, the diameter of the seminiferous tubules was increased after exposure to DBP and decreased after CQ. DBP and DEHP also caused significant changes in the expression of a larger number of gene transcripts than CQ when evaluated by microarray. Liu et al. [80] reported statistically significant alterations in 391 genes after exposure to the endocrine active phthalates BBP, DBP, DEHP, and dipentyl phthalate (500 mg/kg/day). In addition to those regulating testosterone, categories of altered genes included pathways involved in insulin signaling, transcription regulation and oxidative stress. Many of the genes altered in the fetal testes after phthalate treatment are associated with seminiferous tubule structure and Sertoli cells. Phthalates have been shown to have adverse effects on fetal sexual development not related to testosterone, such as cryptorchidism, induction of multinucleated gonocytes, and germ cell detachment in primary cell cultures [35, 165]. These effects on the Sertoli and germ cells were not recapitulated by CQ.

The ability to detect differences in gene expression from the CQ microarray studies was limited by the size of these studies and by the existence of batch effects. For each of the CQ studies, six animals were used for each dose. In the study by Liu et al. [80], where 391 genes were significantly altered, the authors were able to combine results for inactive and active phthalates, giving an effective n of 16 and improving sensitivity. Furthermore, the CQ studies demonstrated a much greater level of toxicity than the phthalates, with significant reductions in maternal and fetal body weight at relatively low doses (50 and 100 mg/kg/day, respectively), which limited the doses at which testes effects could be examined. Nonetheless, the similarity in their effect on the steroidogenic pathway indicates that CQ and the endocrine active phthalates may have a common target in the Leydig cell.

**Table 6.1. Body Weights and Markers of Liver Toxicity**

	Dam		Fetus	
	0	100	0	100
<b>Dose (mg/kg/day)</b>				
<b>Body Weight (g)<sup>a</sup></b>	327.4 (7.1)	281.9 (7.1)**	2.32 (0.17)	2.18 (0.25)*
<b>Liver Weight (g)</b>	14.9 (1.7)	12.3 (1.2)**	0.21 (0.02)	0.173 (0.04)*
<b>Fractional Liver Weight<sup>b</sup></b>	0.045 (0.004)	0.044 (0.005)	0.088 (0.005)	0.082 (0.005)
<b>Liver Centrilobular Degeneration (incidence)<sup>c</sup></b>	Not present = 6	Not present = 3 Grade 2 = 3	Not present = 5	Not present = 5
<b>Liver Lipid Accumulation (incidence)<sup>c</sup></b>	Not present = 6	Grade 1 = 1 Grade 2 = 2 Grade 3 = 2	Not present = 5	Not present = 2 Grade 1 = 3
<b>Serum ALT (U/L)</b>	170.3 (22.2)	148.0 (23.5)	---	---
<b>Serum ALP (U/L)</b>	44.5 (2.5)	43.0 (2.6)	---	---
<b>Serum Creatinine (mg/dL)</b>	0.55 (0.02)	0.55 (0.02)	---	---

Values shown for mean (SE) from dams (n = 6) and their litters.

<sup>a</sup>Mean fetal body weight was calculated from all fetuses for each dose group.

<sup>b</sup>Fetal fractional liver calculated from 1 fetus/litter (liver weight divided by weight of corresponding fetus).

<sup>c</sup>Centrilobular degeneration and lipid accumulation in the maternal (n = 6/dose) and fetal liver (n = 5-6/dose) were evaluated after staining of sections with hematoxylin and eosin or Oil Red O, respectively. Changes in histopathology were evaluated on the following scale: Grade 1 = minimal, Grade 2 = mild, Grade 3 = moderate, and Grade 4 = marked occurrence. \*p<0.05, \*\*p<0.01, Student's t-test.

**Table 6.2. Significantly altered genes in the testes of GD 19 male rat after CQ exposure (adjusted  $p < 0.05$ ).**

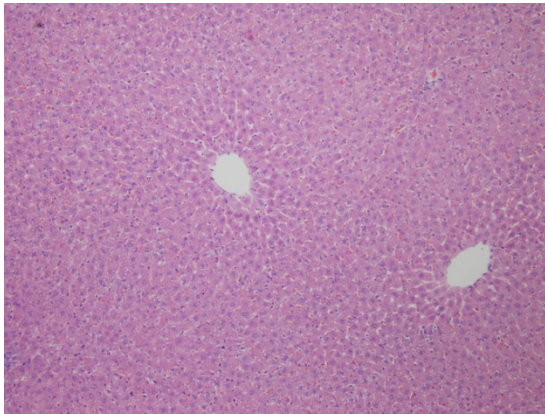
<b>Affymetrix ID</b>	<b>Gene Symbol</b>	<b>Gene Name</b>	<b>Fold-change</b>	<b>Functional Category</b>
1370964_at	Ass	argininosuccinate synthetase	-1.56	NO regulation
1372078_at	Strap	serine/threonine kinase receptor associated protein	-1.08	Regulation of TGF $\beta$ signaling
1372741_at	Sccpdh	saccharopine dehydrogenase (putative)	-1.08	Oxidoreductase activity
1372774_at	Coq6	Coenzyme Q6 homolog (yeast)	-1.67	Oxidoreductase activity
1383472_at	Aldh1b1	aldehyde dehydrogenase 1 family, member B1	-1.93	Oxidoreductase activity
1381684_at	---	Transcribed locus	1.08	Uncharacterized

**Table 6.3. Characterized genes with changes in fetal testis expression of at least a 1.5 fold after maternal CQ treatment.**

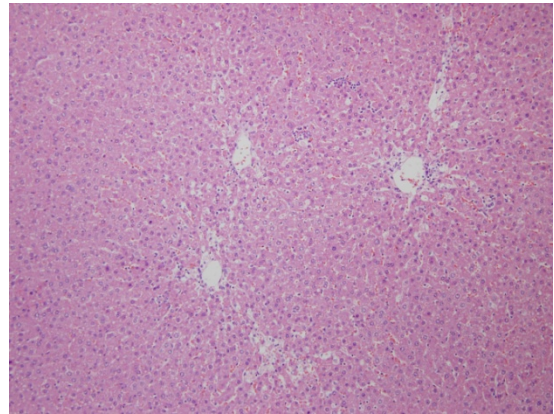
Affymetrix ID	Gene Symbol	Fold-Change	Raw P Value	Adjusted P Value	Putative Function
1368406_at	Star	-1.94	5.1e-5	0.1	Steroid synthesis
1368453_at	Fads2	-1.53	2.0e-4	0.1	Long chain fatty acid synthesis
1368854_at	Vsnl1	-2.18	0.006	0.3	Calcium regulation/signaling
1369579_at	Stc2	-1.54	9.2E-5	0.1	Calcium regulation
1369951_at	Ctrb	-2.34	0.009	0.4	Apoptosis signaling
1370336_at	Okl38	-1.54	0.001	0.2	Inhibit cell growth
1370355_at	Scd1	-1.59	0.003	0.3	Long chain fatty acid synthesis
1370384_a_at	Prlr	-1.57	0.003	0.3	Steroid regulation
1370964_at	Ass	-1.56	5.0e-6	0.0	NO regulation
1373386_at	Gjb2	-1.66	0.182	0.7	Gap junction
1374787_at	kcnfl	-1.63	0.007	0.3	Putative K <sup>+</sup> channel
1376944_at	Prlr	-1.54	0.002	0.3	Steroid regulation
1387174_a_at	Star	-1.79	0.185	0.2	Steroid regulation
1387744_at	Nppc	-2.35	0.001	0.2	Steroid regulation, angiogenesis
1388269_at	Hbg1	-1.69	0.001	0.7	heme binding, oxygen transport
1389725_at	Tm7sf2	-1.81	0.191	0.2	Cholesterol synthesis
1382431_at	ABCA1	-1.66	0.001	0.7	Lipid efflux from Sertoli cells
1391519_at	RGD13063 49_pred	-1.68	0.030	0.5	Cytoskeleton organization
1392664_at	Admr	-1.52	0.001	0.2	Vasodilation, NO response
1396877_at	LAMC1	-1.69	0.139	0.7	Extracellular matrix protein, oxidative stress response
1368187_at	Gpnmb	1.71	2.0e-4	0.1	Melanoprotein
1368290_at	Cyr61	1.77	0.184	0.7	Angiogenesis, cell proliferation/adhesion
1370428_x_at	RT1-A2 /// RT1-A3 /// RT1-Aw2	1.74	0.260	0.8	Antigen presentation to immune system
1373130_at	Myom2	1.73	0.012	0.4	Cytoskeleton structure
1387011_at	Lcn2	1.51	0.428	0.9	Reactive oxygen species response, apoptosis

**Figure 6.1. Sections of (A-B) maternal or (C-D) fetal liver after exposure to 0 or 100 mg/kg/day CQ.**

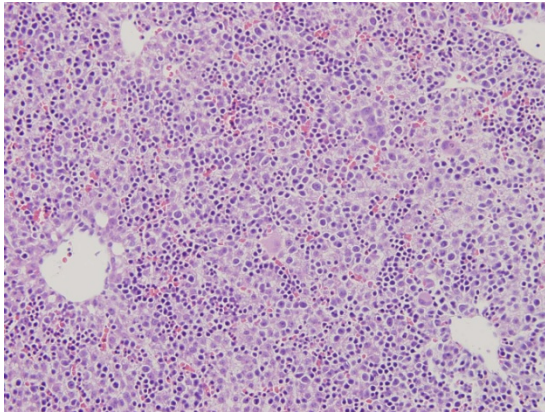
(A) Maternal liver from control animal. (B) Maternal liver from CQ treated animal. (C) Fetal liver from control group. (D) Fetal liver from CQ treated group. Livers were fixed 10% formalin, embedded in paraffin, sectioned at 5  $\mu\text{m}$  and stained with hematoxylin and eosin.



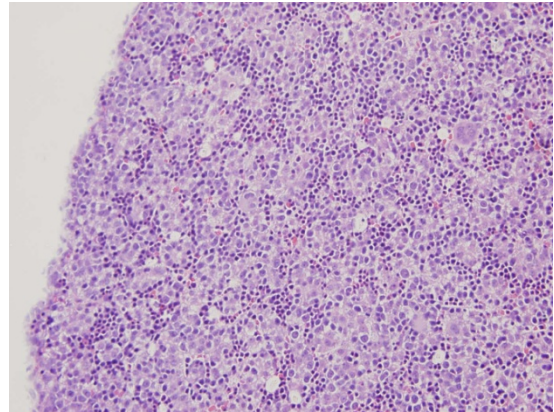
A



B



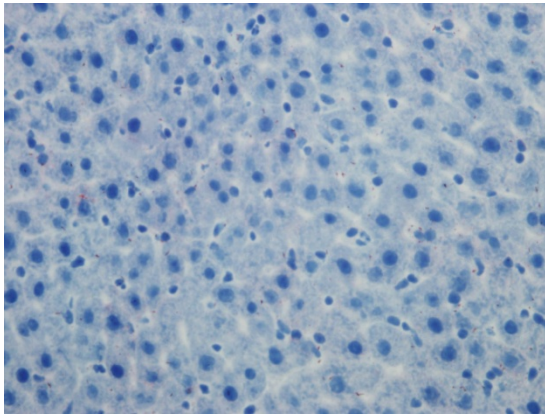
C



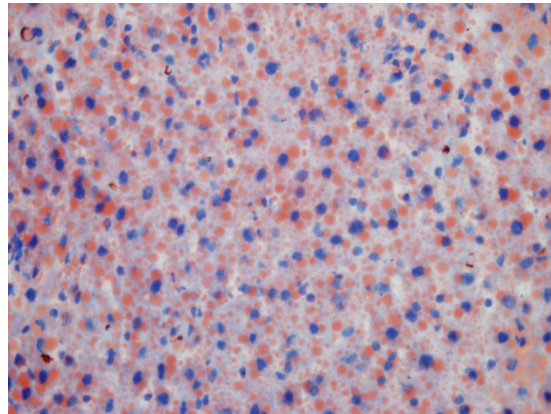
D

**Figure 6.2. Lipid accumulation in the (A-B) maternal or (C-D) fetal liver after exposure to 0 or 100 mg/kg/day CQ.**

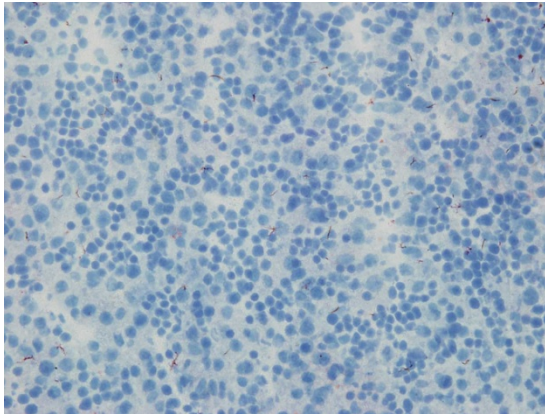
(A) Maternal liver from control animal. (B) Maternal liver from CQ treated animal. (C) Fetal liver from control group. (D) Fetal liver from CQ treated group. Livers were frozen, sectioned at 5  $\mu\text{m}$  and stained with Oil Red O. Arrow indicates small lipid droplets in fetal liver.



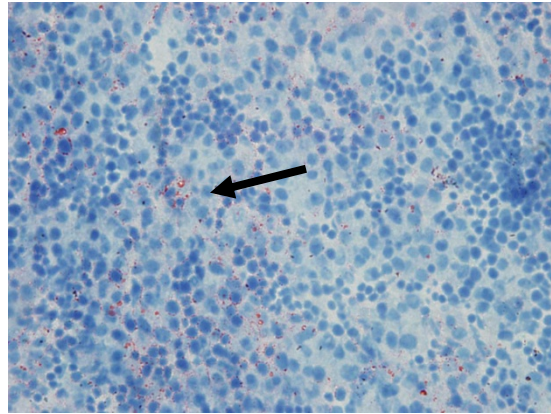
A



B



C



D

**Figure 6.3. Maternal serum estradiol and progesterone levels on GD 19 after maternal CQ exposure to 0 or 100 mg/kg/day from GD 16 – 18.**

Bars represent mean  $\pm$  SE of the measured data. \* $p < 0.05$ , Student's t-test for comparison of treatment vs. control groups. Black bars indicate control hormone levels. Gray bars indicate hormone levels in CQ treated dams.

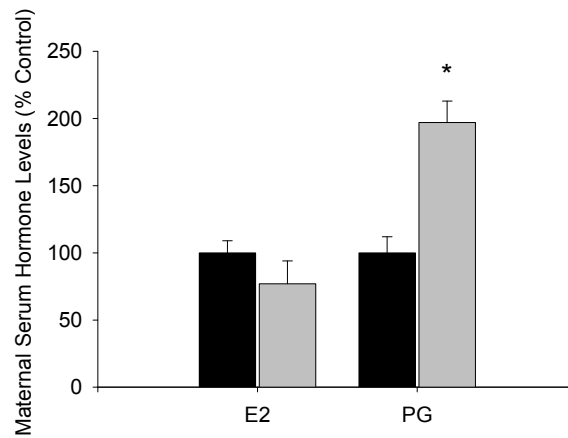




**Figure 6.4. Fetal testes testosterone levels on GD 19 after maternal CQ exposure to 0 or 100 mg/kg/day from GD 16 – 18.**

Bars represent mean  $\pm$  SE of the measured data. \* $p < 0.05$ , Student's t-test for comparison of treatment vs. control groups.

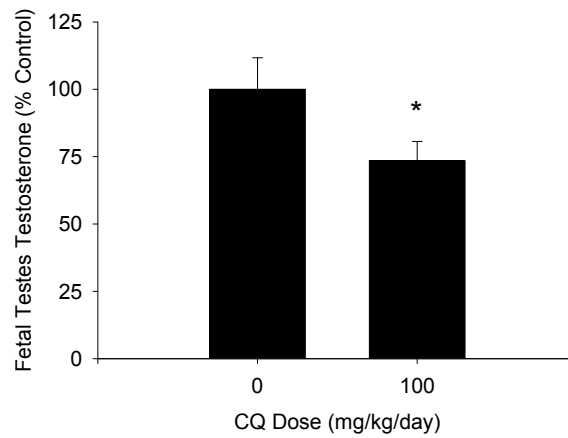


**Figure 6.5. Effect of CQ treatment on fetal anogenital distance (AGD) after maternal exposure to 0 or 100 mg/kg/day from GD 16-18.**

Bars represent mean  $\pm$  SE of the measured values for male (black) or female (gray) fetal rats.

\* $p < 0.05$ , Student's t-test for comparison of treatment vs. control groups.

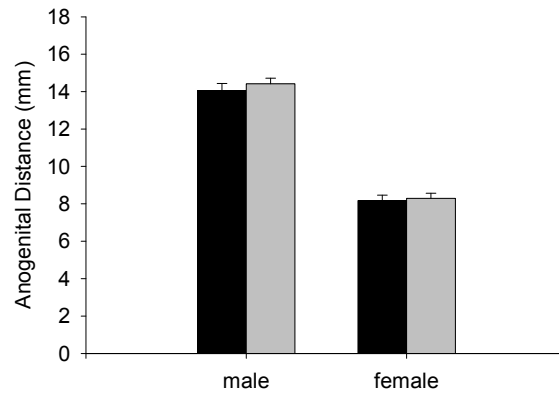
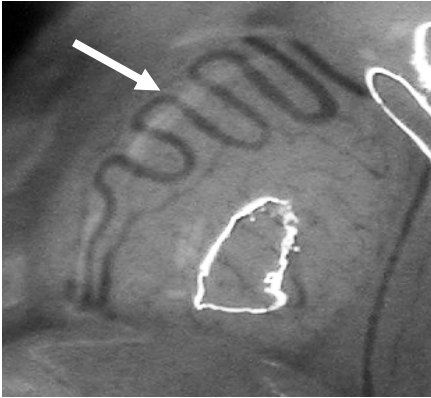
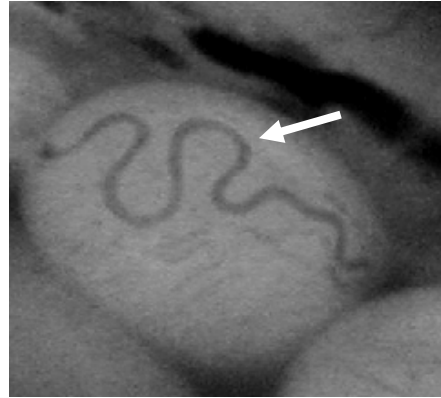


**Figure 6.6. Testicular artery after maternal CQ administration at 0 or 100 mg/kg/day from GD 16-18.**

(A) Testicular artery in control fetus shows several regular loops. (B) Testicular artery in high dose fetus has fewer convolutions and irregular loops. White arrows indicate the testicular artery.



A



B

**Figure 6.7. Effect of CQ treatment on expression of selected steroidogenic genes in fetal testes testosterone after maternal administration of 0 or 100 mg/kg/day from GD 16-18.**

Bars represent mean  $\pm$  SE of the values measured via RT-PCR. \* $p < 0.05$ , Student's t-test for comparison of treatment vs. control groups.

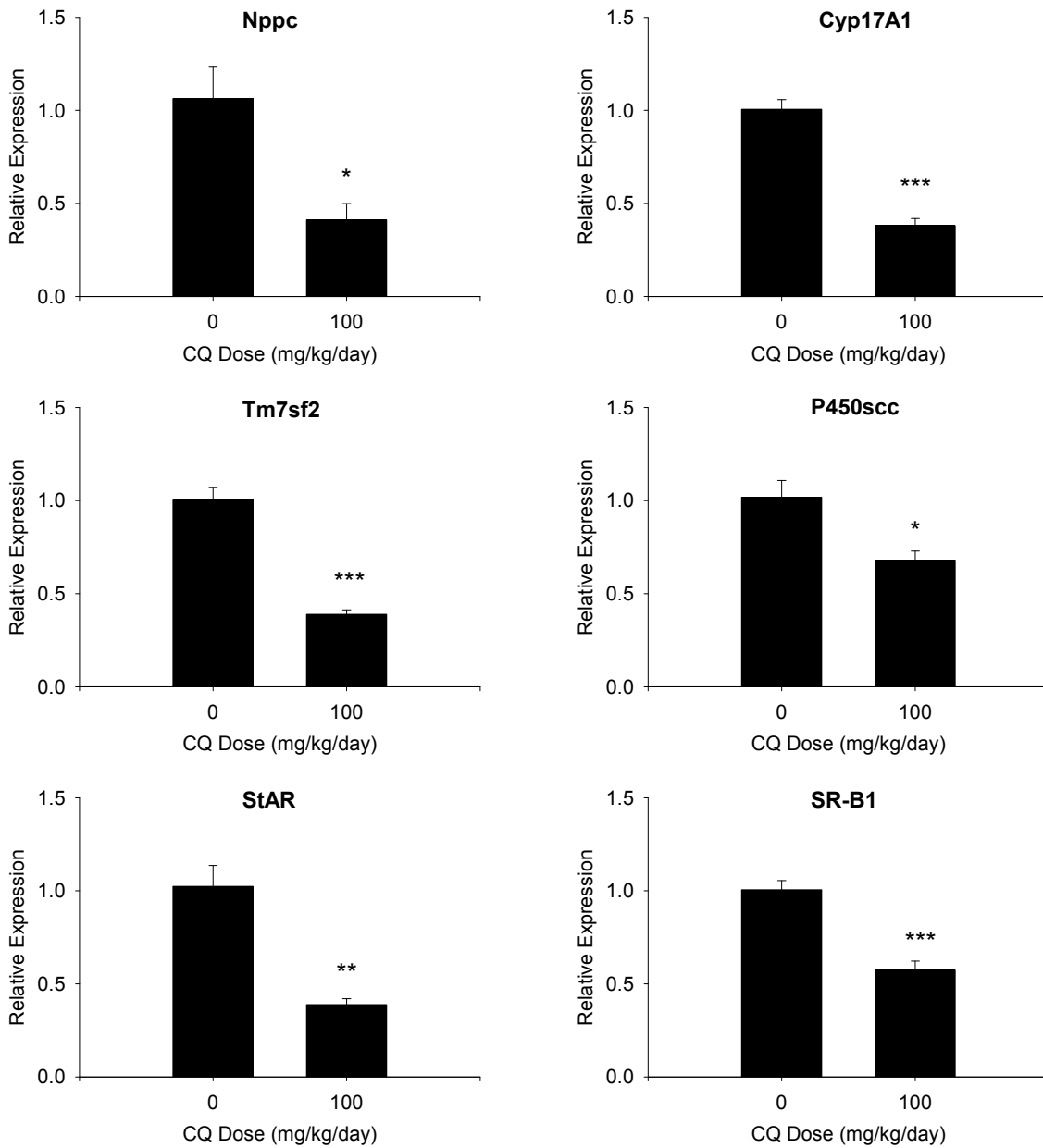


**Figure 6.8. Testosterone in fetal testes after maternal CQ administration at 0, 10, 50, or 100 mg/kg/day from GD 16-18.** Open circles represent Group I. Triangles represent Group II. \* $p < 0.05$ , 2-way ANOVA for dose and treatment group with Tukey's post-test.

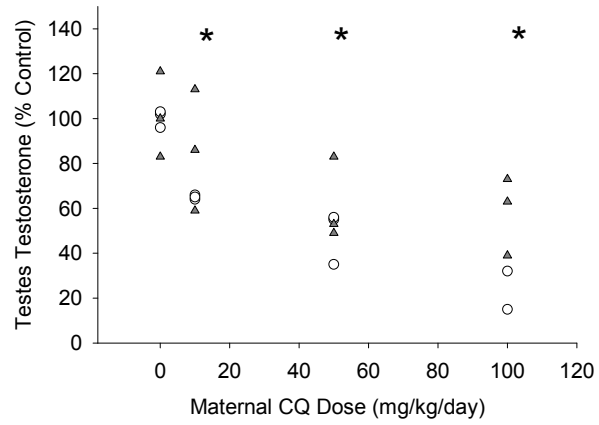
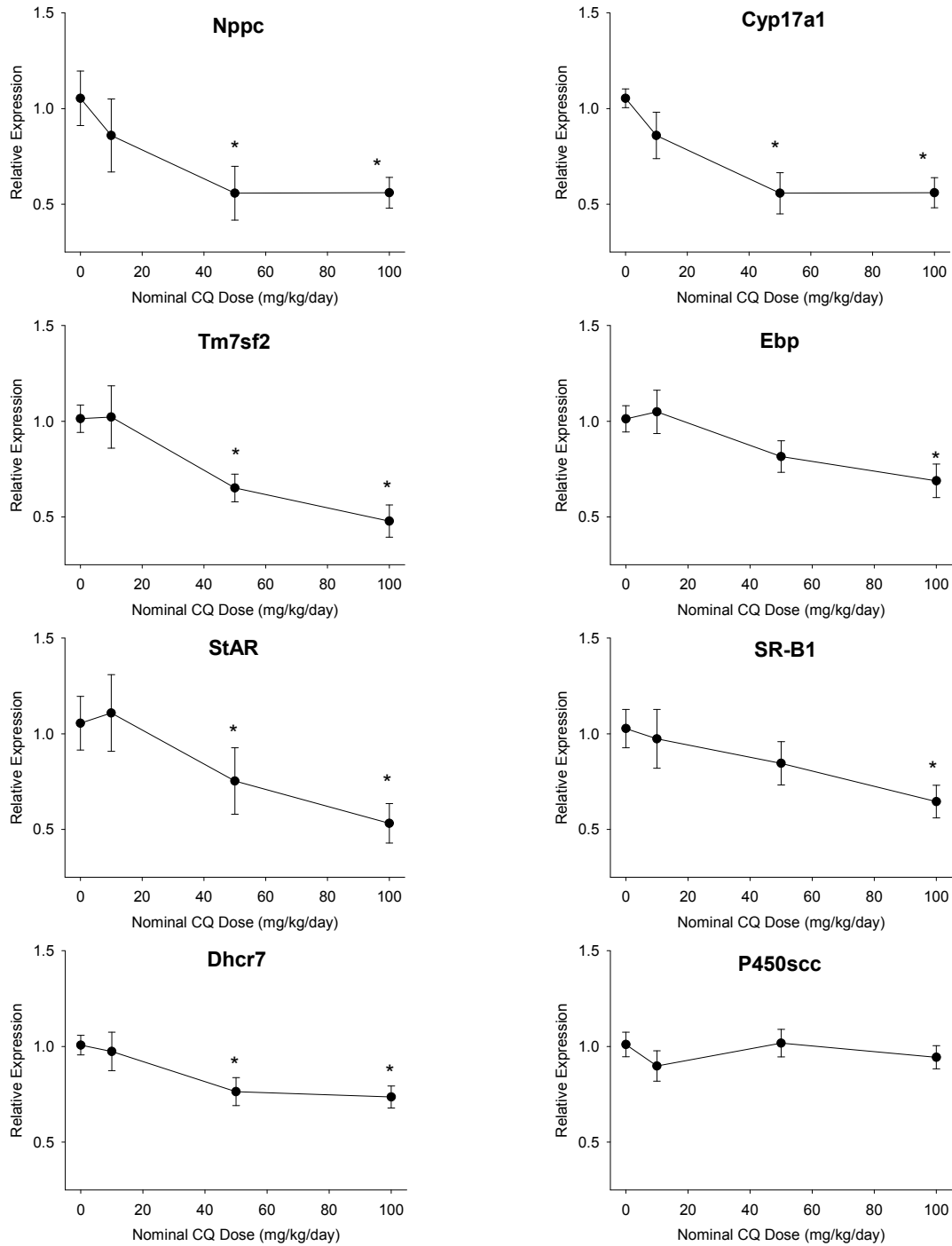


**Figure 6.9. Expression of selected steroidogenic genes in fetal testes after maternal CQ administration at 0, 10, 50, or 100 mg/kg/day from GD 16-18. \*p< 0.05, 2-way ANOVA for dose and treatment group with Tukey's post-test.**



## **CHAPTER 7**

### **GENERAL DISCUSSION**

## A. Summary of Experiments

The purpose of this project was to provide data and quantitative tools that could be used to improve risk assessments for phthalates. To that end, a series of *in vivo*, *in vitro* and *in silico* experiments were performed to evaluate the pharmacokinetic and pharmacodynamic factors controlling the phthalates' anti-androgenic effects. Chapters 2 and 3 focused on better defining phthalate distribution during gestation, using DBP as the representative endocrine active phthalate. The kinetic studies in Chapter 2 served two purposes. First, the dose-response study was the first in which phthalate and testosterone concentrations were simultaneously measured in the fetus. The publication of the plasma and tissue metabolite levels following repeated DBP exposure allowed the observed adverse effect (testosterone reduction) to be directly related to the concentration of the active metabolite in the target tissue (fetal plasma, testes).

The second purpose of the time-course data collected across doses was to provide the data needed to develop a PBPK model for DBP in the pregnant and fetal rat, which could later be extended to other phthalates of interest (*e.g.*, DEHP). Chapter 3 describes the development and validation of a PBPK model for DBP and its metabolites MBP and MBP-glucuronide in the adult male, pregnant female and fetal rat. The model, which was tested against a wide variety of data collected in different rat strains and life-stages, and across different doses and exposure routes, is able to accurately predict maternal and fetal plasma levels of the active metabolite (MBP) with both acute and repeated dosing. Thus, the model allows fetal dose to be calculated for studies in which kinetic data were not collected. Furthermore, incorporation of the various metabolic pathways into the model allowed identification of the important determinants of the non-linear kinetics observed *in vivo*.



Importantly, glucuronidation, a major clearance pathway for MBP, is saturated at very high DBP doses (500 mg/kg/day), which may account for the large number of developmental effects seen at this dose. Successful extrapolation of the DBP model to DEHP allowed fetal concentrations of the active metabolites, MBP and MEHP, to be calculated based on toxicity studies and compared. While DBP appears to induce developmental effects at lower administered doses than DEHP [46, 113], comparison of the fetal metabolite concentrations demonstrates that these two monoesters are equally potent.

Chapter 4 evaluated the pharmacokinetic and pharmacodynamic factors affecting the different potency across phthalates. Measured monoester concentrations in the fetal testes after repeated doses of BBP, DEP, DBP, DEHP, and DMP revealed that all of the corresponding monoesters were transferred to the fetus. When considered together with the results of testosterone inhibition in MA-10 Leydig cells, it became clear that the difference in the ability of the monoesters to cause developmental toxicity resides in pharmacodynamics, *i.e.*, similar target tissue concentrations have significantly different outcomes in the developing testes. The *in vitro* assay developed in Chapter 4 also provided a model for subsequent investigations into the mechanism of phthalate disruption of testosterone signaling in the Leydig cell.

Few studies have attempted to identify the molecular target for the phthalates in the Leydig cell, despite numerous studies indicating their effect on steroid synthesis and steroidogenic gene expression [33, 46, 55, 72, 80, 122]. Based on the available data with chloroquine (CQ), regarding its action on steroidogenesis, and a fairly simple comparison of the two-dimensional chemical structures of phthalate monoesters, CQ and the natural ligand of cPLA<sub>2</sub> (Figure 5.9), we hypothesized that the phthalates disrupted steroid signaling

through inhibition of AA release by cPLA<sub>2</sub>. Chapter 5 examined the ability of the PLA<sub>2</sub> inhibitor CQ and MEHP to inhibit testosterone production, steroidogenic gene expression and AA release in the LH-stimulated Leydig cell. Like MEHP, CQ was able to inhibit testosterone production *in vitro*, and CQ and MEHP caused similar changes in LH-stimulated gene expression and AA release. The ability of CQ and MEHP to interfere with cPLA<sub>2</sub> translocation after activation by calcium stimulation was also confirmed.

In Chapter 6, the *in vivo* effects of AA inhibition by CQ were evaluated in the fetal rat. While the liver effects were vastly different from those seen with phthalate administration (phthalates are hypolipidemic; CQ causes steatosis), the effects on steroidogenesis were similar. CQ reduced fetal testes testosterone levels in a dose-dependent manner. CQ treatment also led to down-regulation of steroidogenic genes that were also down-regulated in studies with the active phthalates [80]. The similarity in steroidogenic response to phthalate and CQ treatment further supports the possible role of cPLA<sub>2</sub> in phthalate-induced inhibition of testosterone production.

Improved understanding of the molecular target(s) for phthalates in the testes is vitally important to future risk assessment efforts, as these assessments are likely to be focused on the developmental effects of phthalate exposure. Together, the studies described in this thesis provide the initial evidence that cPLA<sub>2</sub> is a key target of these phthalates leading to decreased arachidonic acid release and decreased testosterone production. Overall the results of our work can be used to support a more quantitative evaluation of the potential molecular targets for the phthalates using the dose-response data collected in the previous chapters.

## **B. Using Dose-response Modeling to Evaluate Potential Molecular Targets of the Phthalate Monoesters in the Leydig Cell**

The previous studies confirm the ability of MEHP to interfere with the arachidonic acid release and cPLA<sub>2</sub> translocation. Together with the published data showing that arachidonic acid pathways are necessary for testosterone signaling in the Leydig cell, these studies suggest that the phthalate monoesters reduce the production of testosterone by inhibiting cPLA<sub>2</sub> activity. However, cPLA<sub>2</sub> is clearly not the only possible molecular target within the Leydig cell. MEHP binds to and activates PPAR $\alpha$ , a nuclear receptor that induces expression of enzymes that regulate lipid homeostasis and is present in the Leydig cell. In order to evaluate the feasibility of these proposed molecular targets, a series of quantitative models were applied to the various *in vivo* and *in vitro* data collected in the previous studies. Using several pharmacokinetic models, ranging from simple one-compartment structures to more complex physiological (PBPK) models, we compared the potency of the phthalates of interest for different endpoints in the steroidogenic pathway (Table 7.1). The purpose of this analysis was to help pin-point the molecular target of the phthalates, based on the premise that the phthalates should have a potency for the terminal and precursor effects similar to that for interaction with the molecular target.

Maternal DEHP and DBP exposure causes decreased testosterone production in the testes of male fetal rats, which results in a variety of developmental effects. However, for the purpose of this work, decreased testosterone production was considered the key terminal effect. Dose-response data for inhibition of fetal testosterone by both DEHP and DBP have been published [46, 55, 72]. The external dose required to yield 50% inhibition (ED<sub>50</sub>) was calculated to be 35 and 63 mg/kg-day for DBP and DEHP, respectively. Because the fetal

monophthalate concentrations were not measured in these experiments, the PBPK models were used to convert the ED<sub>50</sub> values to the corresponding values for the monophthalate concentrations in fetal plasma (as described in Chapter 3). The resulting plasma IC<sub>50</sub> values for the two phthalates were 1.9 and 1.4 μM for MBP and MEHP, respectively. These values served as points of comparison for the various precursor effects. Phthalate concentrations required for inhibition of testosterone synthesis in MA-10 cells were similar to the IC<sub>50</sub>s estimated from the *in vivo* diester exposure data. The IC<sub>50</sub>s for MBP and MEHP inhibition of testosterone production *in vitro* were 4.4 and 5.1 μM, respectively.

It has been suggested that the PPAR family of nuclear receptors may mediate the anti-steroidogenic effects associated with phthalates [58, 166]. MEHP is a well-known activator of the PPAR family, particularly PPAR $\alpha$ , which leads to induction of a variety of lipid metabolizing enzymes. While the role of PPAR activation in phthalate-induced testicular effects was not within the scope of the current work, the pharmacokinetic tools that were developed for evaluating target tissue dose can be used to evaluate the published PPAR data. Information on the dose-response for PPAR activation by the phthalates in the testes is not available in the published literature. Activation of PPAR $\alpha$  in the liver, however, has been studied extensively and dose-response data are available for both DEHP and DBP administration *in vivo*. The relationship between external phthalate dose and induction of the peroxisomal enzyme carnitine acetyltransferase (CAT) in the liver of exposed adult rats [25] was modeled with a rectangular hyperbola increasing from a basal level to a fully induced response. The external dose required to cause half-maximal induction (ED<sub>50</sub>) was determined for DEHP and DBP (Table 7.1). The PBPK models for DEHP and DBP in the adult rat were then used to convert the ED<sub>50</sub>s to plasma monoester concentrations as

described previously for *in vivo* testosterone inhibition (Chapter 3). The resulting  $IC_{50}$ s for CAT induction by MEHP and MBP were 36 and 323  $\mu$ M, respectively.

In contrast to the trend seen in testosterone inhibition, CAT induction was not similar between the two phthalates. DBP is a much weaker peroxisome proliferator *in vivo*, even after accounting for differences in monoester kinetics. Activation of both mouse PPAR $\alpha$  and PPAR $\gamma$  by MEHP and MBP in transfected COS-1 cells [59] showed a similar trend to that seen in the *in vivo* study in the rat. MEHP was a potent activator of mouse PPAR $\alpha$  and  $\gamma$  ( $IC_{50}$  = 0.6 - 10  $\mu$ M), but MBP showed no significant activation at concentrations up to 300  $\mu$ M. The ability of MBP to inhibit testosterone at similar concentrations to MEHP, despite its lack of effect on PPAR, indicates that the nuclear receptor is not likely to be the primary mediator of the anti-androgenic effects of phthalates. This is not to say that PPAR activation does not have any effect on steroid homeostasis. In fact, up-regulation of PPAR dependent testosterone metabolizing enzymes has been measured in liver microsomes after 13 weeks of PP exposure [166]. Nonetheless, when all of the dose-response information is taken into consideration, direct activation of the nuclear receptor through phthalate/PPAR binding does not appear to be the driving force behind phthalate inhibition of steroid synthesis in the testes.

We have hypothesized that cPLA<sub>2</sub> may be the molecular target for the phthalates within the testes. Our studies on the phthalate-induced inhibition of AA release and cPLA<sub>2</sub> translocation, and those comparing the effects of CQ and MEHP (Chapter 5 and 6), indicate that inhibition of this enzyme's activity is likely to be responsible for the reduced testosterone observed with phthalate exposure *in vivo* and *in vitro*. The measured dose-response for AA inhibition in Leydig cells with monoester phthalate treatment is given in

Chapter 5. In order to quantitatively compare this dose-response data to testosterone inhibition data, the AA inhibition data were modeled using one-site inhibition curves. As is the case with testosterone inhibition, MEHP and MBP have a similar ability to inhibit AA release. Average measured  $IC_{50}$  values were 4.7 and 5.2  $\mu$ M for MBP and MEHP, respectively. These  $IC_{50}$ s were also remarkably similar to those calculated for testosterone inhibition (Table 7.1). The similarity in AA and testosterone response in the Leydig cell to phthalate administration strongly supports our hypothesis that the anti-androgenic activity of the phthalates is mediated through cPLA<sub>2</sub>.

While additional studies are needed to confirm cPLA<sub>2</sub> as the molecular target for the phthalates in the testes, this hypothesis is in agreement with a data large body of research. Specifically, the inhibition of steroidogenesis through inactivation of cPLA<sub>2</sub> and subsequent stimulation of steroidogenic gene expression is consistent with the following information. 1) Both MEHP and MBP reduce testosterone production in the fetal testes *in vivo* and in the isolated Leydig cell *in vitro*. 2)  $IC_{50}$ s based on dose-response modeling are similar for MEHP and MBP inhibition of steroid synthesis and AA release from Leydig cells, but not for effects of these monoesters on hepatic PPAR induction. 3) Inhibition of AA by known PLA<sub>2</sub> inhibitors decreases steroidogenesis *in vivo* and in cells *in vitro* through disruption of LH-induced gene transcription of steroid regulatory proteins that are also down-regulated by the phthalates. 4) Phthalate perturbation of LH signaling in the Leydig cell occurs independently, or at least down-stream, of c-AMP [55].

### C. Implications for Phthalate Risk Assessment

The studies performed during the completion of this dissertation were ultimately intended to aid in the development of a more accurate risk assessment for the phthalates based on their ability to adversely affect sexual development in the male fetus. Prior to the onset of this work, three key areas were identified where information required for an informed risk assessment was lacking: 1) data relating target tissue concentrations and observed effects, 2) understanding of the relative potency and combined effects of phthalates other than DEHP and DBP, and 3) knowledge of the mechanism of action of the phthalates within the Leydig cell. The studies described here, which range from *in vivo* kinetic evaluations and PBPK model development to the examination of potential mechanisms of action, provide important new data and novel quantitative tools for increasing our understanding of these issues and improving the current state of the phthalate risk assessment.

#### *Relating target tissue doses and observed effects*

The kinetic studies in Chapter 2 served two purposes. First, the dose-response study was the first in which phthalate and testosterone concentrations were simultaneously measured in the fetus. The publication of the plasma and tissue metabolite levels following repeated DBP exposure allowed the observed adverse effect (testosterone reduction) to be directly related to the concentration of the active metabolite in the target tissue (fetal plasma, testes). This data is itself important to risk assessment, in that it allows a direct comparison of human blood concentrations to those concentrations associated with adverse effects in animals. The second purpose of the time-course data collected across doses was to enable

the development of a PBPK model for DBP, and eventually DEHP, in the pregnant and fetal rat (Chapter 3).

PBPK models incorporate information on physiology, chemical specific kinetics and biochemical interactions obtained from experiments. When the structures of these models reflect the important determinants of the chemical kinetics, they can be used to predict the qualitative and quantitative behavior of a chemical *in vivo*. In particular, a properly validated PBPK model can be used to perform the high-to-low dose, dose-route, and interspecies extrapolations necessary for estimating human risk on the basis of animal toxicology studies. In recent years, the use of PBPK modeling with environmental chemicals and drugs and their incorporation in chemical risk assessment efforts has increased dramatically (Reddy et al., 2005). The phthalate models developed in Chapter 3 provide a means for calculating the target tissue dose for exposures where kinetic data has not been measured – a particularly useful tool in comparing potency across endpoints and chemicals as done in Table 7-1. Furthermore, the validated model can also serve as a basis for extrapolation across species, life-stages, and exposure scenarios (acute v. repeated dosing) to provide quantitative measures of target tissue dosimetry in the population of interest. Work is already underway to apply the models developed in Chapter 3 for the rat to the human adult and fetus (J. Campbell, personal communication). By accounting for species differences in physiology and metabolism, these validated PBPK models can predict target tissue dose in the human population and increase the accuracy of predictions of human risk from environmental exposure.



### *Determining relative potency of the phthalates*

While the majority of animal toxicity studies and the previous risk assessment efforts have focused on individual phthalates, human exposure actually occurs as mixture of a variety of parent diester phthalates, as well as their monoester metabolites. The Centers for Disease Control currently monitors the general population for exposure to several of the more highly used phthalates, including BBP, DBP, DEP, DEHP and DOP through detection of their monoester metabolites in urine [6]. Several phthalates (BBP, DBP, DEHP, dipentyl phthalate, diisobutylphthalate) have similar effects on the male reproductive tract in the rat when administered to the pregnant rat from GD 12-19 (500 mg/kg/day) and share a common mechanism. Other phthalates (DEP, DMP), however, do not affect male rat reproductive tract development [33, 80]. Because human exposure occurs as a mixture of active and inactive phthalates, one of the more important considerations in a comprehensive risk assessment is accounting for the differences in potency among phthalates, as well as the potential additivity of response.

The experiments in Chapter 4 were designed to address these issues specifically, by testing whether differences in potency were a result of PK or PD differences and by providing a possible model for testing relative potency *in vitro*. The fetal testes data showing that the inactive phthalates (MEP, MMP) are transferred efficiently to the fetal testes confirm that they have much reduced potency for causing inhibition of steroid synthesis than do the endocrine active phthalates. Ideally, the cumulative risk assessment for a family of chemicals such as the phthalates would attempt to account for the combined exposure to only those chemicals with the same molecular targets and to account for differing potencies.

The *in vitro* testosterone assay in MA-10 cell should be particularly useful to risk assessment efforts, in that it provides a method for determining the anti-androgenic activity of the different phthalates without the necessity of conducting expensive, time-consuming *in vivo* developmental studies. Identification of active and inactive phthalates *in vitro* eliminates confounding PK factors inherent in *in vivo* toxicity studies and simplifies decisions regarding which phthalates to include in a cumulative risk assessment. The *in vitro* model would also be useful for testing the effect of combined exposures on testosterone production and assumptions of additivity.

*Improving understanding of the phthalates' mechanism of action in the testes*

Without knowledge of the mechanism of action for a chemical, it is impossible to know whether animal toxicity studies are applicable to the human. This is particularly true when, as in the case of the phthalates, the human epidemiological data is not straightforward. While phthalate inhibition of steroid synthesis in the fetal testes has been demonstrated to be the likely cause of the androgen-dependent effects in rat sexual development, the mechanism by which testosterone is inhibited is not known. The studies performed in Chapters 5 and 6 were designed to specifically test the hypothesis that the phthalates may work through cPLA<sub>2</sub> to inhibit testosterone synthesis in the Leydig cell. The similarity in effects between MEHP and the PLA<sub>2</sub> inhibitor CQ on gene expression, testosterone production and arachidonic release support this hypothesis. Quantitative comparison of these endpoints, as well as activation of PPAR by different phthalates, indicates that cPLA<sub>2</sub> is the more likely mediator of testosterone inhibition. With a better understanding of the molecular mode of action for these compounds, targeted experiments

can be performed to determine whether the phthalates are likely to have similar effects in the human.

#### **D. Study Limitations and Future Directions**

The studies in this dissertation indicate that the testosterone dependent developmental effects in rats exposed to phthalates involve inhibition of steroidogenesis through the arachidonic acid signaling pathway. However, several important data gaps still exist that limit the use of this information in risk assessment applications. Of particular import to risk assessment efforts is the uncertainty in the human relevance of this particular pathway. Currently, the role of arachidonic acid in the human steroidogenic process has not been defined. Therefore, simply defining the mechanism of testosterone inhibition in the rodent is not sufficient. Studies are needed that examine the signaling pathways responsible for steroid signaling in the human. The successful use of the mouse tumor cell line in predicting testosterone inhibition in the rat indicate that immortal human steroidogenic cell lines may be useful for predicting *in vivo* sensitivity. Currently, no human Leydig cell lines have been created, although steroid producing immortalized adrenal cells are available. The utility of this model for Leydig cell effects is not known, however. Development of a primary or immortalized cell assay will be crucial for defining whether or not the mode of action in rodents applies to humans. Nonetheless, risk assessments would go forward with the assumption that humans are as responsive as rodents to altered testosterone synthesis and consequences of altered testosterone during development.

The database for *in vivo* phthalate effects indicates greater susceptibility in the fetal rat than the adult male rat, though the reason for this difference has not been identified. We were able to use the MA-10 cell line to examine relative phthalate potency *in vivo*. However, this model has three important drawbacks: 1) the cell line is derived from the mouse, which does not exhibit similar anti-androgenic effects as those seen in the rat. 2) The MA-10 cell is

derived from the adult Leydig cell, which is morphologically distinct from the fetal Leydig cell. 3) Stimulation of testosterone was accomplished using luteinizing hormone, which does not regulate fetal steroidogenesis. In order to better understand age-dependent differences in susceptibility, models are needed which allow testing directly in the Fetal Leydig cell. Studies employing fetal testes explants to examine testosterone inhibition have been inconsistent and isolation of Fetal Leydig cells has had little success due their small numbers in fetal rat testes. Development of an immortalized fetal Leydig cell line would be particularly valuable for continued study of fetal steroidogenesis. Use of a more biologically relevant stimulating factor than LH is also needed; the factor that initiates fetal steroidogenesis is not known. Fetal sensitivity may be the result of stimulation of only a portion of the entire steroid pathway or stimulation of a different pathway than the one regulated by LH. In order to test this, however, the mechanisms surrounding fetal testosterone production must first be better defined.

Finally, while we have shown that the anti-androgenic activity of the phthalates appears to involve arachidonic acid release by cPLA<sub>2</sub>, the nature of the interaction between the phthalate monoesters and the cPLA<sub>2</sub> protein remains uncharacterized. The translocation assay was performed in a previously available stably transfected human cell line that is not steroidogenic. Thus activation of cPLA<sub>2</sub> was accomplished by increasing intracellular calcium concentrations with an ionophore. In order to test how LH-stimulation of cPLA<sub>2</sub> activation would be affected, it would be necessary to examine inhibition of translocation in transfected testosterone producing cells, such as the MA-10. Binding assays using purified cPLA<sub>2</sub> are also needed to better define the interaction between the phthalates and cPLA<sub>2</sub>. By identifying the site of interaction for the phthalates and comparing the relative activity across

species, we will better predict species susceptibility to phthalate endocrine effects. Despite the very real opportunity for extending the results from the studies in this thesis by future experimentation, our studies are an important step in reaching the goal of understanding the mechanisms of action of phthalates on steroidogenesis and in describing the dose-response behavior of several developmentally active phthalate monoesters..

**Table 7.1. Estimated Potency of Phthalates: Comparison Across Biological Endpoints.**

Average IC<sub>50</sub> values given were calculated using Prism 4.0 (GraphPad Software, Inc., LaJolla, CA) from experiments described in Chapters 2 – 6 or were available in published literature. Values in parentheses represent the 95% confidence interval of calculated values.

Biological Response	Model	Study Type	IC <sub>50</sub> (μM) <sup>a</sup> MEHP	IC <sub>50</sub> (μM) <sup>a</sup> MBP
Testosterone Inhibition <sup>b</sup>	Rat Testes - Fetus	<i>In vivo</i>	1.4 (0.1-25)	1.9 (1-5)
Testosterone Inhibition	Mouse Leydig Cell	<i>In vitro</i>	4.4 (2-10)	3.5 (1-8)
AA (cPLA <sub>2</sub> ) Inhibition	Mouse Leydig Cell	<i>In vitro</i>	4.7 (1-19)	5.2 (1-20)
CAT (PPAR) Induction <sup>c</sup>	Rat – Adult Male	<i>In vivo</i>	36	323
PPARα Activation <sup>d</sup>	Mouse Gene Overexpression	<i>In vitro</i>	0.6	> 300
PPARγ Activation <sup>d</sup>	Mouse Gene Overexpression	<i>In vitro</i>	10	> 300

<sup>a</sup> Fetal or adult rat plasma concentrations calculated from ED<sub>50</sub> values using the PBPK models as described in Chapter 3.

<sup>b</sup> Inhibition of fetal testes testosterone after 4 days administration of DEHP (Borch et al. 2004; Parks et al., 2000) or DBP (Chapter 2; Lehmann et al., 2004).

<sup>c</sup> Carnitine acetyltransferase induction after 14 days DBP or DEHP administration (Seo et al., 2004).

<sup>d</sup> Mouse PPARα and γ overexpressed in COS-1 cells and measured by luciferase assay (Hurst and Waxman, 2003). Cells were treated with MEHP or MBP.

## REFERENCES

1. ATSDR, *Toxicological profile for di-n--butyl phtalate*. 2001, Agency for Toxic Disease Registry: Atlanta, GA.
2. Schettler, T., *Human exposure to phthalates via consumer products*. Int J Androl, 2006. **29**(1): p. 134-9; discussion 181-5.
3. Wormuth, M., et al., *What are the sources of exposure to eight frequently used phthalic acid esters in Europeans?* Risk Anal, 2006. **26**(3): p. 803-24.
4. Brock, J.W., et al., *Phthalate monoesters levels in the urine of young children*. Bull Environ Contam Toxicol, 2002. **68**(3): p. 309-14.
5. Kohn, M.C., et al., *Human exposure estimates for phthalates*. Environ Health Perspect, 2000. **108**(10): p. A440-2.
6. Silva, M.J., et al., *Urinary levels of seven phthalate metabolites in the U.S. population from the National Health and Nutrition Examination Survey (NHANES) 1999-2000*. Environ Health Perspect, 2004. **112**(3): p. 331-8.
7. NTP, *Toxicokinetic Study Report: The Toxicokinetics and Metabolism of Di-n-butyl Phthalate*. 1995, National Institute of Environmental Health Sciences: Research Triangle Park, NC.
8. Franco, A., et al., *Comparison and analysis of different approaches for estimating the human exposure to phthalate esters*. Environ Int, 2007. **33**(3): p. 283-91.
9. White, R.D., et al., *Absorption and metabolism of three phthalate diesters by the rat small intestine*. Food Cosmet Toxicol, 1980. **18**(4): p. 383-6.
10. Kluwe, W.M., *Overview of phthalate ester pharmacokinetics in mammalian species*. Environ Health Perspect, 1982. **45**: p. 3-9.
11. Tanaka, A., A. Matsumoto, and T. Yamaha, *Biochemical studies on phthalic esters. III. Metabolism of dibutyl phthalate (DBP) in animals*. Toxicology, 1978. **9**(1-2): p. 109-23.
12. Albro, P.W. and S.R. Lavenhar, *Metabolism of di(2-ethylhexyl)phthalate*. Drug Metab Rev, 1989. **21**(1): p. 13-34.
13. Albro, P.W., *Absorption, metabolism, and excretion of di(2-ethylhexyl) phthalate by rats and mice*. Environ Health Perspect, 1986. **65**: p. 293-8.
14. Klaunig, J.E., et al., *PPARalpha agonist-induced rodent tumors: modes of action and human relevance*. Crit Rev Toxicol, 2003. **33**(6): p. 655-780.



15. Mandard, S., M. Muller, and S. Kersten, *Peroxisome proliferator-activated receptor alpha target genes*. Cell Mol Life Sci, 2004. **61**(4): p. 393-416.
16. Oliver, J.D. and R.A. Roberts, *Receptor-mediated hepatocarcinogenesis: role of hepatocyte proliferation and apoptosis*. Pharmacol Toxicol, 2002. **91**(1): p. 1-7.
17. Shaban, Z., et al., *AhR and PPARalpha: antagonistic effects on CYP2B and CYP3A, and additive inhibitory effects on CYP2C11*. Xenobiotica, 2005. **35**(1): p. 51-68.
18. Cattley, R.C., *Peroxisome proliferators and receptor-mediated hepatic carcinogenesis*. Toxicol Pathol, 2004. **32 Suppl 2**: p. 6-11.
19. Cattley, R.C., et al., *Do peroxisome proliferating compounds pose a hepatocarcinogenic hazard to humans?* Regul Toxicol Pharmacol, 1998. **27**(1 Pt 1): p. 47-60.
20. Reddy, J.K., et al., *Transcription regulation of peroxisomal fatty acyl-CoA oxidase and enoyl-CoA hydratase/3-hydroxyacyl-CoA dehydrogenase in rat liver by peroxisome proliferators*. Proc Natl Acad Sci U S A, 1986. **83**(6): p. 1747-51.
21. Nemali, M.R., et al., *Differential induction and regulation of peroxisomal enzymes: predictive value of peroxisome proliferation in identifying certain nonmutagenic carcinogens*. Toxicol Appl Pharmacol, 1989. **97**(1): p. 72-87.
22. Moody, D.E. and J.K. Reddy, *The hepatic effects of hypolipidemic drugs (clofibrate, nafenopin, tibric acid, and Wy-14,643) on hepatic peroxisomes and peroxisome-associated enzymes*. Am J Pathol, 1978. **90**(2): p. 435-46.
23. Lake, B.G., et al., *Structure activity studies on the induction of peroxisomal enzyme activities by a series of phthalate monoesters in primary rat hepatocyte cultures*. Arch Toxicol Suppl, 1986. **9**: p. 386-9.
24. Okita, J.R., P.J. Castle, and R.T. Okita, *Characterization of cytochromes P450 in liver and kidney of rats treated with di-(2-ethylhexyl)phthalate*. J Biochem Toxicol, 1993. **8**(3): p. 135-44.
25. Seo, K.W., et al., *Comparison of oxidative stress and changes of xenobiotic metabolizing enzymes induced by phthalates in rats*. Food Chem Toxicol, 2004. **42**(1): p. 107-14.
26. Lapinskas, P.J., et al., *Role of PPARalpha in mediating the effects of phthalates and metabolites in the liver*. Toxicology, 2005. **207**(1): p. 149-63.

27. Mukherjee, R., et al., *Human and rat peroxisome proliferator activated receptors (PPARs) demonstrate similar tissue distribution but different responsiveness to PPAR activators*. J Steroid Biochem Mol Biol, 1994. **51**(3-4): p. 157-66.
28. Sher, T., et al., *cDNA cloning, chromosomal mapping, and functional characterization of the human peroxisome proliferator activated receptor*. Biochemistry, 1993. **32**(21): p. 5598-604.
29. Woodyatt, N.J., et al., *The peroxisome proliferator (PP) response element upstream of the human acyl CoA oxidase gene is inactive among a sample human population: significance for species differences in response to PPs*. Carcinogenesis, 1999. **20**(3): p. 369-72.
30. Cheung, C., et al., *Diminished hepatocellular proliferation in mice humanized for the nuclear receptor peroxisome proliferator-activated receptor alpha*. Cancer Res, 2004. **64**(11): p. 3849-54.
31. Yang, Q., et al., *The PPAR alpha-humanized mouse: a model to investigate species differences in liver toxicity mediated by PPAR alpha*. Toxicol Sci, 2008. **101**(1): p. 132-9.
32. Gray, L.E., Jr., et al., *Administration of potentially antiandrogenic pesticides (procymidone, linuron, iprodione, chlozolinate, p,p'-DDE, and ketoconazole) and toxic substances (dibutyl- and diethylhexyl phthalate, PCB 169, and ethane dimethane sulphonate) during sexual differentiation produces diverse profiles of reproductive malformations in the male rat*. Toxicol Ind Health, 1999. **15**(1-2): p. 94-118.
33. Gray, L.E., Jr., et al., *Perinatal exposure to the phthalates DEHP, BBP, and DINP, but not DEP, DMP, or DOTP, alters sexual differentiation of the male rat*. Toxicol Sci, 2000. **58**(2): p. 350-65.
34. Mylchreest, E., et al., *Disruption of androgen-regulated male reproductive development by di(n-butyl) phthalate during late gestation in rats is different from flutamide*. Toxicol Appl Pharmacol, 1999. **156**(2): p. 81-95.
35. Gaido, K.W., et al., *Fetal mouse phthalate exposure shows that Gonocyte multinucleation is not associated with decreased testicular testosterone*. Toxicol Sci, 2007. **97**(2): p. 491-503.
36. Foster, P.M., *Mode of action: impaired fetal leydig cell function--effects on male reproductive development produced by certain phthalate esters*. Crit Rev Toxicol, 2005. **35**(8-9): p. 713-9.

37. Meeker, J.D., A.M. Calafat, and R. Hauser, *Urinary Metabolites of di(2-ethylhexyl) phthalate Are Associated with Decreased Steroid Hormone Levels in Adult Men*. J Androl, 2008.
38. Pant, N., et al., *Correlation of phthalate exposures with semen quality*. Toxicol Appl Pharmacol, 2008. **231**(1): p. 112-6.
39. Swan, S.H., et al., *Decrease in anogenital distance among male infants with prenatal phthalate exposure*. Environ Health Perspect, 2005. **113**(8): p. 1056-61.
40. Main, K.M., et al., *Human breast milk contamination with phthalates and alterations of endogenous reproductive hormones in infants three months of age*. Environ Health Perspect, 2006. **114**(2): p. 270-6.
41. Sharpe, R.M., *Phthalate exposure during pregnancy and lower anogenital index in boys: wider implications for the general population?* Environ Health Perspect, 2005. **113**(8): p. A504-5.
42. Fennell, T.R., et al., *Pharmacokinetics of dibutylphthalate in pregnant rats*. Toxicol Sci, 2004. **82**(2): p. 407-18.
43. Saillenfait, A.M., et al., *Assessment of the developmental toxicity, metabolism, and placental transfer of Di-n-butyl phthalate administered to pregnant rats*. Toxicol Sci, 1998. **45**(2): p. 212-24.
44. Calafat, A.M., et al., *Urinary and amniotic fluid levels of phthalate monoesters in rats after the oral administration of di(2-ethylhexyl) phthalate and di-n-butyl phthalate*. Toxicology, 2006. **217**(1): p. 22-30.
45. Kessler, W., et al., *Blood burden of di(2-ethylhexyl) phthalate and its primary metabolite mono(2-ethylhexyl) phthalate in pregnant and nonpregnant rats and marmosets*. Toxicol Appl Pharmacol, 2004. **195**(2): p. 142-53.
46. Lehmann, K.P., et al., *Dose-dependent alterations in gene expression and testosterone synthesis in the fetal testes of male rats exposed to di (n-butyl) phthalate*. Toxicol Sci, 2004. **81**(1): p. 60-8.
47. Mylchreest, E., et al., *Dose-dependent alterations in androgen-regulated male reproductive development in rats exposed to Di(n-butyl) phthalate during late gestation*. Toxicol Sci, 2000. **55**(1): p. 143-51.
48. Kremer, J.J., et al., *Pharmacokinetics of monobutylphthalate, the active metabolite of di-n-butylphthalate, in pregnant rats*. Toxicol Lett, 2005. **159**(2): p. 144-53.
49. Payan, J.P., et al., *In vivo and in vitro percutaneous absorption of [(14)C]di-N-butylphthalate in rat*. Drug Metab Dispos, 2001. **29**(6): p. 843-54.

50. Okita, R.T. and J.R. Okita, *Characterization of a cytochrome P450 from di(2-ethylhexyl) phthalate-treated rats which hydroxylates fatty acids*. Arch Biochem Biophys, 1992. **294**(2): p. 475-81.
51. Okita, R.T. and J.R. Okita, *Effects of diethyl phthalate and other plasticizers on laurate hydroxylation in rat liver microsomes*. Pharm Res, 1992. **9**(12): p. 1648-53.
52. Wyde, M.E., et al., *Di-n-butyl phthalate activates constitutive androstane receptor and pregnane X receptor and enhances the expression of steroid-metabolizing enzymes in the liver of rat fetuses*. Toxicol Sci, 2005. **86**(2): p. 281-90.
53. Pollack, G.M., et al., *Effects of route of administration and repetitive dosing on the disposition kinetics of di(2-ethylhexyl) phthalate and its mono-de-esterified metabolite in rats*. Toxicol Appl Pharmacol, 1985. **79**(2): p. 246-56.
54. Teirlynck, O.A. and F. Belpaire, *Disposition of orally administered di-(2-ethylhexyl) phthalate and mono-(2-ethylhexyl) phthalate in the rat*. Arch Toxicol, 1985. **57**(4): p. 226-30.
55. Wang, X., L.P. Walsh, and D.M. Stocco, *The role of arachidonic acid on LH-stimulated steroidogenesis and steroidogenic acute regulatory protein accumulation in MA-10 mouse Leydig tumor cells*. Endocrine, 1999. **10**(1): p. 7-12.
56. Cooke, B.A., et al., *Release of arachidonic acid and the effects of corticosteroids on steroidogenesis in rat testis Leydig cells*. J Steroid Biochem Mol Biol, 1991. **40**(1-3): p. 465-71.
57. Moraga, P.F., M.N. Llanos, and A.M. Ronco, *Arachidonic acid release from rat Leydig cells depends on the presence of luteinizing hormone/human chorionic gonadotrophin receptors*. J Endocrinol, 1997. **154**(2): p. 201-9.
58. Gazouli, M., et al., *Effect of peroxisome proliferators on Leydig cell peripheral-type benzodiazepine receptor gene expression, hormone-stimulated cholesterol transport, and steroidogenesis: role of the peroxisome proliferator-activator receptor alpha*. Endocrinology, 2002. **143**(7): p. 2571-83.
59. Hurst, C.H. and D.J. Waxman, *Activation of PPARalpha and PPARgamma by environmental phthalate monoesters*. Toxicol Sci, 2003. **74**(2): p. 297-308.
60. Labow, R.S., et al., *Inhibition of human platelet phospholipase A2 by mono(2-ethylhexyl)phthalate*. Environ Health Perspect, 1988. **78**: p. 179-83.
61. Romanelli, F., et al., *Arachidonic acid and its metabolites effects on testosterone production by rat Leydig cells*. J Endocrinol Invest, 1995. **18**(3): p. 186-93.

62. Gupta, C., *The role of prostaglandins in masculine differentiation: modulation of prostaglandin levels in the differentiating genital tract of the fetal mouse.* Endocrinology, 1989. **124**(1): p. 129-33.
63. Kim, H.S., et al., *Neonatal exposure to di(n-butyl) phthalate (DBP) alters male reproductive-tract development.* J Toxicol Environ Health A, 2004. **67**(23-24): p. 2045-60.
64. Heudorf, U., V. Mersch-Sundermann, and J. Angerer, *Phthalates: toxicology and exposure.* Int J Hyg Environ Health, 2007. **210**(5): p. 623-34.
65. Ema, M., E. Miyawaki, and K. Kawashima, *Further evaluation of developmental toxicity of di-n-butyl phthalate following administration during late pregnancy in rats.* Toxicol Lett, 1998. **98**(1-2): p. 87-93.
66. Ema, M., E. Miyawaki, and K. Kawashima, *Critical period for adverse effects on development of reproductive system in male offspring of rats given di-n-butyl phthalate during late pregnancy.* Toxicol Lett, 2000. **111**(3): p. 271-8.
67. Fisher, J.S., et al., *Human 'testicular dysgenesis syndrome': a possible model using in-utero exposure of the rat to dibutyl phthalate.* Hum Reprod, 2003. **18**(7): p. 1383-94.
68. Mylchreest, E., R.C. Cattley, and P.M. Foster, *Male reproductive tract malformations in rats following gestational and lactational exposure to Di(n-butyl) phthalate: an antiandrogenic mechanism?* Toxicol Sci, 1998. **43**(1): p. 47-60.
69. Mylchreest, E. and P.M. Foster, *DBP exerts its antiandrogenic activity by indirectly interfering with androgen signaling pathways.* Toxicol Appl Pharmacol, 2000. **168**(2): p. 174-5.
70. Akingbemi, B.T., et al., *Phthalate-induced Leydig cell hyperplasia is associated with multiple endocrine disturbances.* Proc Natl Acad Sci U S A, 2004. **101**(3): p. 775-80.
71. Oishi, S. and K. Hiraga, *Effects of phthalic acid monoesters on mouse testes.* Toxicol Lett, 1980. **6**(4-5): p. 239-42.
72. Parks, L.G., et al., *The plasticizer diethylhexyl phthalate induces malformations by decreasing fetal testosterone synthesis during sexual differentiation in the male rat.* Toxicol Sci, 2000. **58**(2): p. 339-49.
73. Kim, H.S., et al., *Alterations of activities of cytosolic phospholipase A2 and arachidonic acid-metabolizing enzymes in di-(2-ethylhexyl)phthalate-induced testicular atrophy.* J Vet Med Sci, 2004. **66**(9): p. 1119-24.

74. Albro, P.W. and B. Moore, *Identification of the metabolites of simple phthalate diesters in rat urine*. J Chromatogr, 1974. **94**(0): p. 209-18.
75. Foster, P.M., et al., *Differences in urinary metabolic profile from di-n-butyl phthalate-treated rats and hamsters. A possible explanation for species differences in susceptibility to testicular atrophy*. Drug Metab Dispos, 1983. **11**(1): p. 59-61.
76. Furuta, T., K. Kusano, and Y. Kasuya, *Simultaneous measurements of endogenous and deuterium-labelled tracer variants of androstenedione and testosterone by capillary gas chromatography-mass spectrometry*. J Chromatogr, 1990. **525**(1): p. 15-23.
77. Habert, R. and R. Picon, *Testosterone, dihydrotestosterone and estradiol-17 beta levels in maternal and fetal plasma and in fetal testes in the rat*. J Steroid Biochem, 1984. **21**(2): p. 193-8.
78. NTP, *Prestart Toxicokinetic Study Report: Di-n-butyl Phthalate in Rodent Plasma*. 1994, National Institute of Environmental Health Sciences: Research Triangle Park, NC.
79. Wishart, G.J., *Functional heterogeneity of UDP-glucuronosyltransferase as indicated by its differential development and inducibility by glucocorticoids. Demonstration of two groups within the enzyme's activity towards twelve substrates*. Biochem J, 1978. **174**(2): p. 485-9.
80. Liu, K., et al., *Gene expression profiling following in utero exposure to phthalate esters reveals new gene targets in the etiology of testicular dysgenesis*. Biol Reprod, 2005. **73**(1): p. 180-92.
81. Koch, H.M., et al., *New metabolites of di(2-ethylhexyl)phthalate (DEHP) in human urine and serum after single oral doses of deuterium-labelled DEHP*. Arch Toxicol, 2005. **79**(7): p. 367-76.
82. Latini, G., et al., *In utero exposure to di-(2-ethylhexyl)phthalate and duration of human pregnancy*. Environ Health Perspect, 2003. **111**(14): p. 1783-5.
83. Mylchreest, E., et al., *Fetal testosterone insufficiency and abnormal proliferation of Leydig cells and gonocytes in rats exposed to di(n-butyl) phthalate*. Reprod Toxicol, 2002. **16**(1): p. 19-28.
84. Kim, H.S., et al., *Short period exposure to di-(2-ethylhexyl) phthalate regulates testosterone metabolism in testis of prepubertal rats*. Arch Toxicol, 2003. **77**(8): p. 446-51.
85. Rowland, I.R., R.C. Cottrell, and J.C. Phillips, *Hydrolysis of phthalate esters by the gastro-intestinal contents of the rat*. Food Cosmet Toxicol, 1977. **15**(1): p. 17-21.

86. Dickinson, R.G., D.W. Fowler, and R.M. Kluck, *Maternofetal transfer of phenytoin, p-hydroxy-phenytoin and p-hydroxy-phenytoin-glucuronide in the perfused human placenta*. Clin Exp Pharmacol Physiol, 1989. **16**(10): p. 789-97.
87. Fowler, D.W., M.J. Eadie, and R.G. Dickinson, *Transplacental transfer and biotransformation studies of valproic acid and its glucuronide(s) in the perfused human placenta*. J Pharmacol Exp Ther, 1989. **249**(1): p. 318-23.
88. Reynolds, F. and C. Knott, *Pharmacokinetics in pregnancy and placental drug transfer*. Oxf Rev Reprod Biol, 1989. **11**: p. 389-449.
89. Keys, D.A., et al., *Quantitative evaluation of alternative mechanisms of blood disposition of di(n-butyl) phthalate and mono(n-butyl) phthalate in rats*. Toxicol Sci, 2000. **53**(2): p. 173-84.
90. Gentry, P.R., T.R. Covington, and H.J. Clewell, 3rd, *Evaluation of the potential impact of pharmacokinetic differences on tissue dosimetry in offspring during pregnancy and lactation*. Regul Toxicol Pharmacol, 2003. **38**(1): p. 1-16.
91. Lucier, G.W., et al., *Postnatal stimulation of hepatic microsomal enzymes following administration of TCDD to pregnant rats*. Chem Biol Interact, 1975. **11**(1): p. 15-26.
92. Lucier, G.W. and O.S. McDaniel, *Steroid and non-steroid UDP glucuronyltransferase: glucuronidation of synthetic estrogens as steroids*. J Steroid Biochem, 1977. **8**(8): p. 867-72.
93. Brown, R.P., et al., *Physiological parameter values for physiologically based pharmacokinetic models*. Toxicol Ind Health, 1997. **13**(4): p. 407-84.
94. Dedrick, R.L., *Animal scale-up*. J Pharmacokinet Biopharm, 1973. **1**(5): p. 435-61.
95. Williams, D.T. and B.J. Blanchfield, *The retention, distribution, excretion, and metabolism of dibutyl phthalate-7-14 C in the rat*. J Agric Food Chem, 1975. **23**(5): p. 854-8.
96. Hanwell, A. and J.L. Linzell, *The time course of cardiovascular changes in lactation in the rat*. J Physiol, 1973. **233**(1): p. 93-109.
97. Knight, C.H. and M. Peaker, *Mammary cell proliferation in mice during pregnancy and lactation in relation to milk yield*. Q J Exp Physiol, 1982. **67**(1): p. 165-77.
98. Naismith, D.J., D.P. Richardson, and A.E. Pritchard, *The utilization of protein and energy during lactation in the rat, with particular regard to the use of fat accumulated in pregnancy*. Br J Nutr, 1982. **48**(2): p. 433-41.

99. Clewell, R.A., et al., *Predicting fetal perchlorate dose and inhibition of iodide kinetics during gestation: a physiologically-based pharmacokinetic analysis of perchlorate and iodide kinetics in the rat*. Toxicol Sci, 2003. **73**(2): p. 235-55.
100. O'Flaherty, E.J., et al., *A physiologically based kinetic model of rat and mouse gestation: disposition of a weak acid*. Toxicol Appl Pharmacol, 1992. **112**(2): p. 245-56.
101. LaBorde, J.B., et al., *Prenatal dexamethasone exposure in rats: effects of dose, age at exposure, and drug-induced hypophagia on malformations and fetal organ weights*. Fundam Appl Toxicol, 1992. **19**(4): p. 545-54.
102. Naessany, S. and R. Picon, *Onset of a feedback inhibition by testosterone in male rat fetuses*. Biol Neonate, 1982. **41**(5-6): p. 234-9.
103. Park, H.W. and T.H. Shepard, *Volume and glucose concentration of rat amniotic fluid: effects on embryo nutrition and axis rotation*. Teratology, 1994. **49**(6): p. 465-9.
104. Wykoff, M.H., *Weight changes of the developing rat conceptus*. Am J Vet Res, 1971. **32**(10): p. 1633-5.
105. Luquita, M.G., et al., *Molecular basis of perinatal changes in UDP-glucuronosyltransferase activity in maternal rat liver*. J Pharmacol Exp Ther, 2001. **298**(1): p. 49-56.
106. Sjoberg, P., U. Bondesson, and J. Gustafsson, *Metabolism of mono-(2-ethylhexyl)phthalate in fetal, neonatal and adult rat liver*. Biol Neonate, 1988. **53**(1): p. 32-8.
107. Alcorn, J., et al., *Evaluation of the assumptions of an ontogeny model of rat hepatic cytochrome P450 activity*. Drug Metab Dispos, 2007. **35**(12): p. 2225-31.
108. Soucy, N.V., et al., *Kinetics of genistein and its conjugated metabolites in pregnant Sprague-Dawley rats following single and repeated genistein administration*. Toxicol Sci, 2006. **90**(1): p. 230-40.
109. Isaksson, A., B. Hultberg, and M. Bergenfeldt, *Lysosomal enzymes in pregnant and steroid treated rats*. Horm Metab Res, 1988. **20**(5): p. 274-7.
110. Anderson, W.A., et al., *A biomarker approach to measuring human dietary exposure to certain phthalate diesters*. Food Addit Contam, 2001. **18**(12): p. 1068-74.
111. Albro, P.W., R. Thomas, and L. Fishbein, *Metabolism of diethylhexyl phthalate by rats. Isolation and characterization of the urinary metabolites*. J Chromatogr, 1973. **76**(2): p. 321-30.



112. Neale, M.G. and D.V. Parke, *Effects of pregnancy on the metabolism of drugs in the rat and rabbit*. *Biochem Pharmacol*, 1973. **22**(12): p. 1451-61.
113. Borch, J., et al., *Steroidogenesis in fetal male rats is reduced by DEHP and DINP, but endocrine effects of DEHP are not modulated by DEHA in fetal, prepubertal and adult male rats*. *Reprod Toxicol*, 2004. **18**(1): p. 53-61.
114. Thompson, R.C. and O.L. Hollis, *Irradiation of the gastrointestinal tract of the rat by ingested ruthenium-106*. *Am J Physiol*, 1958. **194**(2): p. 308-12.
115. Altman, P.L. and D.S. Dittmer, *Volume of blood in tissue: Vertebrates*, in *Respiration and Circulation*. 1971, Federation of American Societies for Experimental Biology: Bethesda, Md. p. pp.383-387.
116. Buelke-Sam, J., J.F. Holson, and C.J. Nelson, *Blood flow during pregnancy in the rat: II. Dynamics of and litter variability in uterine flow*. *Teratology*, 1982. **26**(3): p. 279-88.
117. Sjoberg, P., et al., *Kinetics of di-(2-ethylhexyl) phthalate in immature and mature rats and effect on testis*. *Acta Pharmacol Toxicol (Copenh)*, 1985. **56**(1): p. 30-7.
118. Chu, I., et al., *Metabolism and tissue distribution of mono-2-ethylhexyl phthalate in the rat*. *Drug Metab Dispos*, 1978. **6**(2): p. 146-9.
119. Jones, H.B., et al., *The influence of phthalate esters on Leydig cell structure and function in vitro and in vivo*. *Exp Mol Pathol*, 1993. **58**(3): p. 179-93.
120. Ascoli, M., *Characterization of several clonal lines of cultured Leydig tumor cells: gonadotropin receptors and steroidogenic responses*. *Endocrinology*, 1981. **108**(1): p. 88-95.
121. Livak, K.J. and T.D. Schmittgen, *Analysis of relative gene expression data using real-time quantitative PCR and the 2(-Delta Delta C(T)) Method*. *Methods*, 2001. **25**(4): p. 402-8.
122. Dees, J.H., M. Gazouli, and V. Papadopoulos, *Effect of mono-ethylhexyl phthalate on MA-10 Leydig tumor cells*. *Reprod Toxicol*, 2001. **15**(2): p. 171-87.
123. Shultz, V.D., et al., *Altered gene profiles in fetal rat testes after in utero exposure to di(n-butyl) phthalate*. *Toxicol Sci*, 2001. **64**(2): p. 233-42.
124. Nativelle, C., et al., *Metabolism of n-butyl benzyl phthalate in the female Wistar rat. Identification of new metabolites*. *Food Chem Toxicol*, 1999. **37**(8): p. 905-17.
125. Oishi, S., *Effects of phthalic acid esters on testicular mitochondrial functions in the rat*. *Arch Toxicol*, 1990. **64**(2): p. 143-7.

126. Akingbemi, B.T., et al., *Modulation of rat Leydig cell steroidogenic function by di(2-ethylhexyl)phthalate*. Biol Reprod, 2001. **65**(4): p. 1252-9.
127. Wang, X., et al., *The role of arachidonic acid in steroidogenesis and steroidogenic acute regulatory (StAR) gene and protein expression*. J Biol Chem, 2000. **275**(26): p. 20204-9.
128. Berenbaum, F., et al., *Concomitant recruitment of ERK1/2 and p38 MAPK signalling pathway is required for activation of cytoplasmic phospholipase A2 via ATP in articular chondrocytes*. J Biol Chem, 2003. **278**(16): p. 13680-7.
129. Six, D.A. and E.A. Dennis, *The expanding superfamily of phospholipase A(2) enzymes: classification and characterization*. Biochim Biophys Acta, 2000. **1488**(1-2): p. 1-19.
130. Kudo, I. and M. Murakami, *Phospholipase A2 enzymes*. Prostaglandins Other Lipid Mediat, 2002. **68-69**: p. 3-58.
131. Lin, T., *Mechanism of action of gonadotropin-releasing hormone stimulated Leydig cell steroidogenesis. III. The role of arachidonic acid and calcium/phospholipid dependent protein kinase*. Life Sci, 1985. **36**(13): p. 1255-64.
132. Didolkar, A.K. and K. Sundaram, *Mechanism of LHRH-stimulated steroidogenesis in rat Leydig cells: lipoxygenase products of arachidonic acid may not be involved*. J Androl, 1989. **10**(6): p. 449-55.
133. Das, S., et al., *Mechanism of group IVA cytosolic phospholipase A(2) activation by phosphorylation*. J Biol Chem, 2003. **278**(42): p. 41431-42.
134. Nosten, F., et al., *Antimalarial drugs in pregnancy: a review*. Curr Drug Saf, 2006. **1**(1): p. 1-15.
135. Nord, J.E., et al., *Hydroxychloroquine cardiotoxicity in systemic lupus erythematosus: a report of 2 cases and review of the literature*. Semin Arthritis Rheum, 2004. **33**(5): p. 336-51.
136. Ochsendorf, F.R. and U. Runne, *[Chloroquine and hydroxychloroquine: side effect profile of important therapeutic drugs]*. Hautarzt, 1991. **42**(3): p. 140-6.
137. Ostensen, M., et al., *Anti-inflammatory and immunosuppressive drugs and reproduction*. Arthritis Res Ther, 2006. **8**(3): p. 209.
138. Mgbodile, M.U., *Effects of perinatal exposure of albino rats to chloroquine*. Biol Neonate, 1987. **51**(5): p. 273-6.

139. Okanlawon, A.O., et al., *Chloroquine-induced retardation of foetal lung maturation in rats*. Afr J Med Med Sci, 1993. **22**(2): p. 61-7.
140. Zahid, A. and T.S. Abidi, *Effect of chloroquine on liver weight of developing albino rats*. J Pak Med Assoc, 2003. **53**(1): p. 21-3.
141. Sharma, A. and A.K. Rawat, *Toxicological consequences of chloroquine and ethanol on the developing fetus*. Pharmacol Biochem Behav, 1989. **34**(1): p. 77-82.
142. Matsuzawa, Y. and K.Y. Hostetler, *Studies on drug-induced lipidosis: subcellular localization of phospholipid and cholesterol in the liver of rats treated with chloroquine or 4,4'-bis (diethylaminoethoxy)alpha, beta-diethyldiphenylethane*. J Lipid Res, 1980. **21**(2): p. 202-14.
143. Yamamoto, A., et al., *Studies on drug-induced lipidosis: VII. Effects of bis-beta-diethyl-aminoethylether of hexestrol, chloroquine, homochlorocyclizine, prenylamine, and diazacholesterol on the lipid composition of rat liver and kidney*. Lipids, 1976. **11**(8): p. 616-22.
144. Grabner, R., *Influence of cationic amphiphilic drugs on the phosphatidylcholine hydrolysis by phospholipase A2*. Biochem Pharmacol, 1987. **36**(7): p. 1063-7.
145. Nicola, W.G., *Chloroquine therapy reduces oestrogen production in females*. Boll Chim Farm, 1997. **136**(5): p. 447-9.
146. Nicola, W.G., M.I. Khayria, and M.M. Osfor, *Plasma testosterone level and the male genital system after chloroquine therapy*. Boll Chim Farm, 1997. **136**(1): p. 39-43.
147. Okanlawon, A.O. and O.A. Ashiru, *Effect of chloroquine on oestrus cycle and ovulation in cyclic rats*. J Appl Toxicol, 1992. **12**(1): p. 45-8.
148. Okanlawon, A.O., C.C. Noronha, and O.A. Ashiru, *An investigation into the effects of chloroquine on fertility of male rats*. West Afr J Med, 1993. **12**(2): p. 118-21.
149. Ebong, P.E., et al., *Influence of chronic administration of chloroquine on Leydig cell integrity and testosterone profile albino wistar rats*. Afr J Reprod Health, 1999. **3**(2): p. 97-101.
150. Akintonwa, A., S.A. Gbajumo, and A.F. Mabadeje, *Placental and milk transfer of chloroquine in humans*. Ther Drug Monit, 1988. **10**(2): p. 147-9.
151. Akintonwa, A., M.C. Meyer, and M.K. Yau, *Placental transfer of chloroquine in pregnant rabbits*. Res Commun Chem Pathol Pharmacol, 1983. **40**(3): p. 443-55.
152. Deng, H., et al., *Sensitive fluorescence HPLC assay for AQ-13, a candidate aminoquinoline antimalarial, that also detects chloroquine and N-dealkylated*

- metabolites*. J Chromatogr B Analyt Technol Biomed Life Sci, 2006. **833**(2): p. 122-8.
153. Pearse, A.G.E., *Histotechnology: A Self-instructional Text*. 2006, Chicago: ASCP Press.
154. Bennati, A.M., et al., *Sterol dependent regulation of human TM7SF2 gene expression: role of the encoded 3beta-hydroxysterol Delta14-reductase in human cholesterol biosynthesis*. Biochim Biophys Acta, 2006. **1761**(7): p. 677-85.
155. Miller, W.L., *Steroidogenic acute regulatory protein (StAR), a novel mitochondrial cholesterol transporter*. Biochim Biophys Acta, 2007. **1771**(6): p. 663-76.
156. El-Gehani, F., et al., *Natriuretic peptides stimulate steroidogenesis in the fetal rat testis*. Biol Reprod, 2001. **65**(2): p. 595-600.
157. Collin, O., E. Lissbrant, and A. Bergh, *Atrial natriuretic peptide, brain natriuretic peptide and c-type natriuretic peptide: effects on testicular microcirculation and immunohistochemical localization*. Int J Androl, 1997. **20**(1): p. 55-60.
158. Dobozy, O., O. Brindak, and G. Csaba, *Influence of pituitary hormones (hCG, TSH, Pr, GH) on testosterone level and on the functional activity of the Leydig cell in rat fetuses*. Acta Physiol Hung, 1988. **72**(2): p. 159-63.
159. Acton, S., et al., *Identification of scavenger receptor SR-BI as a high density lipoprotein receptor*. Science, 1996. **271**(5248): p. 518-20.
160. Dass, E.E. and K.K. Shah, *Paracetamol and conventional antimalarial drugs induced hepatotoxicity and its protection by methionine in rats*. Indian J Exp Biol, 2000. **38**(11): p. 1138-42.
161. Ngaha, E.O., *Some biochemical changes in the rat during repeated chloroquine administration*. Toxicol Lett, 1982. **10**(2-3): p. 145-9.
162. McIntyre, B.S., N.J. Barlow, and P.M. Foster, *Androgen-mediated development in male rat offspring exposed to flutamide in utero: permanence and correlation of early postnatal changes in anogenital distance and nipple retention with malformations in androgen-dependent tissues*. Toxicol Sci, 2001. **62**(2): p. 236-49.
163. Foster, P.M., et al., *Effects of phthalate esters on the developing reproductive tract of male rats*. Hum Reprod Update, 2001. **7**(3): p. 231-5.
164. Borch, J., et al., *Diisobutyl phthalate has comparable anti-androgenic effects to di-n-butyl phthalate in fetal rat testis*. Toxicol Lett, 2006. **163**(3): p. 183-90.

165. Sjoberg, P., et al., *Effects of di-(2-ethylhexyl) phthalate and five of its metabolites on rat testis in vivo and in in vitro*. Acta Pharmacol Toxicol (Copenh), 1986. **58**(3): p. 225-33.
166. Fan, L.Q., et al., *Regulation of phase I and phase II steroid metabolism enzymes by PPAR alpha activators*. Toxicology, 2004. **204**(2-3): p. 109-21.
167. Osifo, N. G., *The effect of pyrogen on the in vivo metabolism and intital kinetics of chloroquine in rats*. J Pharm Pharmacol, 1979. **31**: p. 747-51.
168. Wooten, R. E., *Novel translocation responses of cytosolic phospholipase A2alpha fluorescent proteins*. Biochim Biophys Acta, 2008. **1783**(8): p. 1544-50.